UNIVERSIDADE FEDERAL DE JUIZ DE FORA
FACULDADE DE ENGENHARIA
PROGRAMA DE PÓS-GRADUAÇÃO EM ENGENHARIA ELÉTRICA

Patrícia de Sousa Oliveira Silva

Economic Viability of Long-Duration Energy Storage Systems: A State-Wise Study in the United States

Juiz de Fora
2026

Patrícia de Sousa Oliveira Silva

Economic Viability of Long-Duration Energy Storage Systems: A State-Wise Study in the United States

Thesis presented to the Postgraduate Program in Electrical Engineering of Universidade Federal de Juiz de Fora as a partial requirement for obtaining the title of Doctor in Electrical Engineering. Concentration area: Electrical Power Systems.

Adiviser: Prof. André Luís Marques Marcato, D.Sc.

Co-adiviser: Alexandre Moreira da Silva, PhD.

Juiz de Fora

2026

Ficha catalográfica elaborada através do programa de geração
automática da Biblioteca Universitária da UFJF,
com os dados fornecidos pelo(a) autor(a)

de Sousa Oliveira Silva, Patrícia.
Economic Viability of Long-Duration Energy Storage Systems: A State-Wise Study in the United States / Patrícia de Sousa Oliveira Silva. -- 2026.
171 f.

Orientador: André Luís Marques Marcato
Coorientador: Alexandre Moreira da Silva
Tese (doutorado) - Universidade Federal de Juiz de Fora, Faculdade de Engenharia. Programa de Pós-Graduação em Engenharia Elétrica, 2026.

1. Power systems planning and economics. 2. Long-duration storage systems. 3. Valuation of emergent technology. I. Luís Marques Marcato, André, orient. II. Moreira da Silva, Alexandre, coorient. III. Título.

FEDERAL UNIVERSITY OF JUIZ DE FORA
RESEARCH AND GRADUATE PROGRAMS OFFICE

Patrícia de Sousa Oliveira Silva

Economic Viability of Long-Duration Energy Storage Systems: A State-Wise Study in the United States

Thesis submitted to the Graduate Program in Electrical Engineering
of the Federal University of Juiz de Fora as a partial
requirement for obtaining a Doctor's degree in Electrical Engineering.
Concentration area: Electrical Power Systems

Approved on 31 of March of 2026.

EXAMINING BOARD

Prof. Dr. André Luis Marques Marcato – Academic Advisor
Federal University of Juiz de Fora

Prof. Dr. Alexandre Moreira da Silva – Academic Co-Advisor
Lawrence Berkeley National Laboratory

Prof. Dr. Anderson Rodrigo de Queiroz
North Carolina State University

Prof. Dr. Daniel Ramos Louzada
Pontifical Catholic University of Rio de Janeiro

Prof. Dr. João Alberto Passos Filho
Federal University of Juiz de Fora

Prof. Dr. Bruno Henriques Dias
Federal University of Juiz de Fora

Juiz de Fora, 03/31/2026.

Documento assinado eletronicamente por **Joao Alberto Passos Filho**, **Professor(a)**, em 31/03/2026, às 13:19, conforme horário oficial de Brasília, com fundamento no § 3º do art. 4º do Decreto nº 10.543, de 13 de novembro de 2020.

Documento assinado eletronicamente por **Daniel Ramos Louzada**, **Usuário Externo**, em 31/03/2026, às 13:20, conforme horário oficial de Brasília, com fundamento no § 3º do art. 4º do Decreto nº 10.543, de 13 de novembro

de 2020.

Documento assinado eletronicamente por **Bruno Henriques Dias**, **Professor(a)**, em 31/03/2026, às 13:20, conforme horário oficial de Brasília, com fundamento no § 3º do art. 4º do Decreto nº 10.543, de 13 de novembro de 2020.

Documento assinado eletronicamente por **Alexandre Moreira da Silva**, **Usuário Externo**, em 31/03/2026, às 13:24, conforme horário oficial de Brasília, com fundamento no § 3º do art. 4º do Decreto nº 10.543, de 13 de novembro de 2020.

Documento assinado eletronicamente por **Anderson Rodrigo de Queiroz**, **Usuário Externo**, em 27/05/2026, às 12:49, conforme horário oficial de Brasília, com fundamento no § 3º do art. 4º do Decreto nº 10.543, de 13 de novembro de 2020.

Documento assinado eletronicamente por **Andre Luis Marques Marcato**, **Professor(a)**, em 28/05/2026, às 14:12, conforme horário oficial de Brasília, com fundamento no § 3º do art. 4º do Decreto nº 10.543, de 13 de novembro de 2020.

A autenticidade deste documento pode ser conferida no Portal do SEI-Ufjf (www2.ufjf.br/SEI) através do ícone Conferência de Documentos, informando o código verificador **2900214** e o código CRC **4ED108B4**.

I dedicate this work, first and foremost, to God, the source of all light and wisdom. To the Blessed Virgin Mary, for her constant intercession and maternal presence. And to my husband, Wilian, with love and gratitude, for all his support and encouragement throughout this journey.

ACKNOWLEDGMENTS

I thank God, who granted me the wisdom to carry out this research. I am deeply grateful to my husband, Wilian, for his unwavering love, support, and encouragement throughout this entire journey. During our time in the United States, he faced every challenge by my side with strength and generosity. His partnership was essential in balancing doctoral studies and motherhood, and his constant presence as a devoted husband and wonderful father made this achievement possible. I would like to express my sincere appreciation to my advisor, Dr. André Luís Marques Marcato, for his guidance and support throughout this research. I am especially and profoundly grateful to my co-advisor, PhD Alexandre Moreira da Silva, for his remarkable dedication, patience, and unwavering support, as well as for the invaluable knowledge and insights he shared during these years of research. He also served as my supervisor during my time at Lawrence Berkeley National Laboratory (LBNL) in Berkeley, California, United States, where his mentorship was fundamental to the development of this work. I am also sincerely thankful to Dr. Miguel Heleno for his guidance and support during my period at LBNL, which significantly contributed to the direction and advancement of this research. I would also like to acknowledge M.Sc. Felipe Piancó, my colleague at LBNL, for his support in the daily research activities and for sharing both the professional and personal journey during my time in the United States. Finally, I gratefully acknowledge the indispensable support of CAPES (Coordenação de Aperfeiçoamento de Pessoal de Nível Superior), the partial support provided by the Graduate Program in Electrical Engineering at the Federal University of Juiz de Fora, as well as funding from CNPq (404859/2025-9) and FAPEMIG (APQ-02800-23) throughout my doctoral studies.

RESUMO

A necessidade urgente de descarbonização no setor energético tem levado a uma ênfase crescente na integração de fontes de energia renovável, como eólica e solar, nas redes elétricas. Embora esses recursos ofereçam benefícios ambientais significativos, eles também introduzem desafios relacionados à intermitência e variabilidade. As tecnologias de armazenamento de energia de longa duração (LDES - *Long-Duration Energy Storage*) surgiram como uma solução muito promissora para lidar com esses desafios, armazenando o excesso de energia durante os períodos de alta geração e fornecendo-a quando a demanda é alta ou quando os recursos renováveis são escassos por um período de tempo prolongado. Esta pesquisa apresenta uma nova metodologia para estimar o custo limite da tecnologia de sistemas LDES para a viabilidade econômica em sistemas de energia descarbonizados. Nossa metodologia é aplicada para estimar os custos limite em 2050 para cada estado dos Estados Unidos contíguos de acordo com suas características, com o objetivo de alcançar a aposentadoria total de usinas de energia a gás e carvão. As ambiciosas metas de descarbonização dos EUA e a transição para um sistema elétrico baseado em energia renovável apresentam um contexto ideal para examinar o papel do LDES. Os resultados também oferecem *insights* sobre o planejamento necessário para a expansão da capacidade e a contribuição operacional do LDES no cenário energético do estado, levando em consideração os perfis de demanda de energia únicos e a disponibilidade de recursos renováveis da região. Nossas descobertas têm como objetivo fornecer informações complementares para orientar os tomadores de decisão, planejadores de energia e quaisquer outras partes interessadas na tomada de decisões informadas sobre o investimento em LDES no contexto de um futuro de energia descarbonizada. Além disso, descobrimos que apenas 4 estados (de 48) seriam capazes de remover a geração convencional firme apoiada por sistemas LDES sem aumentar os custos totais do sistema, sob a meta de custo atual do Departamento de Energia dos EUA de US$ 1100 kW^{-1} para LDES de "vários dias".

Palavras-chave: Planejamento e economia de sistemas de energia, sistemas de armazenamento de longa duração, avaliação de tecnologias emergentes.

ABSTRACT

The urgent need for decarbonization in the energy sector has led to an increased emphasis on the integration of renewable energy sources, such as wind and solar, into power grids. While these resources offer significant environmental benefits, they also introduce challenges related to intermittency and variability. Long-duration energy storage (LDES) technologies have emerged as a very promising solution to address these challenges by storing excess energy during periods of high generation and delivering it when demand is high or renewable resources are scarce for a sustained amount of time. This research introduces a novel methodology for estimating the boundary technology cost of LDES systems for economic viability in decarbonized energy systems. Our methodology is applied to estimate the boundary costs in 2050 for each state of the contiguous United States according to its characteristics to achieve full retirement of gas and coal power plants. The U.S.'s ambitious decarbonization goals and transition to a renewable energy-based power system present an ideal context for examining the role of LDES. The results also offer insights into the needed capacity expansion planning and the operational contribution of LDES in the state's energy landscape, taking into account the unique energy demand profiles and renewable resource availability of the region. Our findings are intended to provide complementary information to guide decision-makers, energy planners, and any other stakeholders in making informed choices about LDES investment in the context of a decarbonized energy future. In addition, we find that only 4 states (out of 48) would be able to remove firm conventional generation supported by LDES systems without increasing their total system costs under the current US Department of Energy cost target of US$ 1100 kW^{-1} for multi-day LDES.

Keywords: Power systems planning and economics, long-duration storage systems, valuation of emergent technology.

LIST OF FIGURES

Figure 1 – Flowchart of the main steps of the proposed methodology. 35
Figure 2 – Methodology graphical abstract. 37
Figure 3 – Overview of the analytical structure adopted in the case studies, progressing from a detailed operational analysis in California to a nationwide expansion. 57
Figure 4 – Map of California with BA representatives covered by the model. Source: Adapted from [44]. 60
Figure 5 – Composition of the energy matrix for generating electrical energy in California through the years. Source: Adapted from [58]. 65
Figure 6 – The boundary costs of LDES below which these technologies will be economically viable for the California's system in 2050. 67
Figure 7 – Opportunity values (in purple) associated with different power capacities of 100-hour LDES. For illustration purposes, the FO&M cost of some existing generators and storages are omitted from the figure. 67
Figure 8 – Comparison between (i) the reference costs from the *baseline model*, (ii) the resulting costs from the *opportunity value maximization model* when the gas is replaced by a combination of 17 GW 100-hour LDES, SDES, and RES, and (iii) the resulting costs from the *opportunity value maximization model* when the gas is replaced by a combination of SDES and RES only. 68
Figure 9 – Additional investment required in California in 2050 to have a system without gas energy sources. 69
Figure 10 – The cost reduction in the California system in 2050 for different quantities of LDES when the gas plants are retired. The base net cost reduction refers to the decrease in overall costs once 8.7 GW of LDES are included in the system compared to when gas units are still present. 70

Figure 11 – (a) Aggregate hourly dispatch of all gas power plants from the *baseline model*'s solution. (b) 100-hour LDES system with 8.7 GW of power capacity – state of charge according to the *opportunity value maximization model*'s solution. (c) 4-hour SDES system with 5.3 GW of power capacity – state of charge according to the *opportunity value maximization model*'s solution. 72
Figure 12 – Average hourly availability per month of all installed renewable sources in California per month in 2050 according to the solution of the *opportunity value maximization model* when the 100-hour LDES power capacity is 8.7 GW. 73
Figure 13 – Annual generation contribution per technology for California in 2050 – (a) results of the *baseline model* and (b) results of the *opportunity value maximization model* when the 100-hour LDES power capacity is 8.7 GW. 74
Figure 14 – Annual reserve provision per technology for California in 2050 – (a) results of the *baseline model* and (b) results of the *opportunity value maximization model* when the 100-hour LDES power capacity is 8.7 GW. 74
Figure 15 – Heat map showing the number of hours that SDES discharges consecutively for different quantities of LDES. 75
Figure 16 – Heat map showing the number of hours that SDES charges consecutively for different quantities of LDES. 76
Figure 17 – Heat map showing the number of hours that LDES discharges consecutively for different quantities of LDES. 77
Figure 18 – Heat map showing the number of hours that LDES charges consecutively for different quantities of LDES. 78
Figure 19 – Maximum, minimum, and average monthly energy prices resulting from operating the *baseline model* and the modified system with 17 GW of 100-hour LDES power capacity. 79
Figure 20 – Maximum, minimum, and average monthly, charging and discharging energy prices taken by SDES when operating the *baseline model*. 81

Figure 21 – Maximum, minimum, and average monthly, charging and discharging energy prices taken by SDES when operating the modified system with 17 GW of 100-hour LDES power capacity. 81
Figure 22 – Maximum, minimum, and average monthly, charging and discharging energy prices taken by LDES when operating the modified system with 17 GW of 100-hour LDES power capacity. 82
Figure 23 – Additional six curves of the boundary costs of LDES below which these technologies will be economically viable for the California's system in 2050 given gas price fluctuations around the reference value. 83
Figure 24 – Heat map of various boundary costs of LDES (for 17 GW 100-hour LDES power capacity) considering price fluctuations in natural gas fuel price and solar investment costs compared to their respective reference values. 85
Figure 25 – The boundary costs of LDES below which these technologies will be economically viable for the California's system in 2050 for three different LDES duration: (a) 40-hour LDES; (b) 100-hour LDES; (c) 160-hour LDES. 86
Figure 26 – LDES maximum boundary cost and power capacity distribution across US states in 2050. (a) Maximum boundary cost of 100-hour LDES ($/kW) for each US state, considering the power capacity that maximizes the boundary cost. (b) Histogram of the LDES maximum boundary cost ($/kW) across states with positive values. (c) Histogram of the LDES power capacity (GW) that maximizes the boundary cost in states with positive values. 90
Figure 27 – Comparison between the national LDES capacity projected by the US-DOE and the 100-hour LDES capacity required for thermal replacement according to the findings of this thesis. . . . 92
Figure 28 – The boundary costs of LDES below which these technologies will be economically viable for the system in 2050, for: (a) Colorado, (b) Florida, (c) Iowa, and (d) Michigan. 93

Figure 29 – (a) US total system capacity by technology in 2050 under the *baseline* and *opportunity value maximization models*, shown from two perspectives: total installed capacity (left) and thermal replacement effects (right), with and without LDES. (b) Same analysis for total system costs. Results are based on 43 states with positive boundary costs. 94
Figure 30 – Box plots comparing key system metrics for US states categorized by boundary costs. Figure (a) compares the top 10 and bottom 10 states in terms of boundary cost, and figure (b) extends to the top 24 and bottom 24, encompassing all states. . . . 98
Figure 31 – Relationship between solar generation share and average RES capacity factor across US states. 99
Figure 32 – Interactive dashboard interface developed for exploring state-level economic and operational results. 104
Figure 33 – Annual generation mix and reserve allocation for Georgia (a) and Texas (b) under the *baseline* and *opportunity value models*. 105
Figure 34 – Comparison of seasonal SoC differences: (a) Spring and (b) Winter. 106
Figure 35 – Comparison of seasonal SoC differences: (a) Summer and (b) Fall. 107
Figure 36 – Average relative availability of RES (in % of total demand) among the 48 states for each meteorological season. 108
Figure 37 – Different LDES SOC patterns. (a) LDES SoC in Utah throughout the year. (b) LDES SoC throughout the year in Vermont. 109
Figure 38 – Boundary cost curves for states that achieved positive values under varying LDES round-trip efficiencies. 111
Figure 39 – Alabama (AL). 123
Figure 40 – Arkansas (AR). 124
Figure 41 – Arizona (AZ). 125
Figure 42 – California (CA). 126
Figure 43 – Colorado (CO). 127
Figure 44 – Connecticut (CT). 128
Figure 45 – Delaware (DE). 129

Figure 46 – Florida (FL). 130
Figure 47 – Georgia (GA). 131
Figure 48 – Iowa (IA). 132
Figure 49 – Idaho (ID). 133
Figure 50 – Illinois (IL). 134
Figure 51 – Indiana (IN). 135
Figure 52 – Kansas (KS). 136
Figure 53 – Kentucky (KY). 137
Figure 54 – Louisiana (LA). 138
Figure 55 – Massachusetts (MA). 139
Figure 56 – Maryland (MD). 140
Figure 57 – Maine (ME). 141
Figure 58 – Michigan (MI). 142
Figure 59 – Minnesota (MN). 143
Figure 60 – Missouri (MO). 144
Figure 61 – Mississippi (MS). 145
Figure 62 – Montana (MT). 146
Figure 63 – North Carolina (NC). 147
Figure 64 – North Dakota (ND). 148
Figure 65 – Nebraska (NE). 149
Figure 66 – New Hampshire (NH). 150
Figure 67 – New Jersey (NJ). 151
Figure 68 – New Mexico (NM). 152
Figure 69 – Nevada (NV). 153
Figure 70 – New York (NY). 154
Figure 71 – Ohio (OH). 155
Figure 72 – Oklahoma (OK). 156
Figure 73 – Oregon (OR). 157
Figure 74 – Pennsylvania (PA). 158
Figure 75 – Rhode Island (RI). 159
Figure 76 – South Carolina (SC). 160
Figure 77 – South Dakota (SD). 161
Figure 78 – Tennessee (TN). 162

Figure 79 – Texas (TX). 163
Figure 80 – Utah (UT). 164
Figure 81 – Virginia (VA). 165
Figure 82 – Vermont (VT). 166
Figure 83 – Washington (WA). 167
Figure 84 – Wisconsin (WI). 168
Figure 85 – West Virginia (WV). 169
Figure 86 – Wyoming (WY). 170

LIST OF TABLES

Table 1 – Summary of the literature review on LDES cost and performance parameters. 29
Table 2 – Minimum required inputs to characterize the energy matrix and apply the proposed modeling framework. 34
Table 3 – Sets used in the mathematical model. 37
Table 4 – Parameters used in the mathematical model. 38
Table 5 – Decision variables used in the model. 39
Table 6 – Installed capacity, investment limits, and number of generators by technology in the initial California implementation. . . 63
Table 7 – Power capacity and the limit of investment by technology with the respective number of storage. 64
Table 8 – Top 10 and bottom 10 boundary cost: insights from the *baseline model* run. 96
Table 9 – All values of key parameters for US states. 100
Table 10 – Maximum boundary costs ($/kW) and their corresponding optimal LDES power capacities (GW) under different round-trip efficiencies. 110

LIST OF ABBREVIATIONS AND ACRONYMS

ACAES	Adiabatic Compressed Air Energy Storage
AEO	Annual Energy Outlook
AI	Artificial Intelligenc
ATB	Annual Technology Baseline
BA	Balancing Area
BCV	Boundary Cost Values
CAES	Compressed Air Energy Storage
CAISO	California Independent System Operator
CAPEX	Capital Cxpenditures
CEM	Capacity Expansion Model
CES	Carbonates Energy Storage
CF	Capacity Factor
CH4	Methane
CO2	Carbon Dioxide
CPI	Consumer Price Index
DoD	Depth of Discharge
ES	Energy Storage
FO&M	Fixed Operation and Maintenance
GHG	Greenhouse Gases
GW	Gigawatt
HES	Hydroxides Energy Storage
LAES	Liquid Air Energy Storage
LCOE	Levelized Cost of Energy
LCOS	Levelized Cost of Storage
LDES	Long-Duration Energy Storage
MW	Megawatt
N2O	Nitrous Oxide
OES	Oxides Energy Storage
ONS	National System Operator
PHS	Pumped Hydroelectric Storage
PTES	Pumped Thermal Energy Storage
ReEDS	Regional Energy Deployment System
RES	Renewable Energy Sources

RoCoF	Rates of Change of Frequency
SB 100	Senate Bill 100
SDES	Short-Duration Energy Storage
SoC	State-of-Charge
TMES	Thermo-Mechanical Energy Storage
US-DOE	US Department of Energy

CONTENTS

1	**Introduction**	**20**
1.1	Motivation	20
1.2	LDES main technologies	23
1.3	Literature review	24
1.4	Contributions and objectives	30
1.5	Related Publications	31
1.6	Organization of the Thesis	32
2	**Proposed Methodology**	**33**
2.1	Methodology objective	36
2.2	Sets, parameters and variables	36
2.3	Baseline model	39
2.3.1	Objective function	40
2.3.2	Balance	42
2.3.3	Reserve margin	42
2.3.4	Storage devices	43
2.3.5	Generators	46
2.4	Opportunity value maximization model	50
2.4.1	Objective function	50
2.4.2	Overall cost	51
2.4.3	Balance, reserve margin, storage devices, and generators	52
2.5	Solution framework	52
2.6	Conclusion	54
3	**Results and Discussions**	**55**
3.1	Initial definitions and assumptions	55
3.1.1	Model application	55
3.1.2	Data source	57
3.1.3	Spatial and temporal resolution	59
3.1.4	Fixed and candidate generators	61
3.1.5	Fixed and candidate batteries	62
3.2	Case Study –California	63
3.2.1	Economic results	66

3.2.2 Operational results 71
3.2.3 Contrasting charge-discharge behavior 73
3.2.4 Energy price analysis 77
3.2.5 Sensitivity analyses 81
3.2.5.1 Analysis of natural gas fuel prices 82
3.2.5.2 Analysis of gas prices and solar investment costs 84
3.2.5.3 Analysis of LDES duration impacts 84
3.3 Case Study – United States 86
3.3.1 National overview of boundary costs across the states 88
3.3.2 LDES capacity required for thermal replacement 91
3.3.3 Reasons for high and low boundary costs 95
3.3.4 Comparative analysis of representative state cases 98
3.3.5 Seasonal state of charge dynamics of LDES 104
3.3.6 Analysis of LDES round-trip efficiency impacts on states with negative boundary costs 109
4 Conclusion and future work 112
BIBLIOGRAPHY 117
ANNEX A – Graphs on the operation of all the states of the US 123

1 Introduction

1.1 Motivation

Climate concerns motivated a necessary global movement towards decarbonization, with countries all over the world pledging to reduce carbon emissions and reach net-zero emissions in the following years [1]. The United States (US) has set an ambitious path toward a fully sustainable decarbonized future, committing to reduce greenhouse gases (GHG) emissions by 50–52 % from 2005 levels by 2030 [2] and to achieve net-zero emissions by 2050 [3]. Achieving net-zero CO_2 emissions by 2050 is particularly critical to limiting the global temperature rise to 1.5 °C above pre-industrial levels, contributing significantly to achieving the common global climate objectives [1]. However, it is important to note that at the time of the publication of this thesis, the United States is no longer part of the Paris Agreement and therefore is not formally bound by its decarbonization commitments [4]. Nevertheless, the transition toward a decarbonized power system remains a relevant scenario, driven primarily by state-level policies and market dynamics.

A state in the US, California, as the fifth-largest economy in the world, serves as a prime example, demonstrating that a clean energy future is not only feasible but also beneficial to both its residents and its economy, leading the way toward carbon neutrality and a sustainable future [5]. In this state, the targets are even more aggressive according to the 100 Percent Clean Energy Act of 2018, also known as Senate Bill 100 (SB 100). The SB 100 essentially establishes that: (i) renewable energy sources (RES) will supply 60 % of California's total energy demand by 2030 and (ii) carbon neutrality must be achieved by 2045 [5]. These targets remain in effect, with the state continuing to uphold its long-term decarbonization commitment at the time of this study.

In this context, to achieve net-zero emissions, a global transition to RES is essential [6, 7]. In response, solar, hydropower, and wind power plants are being rapidly developed worldwide [8, 9]. However, the intermittent and fluctuating nature of renewable energy sources, such as solar and wind, represents a major challenge to maintaining a stable and reliable energy system [10], as stability has traditionally been ensured by firm and dispatchable resources, including, for example, hydro

power plants, natural gas units, and coal generators [11]. While natural gas and coal units offer relatively low costs when fully utilized [12], are a significant source of CO_2 emissions and climate change [13], and for true decarbonization to occur, fossil fuel-based power stations must gradually be retired.

Therefore, the strategic deployment of energy storage (ES) systems is crucial to provide the necessary flexibility and to support the continued growth of renewable energy generation [14]. As renewable energy becomes a larger part of the energy mix, integrating energy storage solutions becomes increasingly vital, because these systems can compensate for the variability by shifting surplus energy generated during peak production periods to times of high demand, ensuring flexibility and supporting the stable development of renewable power generation [9, 12]. Furthermore, deploying Battery Energy Storage Systems (BESS) has proven to be an effective strategy to address load-following requirements and post-contingency management, significantly alleviating the ramping burden on conventional thermal generators [15]. Consequently, ES is indispensable for achieving a decarbonized and sustainable energy system [10]. Currently, the participation of short-duration energy storage (SDES) systems has been essential; however, they can only discharge energy for a few hours per day, which limits their ability to ensure continuous system operation.

In addition to ES, emerging technologies referred to as “Firm” low-carbon resources that can provide consistent power across all seasons and extended periods have been examined by [16] to push toward decarbonization. These technologies include nuclear plants with flexible operations, hydropower plants with large reservoirs, coal and natural gas plants with carbon capture and sequestration (CCS), geothermal energy, and power plants fueled by biomass and biogas [16]. Some researchers focused their research mainly on technologies with CCS as an option for word net-zero emissions [17, 16, 9], however, they found that these technologies can increase the costs of decarbonizing the electric sector [17], and the specific role that CCS will play remains uncertain and immaturity [18, 16]. [16] highlights that, while variable renewables receive strong policy support, firm low-carbon resources like nuclear, geothermal, biofuels, and CCS face limited support in most regions and require greater backing for future viability.

In light of these challenges, long-duration energy storage (LDES) is an emerging technology that holds significant promise for the future. By enabling greater integration of renewable energy sources, LDES can help reduce carbon emissions and decrease reliance on fossil fuels, making it a crucial component in the transition to a cleaner energy system [9]. It can charge over extended periods when excess renewable energy is available and discharge during periods of high demand or renewable energy shortages. This capability allows LDES to function similarly to firm low-carbon technologies, providing reliable power when needed, stabilizing the grid, and reducing reliance on fossil fuel-based generation.

Moreover, unlike SDES, LDES provides key benefits that can be sustained over weeks or even months in high-renewable systems, such as: (i) enhanced system resilience and supply adequacy during prolonged weather-related events, enabling the grid to withstand extended periods of low renewable generation and demand uncertainty [19]; (ii) the ability to store excess variable renewable energy and strategically discharge, prioritizing discharge capacity, which is more valuable in a decarbonized grid [20]; (iii) the provision of firm and reliable energy over extended timescales, enabling system adequacy and cost-effective operation in power systems with very high renewable penetration, where short-duration storage is insufficient and alternative firm low-carbon resources face technical, economic, or deployment constraints [16, 21]; and (iv) the mitigation of severe low-inertia challenges, such as high Rates of Change of Frequency (RoCoF) induced by the retirement of conventional thermal plants [22, 23]. As grid-forming batteries provide synthetic inertia and help limit RoCoF [24, 25], we highlight that LDES will act as a vital stabilizing asset, providing the essential power reserves to arrest rapid frequency drops and ensure system reliability.

Additionally, some authors suggest that as variable renewable energy penetration increases to 70-80 %, LDES becomes essential to ensure grid flexibility, cost minimization, and reliable supply-demand balancing, enabling the transition to clean and high-renewable power systems [21, 26, 27, 28]. On the other hand, LDES technologies are not yet mature [19] and according to [9] the major challenge for their deployment includes high initial capital costs and the need to demonstrate cost competitiveness with alternative energy storage and flexibility solutions. Therefore,

to adequately inform policies and programs that aim to make LDES economically viable (such as the DOE's Long Duration Storage Shot [29]), there is a strong need for a systematic methodology that can estimate target LDES technology costs that will enable a cost-effective and beneficial adoption of LDES systems.

1.2 LDES main technologies

Currently, there is no consensus on the best technology to provide LDES services, with many different options to play this role under development [30], and it is unclear what the thresholds of costs and specifications should be for significant adoption [20]. For instance, lithium-ion is currently the most popular storage technology and it is able to provide a sustained output over a long period of time [20]. However, lithium-ion has a high cost per kWh of energy storage capacity, which hinders its scalability for long-duration storage applications [31]. In addition, the ideal duration of an LDES system is still a matter of discussion. Most works consider that LDES has a minimum duration of 10 hours [31, 32, 11, 33]. The US Department of Energy (US-DOE), in its turn, splits LDES technologies according to the following duration categories: (i) inter-day LDES (10–36 hours), (ii) multi-day/week LDES (36–160 hours), (iii) and seasonal shifting (160+ hours) [33]. Within these different categories, several technologies of LDES are under development with diverse cost and performance characteristics. Moreover, LDES technologies can be divided into four main types, namely, mechanical, chemical, electrochemical, and thermal [30]. The round-trip efficiencies (RTE) of these systems vary widely, typically ranging from 30 % to 90 %, depending on the technology and design optimizations [30]. Some examples of each of these types are listed as follows.

- Mechanical: the mechanical type of storage converts excess electricity into potential or kinetic energy to be reconverted and used later when the system is in need of electricity. Popular examples of mechanical storage are the Pumped Hydroelectric Storage (PHS) and the Compressed Air Energy Storage (CAES), which can be used for inter-day services, however both of them are geographically constrained [33].

- Electrochemical: the electrochemical type of storage leverages chemical reactions to store and then provide energy [1]. Typical examples include zinc or vanadium flow batteries as well as lithium-ion, sodium, and iron-air batteries [34]. This type of storage is projected to provide significant improvements for both inter-day and multi-day/week LDES use cases [33].
- Thermal: the thermal type of storage captures excess electricity in the form of heat or cold, and the most common application is the storage of molten salt in concentrating solar power (CSP) plants [1]. These systems are well-suited for multi-day/week and seasonal shifting [33].
- Chemical: the chemical type of storage involves storing energy for later use as chemical bonds [1]. One notable example is the hydrogen storage, which has the potential to provide a path for seasonal shifting services [33].

Furthermore, hybrid systems can also provide LDES services. For example, in [7], the authors explored six Thermo-Mechanical Energy Storage (TMES) technologies: adiabatic compressed air energy storage (ACAES), liquid air energy storage (LAES), pumped thermal energy storage (PTES), oxides energy storage (OES), carbonates energy storage (CES), and hydroxides energy storage (HES).

1.3 Literature review

Given the growing diversity of LDES technologies and their potential applications, understanding their role in power system planning has become a key research topic. In this context, several studies have analyzed the participation of LDES in Capacity Expansion Model (CEM), such as in [35], the authors described an analysis that focused on the minimum cost of electricity of systems using renewable sources and storage at the individual facility level in four locations, Arizona, Iowa, Massachusetts, and Texas, over 20 years with hourly resolution. This study used storage value ranges in its analysis; such costs associated with power capacity for storage systems range from 0 to US$ 2000 kW^{-1}, while energy capacity costs vary between 0 and US$ 300 kWh^{-1}. They concluded that a power and energy capacity cost of US$ 1000 kW^{-1} and US$ 20 kWh^{-1}, respectively are necessary to

provide cost-competitive. [35] reports that storage with a duration of 100 hours is sufficient to permit continuous power output 100 % of the time.

Analyzing the impact of LDES on a system in a different context, [31] discusses technical aspects of economics for LDES systems, and they explore the general LDES cost-performance parameter using the discounted cash flow framework. The main findings of the authors were that the capital cost of the energy must be substantially reduced to US$ 3 kWh^{-1} for a duration of 100 h, and US$ 7 kWh^{-1} for a duration of 50 h on a fully installed basis. Furthermore, an RTE of greater than 50 % is likely required to provide enough revenue to finance the up-front capital costs. Also, they comment that assuming such low energy capital costs can be accomplished, capital costs for the power can vary from US$ 500 kW^{-1} to US$ 1000 kW^{-1}, which they consider challenging.

Options of LDES with a range of US$ 1–20 kWh^{-1} of energy cost, power cost of US$ 500 kW^{-1} and US$ 1000 kW^{-1}, and RTE of 50 % and 80 % was considered in the context of the entire US electricity grid from 2020 through 2050 using a CEM, the Regional Investment and Operations model combined with EnergyPATHWAYS, presented in [36]. In order to meet the zero emissions target by 2050 under growing electricity demand (from 3775 TWh in 2020 to 7000 TWh in 2050), the goal was to determine how much of the gas resource and LDES is maintained in the least expensive resource portfolio across the various combinations of storage costs mentioned, while optimizing investments in renewables, gas, and LDES. According to the analysis of authors in 2050 scenarios, LDES adoption increases with lower energy costs – e.g., 10–12 h duration at US$ 20 kWh^{-1} (displacing little gas capacity), rising to approximately 45 hours at US$ 5 kWh^{-1} and up to 345 h at US$ 1 kWh^{-1} such that a storage device with between 10 and 100 hours of storage can become competitive at a marginal capital cost of between US$ 2.5–20 kWh^{-1}.

In [37], the economic viability of seasonal storage technologies Hydrogen (RTE: 40 %), CAES (RTE: 60 %), and PHS (RTE: 80 %) is assessed for the Western US power system. This is done using a multi-model 3-step approach: (i) capacity expansion planning problem, (ii) production cost analysis without seasonal storage, and (iii) re-running step 2 with optimized seasonal storage dispatch. The analysis relies on pre-established fixed cost ranges from their Table 1 for two discrete

time horizons: 2025 reference costs (hydrogen power: US$ 1507/3013/4520 kW^{-1}; energy: US$ 1.8/3.7/5.5 kWh^{-1} | CAES power: US$ 434/817/984 kW^{-1}; energy: US$ 9.1/34.9/80.8 kWh^{-1} | PHS power: US$ 573/1156/1819 kW^{-1}; energy: US$ 17.4/50.3/101.8 kWh^{-1}) for 2025–2045 analysis, and projected 2050 reference costs (hydrogen power: US$ 650/1300/1950 kW^{-1}; energy: US$ 0.5/1.0/1.5 kWh^{-1} | CAES power: US$ 415/755/947 kW^{-1}; energy: US$ 8.9/31.0/81.6 kWh^{-1} | PHS power: US$ 573/1164/2807 kW^{-1}; energy: US$ 17.3/50.9/97.4 kWh^{-1}) for 2050–2070 analysis. They find that CAES and PHS with 1-day discharge are already economically viable using 2025 reference costs, while hydrogen storage requires power/energy costs to fall to the minimum values considered ($\leq$US$ 1507 kW^{-1} and $\leq$US$ 1.8 kWh^{-1}) to become competitive up to 1-week discharge duration by 2025, or becomes viable with 2050 projected reference costs for up to 2-week discharge duration.

[20] employed an electricity system CEM to evaluate the reduction cost of different combinations of LDES design parameters, such as charge and discharge power capacity costs of US$ 100, 300, 600, and 900 kW^{-1}, energy capacity costs of US$ 1, 5, 10, 20, and 50 kWh^{-1}, charge efficiencies of 30, 50, 70, and 90 %, and discharge efficiencies of 20, 40, 60, and 80 %. To cover different spatial resolutions, they considered two systems, referred to as the Northern System and the Southern System, which consist of climatic and demand conditions typical of New England and a system with climatic and demand conditions typical of Texas, respectively. The results indicated that the cost of energy storage capacity must be less than US$ 20 kWh^{-1}, power cost of US$ 1000 kW^{-1}, and RTE of 72 % for LDES technologies to reduce carbon-free electricity generation system costs by at least 10 %, i.e., considering low-carbon energy sources. To completely replace established low-carbon generation technologies, LDES technologies would need energy capacity costs of US$ 1 kWh^{-1} and a combination of very low power costs and high efficiencies. All capacity costs are based on a fully installed system. Lastly, the findings demonstrate that in situations where there is the greatest displacement of firm generation and the greatest system cost reductions due to LDES, the ideal storage discharge durations fall between 100 and 650 hours.

[38] examined a novel technology solution for LDES called compressed air

seesaw energy storage (Seesaw), proposing its application in coastal regions near deep oceans, such as a floating offshore wind project close to Tokyo, Japan. Using a theoretical-analytical model, the authors provide a preliminary cost estimation based on low-cost high-density polyethylene pipes balanced by ocean pressure, without needing pressurized tanks or caverns. While this system's costs have not been reported in other works, according to their findings, Seesaw projects typically range in size from 1 MW to 100 MW, with Capital Expenditures (CAPEX) for installed power capacity estimated between US$ 800 and US$ 1500 kW^{-1} and energy storage costs ranging from US$ 10 to US$ 50 kWh^{-1}, varying with ocean depth and discharge duration. In one example, a system with an energy storage capacity of 1.5 GWh and a power capacity of 10 MW, capable of discharging continuously for 6.3 days (150 hours), has a total CAPEX of US$ 23 million, or approximately US$ 15 kWh^{-1} for energy storage and US$ 1300 kW^{-1} for power. Reducing the installed capacity to 1 MW extends the discharge period to approximately 63 days, resulting in a lower storage cost of US$ 8 kWh^{-1}. The study highlights Seesaw's potential for weekly, monthly, or seasonal cycles, with round-trip efficiencies of 68–80 %, making it a cost-competitive alternative to pumped hydro and hydrogen in islands and coastal areas.

Another study highlights the importance of understanding the economic feasibility of LDES systems in high renewable penetration grids, particularly focusing on 100-hour storage systems, using the RESOLVE capacity expansion model for grids like California in the years 2030, 2035, 2040, and 2045 both alone and combined with Allam cycle oxy-combustion plants with full CCS [39]. To estimate LDES costs, the authors use a methodology that assumes the annualized all-in investment cost per power (US$/kW-yr) of 1 MW LDES is 1.6 times that of 1 MW 4-hour lithium-ion battery with 85 % RTE, so the cost per energy capacity (US$/kWh) of a 100-hour LDES system is 0.06 times that of a 4-hour lithium-ion battery, with tested RTEs of 50 % and 80 % leading to 120 US$/kW-yr (2030) to 105 US$/kW-yr (2045) or total investment 1715 kW^{-1} in 2030 and 1500 in 2045 kW^{-1}. This approach allows them to model investment costs, resulting in the RESOLVE model selecting up to 60 GW of 80 % RTE LDES by 2045 (replacing nearly all 4 h batteries), cutting solar curtailment from 9 % to 2 %; adding 4 GW

oxy-combustion further reduces solar capacity from 153 to 144 GW and LDES from 60 to 54 GW.

Recently, [18] examined the value of LDES technologies under various grid conditions using a Western Interconnect model with high geographic resolution, analyzing 39 scenarios with differing generation mixes, transmission expansions, storage costs, and storage mandates. Among these scenarios, the study explores the influence of varying storage energy capacity costs, using a baseline of US$ 22.43 kWh^{-1} compared to 10 alternate scenarios where costs range from 0.5 to US$ 102 kWh^{-1} and round-trip efficiency of 85 %. These values reflect overnight energy installation costs (US$/kWh), which differ from conventional CAPEX measures. Furthermore, across all scenarios, the study assumes the overnight power installation costs of US$ 19.58 kW^{-1}, along with annual operation and maintenance costs of US$ 6.10 kW^{-1}. The results highlight that the longest duration storage plants vary significantly with these costs, from 8.9 hours to 825 hours. Furthermore, the study concludes that achieving storage energy capacity costs below US$ 5 kWh^{-1} makes extra-long-duration energy storage, which includes a range of 20 to 400 hours, operated on seasonal cycles, economically viable. Notably, if costs drop to US$ 1 kWh^{-1}, LDES could entirely replace other firm low-carbon generation technologies, underscoring the critical role of cost reduction in enabling widespread LDES deployment.

In general, the models developed and the studies discussed in the previous paragraphs evaluated the contribution of LDES to power systems while fixing different projections of technology costs in a fair attempt to answer the question: "*Given their projected costs, what is the value that LDES technologies can bring to a future system?*", which assumes the cost of LDES is known. Despite all the reported relevant findings, however, they do not provide a systematic methodology where the outcome directly informs boundary technology costs of LDES for economic viability. Such systematic methodology would be particularly important for technologies that are still undergoing a major maturation process. Typically, the future (potentially competitive) cost of an non-mature technology is not yet defined. For instance, technology development policies and programs can bring dramatically down the costs of non-mature technologies in the course of a decade [29]. Therefore, for

non-mature technologies such as LDES, the valuation question is the opposite: "*How much does a technology need to cost to become economically viable to support a given policy target (e.g. decarbonization)?*". In this work, we propose an approach to address the aforementioned question. Our framework is general enough to consider different policy targets and can be applied for the valuation of any non-mature technology to be included in power systems. Nonetheless, here we focus on computing the LDES boundary technology costs to support decarbonization.

To summarize the findings from the literature reviewed in this section and highlight the positioning of this research, Table 1 presents a comprehensive comparison of the main characteristics, models, and cost assumptions of LDES systems found in previous studies, contrasting them with the approach adopted in this thesis.

Table 1 – Summary of the literature review on LDES cost and performance parameters.

Study	**Model**	**Region**	**LDES duration (h)**	**RTE (%)**	**Energy Cost (US$/kWh)**	**Power Cost (US$/kW)**
Ziegler et al. (2019)	CEM	US (AZ, IA, MA, TX)	100	-	0–300	0–2 000
Albertus et al. (2020)	Discounted cash flow	-	50–100	>50	3–7	500–1 000
Hargreaves et al. (2020)	CEM	US	10–100	50–80	1–20	500–1 000
Guerra et al. (2020)	CEM + dispatch (3 steps)	US (Western Interconnect)	Up to 336 (2 weeks)	40–80	0.5–17.4	415–4 520
Sepulveda et al. (2021)	CEM	US (New England, TX)	100–650	20–90	1–50	100–900
Hunt et al. (2023)	-	Japan (Tokyo)	150–1 500 (∼63 days)	-	10–50	800–1 500
Colombo et al. (2023)	CEM	US (CA)	100	50 and 80	0.06 × cost of 4 h Li-ion	1.6 × cost of 4 h Li-ion
Staadecker et al. (2024)	CEM	US (Western Interconnect)	8.9–825	85	0.5–102 (overnight cost)	19.58 (overnight cost)
This thesis (2026)	Dispatch + CEM (2 steps)	US (48 states)	100	42.5	Boundary cost	Boundary cost

To conclude this review, it is important to clarify why traditional economic metrics, such as the Levelized Cost of Energy (LCOE) and the Levelized Cost of Storage (LCOS), are not employed in this study. While LCOE is the most universally recognized standard for evaluating power generation, energy storage systems require its specialized counterpart, LCOS, to accurately account for charging costs and cycle efficiencies [40, 41]. However, both metrics share a fundamental limitation: they are restricted to technology-level assessments and do not reflect system-level value [42]. Consequently, they fail to capture the broader, system-wide externalities of LDES, overlooking crucial grid integration benefits such as avoided capacity

costs, operational security, and deep decarbonization savings [41, 43]. As evidenced by the key studies summarized in Table 1, properly evaluating emerging LDES technologies requires a shift from this isolated operational cost approach to a global power system perspective. Distancing itself from the LCOE and LCOS paradigms, this research aims to determine the LDES boundary cost, representing the maximum opportunity value the entire system can afford to pay for the battery to become economically viable without increasing overall system expenditures.

1.4 Contributions and objectives

The main objective of this research is to propose a valuation methodology that estimates the boundary technology costs of LDES technologies for economic viability. We define this boundary as the technology cost below which the overall system costs (investment plus operations) will not exceed a reference value obtained when firm conventional (and already economically viable) generators perform the needed long-duration services instead of LDES.

Our methodology combines the solution of two optimization problems. They are called the *baseline model* and the *opportunity value maximization model*, which are solved in sequence. First, the *baseline model* is solved with the goal of minimizing both operational and investment expenditures associated with the selected system. Following this, given the cost discovered, the *opportunity value maximization model* is solved and aims to maximize LDES's opportunity value while keeping the same cost of *baseline model*. These models are used in a realistic case study with high temporal resolution (8760 hours), analyzing the power systems of the 48 contiguous US states individually (excluding Hawaii and Alaska). In essence, we estimate the boundary costs of LDES technologies for economic viability in each of these states independently, for the year 2050, and considering a reference energy matrix developed by NREL's Cambium, of scenario mid-case: without tax credit phaseout [44].

To conduct this evaluation across the states, this study models candidate LDES systems with a duration of 100 hours and a round-trip efficiency of 42.5%. The literature indicates that storage with this duration is required to provide continuous power and fully replace firm thermal generation [35, 20]. Moreover, these parameters

are consistent with the technical characteristics of iron air batteries currently under commercial development [45, 46]. For instance, the U.S. Department of Energy is supporting the deployment of such systems at retiring coal plants to replace baseload generation [47]. Similarly, a system with comparable specifications is being deployed in New England to ensure grid reliability during extended periods of cold weather [48]. Therefore, these assumptions provide a realistic and empirically grounded basis for estimating the boundary cost.

The main contributions of this work can be summarized as follows.

1. To propose a novel valuation methodology that computes the boundary technology cost of LDES systems below which these technologies become economically viable based on the opportunity value maximization.

2. To estimate the ideal technology costs required to make 100-hour LDES systems economically viable in support of the decarbonization goals of the power systems across the 48 contiguous US states.

3. To improve the understanding of the operation of LDES systems as means of achieving a GHG emissions-free future.

4. To provide additional information to guide decision-makers, energy planners, and other stakeholders to make informed decisions about LDES investment in the context of a low-carbon energy future.

1.5 Related Publications

To date, one paper has been published to a journal, as listed below:

- "Boundary Technology Costs for Economic Viability of Long-Duration Energy Storage Systems." Silva, P., Moreira, A., Heleno, M., and Marcato, A. L., IEEE Transactions on Energy Markets, Policy, and Regulation, 2024.

  The paper presents a methodology that estimates the boundary technology costs of long-duration energy storage technologies. The results show how much this technology needs to cost to become economically viable to support

a policy goal (e.g., decarbonization). Furthermore, this methodology can be applied to any emerging energy technology with a variety of targets.

To date, one paper has been submitted to a journal, as listed below:

- "State-wise Economic Viability of Long-Duration Energy Storage Systems in the United States." Moreira, A., Silva, P., Heleno, M., and Marcato, A. L., Nature Communications, 2026.

  The paper evaluates the economic viability of long-duration energy storage systems across the 48 contiguous United States. It estimates the maximum technology costs, referred to as boundary costs, under which LDES can replace firm conventional generation without increasing total system costs. Results show that only a few states would meet this condition under the current US-DOE cost target of US$ 1100 kW^{-1} for multi-day LDES. Additionally, states with higher LDES viability tend to have lower shares of thermal generation, greater wind penetration, and higher fixed costs in existing thermal assets.

1.6 Organization of the Thesis

In addition to this introductory chapter, this doctoral thesis is divided into four further chapters. Section 2 presents the proposed methodology, detailing the mathematical formulation, including the *baseline model*, the *opportunity value maximization model*, and the solution framework. Section 3 presents the results and discussion and is divided into three main parts. Section 3.1 introduces the initial definitions and assumptions adopted in the modeling framework, Section 3.2 analyzes the California case study to illustrate the economic and operational role of LDES in a future decarbonized power system, and Section 3.3 extends the analysis to the contiguous United States, examining the systemic drivers behind the variation in LDES boundary costs across states. Finally, Section 4 summarizes the main conclusions of the thesis and outlines directions for future work. Supplementary figures with additional results are provided in the Annex A.

2 Proposed Methodology

The evaluation of emerging technologies, such as long-duration energy storage, requires a systematic approach to identify the conditions under which they become economically competitive. This chapter presents the methodological framework developed to assess the economic viability of LDES by determining its boundary cost. The approach is based on the sequential execution of two optimization models:

- **1. The *Baseline Model*:** First, a reference scenario is established. This model simulates the power system without the inclusion of LDES and without retiring any existing firm generators (e.g., gas and coal power plants). Its objective is to find the minimum overall cost (investment and operation) required to meet the energy demand reliably.
- **2. The *Opportunity Value Maximization Model*:** Next, a scenario driven by a predefined policy target is simulated. In the context of this study, this target involves enforcing the retirement of thermal power plants and introducing a predefined capacity of LDES into the system, alongside potential new investments in RES and SDES. The objective is to calculate the maximum value the system can afford to pay for the LDES, its "opportunity value" or "boundary cost", ensuring that the total system cost never exceeds the benchmark established by the *baseline model*.

Before introducing the mathematical formulation of these models, a high-level overview of the framework is provided. A key advantage of the proposed approach is its adaptability, as it can be applied to different countries or regions beyond the United States, such as Brazil and European countries, as long as the necessary input data are available. The implementation requires a set of technical and economic parameters describing the power system under analysis. These inputs are summarized in Table 2, which are directly related to the mathematical symbols used in the optimization models of this work.

Once the input data are defined, the modeling framework is executed through a structured computational procedure, progressing from data preprocessing to result

Table 2 – Minimum required inputs to characterize the energy matrix and apply the proposed modeling framework.

Parameter Group	**Input Description**	**Mathematical Symbol**
System-Level Requirements	Hourly electricity demand	D_t
	Minimum required reserve margin	$r_t^{up,min}$
Generators (Firm & RES)	Power generation capacity	$\overline{P}_g$
	Annual fixed operation and maintenance (FO&M) cost	$C_g^{fom,gen}$
	Generation cost (fuel prices and variable operation and maintenance (VO&M) cost)	C_{gt}^{p}
	Ramp-up capability factor	RU_g^{factor}
	Ramp-down capability factor	RD_g^{factor}
RES	Hourly availability factor (Capacity Factor for Solar, Wind, and Hydro)	$f_{g,t}^{available}$
SDES	Maximum power charge/discharge limit	$\overline{P}_h^{st,power}$
	Storage duration limit	$\overline{S}_h$
	Round-trip efficiency	η_h
	Annual fixed operation and maintenance (FO&M) cost	$C_h^{fom,st,power}$
Candidate Technologies (Expansion)	Equivalent annual investment cost for candidate generators	$C_g^{inv,gen}$
	Equivalent annual investment cost in power capacity for SDES	$C_h^{st,power}$
	Equivalent annual investment cost in energy capacity for SDES	$C_h^{st,energy}$

extraction. This process is illustrated in Fig. 1 and is described as follows:

- **Step 1: Initialization and Global Configuration.** Defines general economic parameters (e.g., inflation rate and asset lifetimes), temporal parameters (e.g., 8760 hourly periods), and the specific investment, reserve, and retirement rules for both models.
- **Step 2: State-Specific Input Data Loading.** Loads the hourly demand, reserve margins, and the technical and economic specifications for all fixed and candidate units (generators and SDES), as well as the predefined candidate LDES configurations to be analyzed.

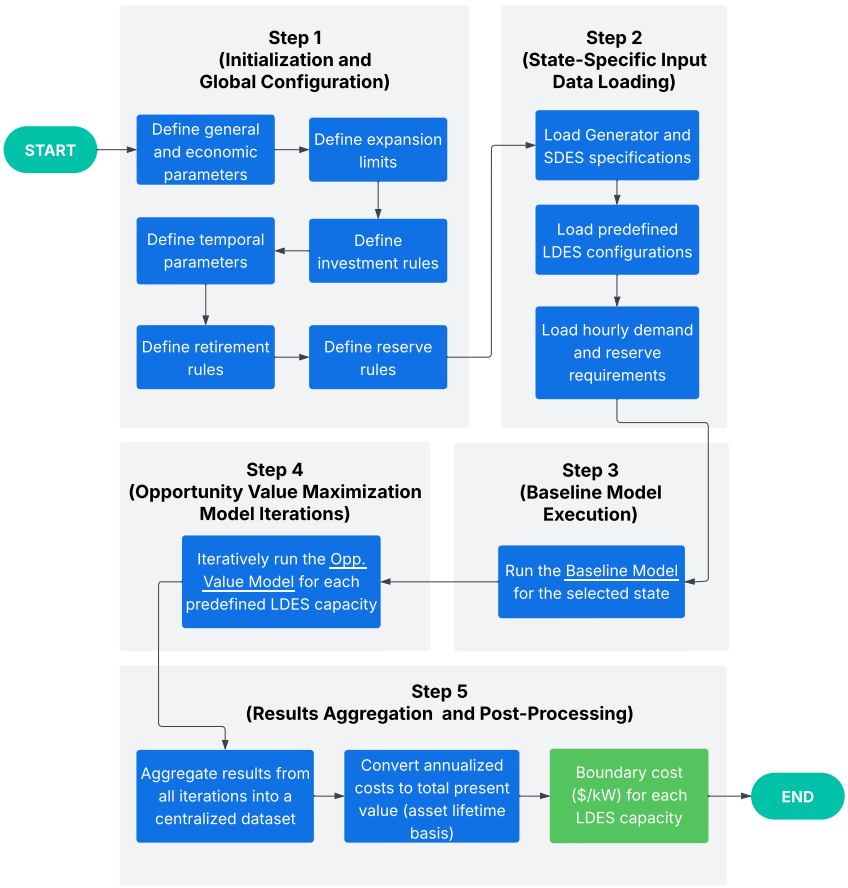

Figure 1 – Flowchart of the main steps of the proposed methodology.

- **Step 3: *Baseline Model* Execution.** Run the *baseline model* for the selected state. This step evaluates the existing system, saving the minimized overall system cost (q^*) to serve as the benchmark bound.
- **Step 4: *Opportunity Value Maximization Model* Iterations.** Iteratively runs the *opportunity value maximization model* for each predefined candidate LDES capacity. This step enforces the retirement of specific technologies and optimizes new investments (RES and SDES), ensuring the overall system cost does not exceed the *baseline model* cost (q^*).
- **Step 5: Results Aggregation and Post-Processing.** Compiles the outcomes from all iterative runs into a centralized dataset, converts annualized

costs to total present values over the assets' lifetimes, and calculates the exact boundary cost (in $/kW) for each evaluated LDES capacity.

Following this overview, the mathematical formulation of the proposed methodology is presented. The remainder of this chapter is organized as follows: Section 2.1 defines the objective of the methodology. Section 2.2 describes the key sets, parameters, and variables used in the modeling process. We then detail the formulation of the *baseline model* (Section 2.3) and the *opportunity value maximization model* (Section 2.4), followed by an explanation of the overall solution framework (Section 2.5). The chapter concludes with a summary of the methodology in Section 2.6.

2.1 Methodology objective

The main objective of the methodology proposed in this research is to determine the boundary cost of LDES, which is the cost below which LDES becomes economically viable. Our methodology consists of a *baseline model* and an *opportunity value maximization model* which are solved in sequence as depicted in Fig. 2. Firstly, the *baseline model* is solved with the goal of minimizing both operational and investment expenditures associated with the selected system. Following this, given the cost discovered, the *opportunity value maximization model* is solved and aims to maximize LDES's opportunity value while keeping the same cost of *baseline model*. The use of LDES allows the new system to retire wished technologies, such as pollutants, but investment in renewable sources must be allowed, i.e., it is about a capacity expansion model.

Therefore, we define the maximum reduction in overall costs provided by a given quantity (energy and power) of LDES as the maximum *opportunity value* for LDES. This value is directly related to its boundary cost, which is in $/MW, and more details are provided in the following subsections, along with each of the models mentioned previously.

2.2 Sets, parameters and variables

The sets used in the mathematical model are presented in Table 3.

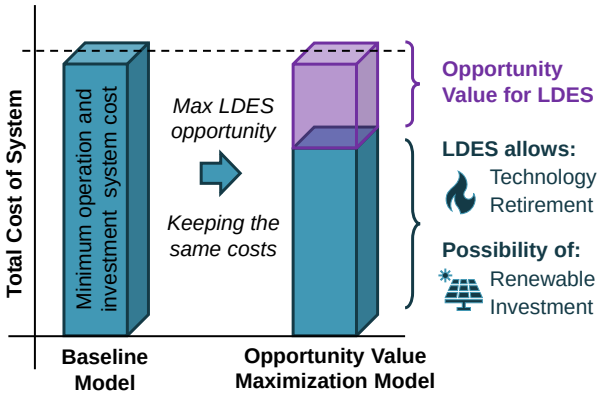

Figure 2 – Methodology graphical abstract.

Table 3 – Sets used in the mathematical model.

Set	Description
G	Set of indexes of all generators.
G^{cand}	Set of indexes of generators that are candidate for investment.
G^{fixed}	Set of indexes of fixed existing generators.
G^{firm}	Set of indexes of generators able to provide firm dispatchable generation.
G^{renew}	Set of indexes of renewable generators.
$G^{firm,fixed}$	Generators in $G^{firm} \cap G^{fixed}$.
$G^{renew,fixed}$	Generators in $G^{renew} \cap G^{fixed}$.
$G^{renew,cand}$	Generators in $G^{renew} \cap G^{cand}$.
$G^{res,providers}$	Set of indexes of generators that can provide reserve.
H	Set of indexes of all energy storage systems.
H^{cand}	Set of indexes of storage systems that are candidate for investment.
H^{fixed}	Set of indexes of fixed existing storage systems.
H^{long}	Set of indexes of long-duration storage systems.
H^{short}	Set of indexes of short-duration storage systems.
$H^{short,fixed}$	Storage systems in $H^{short} \cap H^{fixed}$.
$H^{long,cand}$	Storage systems in $H^{long} \cap H^{cand}$.
$H^{short,cand}$	Storage systems in $H^{short} \cap H^{cand}$.
T	Set of indexes of time periods.

The parameters used in the mathematical model are presented in Table 4.

Table 4 – Parameters used in the mathematical model.

Parameter	**Description**
η_h	Round trip efficiency of storage system h.
C^I	System power imbalance cost.
C^{short}	Reserve shortage cost.
$C_g^{inv,gen}$	Equivalent annual investment cost of candidate generator g.
$C_g^{fom,gen}$	Annual fixed operation and maintenance cost of generator g.
$C_h^{fom,st,power}$	Annual fixed operation and maintenance cost of storage system h.
C_{gt}^{p}	Generation cost of generator g.
$C_h^{st,energy}$	Equivalent annual investment cost in energy capacity for storage system h.
$C_h^{st,power}$	Equivalent annual investment cost in power capacity for storage system h.
C_{gt}^{up}	Reserve provision cost of generator g.
$f_{gt}^{available}$	Number between 0 and 1 that determines how much of the generation capacity of renewable unit g is available during time t.
D_t	Demand of the system at time period t.
$\overline{P}_g$	Power generation capacity of generator g.
$\overline{P}_h^{st,power}$	Maximum power charge/discharge limit for existing storage system h.
$\overline{P}_h^{st,power,ini}$	Maximum initial power charge/discharge limit for candidate storage system h.
$\overline{R}_g^{up,factor}$	Number between 0 and 1 that determines how much of the generation capacity of unit g can be used for reserves.
$r_t^{up,min}$	Minimum amount of reserve to be held by the system at time period t.
RD_g^{factor}	Number between 0 and 1 that determines the ramp-down capability of unit g relative to its generation capacity.
RU_g^{factor}	Number between 0 and 1 that determines the ramp-up capability of unit g relative to its generation capacity.
$\overline{S}_h$	Duration of storage system h.
$\underline{V}_h$	Minimum state of charge limit for storage system h.
$\overline{V}_h$	Maximum state of charge limit for storage system h.
$\overline{x}_g^{inv,gen}$	Maximum limit of generation capacity investment for candidate generator g.
$\underline{x}_g^{ret,gen}$	Number between 0 and 1 that determines the minimum reduction in the generation capacity of unit g.
$\overline{x}_g^{ret,gen}$	Number between 0 and 1 that determines the maximum reduction in the generation capacity of unit g.
$\overline{x}_h^{st,energy}$	Maximum limit of energy capacity investment for candidate storage system h.
$\overline{x}_h^{st,power}$	Maximum limit of power capacity investment for candidate storage system h.
$x_h^{st,energy\ddagger}$	Predefined energy capacity for storage h to be considered in the *opportunity value maximization model.*

The decision variables used in the model are presented in Table 5.

Table 5 – Decision variables used in the model.

Variable	**Description**
Δ_t^-	Negative power imbalance during time t.
Δ_t^+	Positive power imbalance during time t.
$\delta_t^{up,short}$	Reserve shortage during time t.
c^{BC}	Boundary cost of LDES.
p_{gt}	Power generation of unit g during time t.
$p_{ht}^{st,ch}$	Power charge of storage h during time t.
$p_{ht}^{st,dis}$	Power discharge of storage h during time t.
$\overline{p}_g^{rem}$	Remaining generation capacity of unit g after reduction.
q^{over}	Budget overrun relative to the overall cost determined by the *baseline model*.
$r_{ht}^{st,up}$	Reserve provisioned by storage h during time t.
r_{gt}^{up}	Reserve provisioned by generator g during time t.
v_{ht}	State of charge of storage h during time t.
$x_g^{inv,gen\dagger}$	Generation capacity of generator g after investment decision.
$x_g^{ret,gen\dagger}$	Generation capacity of generator g to be reduced after retirement decision.
$x_h^{st,energy\dagger}$	Energy capacity of storage system h after investment decision.
$x_h^{st,power\dagger}$	Power capacity of storage system h after investment decision.

2.3 Baseline model

As depicted in Fig. 2, the *baseline model* provides a solution that minimizes the overall system costs. This optimization problem is solved without taking into account any policy related to enforcing the retirement generators of a particular technology. The main outcome of this model is the system overall cost which will be used as a benchmark to maximize the opportunity value of LDES. We describe the formulation of the *baseline model* as follows.

2.3.1 Objective function

$$
\begin{aligned}
q^* = \underset{\substack{\Delta_t^-,\Delta_t^+,\delta_t^{up,short},p_{gt},\\ p_{ht}^{st,ch},p_{ht}^{st,dis},\overline{p}_g^{rem},\\ r_{ht}^{st,up},r_{gt}^{up},v_{ht},\\ x_g^{inv,gen\dagger},x_g^{ret,gen\dagger},\\ x_h^{st,energy\dagger},x_h^{st,power\dagger}}}{\text{Minimize}} & \sum_{g\in G^{cand}} C_g^{inv,gen} x_g^{inv,gen\dagger} \\
& + \sum_{h\in H^{short,cand}} \left[C_h^{st,energy} x_h^{st,energy\dagger} + C_h^{st,power} x_h^{st,power\dagger} \right] \\
& + \sum_{t\in T} \Bigg[\sum_{g\in G} \left[C_{gt}^{p} p_{gt} + C_{gt}^{up} r_{gt}^{up} \right] \\
& + C^I \left(\Delta_t^- + \Delta_t^+ \right) + C^{short} \delta_t^{up,short} \Bigg] \\
& + \sum_{g\in G^{firm,fixed}} C_g^{fom,gen} \overline{p}_g^{rem} + \sum_{g\in G^{renew,fixed}} C_g^{fom,gen} \overline{P}_g \\
& + \sum_{g\in G^{cand}} C_g^{fom,gen} x_g^{inv,gen\dagger} \\
& + \sum_{h\in H^{fixed}} C_h^{fom,st,power} \overline{P}_h^{st,power} \\
& + \sum_{h\in H^{cand}} C_h^{fom,st,power} \left(\overline{P}_h^{st,power,ini} + x_h^{st,power\dagger} \right)
\end{aligned}
\tag{2.1}
$$

The objective function of the *baseline model* (2.1) minimizes expenditures on investments and operations as well as Fixed Operation and Maintenance (FO&M) costs. Each kind of cost is described below.

- Investment expenditures: The investment expenditures are associated with new power plants and short-duration storage systems. This investment, also known as CAPEX (Capital Expenditure), refers to the initial investment required to acquire, construct, and install a new energy generation or storage system, including all associated infrastructure and equipment. The investment in SDES involves considering the cost of power and the cost of energy. The cost of power encompasses the initial investment needed to install and operate a storage system, focusing primarily on expenses associated with its power

capacity. On the other hand, the cost of energy accounts for the total quantity of energy stored by the system throughout its operational lifetime, taking into account the energy capacity of the storage system. This is a cost that is incurred only once and varies depending on the type of technology, i.e., each kind of power plant or storage. All then are described in the first two lines of the objective function.

- Operations expenditures: The operations expenditures are primarily related to generation output, which has an impact on the project's profitability and competitiveness over its operational lifetime, but they also include reserve provision, power imbalance, and reserve shortage costs. The reserve provision cost refers to the availability of additional generating capacity that grid operators maintain to balance supply and demand in real-time; if this does not occur, the reserve shortage cost is incurred. The cost of power imbalance occurs when there is a disparity between electricity supply and demand within a power system. The cost of generation and reserve occurs as a function of generation and time, whereas the cost of power imbalance and reserve shortage occurs only as a function of time. Operating costs are incurred in the third and fourth line of the objective function.

- FO&M costs: The FO&M costs essentially apply for all existing and newly included generation and storage capacity. This type of cost typically includes expenses that are independent of the level of electricity production or energy storage. From the fifth line in the objective function, these costs are divided into 5 terms. The first three are about generators and represent the cost of the fixed and firm-source generators, the fixed generators from renewable energy sources, and the invested generators. An important detail is that for fixed generators from a firm source, the cost is multiplied by the amount of remaining generation capacity; it will be shown later that this happens because these generators can be retired. The cost of fixed generators and renewable sources is multiplied by the value of their installed capacity, while the cost of invested generators is multiplied by the value of the model-determined amount of investment. The last two terms are related to the storage costs, first the

fixed storage group and then the candidate storage group, multiplying the cost by the amount of installed power and invested power, respectively.

2.3.2 Balance

$$\sum_{g \in G} p_{gt} + \sum_{h \in H} \left[p_{ht}^{st,dis} - p_{ht}^{st,ch} \right] = D_t - \Delta_t^- + \Delta_t^+ ; \forall t \in T \tag{2.2}$$

$$\Delta_t^-, \Delta_t^+ \geq 0 ; \forall t \in T \tag{2.3}$$

Power balance is enforced for each period t via constraint (2.2). This constraint states that the sum of power outputs (p_{gt}) from all generators, plus the net power flow out ($p_{ht}^{st,dis}$) or into ($p_{ht}^{st,ch}$) of storage devices, should equal the total demand (D_t). In case the supply is insufficient or excessive, the model introduces two imbalance variables: Δ_t^- represents the amount of unmet demand (load shedding), and Δ_t^+ reflects surplus generation that exceeds demand (overgeneration). These variables allow the model to maintain feasibility when an exact supply-demand match is not possible. Both imbalance terms are penalized in the objective function, typically with high costs, to discourage deviations from the power balance, i.e., the optimizer will only allow imbalances when absolutely necessary to maintain feasibility.

In addition, the non-negative nature of the imbalance variables is imposed by constraints (2.3).

2.3.3 Reserve margin

$$\sum_{g \in G^{res,providers}} r_{gt}^{up} + \sum_{h \in H} r_{ht}^{st,up} \geq r_t^{up,min} - \delta_t^{up,short} ; \forall t \in T \tag{2.4}$$

$$\delta_t^{up,short} \geq 0 ; \forall t \in T \tag{2.5}$$

A minimum amount of reserve to be provisioned during each period t is established by constraints (2.4). The constraint states that the sum of the total

reserve provisioned (r_{gt}^{up}) by set generators that can provide reserve and storage ($r_{ht}^{st,up}$) must be sufficient to meet or exceed the minimum required up-reserve ($r_t^{up,min}$) at each period. If the total available up-reserve capacity falls short of the minimum requirement, the constraint allows for a certain amount of reserve shortage ($\delta_t^{up,short}$) penalized in the objective function.

Moreover, constraints (2.5) enforce non-negativity for reserve shortage variables $\delta_t^{up,short}$, which are penalized in the objective function.

2.3.4 Storage devices

$$v_{ht} = v_{h,t^{ini}} + \eta_h p_{ht}^{st,ch} - p_{ht}^{st,dis}; \forall h \in H, t = 1 \tag{2.6}$$

$$v_{ht} = v_{h,t-1} + \eta_h p_{ht}^{st,ch} - p_{ht}^{st,dis}; \forall h \in H, t \in T | t \geq 2 \tag{2.7}$$

$$v_{h,t^{ini}} = v_{h,t^{end}}; \forall h \in H \tag{2.8}$$

$$\underline{V}_h \leq v_{ht} \leq \overline{V}_h; \forall h \in H^{fixed}, t \in T \tag{2.9}$$

$$\underline{V}_h \leq v_{ht} \leq \left(\overline{V}_h^{ini} + x_h^{st,energy\dagger}\right); \forall h \in H^{cand}, t \in T \tag{2.10}$$

$$0 \leq p_{ht}^{st,ch} \leq \overline{P}_h^{st,power}; \forall h \in H^{fixed}, t \in T \tag{2.11}$$

$$0 \leq p_{ht}^{st,dis} + r_{ht}^{st,up} \leq \overline{P}_h^{st,power}; \forall h \in H^{fixed}, t \in T \tag{2.12}$$

$$0 \leq p_{ht}^{st,ch} \leq \overline{P}_h^{st,power,ini} + x_h^{st,power\dagger}; \forall h \in H^{cand}, t \in T \tag{2.13}$$

$$0 \leq p_{ht}^{st,dis} + r_{ht}^{st,up} \leq \overline{P}_h^{st,power,ini} + x_h^{st,power\dagger}; \forall h \in H^{cand}, t \in T \tag{2.14}$$

$$v_{ht} - r_{ht}^{st,up} \geq \underline{V}_h; \forall h \in H, t \in T \tag{2.15}$$

$$x_h^{st,energy\dagger} = x_h^{st,power\dagger} \overline{S}_h; \forall h \in H^{cand} \tag{2.16}$$

$$0 \leq x_h^{st,power\dagger} \leq \overline{x}_h^{st,power}; \forall h \in H^{cand} \tag{2.17}$$

$$0 \leq x_h^{st,energy\dagger} \leq \overline{x}_h^{st,energy}; \forall h \in H^{cand} \tag{2.18}$$

$$p_{ht}^{st,ch}, p_{ht}^{st,dis}, r_{ht}^{st,up} \geq 0; \forall h \in H, t \in T \tag{2.19}$$

Constraints on storage devices take into account various behaviors to ensure the safe and efficient operation of these systems. These constraints include limitations on energy and power capacities, as well as the state of charge and discharge. These constraints are explained as follows:

- **State of charge constraints:** The constraints (2.6) and (2.7) update the state of charge of each storage system h throughout the time periods t. For the first time instant of the optimization, the constraint (2.6) states that the state of charge (v_{ht}) of each storage h at time t is equal to the initial state of charge ($v_{h,t^{ini}}$) plus the power being stored ($\eta_h p_{ht}^{st,ch}$) minus the power being discharged ($p_{ht}^{st,dis}$). The constraint (2.7) is similar to the first one, however, the initial state of charge is equal to the state of charge at the previous time step ($v_{h,t-1}$). The η_h is the round trip efficiency of each storage system h that is the percentage of electricity that is stored and then retrieved.

- **Initial and final state of charge constraints:** Constraints (2.8) impose equality between the initial ($v_{h,t^{ini}}$) and final ($v_{h,t^{end}}$) states of charge of each storage system h.

- **State of charge limits constraints:** Limits for states of charge are enforced via constraints (2.9) and (2.10) for existing and candidate storage systems, respectively. The equation (2.9) states that for existing storage systems, the state of charge (v_{ht}) of each storage h at time t must be within the predefined lower ($\underline{V}_h$) and upper bounds ($\overline{V}_h$). For candidate storage systems, the upper bound of this group is composed of the sum of the initial upper bound ($\overline{V}_h^{ini}$) and the energy capacity of the storage system after investment decision ($x_h^{st,energy\dagger}$), ensured via constraints (2.10).

- **Power limits constraints for existing storage systems:** The constraints (2.11) and (2.12) express the limits of power charging and discharging capacities for existing storage systems. The charging power ($p_{ht}^{st,ch}$) of each storage h at time t is kept between zero and the maximum power capacity ($\overline{P}_h^{st,power}$) of each storage h by the (2.11) constraint. About discharging power, the (2.12) makes sure that the discharging power ($p_{ht}^{st,dis}$) of each storage h at time t plus provisioned reserve ($r_{ht}^{st,up}$) by each storage h at time t stays between zero and the maximum power capacity.

- **Power limits constraints for candidate storage systems:** Analogous to the constraints in the previous item, the constraints (2.13) and (2.14) express respectively, the limits of power charging and discharging capacities,

for candidate storage systems. The difference is that the maximum limits include the sum of the initial maximum power capacity ($\overline{P}_h^{st,power,ini}$) and the additional investment power capacity ($x_h^{st,power\dagger}$) of each storage h.

- **Reserve provisioned by storage constraint:** The constraint (2.15) ensure that there is a sufficient state of charge to hold the provisioned up-reserve ($r_{ht}^{st,up}$) by storage systems. The state of charge (v_{ht}) of each storage system h throughout each time t it must be greater than or equal to the minimum state of charge ($\underline{V}_h$) for storage system h plus provisioned reserve ($r_{ht}^{st,up}$), ensuring that the storage always has the minimum reserve to serve the system if it is required.

- **Power and energy capacity constraint relationship:** The constraint (2.16) imposes that the energy capacity ($x_h^{st,energy\dagger}$) of each candidate storage h is defined based on the product of the power capacity ($x_h^{st,power\dagger}$) and the specified duration ($\overline{S}_h$) of each candidate storage h, providing the total energy that can be stored and discharged over the specified duration.

- **Investment limits constraint:** The limits for power and energy capacity investment in candidate storage systems are enforced by (2.17) and (2.18), respectively. These constraints are crucial to ensure that the investment decisions for power ($x_h^{st,power\dagger}$) and energy ($x_h^{st,energy\dagger}$) storage capacities are within feasible limits. The upper bounds represent the maximum allowable investments in power ($\overline{x}_h^{st,power}$) and energy ($\overline{x}_h^{st,energy}$) storage capacities respectively for each candidate storage.

- **Non-negativity constraint:** (2.19) enforces the non-negativity of power charging, power discharging, and reserve provision variables ($p_{ht}^{st,ch}, p_{ht}^{st,dis}, r_{ht}^{st,up}$).

2.3.5 Generators

$$0 \leq p_{gt} \leq \overline{p}_g^{rem} - r_{gt}^{up}; \forall g \in G^{firm,fixed}, t \in T \tag{2.20}$$

$$0 \leq p_{gt} \leq \overline{P}_g f_{gt}^{available}; \forall g \in G^{renew,fixed} \mid g \notin G^{res,providers}, t \in T \tag{2.21}$$

$$0 \leq p_{gt} \leq \overline{P}_g f_{gt}^{available} - r_{gt}^{up}; \forall g \in G^{renew,fixed} \cap G^{res,providers}, t \in T \tag{2.22}$$

$$0 \leq p_{gt} \leq x_{gt}^{inv,gen\dagger} - r_{gt}^{up}; \forall g \in G^{firm,cand}, t \in T \tag{2.23}$$

$$0 \leq p_{gt} \leq x_{g}^{inv,gen\dagger} f_{gt}^{available}; \forall g \in G^{renew,cand} \mid g \notin G^{res,providers}, t \in T \tag{2.24}$$

$$0 \leq p_{gt} \leq x_{g}^{inv,gen\dagger} f_{gt}^{available} - r_{gt}^{up}; \forall g \in G^{renew,cand} \cap G^{res,providers}, t \in T \tag{2.25}$$

$$0 \leq r_{gt}^{up} \leq \overline{p}_g^{rem} \overline{R}_g^{up,factor}; \forall g \in G^{firm,fixed}, t \in T \tag{2.26}$$

$$0 \leq r_{gt}^{up} \leq \overline{P}_g f_{gt}^{available} \overline{R}_g^{up,factor}; \forall g \in G^{renew,fixed} \cap G^{res,providers}, t \in T \tag{2.27}$$

$$0 \leq r_{gt}^{up} \leq x_{gt}^{inv,gen\dagger} \overline{R}_g^{up,factor}; \forall g \in G^{firm,cand}, t \in T \tag{2.28}$$

$$0 \leq r_{gt}^{up} \leq x_{g}^{inv,gen\dagger} f_{gt}^{available} \overline{R}_g^{up,factor}; \forall g \in G^{renew,cand} \cap G^{res,providers}, t \in T \tag{2.29}$$

$$p_{gt} - p_{g,t-1} \leq RU_g^{factor} \overline{p}_g^{rem}; \forall g \in G^{firm,fixed}, t \in T | t \geq 2 \tag{2.30}$$

$$p_{g,t-1} - p_{gt} \leq RD_g^{factor} \overline{p}_g^{rem}; \forall g \in G^{firm,fixed}, t \in T | t \geq 2 \tag{2.31}$$

$$p_{gt} - p_{g,t-1} \leq RU_g^{factor} x_{gt}^{inv,gen\dagger}; \forall g \in G^{firm,cand}, t \in T | t \geq 2 \tag{2.32}$$

$$p_{g,t-1} - p_{gt} \leq RD_g^{factor} x_{gt}^{inv,gen\dagger}; \forall g \in G^{firm,cand}, t \in T | t \geq 2 \tag{2.33}$$

$$0 \leq x_{g}^{inv,gen\dagger} \leq \overline{x}_g^{inv,gen}; \forall g \in G^{cand} \tag{2.34}$$

$$\overline{p}_g^{rem} = \overline{P}_g - x_g^{ret,gen\dagger}; \forall g \in G^{firm,fixed} \tag{2.35}$$

$$\underline{x}_g^{ret,gen} \overline{P}_g \leq x_g^{ret,gen\dagger} \leq \overline{x}_g^{ret,gen} \overline{P}_g; \forall g \in G^{firm,fixed} \tag{2.36}$$

Generator constraints play a crucial role in ensuring the stability and reliability of power systems by imposing limitations on various aspects of generation. These constraints, delineated through a series of mathematical expressions, regulate the output capacities of existing firm and renewable units, as well as those of potential candidate units. We set bounds for generation, reserve, and, capacity. Each constraint is described below:

- **Generation limits constraints**: Essentially, the constraints (2.20)–(2.25) ensures that the generation output of each generator g and time t stays

within the bounds of its generation capacity, considering the reserve provision requirements when it exists. This constraint was written in 6 separate groups of generators:

  - Existing firm generators: The generation output (p_{gt}) must be greater than or equal to zero and less than or equal to the maximum remaining generation capacity ($\overline{p}_g^{rem}$) reduced by the reserve provisioned (r_{gt}^{up}) via constraint (2.20).
  - Existing renewable generators that do not provide reserve: The generation output (p_{gt}) must be greater than or equal to zero and less than or equal to the maximum power generation capacity ($\overline{P}_g$) multiplied by the availability factor ($f_{gt}^{available}$) via constraint (2.21).
  - Existing renewable generators that provide reserve: The generation output (p_{gt}) must be greater than or equal to zero and less than or equal to the maximum power generation capacity ($\overline{P}_g$) multiplied by the availability factor ($f_{gt}^{available}$) reduced by the reserve provisioned (r_{gt}^{up}) via constraint (2.22).
  - Candidate firm generators: The generation output (p_{gt}) must be greater than or equal to zero and less than or equal to the generation capacity of the firm generator after investment decision ($x_{gt}^{inv,gen\dagger}$) reduced by the reserve provisioned (r_{gt}^{up}) via constraint (2.23).
  - Candidate renewable generators that do not provide reserve: The generation output (p_{gt}) must be greater than or equal to zero and less than or equal to the renewable generator after investment decision ($x_{gt}^{inv,gen\dagger}$) multiplied by the availability factor ($f_{gt}^{available}$) via constraint (2.24).
  - Candidate renewable generators that provide reserve: The generation output (p_{gt}) must be greater than or equal to zero and less than or equal to the renewable generator after investment decision ($x_{gt}^{inv,gen\dagger}$) multiplied by the availability factor ($f_{gt}^{available}$) reduced by the reserve provisioned (r_{gt}^{up}) via constraint (2.25).

- **Reserve limits constraints:** In summary, the constraints (2.26)–(2.29) regulate the up-reserve provision capacity for both existing and candidate

generators g that can provide reserve at each time t. These constraints ensure that it aligns with specified limits relative to the available generation capacity while considering the maximum provision up-reserve factors. To accomplish this, consider the four constraints listed below according to the generator group:

  - Existing firm generators: For this set of generators, the constraint (2.26) ensures that the up-reserve provision capacity (r_{gt}^{up}) must be greater than or equal to zero and less than or equal to the remaining generation capacity ($\overline{p}_g^{rem}$) multiplied by the maximum provision up-reserve factor ($\overline{R}_g^{up,factor}$).
  - Existing renewable generators that provide reserve: Essentially similar to the previous restriction, but in this group of generators the constraint (2.27) multiplied the up-reserve factor by the maximum power generation capacity ($\overline{P}_g$) multiplied by the availability factor ($f_{gt}^{available}$).
  - Candidate firm generators: In this set, the constraint (2.28) multiplied the up-reserve factor by the generation capacity of the firm generator after investment decision ($x_{gt}^{inv,gen\dagger}$).
  - Candidate renewable generators that provide reserve: The constraint (2.29), like the constraint of existing generators that provide reserve, multiplied the up-reserve factor by the availability factor ($f_{gt}^{available}$), but multiplied this output by the generation capacity of the renewable generator after investment decision ($x_{gt}^{inv,gen\dagger}$).

- **Ramping limits constraints:** The power generation system must be able to ramp up or down quickly enough to meet the change in net demand; therefore, the constraints (2.30)–(2.33) determines the up and down ramping limits. These limits are determined by the real capacity of generators and ramping up and down factors (RU_g^{factor} and RD_g^{factor}), which range from 0 to 1 and determine each generator's ramp-up or ramp-down capability in relation to its generation capacity. Only firm generators are required to simulate ramp constraints. Because this restriction is determined by the previous period's generation, it will only apply from the second period onward.

For up-ramping up limits, that involves increasing the output of a power generation unit, there are the following constraints:

- Exiting generators: The difference between the current period's generation output (p_{gt}) and the previous period's generation output ($p_{g,t-1}$) is limited by the ramping-up factor (RU_g^{factor}) multiplied by the maximum remaining generation capacity ($\overline{p}_g^{rem}$) via constraint (2.30).
- Candidate generators: Similar to the previous constraint, this applies to candidate generators, via constraint (2.32). In this case, the ramping-up factor is multiplied by the generation capacity of the firm generator after the investment decision ($x_{gt}^{inv,gen\dagger}$).

For down-ramping limits, which refers to the process of decreasing the output of a power generation unit, there are the following constraints:

- Exiting generators: The difference between the previous period's generation output ($p_{g,t-1}$) and the current period's generation output (p_{gt}) is limited by the ramping-down factor (RD_g^{factor}) multiplied by the maximum remaining generation capacity ($\overline{p}_g^{rem}$) via constraint (2.31).
- Candidate generators: Similar to the previous constraint, this applies to candidate generators, via constraint (2.33). In this case, the ramping-down factor is multiplied by the generation capacity of the firm generator after the investment decision ($x_{gt}^{inv,gen\dagger}$).

- **Investment limits constraint:** The constraint (2.34) ensures that the investment decision for each candidate generator g stays within certain limits. Specifically, the generation capacity of the generator after the investment decision ($x_g^{inv,gen\dagger}$) must be greater than or equal to zero and less than or equal to the maximum limit of generation capacity investment ($\overline{x}_g^{inv,gen}$) for candidate generator.

- **Retirement constraint:** The constraint (2.35) determines how much generation capacity will be left after the retirement decision has been made, i.e., the remaining generation capacity ($\overline{p}_g^{rem}$) for each fixed firm generator g. It subtracts the generation capacity to be retired ($x_g^{ret,gen\dagger}$) from the

maximum generation capacity ($\overline{P}_g$). Only firm source generators are eligible for retirement in this study.

- **Retirement limits constraint:** The constraint (2.36) determines the amount of capacity that can be retired in order to guarantee that it falls within the predetermined bounds. The lower and upper bounds are set by multiplying the minimum and maximum retirement fractions ($\underline{x}_g^{ret,gen}$ and $\overline{x}_g^{ret,gen}$) by the total maximum generation capacity ($\overline{P}_g$) of each generator g, respectively. These fractions, which range from 0 to 1, indicate how much the generation capacity has been reduced.

2.4 Opportunity value maximization model

The *opportunity value maximization model*, as depicted in Fig. 2, seeks to obtain the maximum technology cost of LDES – formulated as (2.37) – below which the overall costs associated with investments, operations, and maintenance are lower or equal to q^* – formulated as (2.38) – while complying with all technical constraints considered in the *baseline model* – formulated as (2.39). The cost bound q^* is the value of the objective function (2.1) and imposing this bound essentially ensures that the resulting opportunity value of LDES will not imply an overall system cost higher than that attained through the *baseline model*.

2.4.1 Objective function

$$\underset{\substack{\Delta_t^-,\Delta_t^+,\delta_t^{up,short},c^{BC},\\ p_{gt},p_{ht}^{st,ch},p_{ht}^{st,dis},\overline{p}_g^{rem},q^{over}\\ r_{ht}^{st,up},r_{gt}^{up},v_{ht},x_g^{inv,gen\dagger},\\ x_g^{ret,gen\dagger},x_h^{st,energy\dagger},x_h^{st,power\dagger}}}{\text{Maximize}} \quad c^{BC} - C^{over} q^{over} \tag{2.37}$$

For a given predetermined newly installed power capacity of LDES defined by the user in $\sum_{h \in H^{long,cand}} x_h^{st,power\ddagger}$, the objective function of the *opportunity value maximization model* (2.37) is to maximize the variable c^{BC} as much as possible. Additionally, there is an auxiliary variable q^{over}, which relaxes constraint (2.38) in

case it is not possible to comply with constraints (2.39) while respecting the cost bound q^*.

2.4.2 Overall cost

$$\begin{aligned}
&\sum_{h \in H^{long,cand}} c^{BC} x_h^{st,power\ddagger} + \sum_{g \in G^{cand}} C_{ge}^{inv,gen} x_g^{inv,gen\dagger} \\
&+ \sum_{h \in H^{short,cand}} \left[C_h^{st,energy} x_h^{st,energy\dagger} + C_h^{st,power} x_h^{st,power\dagger} \right] \\
&+ \sum_{t \in T} \left[\sum_{g \in G} \left[C_{gt}^{p} p_{gt} + C_{gt}^{up} r_{gt}^{up} \right] + C^{I} \left(\Delta_t^{-} + \Delta_t^{+} \right) + C^{short} \delta_t^{up,short} \right] \\
&+ \sum_{g \in G^{firm,fixed}} C_g^{fom,gen} \overline{p}_g^{rem} \\
&+ \sum_{g \in G^{renew,fixed}} C_g^{fom,gen} \overline{P}_g \\
&+ \sum_{g \in G^{cand}} C_g^{fom,gen} x_g^{inv,gen\dagger} \\
&+ \sum_{h \in H^{fixed}} C_h^{fom,st,power} \overline{P}_h^{st,power} \\
&+ \sum_{h \in H^{cand}} C_h^{fom,st,power} \left(\overline{P}_h^{st,power,ini} + x_h^{st,power\dagger} \right) \leq q^* + q^{over} \qquad (2.38)
\end{aligned}$$

Constraint (2.38) imposes that the inclusion of investment costs related to LDES will not imply an overall system cost higher than q^*. The variable q^{over} exists in case the model is not feasible. Furthermore, supposing that the model is feasible, i.e., $q^{over} = 0$, the optimal solution for the model provides c^{BC^*}, which is the boundary cost of LDES in \$/MW, and the term $\sum_{h \in H^{long,cand}} c^{BC} x_h^{st,power\ddagger}$ is defined as the opportunity value of LDES.

Note that, according to the structure of (2.37) and (2.38), investment, operational, and maintenance costs will be minimized in the *opportunity value maximization model* as they are in the *baseline model*. This cost minimization will occur in order to maximize the variable c^{BC} as much as possible for a given predetermined newly installed capacity of LDES, represented by $x_h^{st,power\ddagger}$ for each storage h. In this context, if $q^{over} = 0$ is a feasible solution and C^{over} is high

enough, in the optimal solution, the term $\sum_{h \in H^{long,cand}} c^{BC^*} x_h^{st,power\ddagger}$ in (2.38) will be equivalent to the maximum reduction in the overall cost of the system (compared to q^*) as a result of the installation of a certain amount, $\sum_{h \in H^{long,cand}} x_h^{st,power\ddagger}$, of LDES in the system. Therefore, (i) the term $\sum_{h \in H^{long,cand}} c^{BC^*} x_h^{st,power\ddagger}$ will be the corresponding maximum opportunity value of LDES and, consequently, (ii) c^{BC^*} will be a threshold or boundary cost in \$/MW below which the integration of a predefined quantity of LDES, $\sum_{h \in H^{long,cand}} x_h^{st,power\ddagger}$, will reduce the investment (not counting LDES), operational, and maintenance costs such that the inclusion of investment costs related to LDES will not imply an overall system cost higher than q^*.

2.4.3 Balance, reserve margin, storage devices, and generators

$$\text{Constraints (2.2)-(2.36)} \tag{2.39}$$

Constraint (2.39) makes sure that the system stays balanced in terms of power, keeps a minimum reserve, maintains the right storage charge, and ensures generators work properly as the *baseline model*.

2.5 Solution framework

As previously mentioned, the *baseline model* and the *opportunity value maximization model* are solved in sequence. Within our proposed framework, different circumstances can be considered to evaluate the boundary cost of LDES. In this work, we focus specifically on determining the opportunity value of LDES to achieve a fully decarbonized power system which entails a complete retirement of gas and coal generators and a potential increase in renewable installed capacity. To ensure this, the following settings were considered:

- We obtain q^* by solving the *baseline model* while enforcing:

  $\rightarrow$ $0 \leq x_h^{st,energy\dagger} \leq 0; \forall h \in H^{long,cand}$ in constraints (2.18), which implies that this model does not allow investment in LDES;

→ $0 \leq x_h^{st,energy\dagger} \leq 0; \forall h \in H^{short,cand}$ in constraints (2.18), which implies that this model does not allow investment in SDES;

→ $0 \leq x_g^{inv,gen\dagger} \leq 0; \forall g \in G^{cand}$ in constraints (2.34), which implies that this model does not allow investment in any type of generator, whether from a firm or renewable source;

→ $0 \leq x_g^{ret,gen\dagger} \leq 0; \forall g \in G^{firm,fixed}$ in constraints (2.36), which implies that this model does not allow retirement of existing firm generators.

- We write the *opportunity value maximization model* with:

→ $x_h^{st,energy\dagger} = x_h^{st,energy\ddagger}; \forall h \in H^{long,cand}$ in constraints (2.18), which implies that the LDES investment corresponds to the predetermined value ($x_h^{st,energy\ddagger}$) provided by the user in this model;

→ $0 \leq x_h^{st,energy\dagger} \leq \overline{x}_h^{st,energy}; \forall h \in H^{short,cand}$ in constraints (2.18), which implies that allow investment in SDES in this model;

→ $0 \leq x_g^{inv,gen\dagger} \leq \overline{x}_g^{inv,gen}; \forall g \in G^{renew,cand}$ in constraints (2.34), which implies that allow investment in generators of renewable source in this model;

→ $0 \leq x_g^{inv,gen\dagger} \leq 0; \forall g \in G^{firm,cand}$ in constraints (2.34), which implies that does not allow investment in generators of firm source in this model.

→ $x_g^{ret,gen\dagger} = \overline{P}_g; \forall g \in G^{gas,fixed} \cup G^{coal,fixed}$ in constraints (2.36), which implies that all generation capacity of gas and coal source generators is retired in this model;

→ $0 \leq x_g^{ret,gen\dagger} \leq 0; \forall g \in G^{firm,fixed} \setminus G^{gas,fixed} \cup G^{coal,fixed}$ in constraints (2.36), which implies that existing generators from firm sources, but not gas and coal sources, are not retired, that is, they remain at their full generation capacity available.

All of the configurations listed above ensured that the *baseline model* required no investment, such as short or long-duration storage or generators. Furthermore, no generators were retired in the *baseline model*. In *opportunity value maximization model*, the configurations ensured that the LDES investment was the

value previously specified by the user, and maximum investment limits were also defined for SDES and candidate generators. It was also ensured that all installed gas and coal generators were retired, but no other fixed or firm generators were retired.

2.6 Conclusion

This chapter presented the methodological framework developed to evaluate the economic viability of LDES in a fully renewable power system. The approach is based on two interconnected models: a *baseline model* and an *opportunity value maximization model*. By comparing systems with and without LDES under the same total cost, the methodology identifies the maximum cost at which LDES can be deployed without increasing the total system cost, which is then used to define its boundary cost.

The proposed framework enables a consistent and flexible analysis of the role of LDES in future energy systems, accounting for investment decisions, operational constraints, and technology retirement. The next chapters will apply this methodology to case studies in order to quantify the boundary cost of LDES across different regions and system configurations.

3 Results and Discussions

3.1 Initial definitions and assumptions

Before analyzing results, it is essential to present the initial definitions and assumptions that guide the modeling process. This section begins by describing how the model is applied, including the tools used, the type of optimization problem solved, and the set of states considered. It also identifies the data sources that support the analysis and explains the spatial and temporal resolution adopted, which establishes the conditions under which the system is evaluated.

The section further details the technologies incorporated into the model, distinguishing between fixed and candidate options for both generators and storage. These details include the criteria used to reduce system dimensionality, the clustering approach applied, and the investment limits defined for candidate technologies. Together, these elements provide the structural basis for interpreting the system behavior and the economic outcomes discussed in later sections.

3.1.1 Model application

The proposed model was implemented in Python using the Pyomo optimization modeling language and solved with the commercial solver Gurobi (version 10.0.1), accessed through a free academic license. All numerical experiments were carried out on a computing workstation equipped with an Intel® Core™ i9-12900K processor (3.20 GHz) and 32 GB of RAM.

The model is formulated as a large-scale Linear Programming (LP) problem, involving only continuous variables and linear constraints. This structure ensures high computational tractability, even under the high temporal resolution and the state-level disaggregation adopted in the study.

In terms of computational performance, the model exhibited satisfactory behavior across all test cases. The *baseline model* required approximately 1 to 10 minutes of processing time per state. In contrast, the *opportunity value maximization model*, which involves a sequence of optimization runs for different values of $x_h^{st,energy\dagger}$ (as described in the chapter 2 – proposed methodology section), ex-

hibited higher computational demands. Depending on the state, each of these cases, i.e., for each energy capacity of a storage system, required between 1 and 60 minutes to converge. This variation reflects differences in system complexity across states, ranging from smaller ones like Virginia (VA), with fewer generators, to large states like Texas (TX), which have a greater quantity of generators. The level of performance was considered acceptable for the scope of the study, given the high temporal resolution of the study.

Initially, the model was implemented and tested using data from the state of California. This state was selected as the first case study due to its high potential for renewable energy sources penetration and ambitious decarbonization goals. The primary objective of this preliminary application was to evaluate the performance of the model, validate its formulation, and provide a comprehensive analysis of the results under realistic conditions. By focusing on a single state, it was possible to examine in detail the operational dynamics of the system, the role of LDES, and the economic interactions between different technological options.

Once the model's performance was verified and the results thoroughly analyzed in the California context, the study was extended to a broader scope. The optimization was subsequently applied to each of the 48 contiguous United States. This expanded application was designed to uncover systemic patterns and regional characteristics that significantly influence the economic viability of LDES. To this end, several factors were analyzed across states, including: the share of thermal generation relative to total demand, the utilization rate of thermal capacity, the capacity factor of renewable resources, and the share of thermal FO&M costs in the overall system cost. Additionally, the composition of renewable generation was considered, particularly the relative contributions of solar and wind. By correlating these variables with the economic outcomes of the optimization, the study provides insights into the conditions under which LDES becomes a competitive and essential asset within a decarbonized grid. In summary, the overall analytical structure of the case studies, progressing from the micro-analysis in California to the macro-expansion across the United States, is illustrated in Fig. 3.

Before running each model, investment costs were annualized to account for the time value of money. We assumed a lifetime of 50 years for conventional

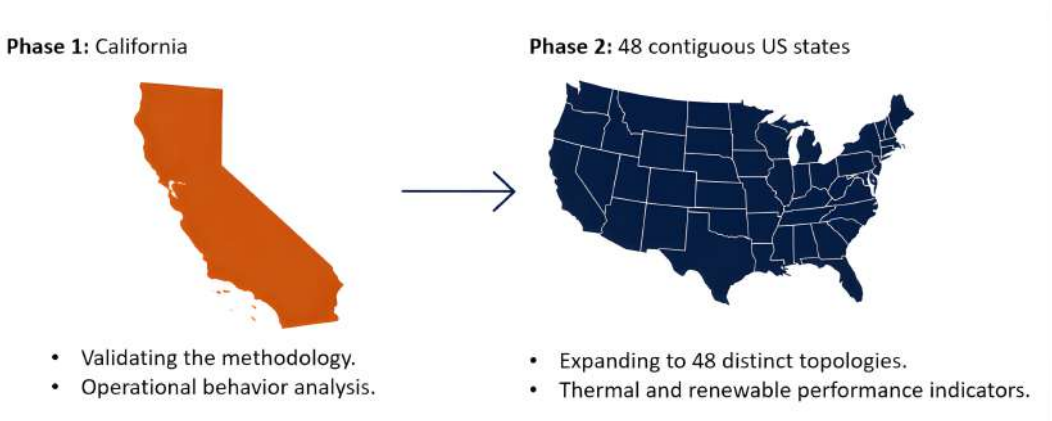

Figure 3 – Overview of the analytical structure adopted in the case studies, progressing from a detailed operational analysis in California to a nationwide expansion.

generators and 20 years for LDES technologies, applying an annual interest rate of 2.5 % to convert capital expenditures into Equivalent Annual Costs (EAC) [49]. The financial results in this study are then expressed in 2022 US dollars.

3.1.2 Data source

The dataset used in our computational experiments is based on a compilation of data from several reliable sources, as described below. These sources provide a comprehensive view of how the energy matrix of the 48 contiguous US states is projected to be in 2050. We accessed information about system load as well as available generation technologies with their respective installed capacities through data made available by NREL's Cambium 2022, without tax credit phaseout scenario [50].

The demand for each state is approximated by the total electricity generation reported by Cambium for that state. This assumption is consistent with Cambium's design, where electricity supply and demand are balanced at the state level. Since the dataset reports hourly generation data for each state, we use this information to represent hourly demand, under the assumption that each state is analyzed individually and interconnections between states, such as electricity imports and exports, are not considered in this study. In addition, our modeling framework considers only one node per state, meaning that the entire demand is aggregated

into a single load point per state.

More specific parameters such as ramp rates of each power plant technology come from the Cambium 2022 documentation [44]. Values of FO&M costs of each generator are provided by the Regional Energy Deployment System (ReEDS[1]) base [51], which is publicly available on GitHub [52], and complemented by information present in the 2022 Annual Technology Baseline (ATB) [53]. In addition, we use fuel prices that are reported in the Annual Energy Outlook (AEO) 2023 [54]. Moreover, from the ATB 2022, we take into account relevant data related to investment costs associated with renewable power plants. Furthermore, specific operational parameters for individual generators (such as maximum and minimum capacities, heat rates, and Variable Operation and Maintenance (VO&M) costs) and storage devices (including power, energy capacity, duration, and round-trip efficiency) were extracted from the underlying PLEXOS database used by the NREL team to simulate the Cambium 2022 scenarios. This detailed dataset was provided directly by the Cambium development team upon request [55]. Monetary values are updated considering the Consumer Price Index (CPI) [56].

Capacity Factor (CF) values for each type of source were constructed at each time period for this case study in order to account for the variability of renewable energy sources. The required data, installed capacity, and generation were acquired from Cambium 2022 [50] of the corresponding scenario discussed. The capacity factor values that ReEDS base [51] provided were also gathered for the wind source. The methods used for each technology are explained in detail below, and the ratio is determined for each Balancing Area (BA) across the 48 contiguous US states. The concept of a BA will be described in the next section 3.1.3.

- Solar: The capacity factor used in the model is the ratio between effective provided generation at each period under consideration and installed capacity

[1] The ReEDS is a long term capacity expansion model developed by NREL that generates projections of how the US electric sector could evolve across a suite of different potential futures, including changes in generation capacity, technology mix, and regional deployment. These ReEDS-based scenarios are then used to produce the Cambium dataset, which provides hourly estimates of marginal emissions, marginal operating costs, marginal energy and capacity values, and other metrics for evaluating the environmental and economic impacts of electricity use.

by the Cambium 2022 output sheets.

- Hydropower: The capacity factor used in the model is defined as the highest generation observed during each season, divided by the installed capacity, based on data from the Cambium 2022 output. This seasonal approach captures the maximum potential availability of hydropower in different parts of the year.

- Wind: For the initial implementation focused on California, wind capacity factors were estimated at each time step using the maximum value between two sources: the ratio of generation to installed capacity from Cambium 2022 output data, and the capacity factor provided by the ReEDS base dataset [51]. This approach aimed to avoid underestimation of availability during certain periods. However, for the nationwide implementation covering all 48 contiguous US states, only the Cambium dataset was used, i.e., the generation to installed capacity ratio. This change was made to better capture the temporal variability of wind resources, as the Cambium data offers hourly resolution and greater consistency across regions, enabling a more accurate representation of seasonal patterns.

3.1.3 Spatial and temporal resolution

The simulation model was first implemented for the state of California to test and validate the proposed methodology, as mentioned before. Following the system representation used in the Cambium and ReEDS datasets, California is divided into four Balancing Areas (BAs) within its territory ('p8', 'p9', 'p10', and 'p11'), as shown in Fig. 4. The analysis adopted an hourly temporal resolution with 8760 intervals throughout the year. To ensure system reliability, a reserve requirement of 15 % of the system demand was imposed for all time periods, consistent with practices adopted by California Independent System Operator (CAISO) [57].

After validating the approach in California, the model was expanded to encompass the entire contiguous United States, covering 48 states. In this broader implementation, each state is analyzed individually, and power plants of different

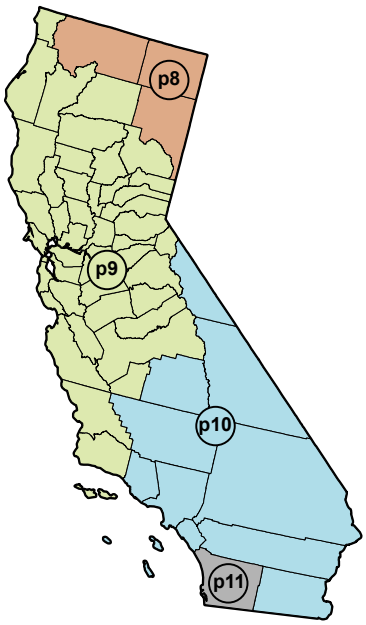

Figure 4 – Map of California with BA representatives covered by the model. Source: Adapted from [44].

technologies are located within specific BA, totaling 134 BAs across the country [44]. The hourly temporal resolution is maintained, and for consistency with national grid planning standards, the reserve requirement is adjusted to 4 % of the system demand across all time periods and states. In this setup, the combined generating capacity of all BAs within a state must meet that state's demand. This value aligns with standard practices in grid planning and operation, where reserve margins are maintained to accommodate fluctuations in generation capacity availability and demand.

It is important to note that, in both the California case study and the national study, a simplified approach was used to model the system, which did not include any representation of transmission lines, not even investments in transmission lines or constraints on transmission. Because of this simplification, the model effectively aggregates each state's demand into a single node. Nevertheless, the spatial division into BAs is purposely maintained. This BA-level granularity is crucial for two main reasons. First, it preserves the spatial diversity and regional accuracy of the intermittent renewable resources, as hourly CF is evaluated individually

for each BA. Second, this high-resolution spatial modeling establishes a robust foundation for future studies, which intend to incorporate intra- and inter-state transmission constraints, power flow dynamics, and localized congestion analyses without requiring structural changes to the model's geographical definitions.

3.1.4 Fixed and candidate generators

The initial implementation of the model that focuses on California, Cambium 2022 projects that 714 generators will be in operation by 2050. To reduce the problem's dimensionality and improve computational tractability, we applied K-means clustering to group generators into three cost-based categories (high, medium, and low) within each BA. The clustering was based on the generation cost of each unit, denoted as C_g^p, defined in equation (3.1). This categorization enables a more manageable yet representative modeling of generation options in each region.

$$C_g^p = C_g^{VO\&M} + C_g^{fuel} \times HR_g \tag{3.1}$$

Where:

- C_g^p: Generation cost of generator g.
- $C_g^{VO\&M}$: Variable operations and maintenance cost of generator g.
- C_g^{fuel}: Fuel price cost of generator g.
- HR_g: Heat Rate (the amount of fuel required to produce one unit of electricity) of generator g.

This clustering process resulted in 75 representative existing generators for the CA case study. In addition to the fixed generators, we defined a set of candidate generators restricted to intermittent renewable technologies (solar, wind-ons, and wind-ofs). For each RES already present in a given balancing area, a corresponding candidate generator was introduced with specifications identical to those of the existing unit, resulting in a set of 17 candidate generators for CA. This same

methodology for defining candidate generators was applied in both the CA study and the national-scale study.

The expansion potential of candidate generators was incorporated into the model to allow for system growth. In the initial implementation focused on California, the quantity of investment in megawatt (MW) of each candidate generator could not exceed the installed capacity of its corresponding fixed generator (i.e., a 1x limit). For the national-scale study covering all 48 contiguous US states, this limit was set to 4x (four times) the capacity of the corresponding fixed generator, providing more flexibility for system expansion. In states with more restrictive geographic or resource conditions, such as Connecticut (CT), Delaware (DE), and Pennsylvania (PA), the expansion limit was further increased to 10x (ten times) to ensure feasibility under more constrained scenarios.

To make the methodology presented in this section clearer, the resulting set of 75 fixed generators and 17 candidate generators used in the California case study is detailed in Table 6.

3.1.5 Fixed and candidate batteries

In this study, fixed batteries in each BA were grouped by type, considering durations of 2 h, 4 h, 6 h, 8 h, PHS, and Compressed Air Energy Storage (CAES). For candidate SDES, a single 4-hour system, with an RTE of 85 %, was defined for each state, and a candidate LDES system with 100-hour duration and 42.5 % RTE (realistic parameters of an iron-air storage [45, 46]) was also included.

In the initial implementation focused on California, the investment limit for the candidate 4-hour SDES was restricted to 1x the existing SDES capacity. The LDES capacity range was limited to 0 to 75 GW, as higher capacities were not required to reach feasible solutions in that case. The resulting fixed and candidate storage systems used in the initial California implementation are summarized in Table 7.

In the national-scale implementation, the same structure was applied; however, the maximum investment capacity for the SDES candidate was set to 10 times the total existing SDES power capacity in the state (excluding PHS). In the national model, the investment capacity limit for LDES ranged from 0 to 150 GW.

Table 6 – Installed capacity, investment limits, and number of generators by technology in the initial California implementation.

Technology	**Installed Capacity (GW)**	**Numb. of Existing Gen.**	**Limit of Invest. (GW)**	**Numb. of Candidate Gen.**
Biopower	0.29	8	-	-
Distributed PV	28.50	4	28.50	4
Distributed utility PV	0.04	3	0.04	3
Natural gas cc	18.39	9	-	-
Natural gas ct	8.99	10	-	-
Geothermal	2.23	3	-	-
Hydropower ED[a]	3.49	2	-	-
Hydropower END[b]	6.70	4	-	-
Hydropower UD[c]	1.09	1	-	-
Hydropower UND[d]	0.15	3	-	-
Landfill gas	0.07	9	-	-
Oil/gas steam	0.15	9	-	-
Utility-scale PV	83.59	4	83.59	4
Offshore Wind	25.00	2	25.00	2
Onshore Wind	9.48	4	9.48	4
Total	**188.16**	**75**	**146.61**	**17**

[a] Existing dispatchable.
[b] Existing non-dispatchable.
[c] Undiscovered dispatchable.
[d] Undiscovered non-dispatchable.

3.2 Case Study –California

This section presents the results of the initial application of the model to California. The case study focuses on the critical role of LDES technologies in supporting the state's transition toward full power sector decarbonization by 2050. Gas power plants are currently the main source of firm generation to counterbalance renewable energy sources in the state. However, in a fully decarbonized future power system, gas units should be replaced by a more environmentally friendly option. This firm generation role can be performed by LDES technologies.

Fig. 5 illustrates the energy matrix for the generation of electrical energy in California. It shows a complex trajectory with significant changes over the

Table 7 – Power capacity and the limit of investment by technology with the respective number of storage.

Technology	Power Capacity (GW)	Numb. of Existing Storage	Limit of Invest. (GW)	Numb. of Candidate Storage
Battery 2 h	0.30	2	-	-
Battery 4 h	17.46	4	43.00	1
Battery 6 h	9.55	3	-	-
Battery 8 h	4.03	4	-	-
PHS (12 h)	11.43	3	-	-
LDES	-	-	0 - 75[a]	1
Total	**42.78**	**16**	**-**	**2**

[a] The range consists of discrete values between 0 and 75.

decades examined. Natural gas power plants are clearly in the lead until the most recent year, with installed capacity increasing until 2010. Nonetheless, the information reveals a significant turning point around 2015, when a decline in natural gas capacity occurred. The reason for this is the application of strict regulations meant to reduce the emissions of greenhouse gases. In response to this decrease, we observed an increase in renewable plants, with notable increases in solar, battery, and wind energy capacities attesting to California's sincere efforts to shift its energy mix toward more sustainable options. These patterns demonstrate the state's dedication to reducing climate change and promoting a more sustainable and resilient energy sector. Looking ahead, California has committed to a future dominated by renewable energy and carbon neutrality, and its ambitious 2030 and 2045 targets further support this commitment, as mentioned in the section 1.1 through the targets proposed by SB 100.

Given this, California provides a real-world illustration of why LDES will be necessary in a decarbonized grid in the future. According to the author [19], a theoretical analysis using 2020 and 2022 data from this state shows that during 61 % of the hours during the year, the generation is less than the load. Moreover, the research highlighted a significant dependence on energy imports originating from regions that will require 100 % clean energy in the future, implying that California is unlikely to be able to obtain firm capacity from these regions. This

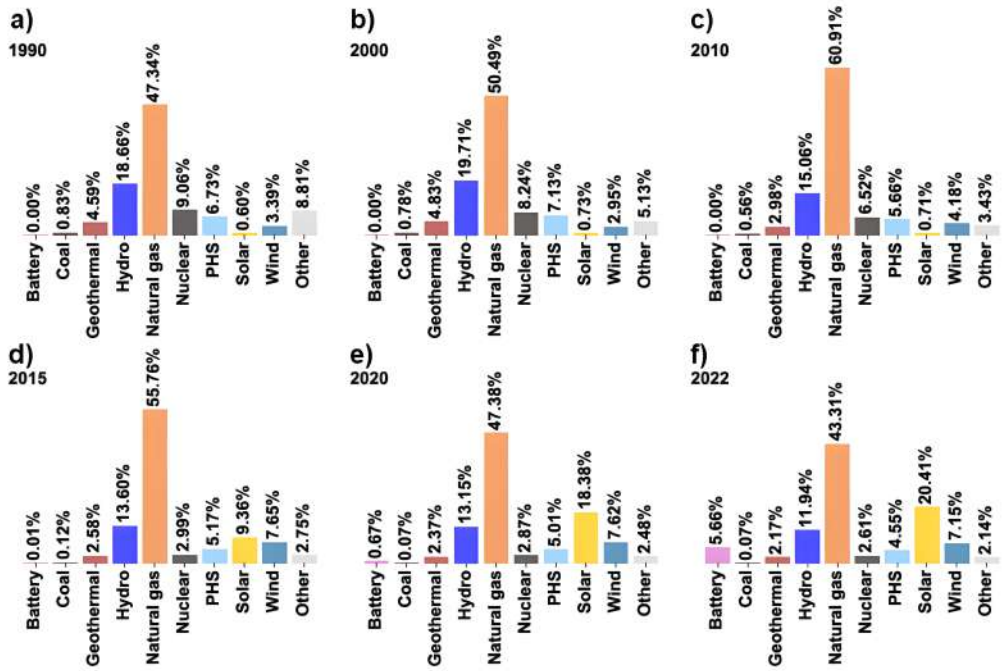

Figure 5 – Composition of the energy matrix for generating electrical energy in California through the years. Source: Adapted from [58].

illustrative analysis consequently makes the assumption that the state will also need to substitute another energy, like LDES, for this one. Since these technologies are still not mature, here we estimate, via the proposed methodology, the boundary costs that would make them economically viable for California's system.

In the next subsections, we analyze the projected energy matrix of California for 2050 in a scenario where polluting energy sources are phased out and replaced with LDES technologies. We then present a comprehensive set of results, including economic and operational outcomes, insights from consecutive charge and discharge behavior of SDES and LDES, electricity price dynamics, and a series of sensitivity analyses covering fuel prices, the trade-off between gas prices and solar investment costs, and variations in LDES duration.

3.2.1 Economic results

The boundary costs of LDES systems are defined in this research as the technology costs below which these technologies become economically viable. To obtain these boundary costs for California, we maximized the opportunity value following our proposed solution framework. As a reference, we consider the previously described data for the projected California's energy matrix in 2050 without any candidate assets to solve the *baseline model*. Then, we run the *opportunity value maximization model* for different amounts of LDES added to the system while bounding overall system costs below those of the *baseline model*, retiring 100 % of the gas power plants and considering candidate investments in SDES and renewable generators.

Results from the modeled scenarios indicate that at least 8.7 GW of 100-hour LDES will be necessary to retire gas power plants and maintain overall system costs limited to the same values determined by the *baseline model*, in which the participation of gas units is still included. According to Fig. 6, the boundary cost of 8.7 GW of 100-hour LDES is US$ 13.74 kW^{-1}. It is worth noting that, as we increase the power capacity of 100-hour LDES in Fig. 6, overall system costs decrease as a result of lower needed operational and investment costs to retire gas units (as will be seen in the next graphs). Therefore, the boundary cost of LDES increases from 8.7 GW to 17 GW, where it reaches a peak of US$ 512.54 kW^{-1}. Then, after its peak, the boundary cost of LDES starts to fall since the rate of reduction in overall system costs per additional kW of LDES power capacity begins to decline.

The opportunity value for various amounts of LDES is shown in Fig. 7. The first bar on the left depicts the reference system costs obtained through the *baseline model*, including the operational and fixed costs of gas plants. The FO&M costs of some existing generators (biopower, geothermal, hydropower, solar, and wind) and existing storages are the same for all bars, therefore they are omitted from Fig. 7. It is worth mentioning that an eventual bar corresponding to a 100-hour LDES power capacity lower than 8.7 GW would result in an overall system cost higher than the reference cost obtained when gas units are still present in the system. In addition, it is interesting to see that, as the amount of 100-hour LDES power

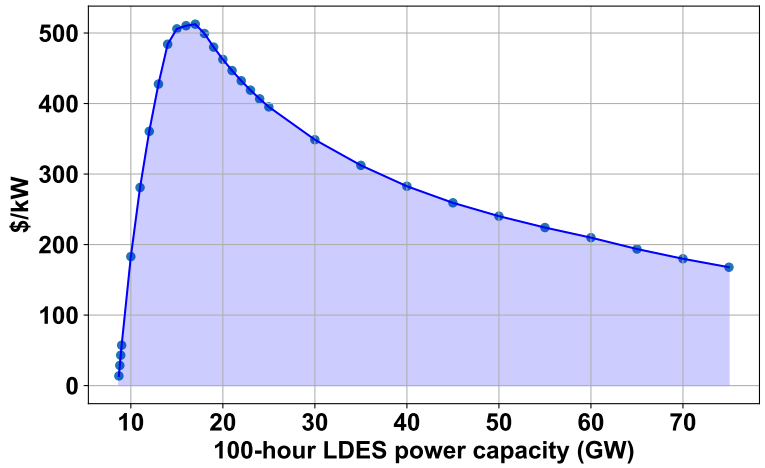

Figure 6 – The boundary costs of LDES below which these technologies will be economically viable for the California's system in 2050.

capacity increases, the need for SDES and renewable investments significantly decreases, which makes room for the opportunity value maximization of the LDES option.

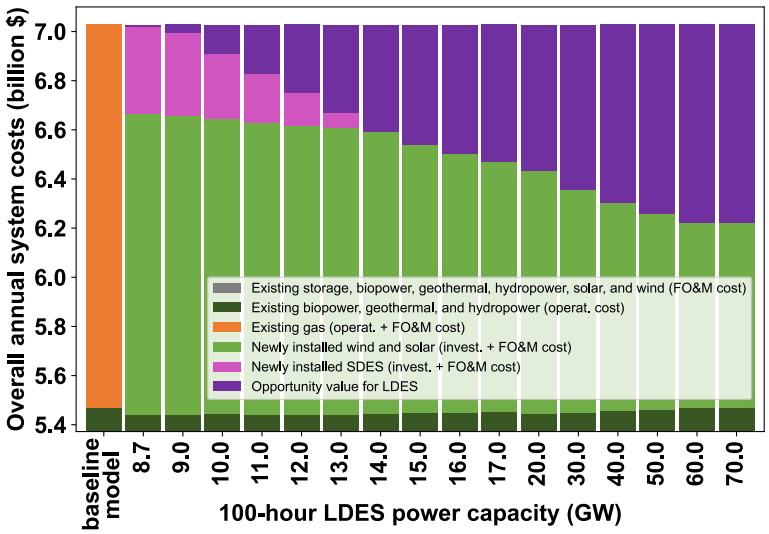

Figure 7 – Opportunity values (in purple) associated with different power capacities of 100-hour LDES. For illustration purposes, the FO&M cost of some existing generators and storages are omitted from the figure.

In Fig. 8, is provided a direct comparison between (i) the reference costs

obtained through the *baseline model*, (ii) the costs obtained via the *opportunity value maximization model* when gas is replaced by a combination of LDES (setting the 100-hour LDES power capacity to 17 GW), SDES and RES, and (iii) the costs obtained via the *opportunity value maximization model* when gas is replaced by a combination of SDES and RES only. From these results, it is clear that the system would be substantially more expensive if we retire gas plants without LDES. On the other hand, when 17 GW of 100-hour LDES is present, overall system costs are the same as the reference cost as long as the cost associated with the LDES is at US$ 512.54 kW^{-1}.

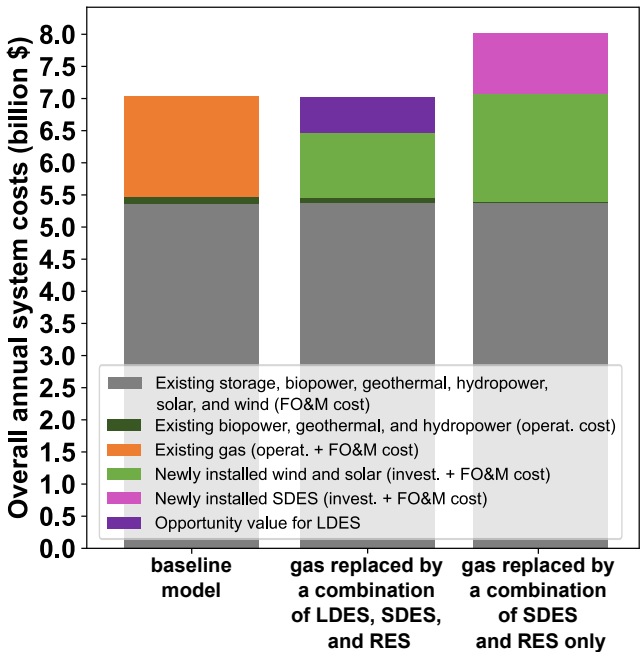

Figure 8 – Comparison between (i) the reference costs from the *baseline model*, (ii) the resulting costs from the *opportunity value maximization model* when the gas is replaced by a combination of 17 GW 100-hour LDES, SDES, and RES, and (iii) the resulting costs from the *opportunity value maximization model* when the gas is replaced by a combination of SDES and RES only.

For each considered amount of 100-hour LDES power capacity, a different mix of renewable energy investment is required, as shown in Fig. 9. The candidate options in the *opportunity value maximization model* are solar, wind-ons, wind-ofs, and SDES (4 h duration) assets. From these options, wind-ofs is never chosen

by the model, and SDES investment is only required for LDES power capacities lower than 14 GW. In general, as LDES power capacity increases, the amount of additional installed capacity from other technologies decreases, with the exception of LDES power capacities ranging between 15 and 20 GW. Within this specific range, LDES provides enough support for the system to choose to invest primarily in solar, which is the less expensive renewable technology in this case study but it is not available at all hours of the day. Furthermore, we observe a saturation in the contribution of LDES to decrease renewable investments when its power capacity reaches 60 and 70 GW. In this case, an amount of 13710 MW (mix of solar and wind-ons) of newly included renewables is the minimum requirement to retire gas units and use LDES as a firm energy source.

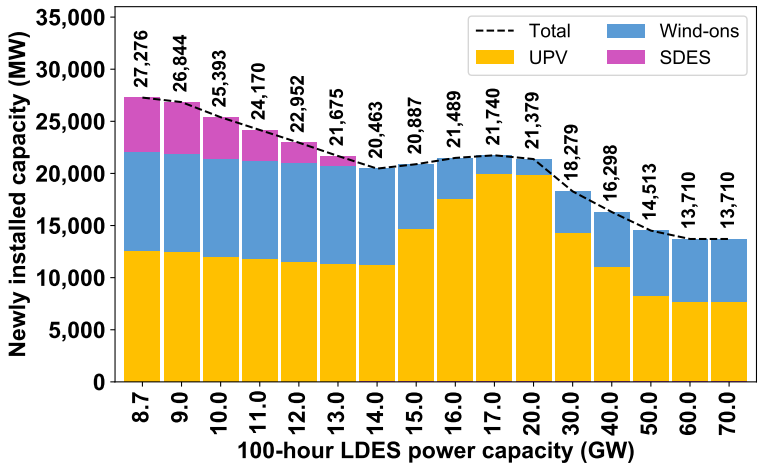

Figure 9 – Additional investment required in California in 2050 to have a system without gas energy sources.

Fig. 10 depicts the reduction in overall system costs as we increase the LDES power capacity once gas units are retired. Essentially, without LDES, the retirement of gas power plants would require substantial investments in SDES and renewable generators. These investments are significantly reduced as we increase the LDES power capacity present in the system. For instance, when the LDES power capacity is 8.7 GW, there is an overall annual system cost reduction of 7.67 million dollars compared to the costs obtained from the *baseline model*. This reduction justifies an investment cost of US$ 13.74 kW^{-1} for LDES. As we increase

the LDES power capacity to 17 GW, the overall annual system cost reduction reaches 558.93 million dollars which can allow the investment cost of LDES to be US$ 512.54 kW^{-1}.

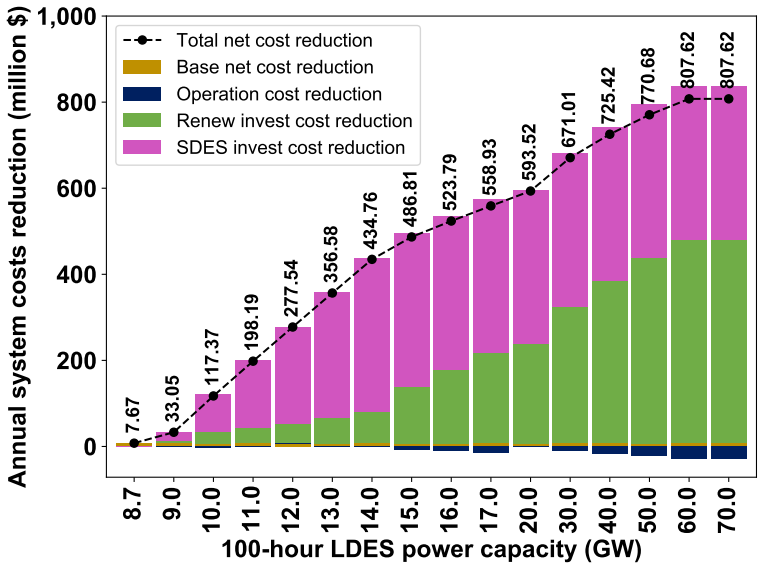

Figure 10 – The cost reduction in the California system in 2050 for different quantities of LDES when the gas plants are retired. The base net cost reduction refers to the decrease in overall costs once 8.7 GW of LDES are included in the system compared to when gas units are still present.

In order to provide even more clarity, we would like to show at the end of this subsection how the Boundary Cost Values (BCV) match if we take the values from the cost reduction, which is the same as opportunity values (seen in purple in the Fig. 7). For that, if the cost reduction values are annual, we need to know the total value throughout an LDES's lifetime. To find out this, see Eq. (3.2), where r is the annual interest rate, and L is the lifetime of storage.

Let's consider an LDES of 10 GW as an example. In 2050, the cost reduction was approximately 117 million dollars (see Fig. 10); however, with a lifetime of 20 years and an annual interest rate of 2.5 %, we can achieve the cost reduction value of around 1.8 billion dollars, and then, as the storage has power quantity of 10 GW, i.e., 10,000 MW, the boundary cost value will be 182,969 US$/MW or 182 US$/kW (see Fig. 6), as shown in the Eq. (3.3)–(3.6). The same logic applies to

other storage amounts and their cost reduction or opportunity value.

$$BCV = \frac{CostReduction}{x^{st,power\ddagger}} \times \frac{1 - \frac{1}{(1+r)^L}}{r} \tag{3.2}$$

$$BCV^{10\ \text{GW}} = \frac{\$117369745}{10000\ MW} \times \frac{1 - \frac{1}{(1+0.025)^{20}}}{0.025} \tag{3.3}$$

$$BCV^{10\ \text{GW}} = \frac{\$117369745}{10000\ MW} \times 15.5891 \tag{3.4}$$

$$BCV^{10\ \text{GW}} = \frac{\$1829696,011}{10000\ MW} \tag{3.5}$$

$$BCV^{10\ \text{GW}} = 182969.60\ \$/MW \tag{3.6}$$

3.2.2 Operational results

The previous subsection illustrated the economic results obtained in this case study, specifically the cost below which LDES becomes economically viable as a firm capacity technology to compensate for renewables variability. However, how does an LDES aid the system's operation? This question has been answered below.

The LDES is an essential component of the system and makes a unique operational contribution that helps to justify the boundary costs that were previously mentioned. For example, Fig. 11 (a) depicts the aggregate dispatch of gas power plants during a year according to the *baseline model*. Meanwhile, Figs. 11 (b) and 11 (c) display the state of charge of LDES and SDES systems, respectively. The 100-hour LDES power capacity is 8.7 GW, and the 4-hour SDES power capacity is 5.3 GW. Additionally, Fig. 12 presents the average hourly renewable availability per month in 2050 in California, reflecting the impact of investments from the *opportunity value maximization model*, also, when the 100-hour LDES power capacity is 8.7 GW.

Notably, renewable generation in California exhibits significant fluctuations, with higher output levels during spring and summer compared to fall and winter. In this context, the participation of SDES systems is very important to balance intraday fluctuations of renewables as indicated by the high frequency in the change of their aggregate state of charge in Fig. 11 (c). On the other hand, SDES systems are not able to help the system cope with seasonal changes in renewable generation

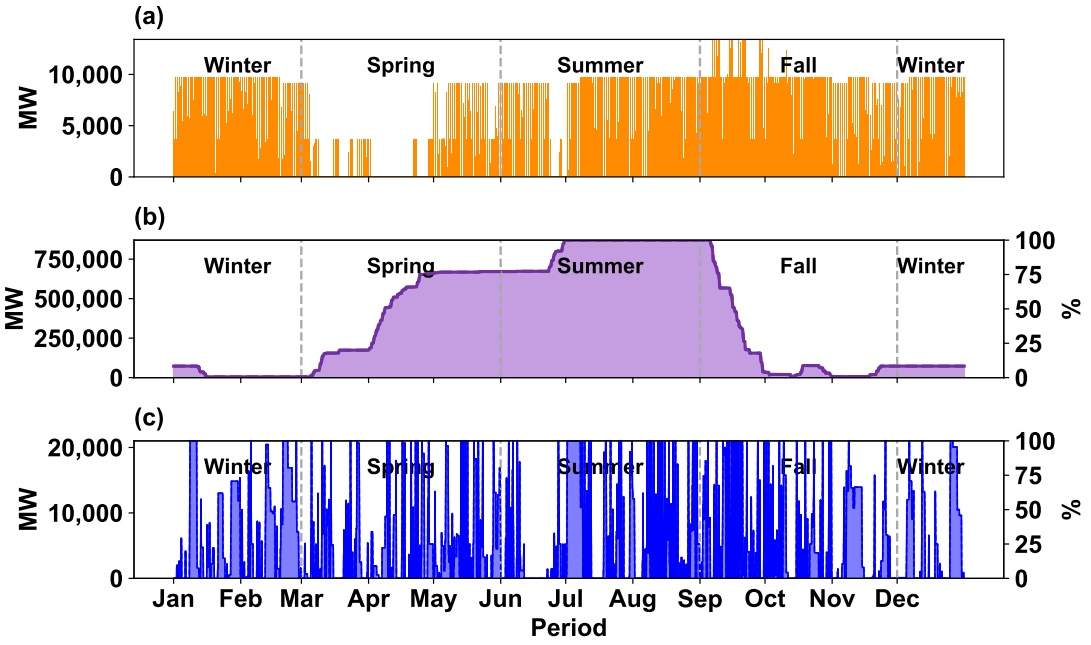

Figure 11 – (a) Aggregate hourly dispatch of all gas power plants from the *baseline model*'s solution. (b) 100-hour LDES system with 8.7 GW of power capacity – state of charge according to the *opportunity value maximization model*'s solution. (c) 4-hour SDES system with 5.3 GW of power capacity – state of charge according to the *opportunity value maximization model*'s solution.

patterns. In the reference system tested through the *baseline model*, gas units provided the firm generation needed especially during September when there is a sharp decline in renewable generation output.

Afterward, it became evident that gas plants are essential for maintaining system reliability, particularly during months with lower renewable output. However, in scenarios without gas plants, LDES systems capitalize on periods of high renewable availability to store energy, ensuring their contribution as a firm resource when needed, behavior clearly observed in Fig. 11 (b). Besides, it is interesting to see in this figure how LDES starts a long period of charge in spring and summer, i.e., when there is a greater abundance of renewable energy available and then a quick discharge happens during the fall, and a comparison with the system without LDES shows that this occurred at the same time the gas plants operated at a higher intensity (see Fig. 11 (a)).

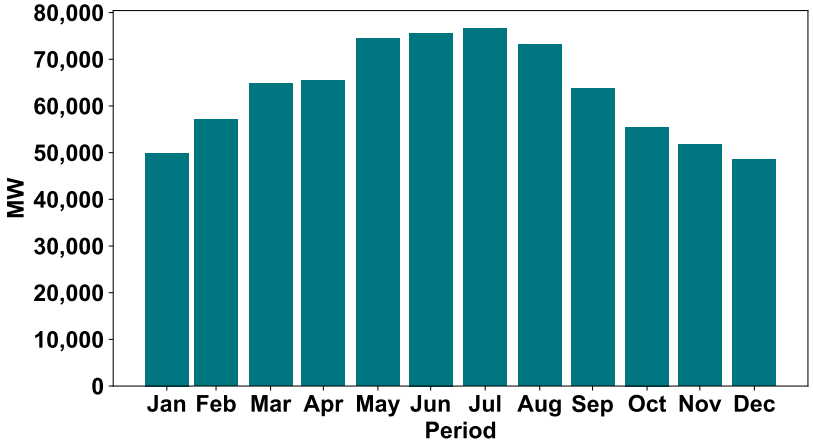

Figure 12 – Average hourly availability per month of all installed renewable sources in California per month in 2050 according to the solution of the *opportunity value maximization model* when the 100-hour LDES power capacity is 8.7 GW.

Finally, the overall annual contribution in terms of generation output and reserve provision from each technology is illustrated in Figs. 13 and 14, respectively, according to the results of (a) the *baseline model* and (b) the *opportunity value maximization model* when the 100-hour LDES power capacity is 8.7 GW (minimum LDES capacities that would be required to retire gas power plants). In both figures, the combined contribution of LDES and SDES, together with the expansion of renewable generation, compensates for the retirement of gas capacity.

3.2.3 Contrasting charge-discharge behavior

Data analysis and interpretation can be made more approachable with the help of heat map charts, which are an effective tool for identifying and presenting patterns and trends in datasets. In order to gather additional insights regarding this emerging technology, LDES, the heat map of the number of hours that an SDES and LDES discharge and charge consecutively[2] for various solutions is displayed in the following figures.

[2] Discharging consecutively aims to depict the duration between the initial discharging and the last discharging before charging; during this time, there might be intervals without discharging, but there was no charging during this computed time. This also applies to consecutively charge.

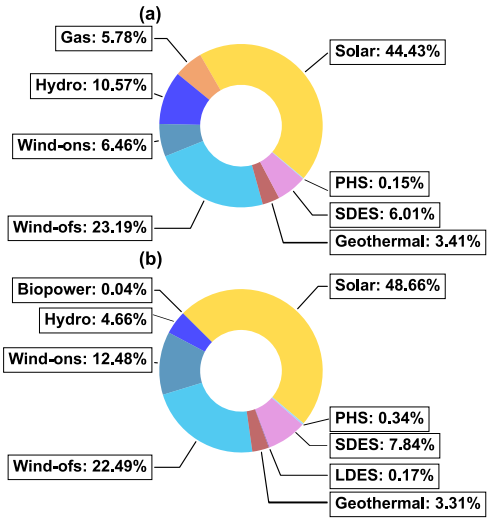

Figure 13 – Annual generation contribution per technology for California in 2050 – (a) results of the *baseline model* and (b) results of the *opportunity value maximization model* when the 100-hour LDES power capacity is 8.7 GW.

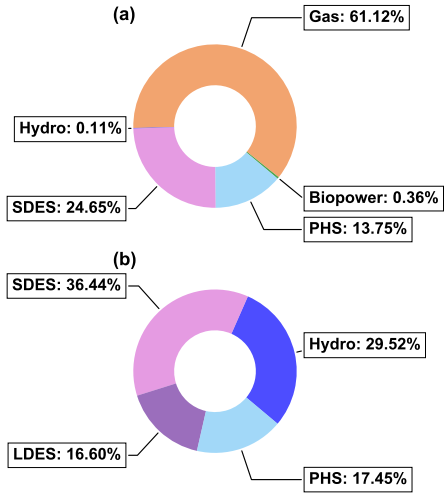

Figure 14 – Annual reserve provision per technology for California in 2050 – (a) results of the *baseline model* and (b) results of the *opportunity value maximization model* when the 100-hour LDES power capacity is 8.7 GW.

In Fig. 15, the SDES behavior profile is depicted, which shows the number of hours of continuous discharge, and Fig. 16, the number of hours of continuous charge. In fact, the heat map graph showed that the storage mostly operated for 4 hours, i.e., occurred up to 92 times. The maximum continuous discharge period found was 8 hours when the system's LDES concentration was lower. About the charging, the maximum time of charging consecutively was 10 hours.

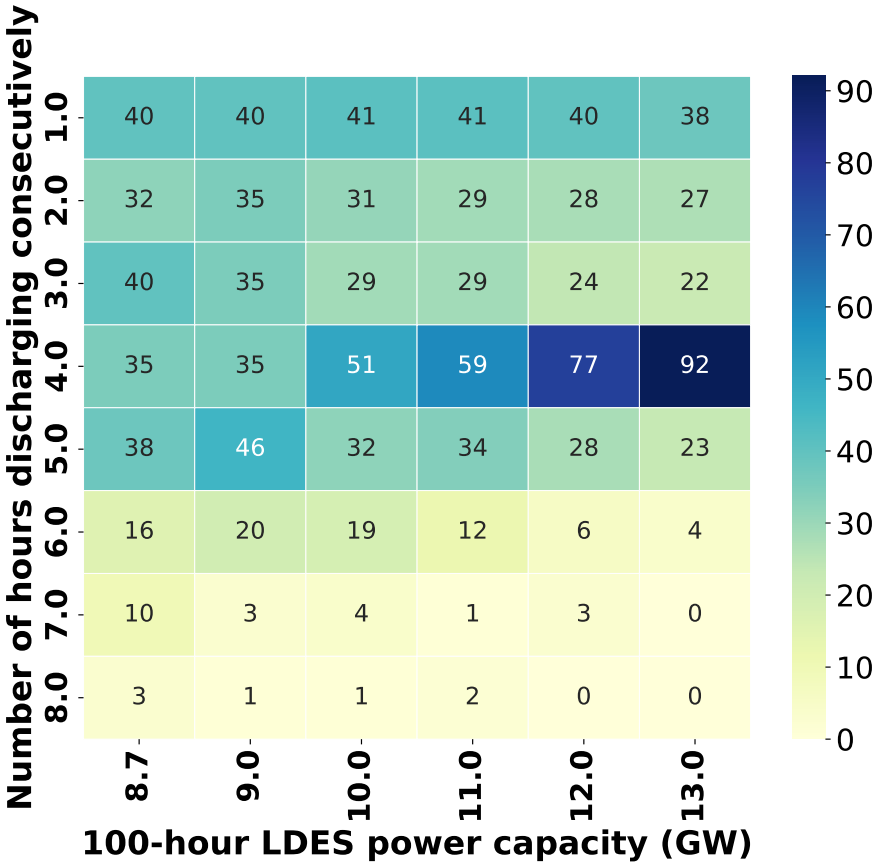

Figure 15 – Heat map showing the number of hours that SDES discharges consecutively for different quantities of LDES.

The behavioral dynamics of LDES stand out in comparison to the previously observed behavior of SDES by the heat maps depicted in Fig. 17 and Fig. 18, which respectively showcase the duration of continuous discharge and charge. These visualizations underscore the significant role that LDES technology plays in systems characterized by prolonged periods of discharging or charging, a significant contrast

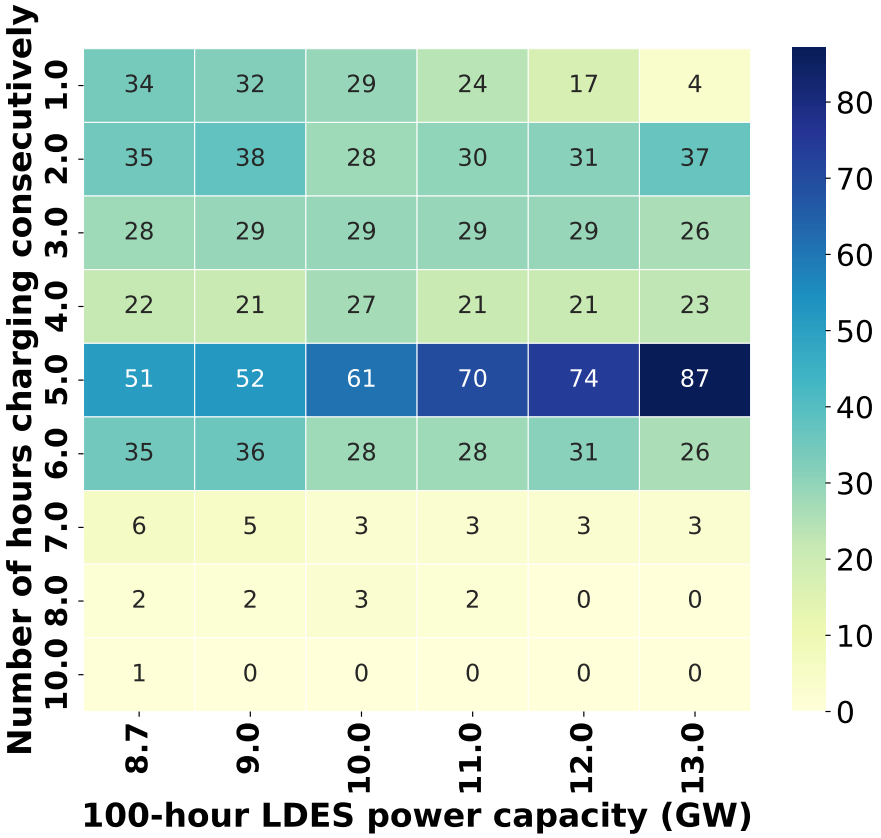

Figure 16 – Heat map showing the number of hours that SDES charges consecutively for different quantities of LDES.

to the behavior observed with SDES. Moreover, as depicted in Fig. 17, long-duration energy storage systems can provide energy to the system for roughly 497 hours annually without requiring charging. Consequently, there have been occasions where the recharging phase for this type of technology extended up to 1470 hours.

Additionally, LDES systems operate with significantly fewer cycles, characterized by long periods without switching between charging and discharging, in contrast to SDES, which undergo more frequent transitions. This lower cycling frequency contributes positively to the overall longevity of LDES technologies. Furthermore, the heat map for LDES suggests that higher power capacity results in extended consecutive periods of energy delivery to the system.

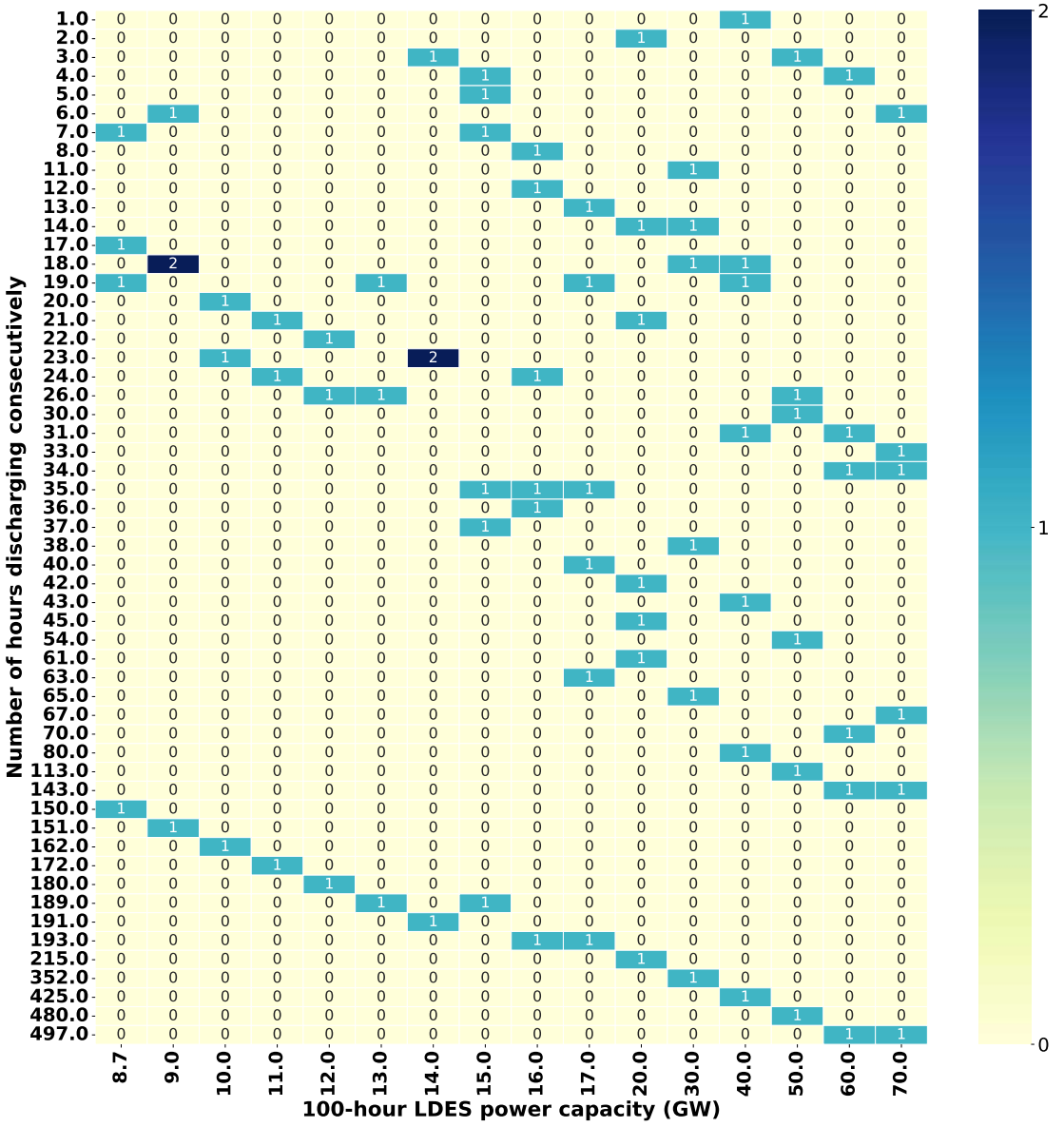

Figure 17 – Heat map showing the number of hours that LDES discharges consecutively for different quantities of LDES.

3.2.4 Energy price analysis

In this study, hourly energy prices are derived from the dual variables associated with the power balance constraint of the optimization model. This constraint, defined in Equation 2.2 in Section 2, ensures that, at every hour, the

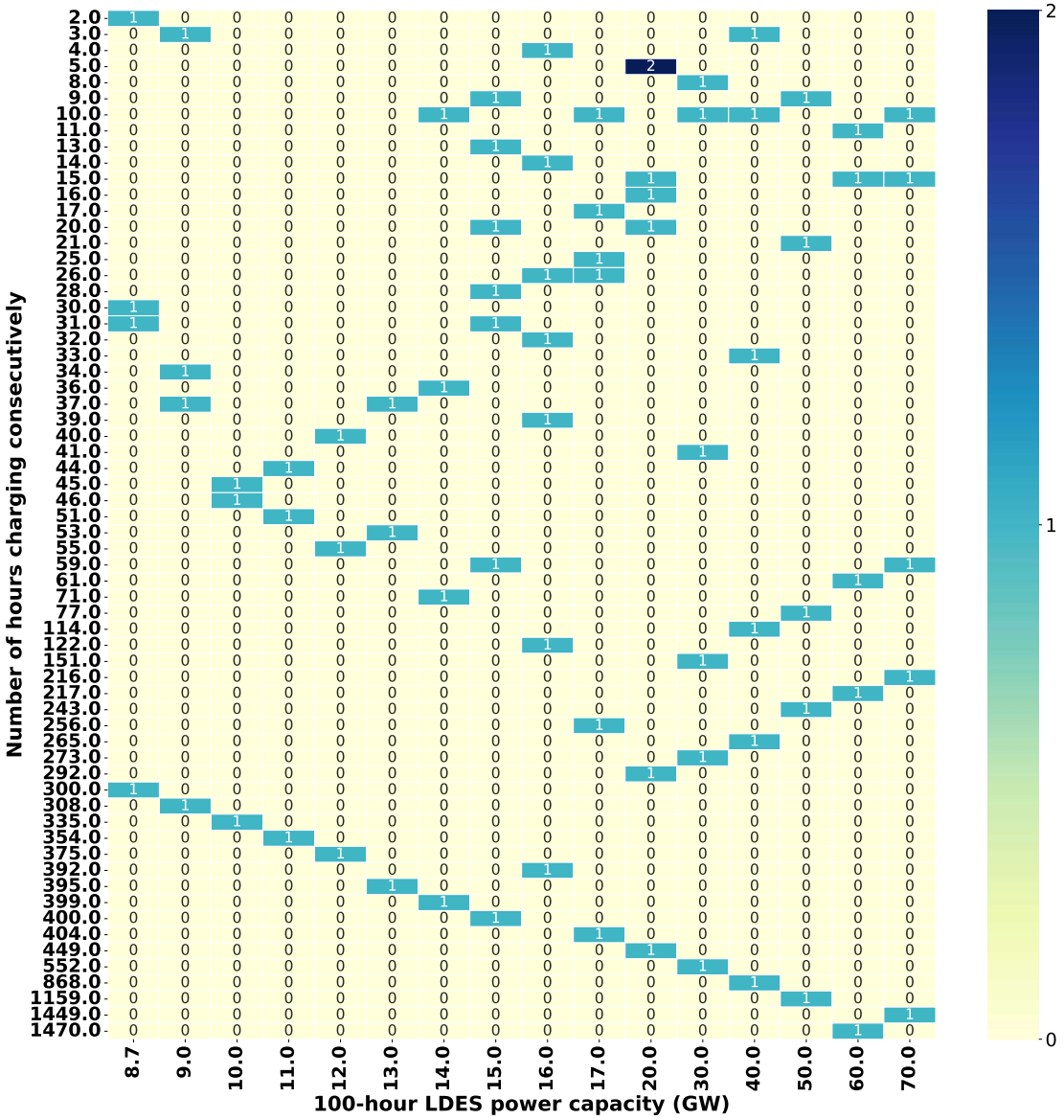

Figure 18 – Heat map showing the number of hours that LDES charges consecutively for different quantities of LDES.

total electricity supply, comprising generation and storage discharge, matches the total demand, adjusted by potential load shedding and overgeneration. The dual variable reflects the marginal cost of supplying an additional unit of electricity at each hour, and this value is used as a proxy for the energy price.

Energy prices can substantially change when the energy matrix is modified.

Here, we compare (i) energy prices that result from simulating the operation of the *baseline model* where gas is still present and LDES is not part of the available resources to (ii) energy prices of the resulting system after placing the investments indicated by the *opportunity value maximization model* to replace gas generators while considering 17 GW of 100-hour LDES power capacity. This comparison is illustrated in Figs. 19, 20, 21, and 22.

In general, Fig. 19 highlights that when gas generators are retired and replaced by a combination of renewables and LDES, there is a greater frequency of very low energy prices throughout the year. This reflects periods of abundant renewable generation and low system marginal costs. However, during the months when the capacity factors of renewables start to decline (August, September, October — see Fig. 12), energy prices exhibit much higher variability and can spike to values significantly above those observed in the *baseline model*. This increased price volatility reflects the system's higher stress and scarcity conditions when renewable output is reduced and reliance on LDES becomes critical.

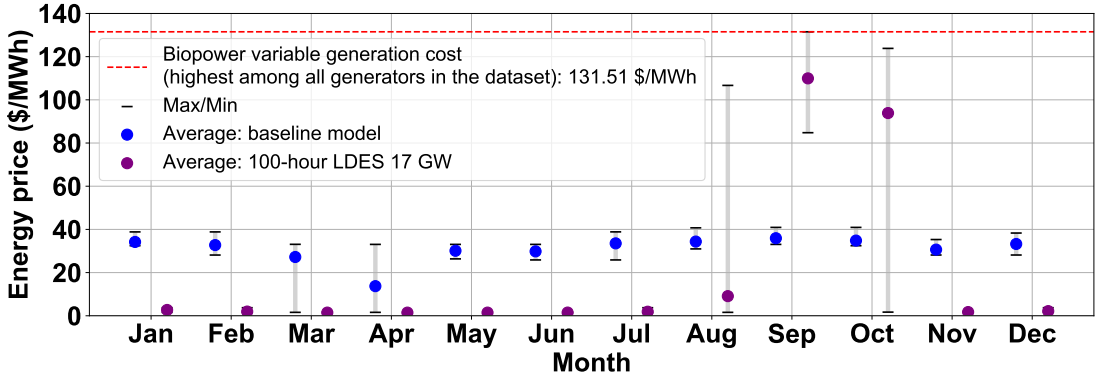

Figure 19 – Maximum, minimum, and average monthly energy prices resulting from operating the *baseline model* and the modified system with 17 GW of 100-hour LDES power capacity.

Figs. 20, 21, and 22 demonstrate that storage resources can profit from energy arbitrage in both power system configurations. To analyze this behavior, we also computed the monthly maximum, minimum, and average energy prices, but only during periods when the storage units were actively charging or discharging. These prices were obtained by filtering the dual values of the power balance

constraint according to the periods when each storage technology was charging or discharging, within the corresponding power system configuration being analyzed (e.g., SDES in the *baseline model* and *opportunity value maximization model*, or 100-hour LDES in the *opportunity value maximization model* with 17 GW of capacity). Specifically, for each technology, we selected the periods when the charging power was negative or the discharging power was positive, and then calculated the corresponding monthly average prices. This approach allows us to capture the actual price signals that storage units face in the market.

Fig.20 shows that, under the *baseline model*, SDES is consistently profitable, as the average discharging price is always higher than the average charging price. In Fig.21, under the *opportunity value maximization model* with 17 GW of 100-hour LDES capacity, energy prices faced by SDES become significantly more volatile, especially between August and October, when RES availability is lower, as mentioned before. Although the average discharging price remains higher than the charging price, indicating that arbitrage is still viable, the difference between charging and discharging prices becomes much larger, reflecting a more stressed system during months of low renewable availability. Fig. 22 presents the monthly charging and discharging energy prices for LDES under the same *opportunity value maximization model*. Most charging and discharging takes place at very low energy prices from January to July. However, between September and October, average discharging prices increase significantly, occasionally approaching the biopower variable cost, which is the highest among all generators in the dataset, highlighting the role of LDES in supporting the system during periods of high price stress and reduced renewable output.

These results suggest that phasing out gas generators and relying on a mix of renewables and LDES significantly changes the price dynamics in the power system. The system experiences more frequent occurrences of very low energy prices during periods of high renewable generation, which may benefit flexible consumers and increase the value of demand-side participation. However, during months of lower renewable availability, energy prices become much more volatile and can reach very high levels, increasing the potential revenues for storage operators but also exposing the system to greater financial risks. In this context, LDES plays a

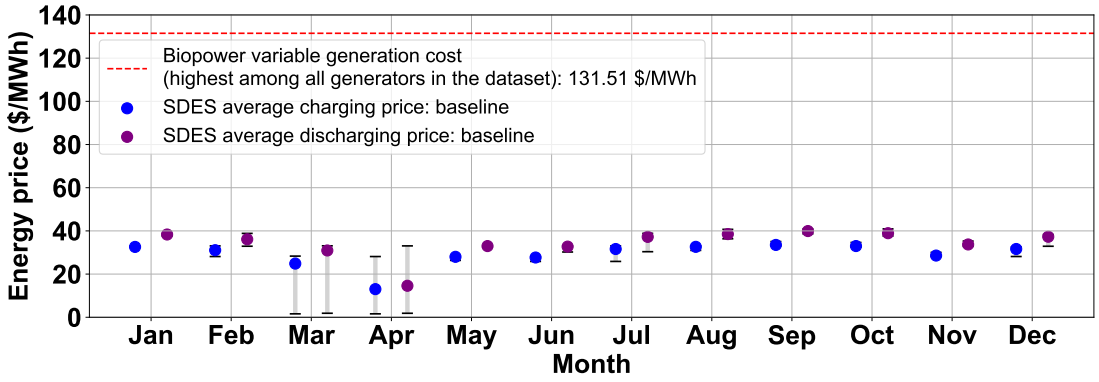

Figure 20 – Maximum, minimum, and average monthly, charging and discharging energy prices taken by SDES when operating the *baseline model*.

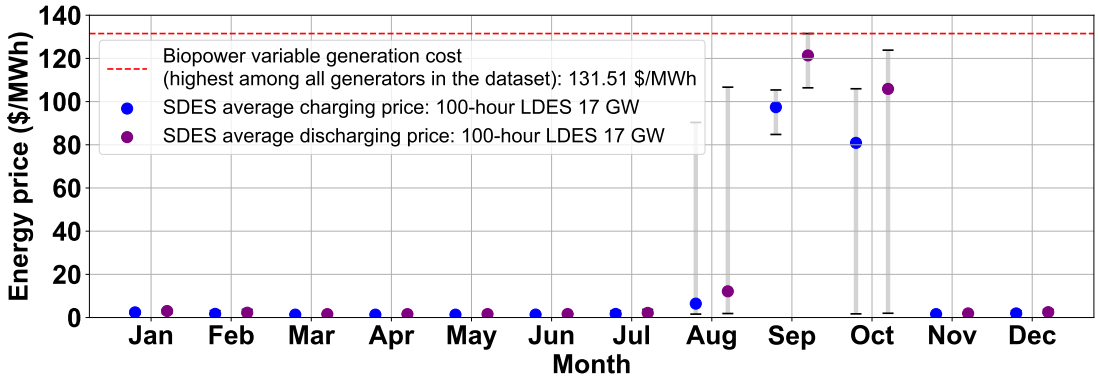

Figure 21 – Maximum, minimum, and average monthly, charging and discharging energy prices taken by SDES when operating the modified system with 17 GW of 100-hour LDES power capacity.

critical role in maintaining system reliability and capturing market value during scarcity events.

3.2.5 Sensitivity analyses

In this section, to better understand the robustness of our results and the key drivers influencing the economic viability of LDES, we conduct a series of sensitivity analyses. These analyses aim to evaluate how variations in external assumptions affect the estimated boundary costs of LDES. In particular, we examine the sensitivity of our findings to (i) changes in natural gas fuel prices, (ii) combined

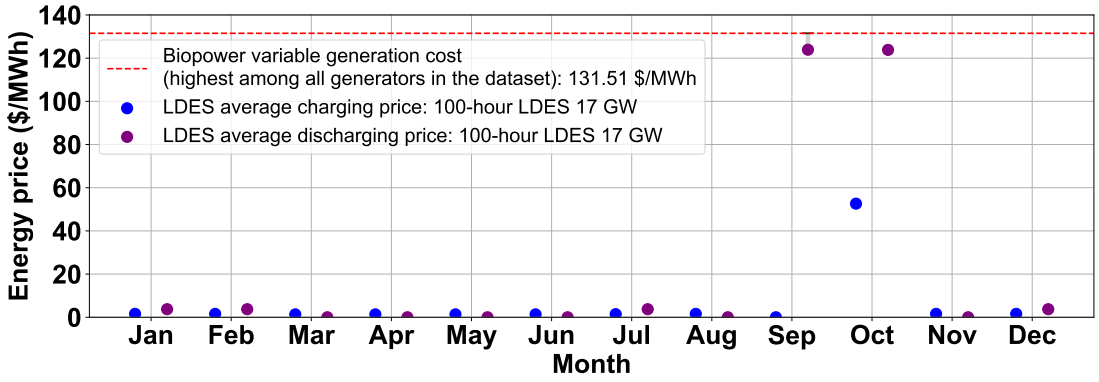

Figure 22 – Maximum, minimum, and average monthly, charging and discharging energy prices taken by LDES when operating the modified system with 17 GW of 100-hour LDES power capacity.

changes in both natural gas prices and solar investment costs, and (iii) different LDES durations, which directly impact storage flexibility and cost effectiveness. The following subsections present and discuss the outcomes of each scenario.

3.2.5.1 Analysis of natural gas fuel prices

In our case study, the natural gas fuel price plays an important role for the estimation of the LDES boundary costs. We obtained this fuel price information from the AEO 2023 study [54], as previously mentioned. In the AEO data, we selected the values from the Reference case scenario, which assumes no new laws or policies are introduced throughout the projected period, i.e., it is based on current laws and regulations as of November 2022 [59]. Nonetheless, while these are valid assumptions, it is totally possible that the natural gas fuel prices will not follow exactly the projections provided by the Reference case. Therefore, we present here a sensitivity analysis around the reference value of the natural gas fuel price (3.98 US$/MMBtu, considering the dollar of 2022) provided by the AEO, exploring alternative projections based on different potential futures. Our sensitivity analysis in based on 5 %, 10 %, and 15 % more expensive or cheaper natural gas fuel prices in 2050 compared to the Reference case. The results can be seen in Fig. 23.

We observe some trends in this fuel price sensitivity such as, in general, an increase in LDES boundary costs and a decrease in the minimum needed 100-hour

LDES power capacity as gas fuel prices rise. For example, when gas prices are 5 % higher than the reference, the maximum boundary cost (associated with 16 GW of 100-hour LDES power capacity in this case) has a 10.98 % increase, with the value being US$ 568.83 kW^{-1}. Moreover, at least 8.0 GW (compared to the 8.7 GW computed for reference) of 100-hour LDES power capacity will be required to replace gas power plants while keeping overall system costs within the same limits as the *baseline model*. For this minimum quantity and the 5 % increased gas prices, the boundary cost is US$ 15.98 kW^{-1}.

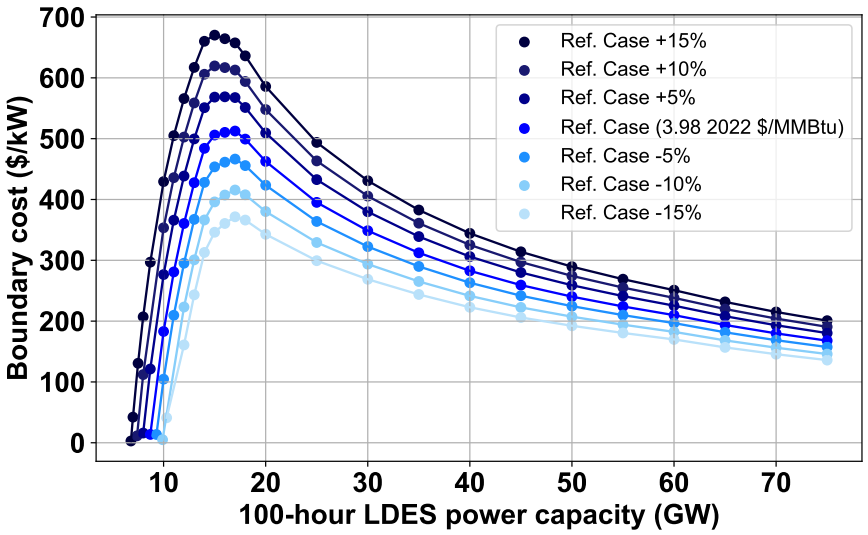

Figure 23 – Additional six curves of the boundary costs of LDES below which these technologies will be economically viable for the California's system in 2050 given gas price fluctuations around the reference value.

In addition, it is worth mentioning the asymmetrical impact of increases and decreases of gas fuel prices on LDES boundary costs. For example, on the one hand, a gas price 10 % higher results in an average (across the considered LDES power capacities) boundary cost increase of 19.4 % compared to the reference case. On the other hand, a 10 % decrease in gas price leads to an average boundary cost 17.22 % lower.

In conclusion, the boundary cost of LDES is sensitive to changes in natural gas fuel prices, with higher prices generally making LDES more economically attractive by raising the cost of conventional generation. As gas prices increase, the

system can rely on smaller amounts of LDES capacity to achieve cost parity with the *baseline model*, while still allowing for higher boundary costs. Conversely, lower gas prices reduce the competitiveness of LDES and require larger deployments to maintain economic feasibility. This asymmetrical effect reinforces the importance of fuel price assumptions when evaluating storage investments and highlights the potential market advantage of LDES.

3.2.5.2 Analysis of gas prices and solar investment costs

In this sensitivity study, we combine variation in gas fuel prices with variation in solar investment costs to analyze both of their impacts together on our estimated LDES boundary costs. As depicted in Fig. 9, solar generators play a major role in the investment plans for different LDES power capacities under consideration while retiring gas units. Therefore, solar investment costs also have a substantial impact on our estimated boundary costs. We obtained solar investment costs from the ATB 2022 [53], where we selected the Moderate scenario. This ATB 2022 scenario assumes that research and development investments will continue at similar levels as today, with current industry technology road maps being achieved and no substantial innovations or new technologies being introduced to the market.

The results of this sensitivity analysis are depicted in Fig. 24. For this analysis, we considered the 100-hour LDES power capacity of 17 GW. Indeed, as can be seen, the LDES boundary costs are significantly influenced by changes in the combination of fluctuation in gas prices and solar investment costs. Essentially, the boundary costs increase when the solar investment cost decreases and the gas fuel price rises. This insight underscores the critical interplay between fuel prices and investment costs in shaping economic outcomes in energy systems, especially when phasing out polluting technologies while integrating renewables with the help of emerging technologies, such as LDES.

3.2.5.3 Analysis of LDES duration impacts

The duration of the LDES is also an important factor to evaluate its boundary cost for economic viability. We have chosen the duration of 100 hours in our case study based on the real LDES system of an iron-air storage [45]. Here, we

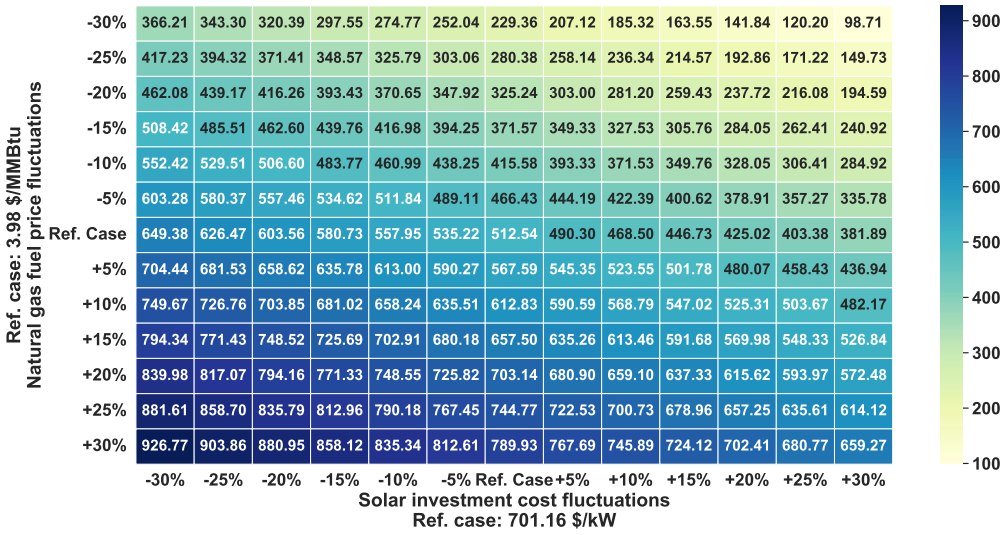

Figure 24 – Heat map of various boundary costs of LDES (for 17 GW 100-hour LDES power capacity) considering price fluctuations in natural gas fuel price and solar investment costs compared to their respective reference values.

also analyze the LDES boundary costs for 40-hour and 160-hour durations, which fall under the previously described category of seasonal shifting according to the US-DOE [33]. The results of this analysis can be seen in Fig. 25.

Essentially, we can observe that as the duration increases, the boundary cost curve shifts upwards. For example, a 40-hour LDES has an energy capacity of 600.0 GWh, a power output of 15.0 GW, and a boundary cost of US$ 365.50 kW^{-1}. Moving to the 100-hour LDES, the energy capacity increases to 1500.0 GWh with the same power output, and the boundary cost goes up to US$ 505.93 kW^{-1}. Furthermore, the 160-hour LDES corresponds to an energy capacity of 2400.0 GWh, keeping the 15.0 GW power output. Accordingly, the boundary cost reaches US$ 610.60 kW^{-1}.

These results reveal that increasing the storage duration can enhance the economic viability of LDES. A higher energy capacity allows the system to achieve greater operational savings, which translates into a higher opportunity value and, consequently, a higher boundary cost threshold. In other words, longer duration contributes more significantly to system cost reduction, which justifies a higher acceptable cost for deployment. On the other hand, if the market is able to offer

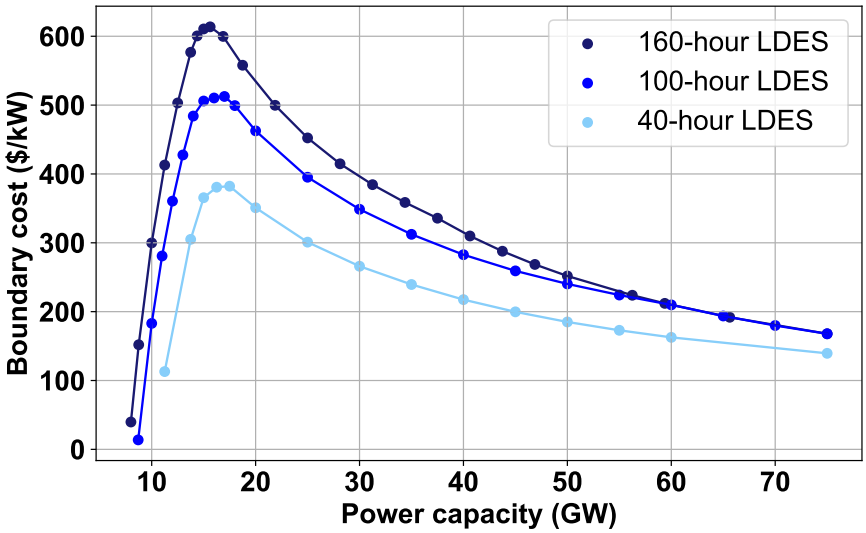

Figure 25 – The boundary costs of LDES below which these technologies will be economically viable for the California's system in 2050 for three different LDES duration: (a) 40-hour LDES; (b) 100-hour LDES; (c) 160-hour LDES.

LDES technologies with shorter durations, such as 40-hour LDES, at costs below US$ 365.50, these options could still meet system needs and provide competitive alternatives for replacing gas generation.

3.3 Case Study – United States

This section expands the scope of the analysis to the entire United States, applying the same modeling framework to all 48 contiguous states. Unlike the study focused on California, which emphasized the operational feasibility and economic competitiveness of LDES in replacing gas fired generation, the objective here is to investigate systemic factors that drive the variation in the resulting LDES boundary cost across different states.

By analyzing a broad set of power systems with distinct renewable resource profiles, demand patterns, and existing generation infrastructure, this case study aims to identify the main drivers that influence whether a state tends to exhibit a higher or lower LDES boundary cost. The results provide insights into how renewable availability, seasonal mismatches, and system flexibility shape the economic

value and viability of LDES in different regional contexts.

To support the interpretation of the results presented in the following sections, we define a set of system level indicators that help characterize the operational context of each state. The metrics are defined as follows:

- **Thermal generation share (% of annual demand):**

$$\text{Thermal gen. share (\%)} = \frac{\text{Total annual thermal gen. (MWh)}}{\text{Total annual demand (MWh)}} \times 100 \tag{3.7}$$

- **Thermal cap.utilization (%):**

$$\begin{aligned}\text{Total annual thermal dispatch (MWh)} = \text{Total annual thermal gen. (MWh)} \\ +\text{Total annual thermal res. (MWh)}\end{aligned} \tag{3.8}$$

$$\text{Total annual thermal cap. (MWh)} = \sum_{g \in \text{THE}} \sum_{t=1}^{8760} \left(\text{Capacity}_g\right) \tag{3.9}$$

$$\text{Thermal cap. util. (\%)} = \frac{\text{Total annual thermal dispatch (MWh)}}{\text{Total annual thermal capacity (MWh)}} \times 100 \tag{3.10}$$

- **CF of RES in *baseline model* (%):**

$$\text{Total annual RES availability (MWh)} = \sum_{g \in \text{RES}} \sum_{t=1}^{8760} \left(\text{Capacity}_g \times \text{CF}_{g,t}\right) \tag{3.11}$$

$$\text{CF RES baseline (\%)} = \frac{\text{Total annual RES availability (MWh)}}{\text{Total annual RES capacity (MWh)}} \times 100 \tag{3.12}$$

- **Thermal FO&M cost share (% of total annual system cost):**

$$\begin{aligned}\text{Total annual thermal FO\&M cost (\$)} = \text{Total annual coal FO\&M cost (\$)} \\ +\text{Total annual gas FO\&M cost (\$)}\end{aligned} \tag{3.13}$$

$$\text{Thermal FO\&M cost share (\%)} = \frac{\text{Total annual thermal FO\&M cost (\$)}}{\text{Total annual system cost (\$)}} \times 100 \tag{3.14}$$

- **Solar generation in *baseline model* (% of total RES generation):**

$$\begin{aligned}\text{Total annual RES gen. (MWh)} = &\ \text{Total annual solar gen. (MWh)} \\ &+ \text{Total annual wind-ons gen. (MWh)} \\ &+ \text{Total annual wind-ofs gen. (MWh)} \quad (3.15)\end{aligned}$$

$$\text{Solar gen. baseline (\%)} = \frac{\text{Total annual solar gen. (MWh)}}{\text{Total annual RES gen. (MWh)}} \times 100 \quad (3.16)$$

- **Wind generation in *baseline model* (% of total RES generation):**

$$\begin{aligned}\text{Total annual wind gen. (MWh)} = &\ \text{Total annual wind-ons gen. (MWh)} \\ &+ \text{Total annual wind-ofs gen. (MWh)} \quad (3.17)\end{aligned}$$

$$\text{Wind gen. baseline (\%)} = \frac{\text{Total annual wind gen. (MWh)}}{\text{Total annual RES gen. (MWh)}} \times 100 \quad (3.18)$$

- **Alpha (relative LDES deployment level at boundary cost maximum):**

$$\alpha = \frac{\text{LDES power capacity at maximum boundary cost (GW)}}{\text{Thermal power capacity (GW)}} \quad (3.19)$$

3.3.1 National overview of boundary costs across the states

In this subsection, we estimate the maximum LDES boundary cost for each state of the contiguous US, considering their 2050 energy matrices according to NREL's Cambium 2022 dataset [50], as also carried out for the first experiment in California. In the California case, gas was retired because it was the only thermal technology expected to remain in the 2050 generation mix. When extending the analysis to the entire contiguous US, some states still rely on coal in 2050, which motivates extending the boundary cost assessment to both gas and coal based thermal generation.

Therefore, the analysis considers the replacement of gas and coal generators with also a combination of RES alongside SDES and LDES resources and computing the maximum avoided costs (with respect to the total costs of the original system), which correspond to the maximum boundary cost values. Remembering that these configuration systems can be achieved by various power capacities of a 100-hour

LDES system, which are varied in this study from 0 to 150 GW with an RTE of 42.5 %.

The results of this study reveal substantial variation in the maximum boundary cost of a 100-hour LDES system across the contiguous US states. Fig. 26 (a) presents the maximum boundary cost in each state, and Fig. 26 (b) shows the distribution of these maximum boundary costs across states with positive values, highlighting substantial variation in economic potential for LDES deployment, ranging from -US$ 11.81 kW^{-1} to US$ 5993.94 kW^{-1}. While some states, such as Virginia (VA) and Nebraska (NE), achieve particularly high boundary cost values, others exhibit low or even negative values, indicating more limited opportunities for cost effective integration of long-duration storage. Notably, we identified that 79.07 % of the states with positive boundary costs (34 out of 43) have a boundary cost between 0 and US$ 500,00 kW^{-1}, suggesting that although extreme values exist, the economic viability of LDES tends to concentrate within a moderate cost range for most states.

Fig. 26 (c) complements the analysis by showing the distribution of LDES power capacities that maximize the boundary cost (only states com positive value). Each cost value in the map and histogram corresponds to a specific optimal power capacity, reinforcing that both the economic value and required scale of LDES vary significantly across the country. In 46.51 % of the states with positive boundary costs (20 out of 43), the optimal power capacity is 10 GW or less, indicating that in nearly half of the states, the maximum economic contribution of LDES can be achieved with more moderate power capacities.

In states where the boundary cost is negative, such as AL, NJ, OH, CT, and DE, which together represent 10.42 % of all states, the system cost in the *opportunity value maximization model* exceeds that of the *baseline model*, meaning that total system costs increase when thermal generation is replaced by intermittent plants. To equalize costs between the two systems, an injection of capital is needed, which is why these values appear as negative. In essence, this value is derived from the additional costs over the *baseline model* cost, divided by the necessary power capacity, representing the minimum required subsidy per kW.

Our studies reveal that the structural characteristics of the generation

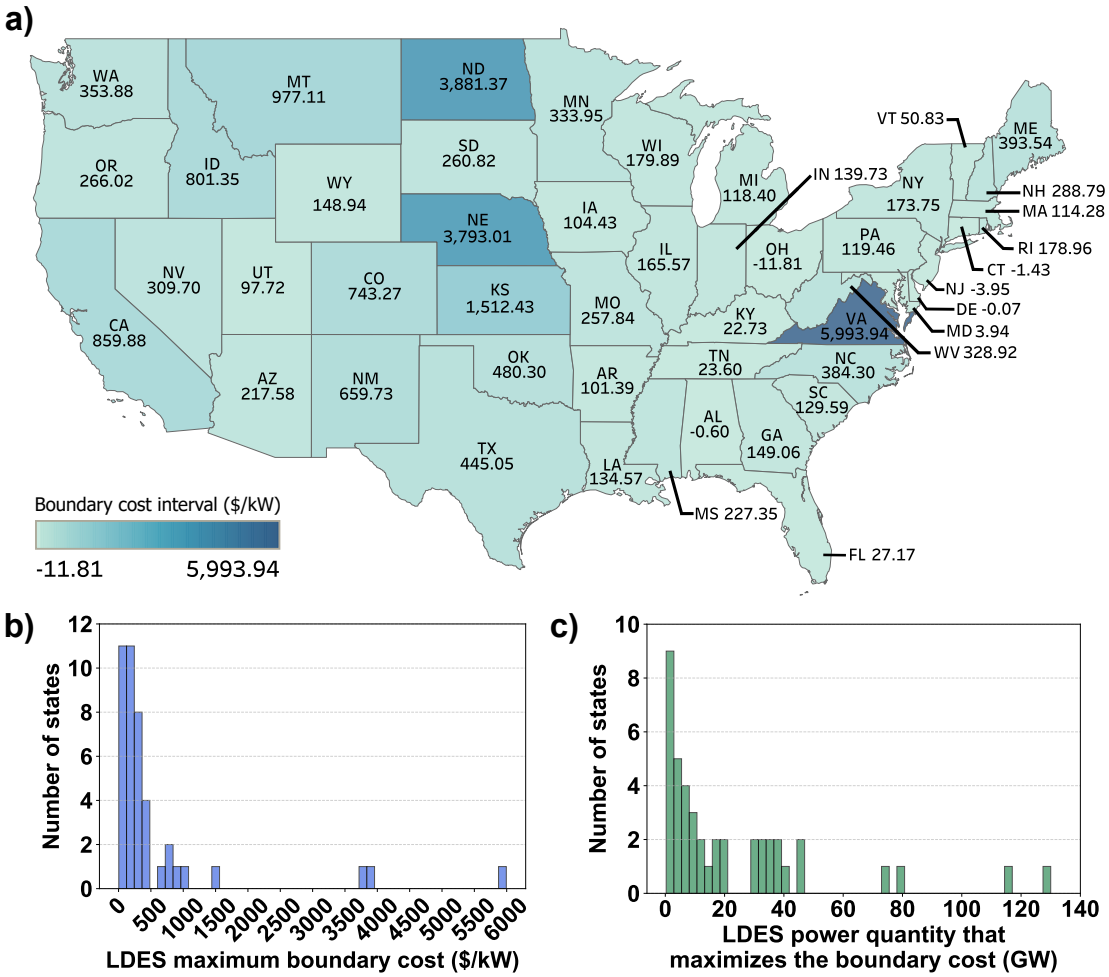

Figure 26 – LDES maximum boundary cost and power capacity distribution across US states in 2050. (a) Maximum boundary cost of 100-hour LDES ($/kW) for each US state, considering the power capacity that maximizes the boundary cost. (b) Histogram of the LDES maximum boundary cost ($/kW) across states with positive values. (c) Histogram of the LDES power capacity (GW) that maximizes the boundary cost in states with positive values.

portfolios in these regions (negative boundary cost) reduce the benefits of retiring thermal power plants, which limits the opportunity value of LDES. The outcomes show that specifically, 4 of these states have an average hourly CF for RES units below 25 % and also 4 of them have solar capacity exceeding 95 % of their intermittent portfolio (solar and wind), which limits the flexibility of charging and discharging cycles. In addition, all of them rely on thermal generation to supply

more than 30.00 % of their annual demand, and 4 of them incur in thermal-related FO&M costs that represent less than 10.00 % of overall costs, indicating dependence on low cost firm generators.

This discussion exemplifies how each state's structural conditions shape the economic value of LDES, highlighting the sensitivity of boundary cost levels to system characteristics. Other drivers behind the variation across states will be discussed later. However, in this context, it is useful to compare our findings with national cost benchmarks. The US-DOE, which is the United States Department of Energy responsible for energy policy, has set a 2030 cost target of US$ 1100 kW^{-1} for multi-day LDES (36–160 hours) in its Pathways to Commercial Liftoff report [33]. Surprisingly, according to our results, 100-hour LDES systems would be economically viable for thermal replacement in only 4 states (KS, ND, NE, and VA) under this cost target. If the US-DOE target falls to US$ 500 kW^{-1} by 2050, 9 states would surpass this threshold, including CA, CO, ID, KS, ND, NE, NM, MT, and VA. A further reduction to US$ 300 kW^{-1} would result in 17 states exceeding this value, expanding the list to include ME, MN, NC, NV, OK, TX, WA, and WV.

3.3.2 LDES capacity required for thermal replacement

At a national scale, our analysis reveals a substantial gap between projected LDES needs and the minimum LDES capacities that would be required to retire thermal generators in the United States while maintaining the same overall system costs. While the Pathways to Commercial Liftoff report [33] suggests that the US grid may need between 225 and 460 GW of LDES capacity in 2050, including multi-day/week LDES (36–160 hours) as well as inter-day storage (10–36 hours), our results estimate that the minimum required 100-hour LDES capacity is approximately 646.09 GW (64.61 TWh) for the 43 states where maximum boundary costs are positive. More specifically, 39.53 % of these 43 states would need more than 10 GW, while only 16.28 % would require less than 1 GW. Considering the 100-hour LDES power capacities that maximize the boundary costs, these numbers increase significantly to 1009.30 GW (100.93 TWh) for these 43 states. In this case, 53.49 % of these states are associated with more than 10 GW, 4.65 % exceeding

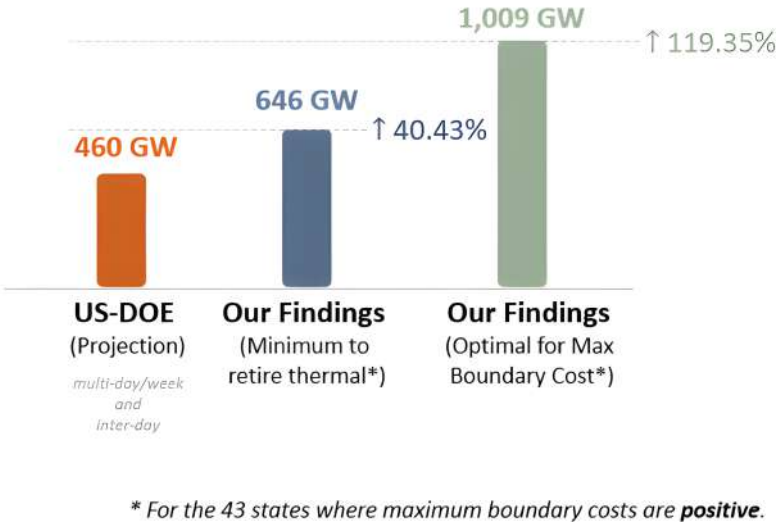

Figure 27 – Comparison between the national LDES capacity projected by the US-DOE and the 100-hour LDES capacity required for thermal replacement according to the findings of this thesis.

100 GW, and only 9.30 % requiring less than 1 GW. A visual comparison between the US-DOE capacity projection and the national 100-hour LDES needs identified in our findings for these 43 states is illustrated in Fig. 27.

Essentially, for each considered LDES power capacity, there is an associated amount of total avoided costs that long-duration systems can achieve while supporting thermal replacement. These total avoided costs, when divided by the LDES power capacity, result in the reported boundary costs, below which LDES would be viable. Examples of boundary cost curves are presented in Fig. 28. The corresponding figures for all US states are provided in the supplementary material, Annex A. The interpretation of this curve behavior was already discussed in the first case study, focused on California, but in summary, illustrated for four additional states as examples, initially, for each kW of LDES capacity, there is an increasing rate of cost reduction, i.e, higher total avoided costs, which explains growing boundary costs at first until a maximum value. As the rate of cost reduction decreases, the boundary costs follow the same pattern.

To better illustrate how LDES contributes to the US energy matrix under thermal replacement, Fig. 29 shows the total US system capacity and cost by

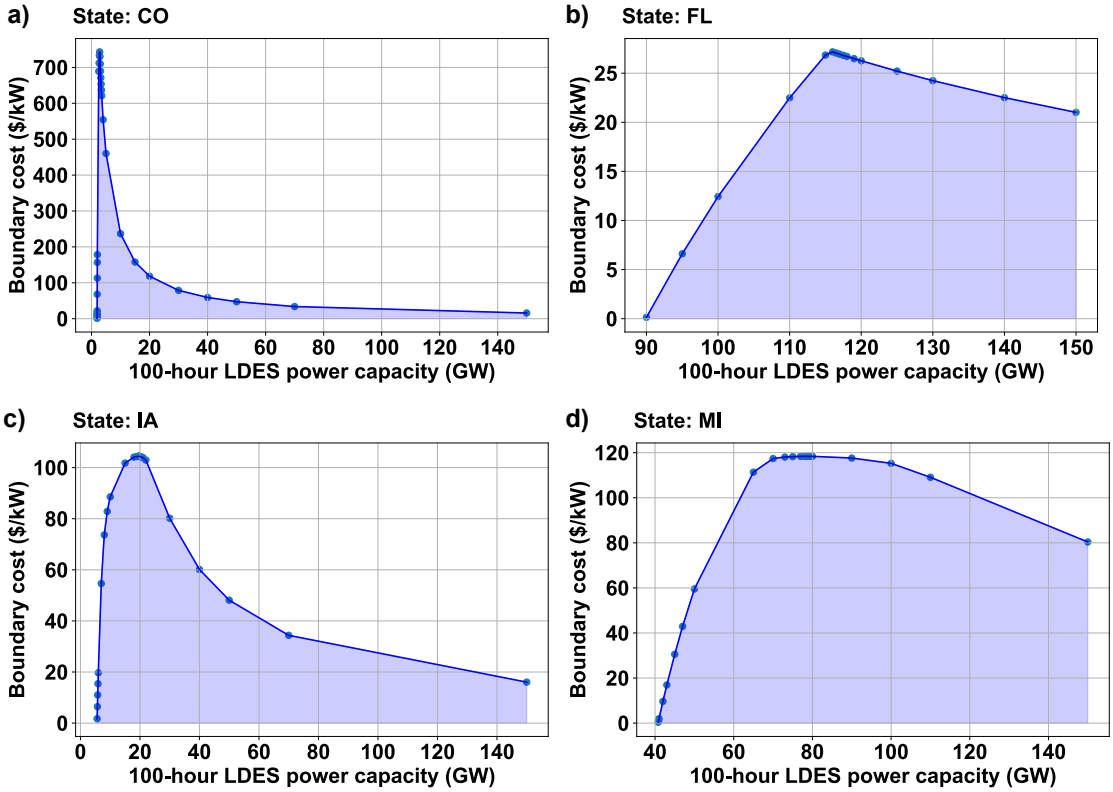

Figure 28 – The boundary costs of LDES below which these technologies will be economically viable for the system in 2050, for: (a) Colorado, (b) Florida, (c) Iowa, and (d) Michigan.

technology in 2050, based on data from the 43 states where the boundary costs are positive. The first bar in each graph represents the *baseline model*, where gas and coal power plants are still part of the system and no LDES is included. The second bar corresponds to the *opportunity value maximization model* with LDES, where gas and coal are replaced by a combination of LDES, SDES, and variable renewable sources, with the LDES capacity set to the amount that maximizes the boundary cost. The third bar shows the same thermal replacement but without LDES, relying only on SDES and RES.

As shown in Fig. 29 (a), the system capacity can be viewed from both its overall expansion (left panel) and its thermal replacement structure (right panel). For the LDES power capacities that maximize the boundary cost (second column), the results indicate a net increase of 1055.62 GW in total installed capacity, resulting

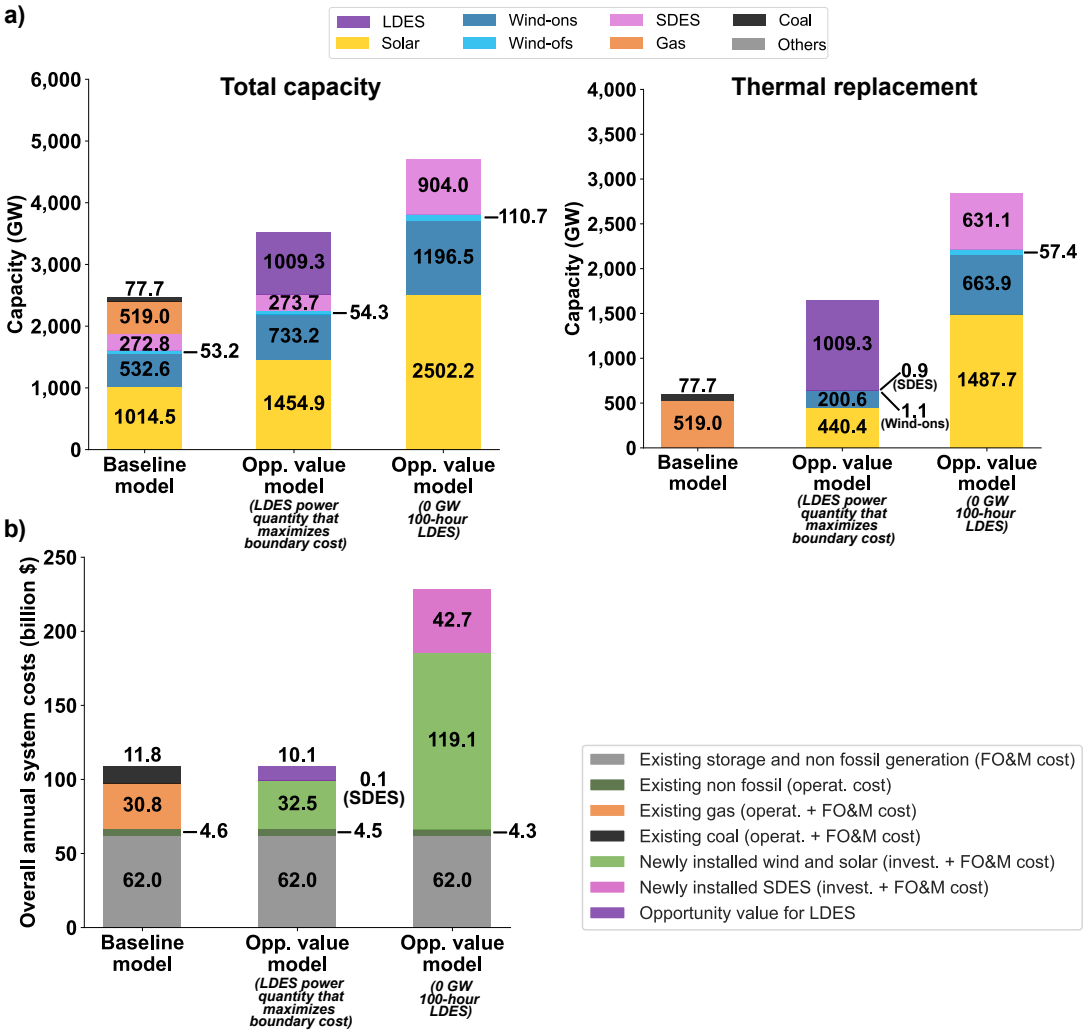

Figure 29 – (a) US total system capacity by technology in 2050 under the *baseline* and *opportunity value maximization models*, shown from two perspectives: total installed capacity (left) and thermal replacement effects (right), with and without LDES. (b) Same analysis for total system costs. Results are based on 43 states with positive boundary costs.

from the retirement of 596.69 GW of gas and coal and the addition of 1652.31 GW in new assets. This includes an expansion of 440.43 GW in solar, representing a 43.4 % increase relative to the baseline, 200.62 GW in wind-ons (37.7 % increase), 1.08 GW in wind-ofs (2.0 % increase), 0.89 GW in SDES (0.3 % increase), and 1009.30 GW in LDES, which in this case reflects a 0 % change relative to its

baseline. In contrast, when gas and coal are retired without the inclusion of LDES (third bar), the net increase in installed capacity jumps to 2243.48 GW, driven by a much higher need for renewable energy sources and SDES to compensate for the lack of firm capacity.

Regarding system costs, Fig. 29 (b) shows that, when LDES is included (second column), the total system cost amounts to approximately 109.21 billion dollars, the same as in the *baseline model*. This means that the opportunity value of LDES, meaning the maximum amount that can be paid for LDES while maintaining system costs equal to the *baseline*, reaches a total of 10.12 billion dollars. Conversely, when gas and coal are replaced without LDES (third column), the total system cost increases sharply to 228.12 billion dollars, representing a 108.88 % rise compared to either the *baseline* or the scenario with LDES. These results clearly demonstrate the strategic role of LDES in enabling the replacement of thermal generation with a balanced and cost-effective expansion of renewable and storage technologies.

3.3.3 Reasons for high and low boundary costs

In this study, we identified that different factors and their combinations influence LDES boundary costs, leading them to high or low values. Table 8 summarizes the main characteristics of the *baseline model* (where gas and coal generators are still present and LDES is not included) behind high and low values of LDES boundary costs in the *opportunity value maximization model*. Essentially, these main characteristics are thermal generation participation in annual load supply, percentage of thermal capacity utilization relative to the available capacity throughout the whole year, average hourly CF of RES in the *baseline model*, gas and coal-related FO&M costs as a percentage of the overall system costs, and the predominant renewable generation source in the *baseline model* (either solar or wind). In addition, we include the parameter α, which we define as the ratio between the LDES capacity that maximizes the boundary cost and thermal capacity present in the *baseline model*.

Notably, all states in the top 10 boundary cost group present an α lower than 1, indicating that the required LDES power capacity to replace thermal

generation is smaller than the baseline installed thermal capacity. In contrast, all states in the bottom 10 boundary cost group exhibit α values greater than or equal to 1, suggesting a higher dependence on LDES power capacity relative to existing thermal capacity. Thermal generation characteristics play a central role in explaining these differences. Among the top 10 boundary cost states, 9 states have thermal generation participation in load supply lower than 10 %, while in the bottom 10 group, 9 of the states show thermal participation higher than 20 %. A similar pattern is observed for thermal capacity utilization, as 70 % of the top 10 boundary cost states present thermal capacity utilization below 20 %, whereas 80 % of the bottom 10 states exhibit utilization levels above this threshold. These results indicate that states with lower reliance and utilization of thermal generation tend to face higher boundary costs.

Renewable energy characteristics further reinforce this contrast, as 70 % of

Table 8 – Top 10 and bottom 10 boundary cost: insights from the *baseline model* run.

Top 10 boundary cost	**Bottom 10 boundary cost**
States: California, Colorado, Idaho, Kansas, Montana, North Dakota, Nebraska, New Mexico, Oklahoma, Virginia	States: Alabama, Connecticut, Delaware, Florida, Kentucky, Maryland, New Jersey, Ohio, Tennessee, Vermont
9 of the 10 states with the highest boundary cost have thermal generation participation lower than 10 %	9 of the 10 states with the lowest boundary cost have thermal generation participation higher than 20 %
7 of the 10 states with the highest boundary cost have thermal capacity utilization participation lower than 20 %	8 of the 10 states with the lowest boundary cost have thermal capacity utilization participation higher than 20 %
7 of the 10 states with the highest boundary cost have average hourly capacity factor (CF) of renewable energy sources (RES) in baseline higher than 25 %	8 of the 10 states with the lowest boundary cost have average hourly capacity factor (CF) of renewable energy sources (RES) in baseline lower than 25 %
6 of the 10 states with the highest boundary cost have thermal FO&M cost participation higher than 10 %	7 of the 10 states with the lowest boundary cost have thermal FO&M cost participation lower than 10 %
6 of the 10 states with the highest boundary cost have wind (ons/ofs) generation participation in baseline higher than 65 % (% RES)	8 of the 10 states with the lowest boundary cost have solar generation participation in baseline higher than 65 % (% RES)
All of the 10 states with the highest boundary cost have $\alpha < 1$	All of the 10 states with the lowest boundary cost have $\alpha >= 1$

the states with the highest boundary costs present average hourly capacity factors of renewable energy sources above 25 %, while 80 % of the states with the lowest boundary costs show values below this level. In addition, wind generation plays a particularly important role in high boundary cost states, with 60 % of these states exhibiting wind participation above 65 % of total renewable generation. Conversely, in the bottom 10 boundary cost group, 80 % of the states have solar generation participation above 65 % of renewable output. This result aligns with previous findings [60], indicating that wind-heavy systems are more reliable, which reduces the required LDES power capacity while increasing to higher boundary costs.

Along the same lines, thermal FO&M cost also differs across groups, with a higher participation in high boundary cost states and a lower participation in low boundary cost states, reinforcing the relevance of thermal fleet characteristics in shaping boundary cost outcomes. To further examine how these differences manifest across the key system indicators discussed in Table 8, not only among the top 10 and bottom 10 boundary cost states but also across all 48 US states, Fig. 30 provides a complementary perspective through box plots.

Fig. 30 sheds more light on the evaluation of the factors analyzed through thresholds in Table 8 by giving a sense of average and dispersion. Interestingly, even considering top and bottom 24 states in terms of boundary costs reaffirms the findings of Table 8. States with lower boundary costs typically exhibit higher thermal generation shares and higher thermal capacity utilization, often associated with lower thermal FO&M cost. Replacing this generation would require significant investments in renewable capacity at costs comparable to or exceeding those of existing gas and coal units, therefore leaving less room for investments in storage systems.

In addition, these states tend to present a higher solar share in their baseline renewable mix, which is associated with systematically lower hourly average RES capacity factors. As illustrated in Fig. 31, the cross state comparison suggests a systematic association between higher solar participation and lower hourly average RES capacity factors, in line with the stronger diurnal variability of solar resources when compared to wind. Lower average capacity factors require additional investments in intermittent capacity to replace thermal generation,

further limiting the viability of storage systems. Conversely, higher RES capacity factors, typically driven by wind dominated mixes, promote periods of excess generation and underutilized thermal plants with higher FO&M costs, which are associated with higher boundary costs.

3.3.4 Comparative analysis of representative state cases

While the previous subsection identified the main factors driving high and low LDES boundary costs across states, it did not examine how these factors

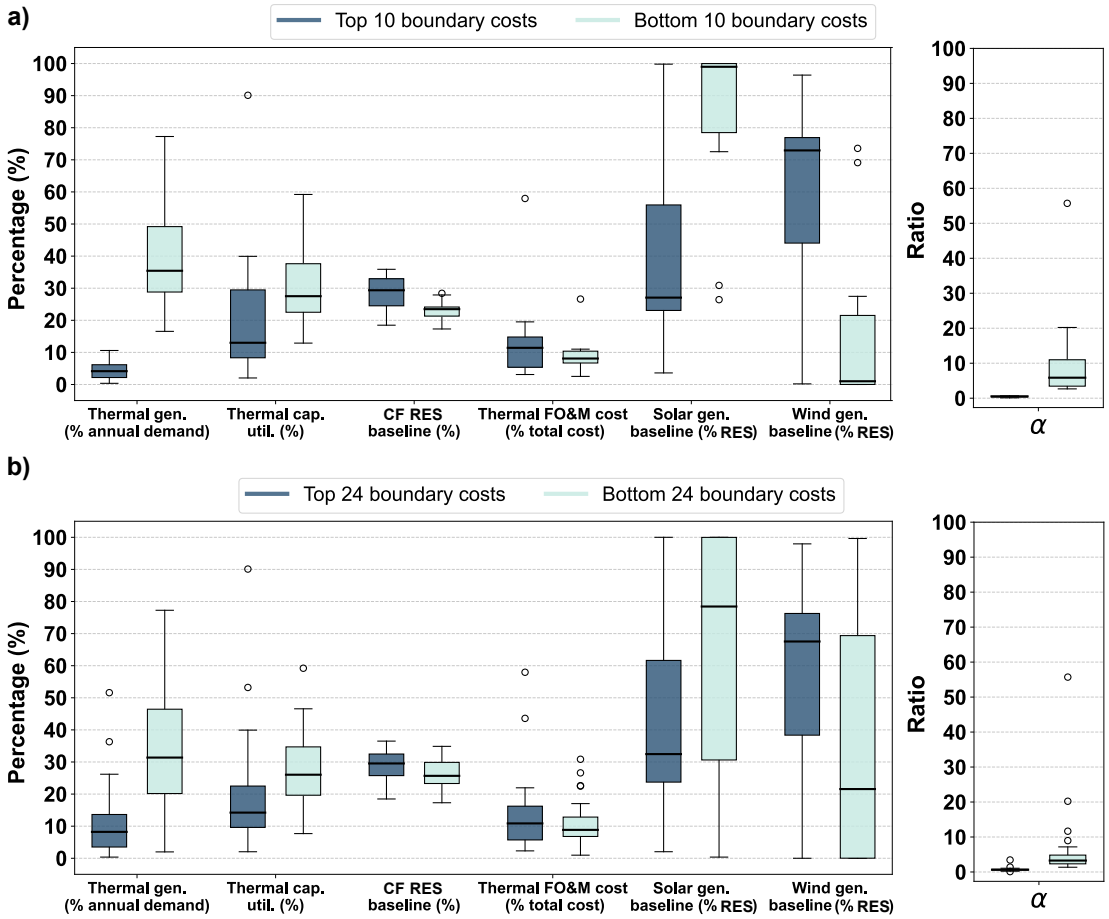

Figure 30 – Box plots comparing key system metrics for US states categorized by boundary costs. Figure (a) compares the top 10 and bottom 10 states in terms of boundary cost, and figure (b) extends to the top 24 and bottom 24, encompassing all states.

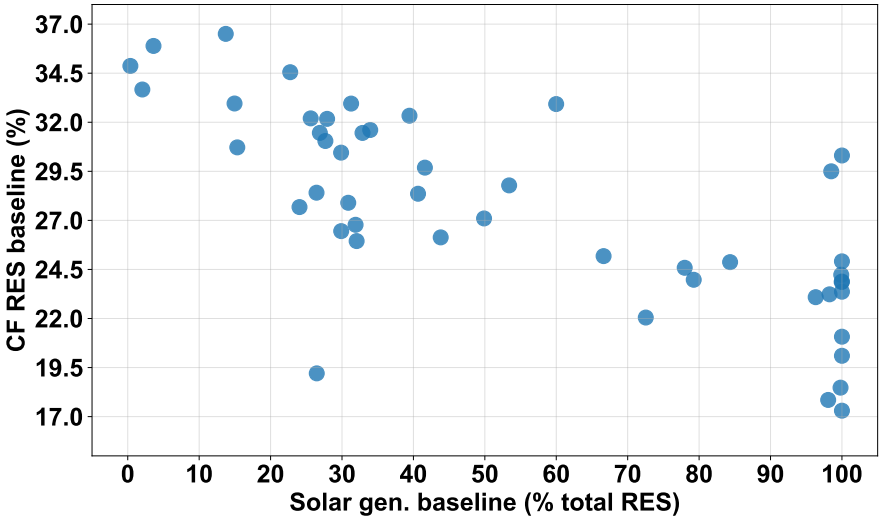

Figure 31 – Relationship between solar generation share and average RES capacity factor across US states.

combine within individual power systems. Therefore, this subsection presents a comparative analysis of selected representative state cases, chosen to illustrate distinct configurations that lead to high and low boundary costs. Rather than providing an exhaustive state-by-state discussion, the focus is on contrasting cases that highlight the interplay between renewable resource composition, thermal plant characteristics, and the resulting economic space for LDES deployment. To begin, Table 9 summarizes the key parameters for all 48 contiguous states, including the maximum LDES boundary cost, the power capacity that maximizes it, and the associated thermal, intermittent, and cost-related indicators, together with the corresponding α ratios.

Concrete first examples for analysis are the cases of Maryland (MD) and Nebraska (NE). MD exhibits a very low LDES boundary cost (US$ 3.94 kW^{-1}), while NE has one of the highest (US$ 3,793.01 kW^{-1}). MD has a substantial reliance on thermal generation, with 28.37 % of thermal generation participation and a thermal capacity utilization of 22.07 %. Additionally, MD's RES exhibits a low CF of 22.05 %, and its RES generation is mostly solar (72.53 %) in the *baseline model*. On the other hand, NE stands at the opposite end of the spectrum, characterized by a limited dependence on thermal generation, with only 3.69 % and

Table 9 – All values of key parameters for US states.

State	Maximum boundary cost ($/kW)	Power qty. (GW) for max boundary cost	Thermal gen. (% annual demand)	Thermal cap. util. (%)	CF RES baseline (%)	Thermal FO&M cost (% total cost)	Solar gen. baseline (% total RES)	Wind gen. baseline (% total RES)	α
OH	-11.81	150.00	50.56	59.21	23.09	6.65	96.32	3.68	4.55
NJ	-3.95	150.00	30.15	28.89	28.41	7.44	26.43	73.57	11.66
CT	-1.43	150.00	56.31	38.97	17.85	8.94	98.07	1.93	20.22
AL	-0.60	150.00	31.97	33.60	23.88	8.75	100.00	0.00	8.96
DE	-0.07	150.00	77.27	23.82	17.30	10.86	100.00	0.00	55.71
MD	3.94	36.40	28.37	22.07	22.05	11.01	72.53	27.47	3.73
KY	22.73	75.00	45.07	15.88	23.86	26.61	99.96	0.04	3.34
TN	23.60	39.80	16.55	26.15	24.23	2.52	99.90	0.10	3.22
FL	27.17	116.00	38.90	46.57	21.07	6.85	100.00	0.00	2.67
VT	50.83	7.10	20.51	12.90	27.90	5.14	30.87	69.13	7.17
UT	97.72	32.50	30.78	26.63	29.50	30.85	98.50	1.50	5.65
AR	101.39	30.20	13.89	7.69	23.36	22.49	100.00	0.00	2.41
IA	104.43	19.70	12.18	32.58	31.46	8.42	26.90	73.10	2.95
MA	114.28	29.90	36.49	39.13	30.45	9.93	29.87	70.13	4.52
MI	118.40	79.30	53.70	41.85	31.61	7.67	33.95	66.05	2.63
PA	119.46	130.00	53.89	38.02	26.45	11.46	29.89	70.11	3.31
SC	129.59	37.90	19.15	21.98	20.10	5.27	100.00	0.00	2.07
LA	134.57	36.40	42.65	19.01	24.87	16.97	84.34	15.66	1.63
IN	139.73	38.50	53.50	22.62	29.69	17.03	41.61	58.39	1.36
WY	148.94	13.20	3.01	13.78	34.87	10.43	0.37	99.63	3.96
GA	149.06	45.00	20.91	25.92	24.91	5.87	100.00	0.00	2.01
IL	165.57	6.00	1.99	19.86	32.95	0.97	31.28	68.72	1.47
NY	173.75	32.90	24.24	29.79	27.10	7.21	49.89	50.11	1.45
RI	178.96	10.30	41.19	18.38	32.17	22.62	27.91	72.09	3.01
WI	179.89	17.90	36.31	11.85	25.18	21.95	66.63	33.37	0.80
AZ	217.58	12.90	11.81	16.14	23.23	12.54	98.26	1.74	0.86
MS	227.35	18.60	26.18	23.17	28.78	15.61	53.40	46.60	1.39
MO	257.84	14.00	7.65	7.44	36.50	19.80	13.72	86.28	0.73
SD	260.82	0.70	0.59	14.18	33.67	2.31	2.04	97.96	0.65
OR	266.02	3.00	3.46	22.28	32.33	6.84	39.44	60.56	1.07
NH	288.79	4.40	21.64	14.22	32.20	7.08	25.62	74.38	0.98
NV	309.70	17.40	23.69	53.22	30.31	5.94	100.00	0.00	3.43
WV	328.92	10.00	51.60	4.92	26.77	43.59	31.90	68.10	0.69
MN	333.95	3.00	8.80	24.78	28.36	4.69	40.65	59.35	0.53
WA	353.88	8.00	1.14	4.99	30.72	10.38	15.34	84.66	0.64
NC	384.30	10.00	13.56	18.77	24.58	5.04	77.98	22.02	0.47
ME	393.54	1.30	10.16	13.84	31.46	18.12	32.87	67.13	0.78
TX	445.05	46.50	13.90	19.64	25.95	11.06	32.05	67.95	0.61
OK	480.30	5.40	3.52	14.23	32.96	12.19	14.95	85.05	0.52
NM	659.73	1.20	5.98	33.83	31.05	3.11	27.67	72.33	0.56
CO	743.27	2.80	1.72	10.27	34.55	14.17	22.75	77.25	0.52
ID	801.35	3.70	4.62	2.04	18.48	57.96	99.80	0.20	0.56
CA	859.88	7.70	6.23	16.40	32.93	6.95	59.99	40.01	0.28
MT	977.11	0.30	0.37	11.77	35.89	4.85	3.61	96.39	0.66
KS	1512.43	2.40	10.60	39.93	26.13	10.66	43.82	56.18	0.46
NE	3793.01	0.50	3.69	7.67	27.68	19.51	24.05	75.95	0.10
ND	3881.37	0.50	0.37	6.73	19.20	15.01	26.47	73.53	0.22
VA	5993.94	1.00	9.09	90.11	23.97	3.73	79.25	20.75	0.67

an extremely low thermal capacity utilization (7.67 %). Unlike MD, NE's energy mix is dominated by wind, accounting for 75.95 % of its total renewable generation in the *baseline model*, while solar plays a minor role, 24.05 %.

West Virginia (WV) represents an intriguing case. Despite its considerable thermal reliance, with thermal generation participation of 51.60 % and a high thermal FO&M cost of 43.59 % of total cost, WV still maintains a relatively high boundary cost of US$ 328.92 kW^{-1}. This outcome is allowed by a favorable renewable resources portfolio, consisting of 68.10 % wind generation in the *baseline model*, and a considerable RES CF of 26.77 %. Additionally, the low thermal capacity utilization of 4.92 % suggests overcapacity of thermal plants, potentially creating opportunities for LDES integration due to the high thermal-related fixed costs.

Comparing Colorado (CO) and California (CA) demonstrates how states with similarly high maximum boundary costs (743.27 kW^{-1} and US$ 859.88 kW^{-1}, respectively) can reach those values through distinct system configurations. Colorado has one of the highest average capacity factors (34.55 %) for renewable resources and can heavily rely on wind generation (around 77 % of its intermittent generation) in the *baseline model*. Additionally, Colorado incurs a thermal FO&M cost equivalent to 14.17 % of its overall costs, while its thermal generation share is only 1.72 % resulting in substantial avoided costs when underutilized thermal plants are retired. California also relies minimally on thermal generation, at only 6.23 % and exhibits a low thermal capacity utilization of 16.40 % while having thermal FO&M costs equivalent to 6.95 % of its overall costs. Unlike Colorado, California's intermittent generation mix is more balanced, having more solar (59.99 %) than wind (40.01 %). Nonetheless, California's high average hourly CF of 32.93 % for RES units allows for the retirement of the thermal generation capacity with a much lower LDES power capacity (α =0.28) and California's thermal-related FO&M costs (in dollars) are nearly three times higher than those of Colorado, which explains the state's higher maximum boundary cost.

Wyoming (WY) is another state that stands out as an exception to the typical pattern, but in this case in the bottom boundary cost states group. Unlike many states in this group, where solar is the predominant RES, WY relies almost

entirely on wind (99.63 %), coupled with an exceptionally high RES capacity factor of 34.87 %, the third highest among the 48 states, which leads us to expect a high boundary cost. However, the state is not dependent on thermal generation, which supplies only 3.01 % of its annual energy demand, while wind-ons units have a much higher participation, addressing 95.89 % of the annual load. As a result, there is little financial room to invest in LDES after retiring thermal plants, since the state is highly dependent on wind-ons. Additionally, similar to states in this group, WY's α ratio of 3.96 indicates that the state requires nearly 4 times more LDES capacity than its current thermal capacity. Since the boundary cost is defined as the savings in dollars per kW of required LDES capacity, this high requirement to maximize the boundary cost, totaling 13.2 GW, and the low-cost saving after thermal retirement, effectively pulls the boundary cost down.

Michigan (MI) and North Carolina (NC) are two states of comparable size in terms of annual demand, with 191799 GWh and 198269 GWh respectively, yet they display strikingly different boundary costs and energy mixes. Michigan has a boundary cost of US$ 118.40 kW^{-1} (bottom 24 boundary costs), driven by its substantial thermal dependence of 53.70 % and a high thermal capacity utilization of 41.85 %. Even though MI boasts a significant wind share of 66.05 % at a relatively high RES capacity factor of 31.61 %, its extraordinarily high reliance on thermal generation pulls its boundary cost down. In contrast, North Carolina reports a boundary cost of US$ 384.30 kW^{-1}, placing it among the higher boundary cost states. Its thermal capacity utilization is yet considerable, 18.77 %, and its thermal generation participation is 13.56 % of the annual demand. Nonetheless, these numbers are considerably lower than those of Michigan, allowing North Carolina to have a higher LDES boundary cost.

Kentucky (KY) and Florida (FL) both exhibit relatively low maximum boundary costs, at US$ 22.73 kW^{-1} and US$ 27.17 kW^{-1} respectively, though they arrive at these values through different system parameters. Kentucky stands out due to its notably higher thermal FO&M cost share of 26.61 %, along with a lower thermal capacity utilization of 15.88 %. However, due to the high solar participation (99.96 %) in its intermittent generation, Kentucky needs a substantially high 100-hour LDES power capacity (75 GW) to maximize its LDES boundary cost and

retire thermal plants. Florida, on the other hand, has a low maximum boundary cost due to its high thermal capacity utilization of 46.56 %.

Georgia (GA), in addition to a considerable reliance on thermal generation (with 20.91 % of the total demand and a thermal capacity utilization of 25.92 %), has low thermal FO&M cost, which represents just 5.87 %. This limits the potential economic benefits of retiring underutilized thermal plants, resulting in a relatively low boundary cost of US$ 149.06 kW^{-1}. Moreover, RES in Georgia is exclusively solar, comprising 100 % of the RES mix. Texas (TX) also exhibits a relative dependency on thermal generation, with thermal generation participation accounting for 13.90 % and a thermal capacity utilization of 19.64 %. However, Texas achieves a substantially higher LDES boundary cost of US$ 445.05 kW^{-1} due to two key factors. First, its thermal FO&M cost is higher at 11.06 % of the total cost, nearly double that of Georgia, resulting in greater potential savings when retiring underutilized thermal plants. Second, Texas relies heavily on wind energy, which comprises 67.95 % of the RES generation in the *baseline model*.

Alongside the provided comparative analysis, we prepared a dashboard available at [61] to provide detailed absolute values for key parameters, enhancing the understanding of each state's energy profile. The dashboard interface, highlighting its main features such as side-by-side comparison and downloadable data export, is illustrated in Fig. 32. For example, the α values in Georgia (2.01) and Texas (0.61) highlight differences in the efficiency of LDES compared to thermal plants. Despite this, both states require nearly the same installed capacity of LDES, with 45 GW in Georgia and 46.5 GW in Texas. The thermal costs also vary significantly, with Georgia incurring in US$ 1.95 billion, compared to US$ 4.41 billion in Texas, emphasizing the greater potential for cost savings in Texas through the retirement of underutilized thermal plants. These savings are evident not only in the FO&M costs but also in the variable costs associated with thermal generation, as shown in the dashboard, which presents total gas and coal capacity, average FO&M cost, and average fuel price. In Georgia, the average fuel price is 2.19 $/MMBtu for coal and 4.08 $/MMBtu for gas, while in Texas, it is 1.89 $/MMBtu for coal and 3.79 $/MMBtu for gas. Additionally, the average FO&M cost is 33863.46 $/MW for coal and 8413.28 $/MW for gas in Georgia, and 45552.40 $/MW for coal and

Figure 32 – Interactive dashboard interface developed for exploring state-level economic and operational results.

14099.95 $/MW for gas in Texas. The opportunity value cost quantifies the savings achieved with LDES integration, amounting to US$ 430.3 million in Georgia and US$ 1,327.5 million in Texas.

Finally, Fig. 33 presents one of the visualizations available in the dashboard, comparing the annual generation mix and reserve allocation for Georgia and Texas under both the *baseline* and *opportunity value* models. In Georgia, solar generation clearly dominates the energy mix in both models, while batteries play a central role in reserve provision. In Texas, wind generation is the primary energy source, with solar also contributing, whereas gas remains an important component of the reserve mix in the *baseline model*. This model also exhibits a higher total annual generation compared to the *baseline model*, as it accounts for energy discharged from storage systems that were predominantly charged using renewable energy sources. This distinction highlights the contribution of LDES to both energy supply and system adequacy following the retirement of firm thermal capacity.

3.3.5 Seasonal state of charge dynamics of LDES

The seasonal operation of LDES systems can be characterized by their state of charge (SoC) behavior, which reflects how energy is shifted across seasons in

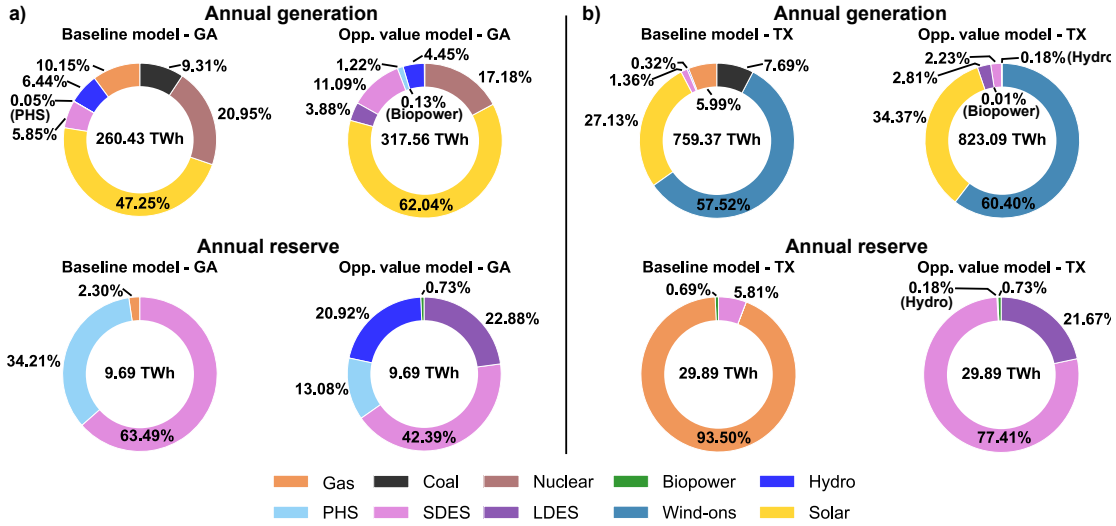

Figure 33 – Annual generation mix and reserve allocation for Georgia (a) and Texas (b) under the *baseline* and *opportunity value models*.

response to variations in renewable resource availability. The impact of LDES systems varies across states depending on the season, as depicted in Fig. 34 for spring and winter. The figure illustrates the seasonal relative differences in state of charge, computed as the SoC at the end of a season minus its initial SoC and normalized by the SoC capacity for each state, with more intense colors in spring indicating higher charging levels and lighter colors in winter reflecting greater discharging. Fig. 35 extends the seasonal analysis to summer and fall, complementing the spring and winter results and highlighting interseasonal state of charge variability across US states. Across the 48 states, 36 states exhibit their highest net charging during spring, while 6 in summer, 4 in fall, and 2 in winter. Conversely, the discharging is most pronounced in winter for 28 states, followed by summer for 12 states, fall for 5 states, and spring for 3 states.

In fact, 22 states charge more during spring and discharge more during winter. To contextualize this behavior, we compute the average relative availability of RES expressed as a percentage of total demand for each meteorological season, as shown in Fig. 36. For these 22 states, the median across states of the seasonal average relative availability of RES, expressed as a percentage of total demand, is 64.8 % in spring, 60.0 % in summer, 52.5 % in fall, and 46.0 % in winter. This

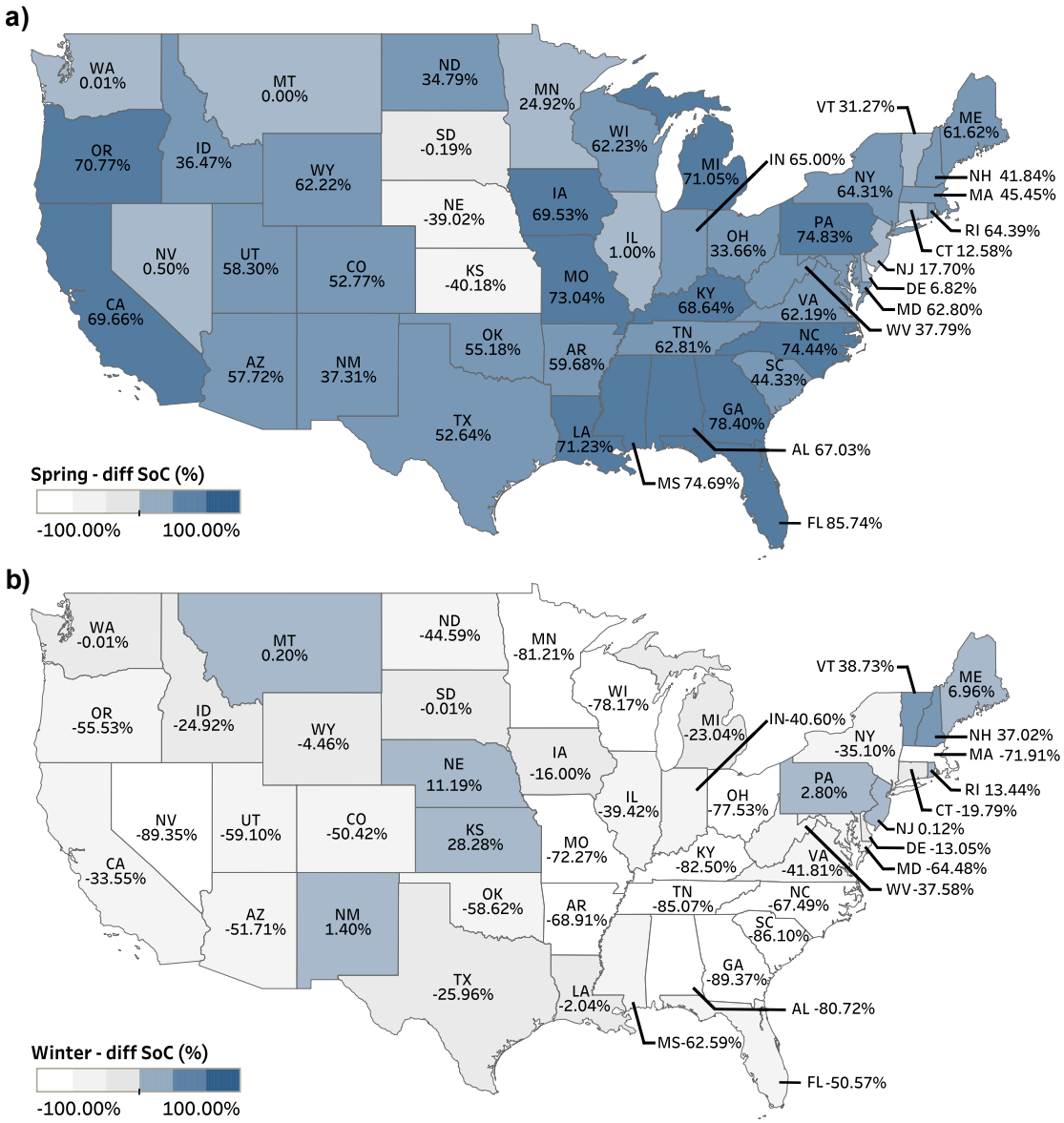

Figure 34 – Comparison of seasonal SoC differences: (a) Spring and (b) Winter.

progressive reduction from spring to winter is consistent with the observed SoC behavior and helps explain the tendency toward higher charging during spring and higher discharging during winter. Other states also exhibit seasonal variations, but maintain higher average relative availability levels, ranging from a median of 72.4 % in spring to 60.5 % in winter, and 58.7 % in fall, with a smaller seasonal contrast of approximately 13.7 %, compared to about 18.8 % for the 22 states.

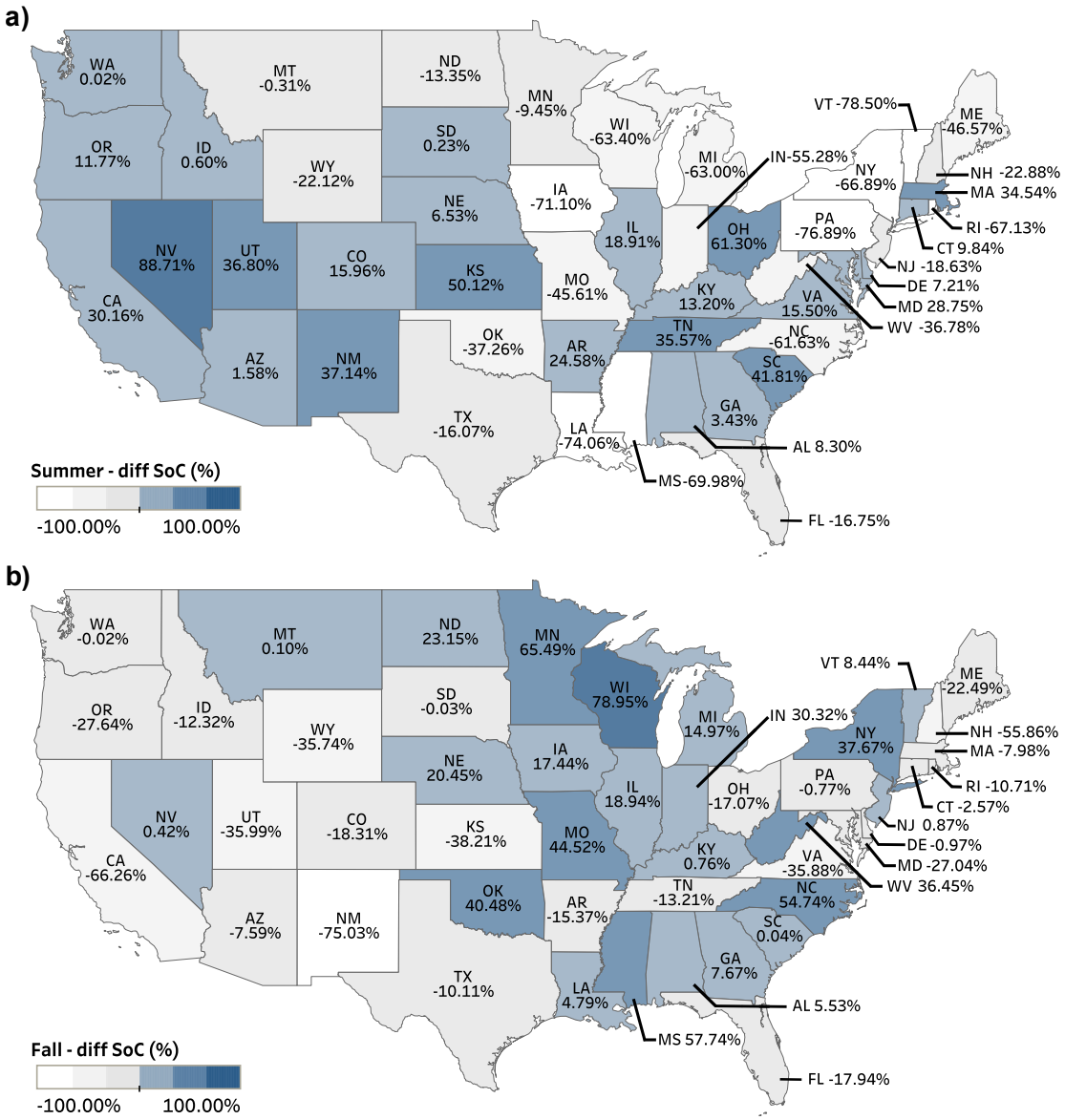

Figure 35 – Comparison of seasonal SoC differences: (a) Summer and (b) Fall.

This combination of higher availability levels and greater dispersion indicates a more heterogeneous interseasonal state of charge behavior.

To further illustrate the seasonal SoC patterns discussed above, two contrasting state level examples are presented. Figure 37 shows the annual state of charge profiles for Utah and Vermont (the remaining SoC profiles are illustrated in the supplementary material, Annex A), which represent distinct seasonal operational

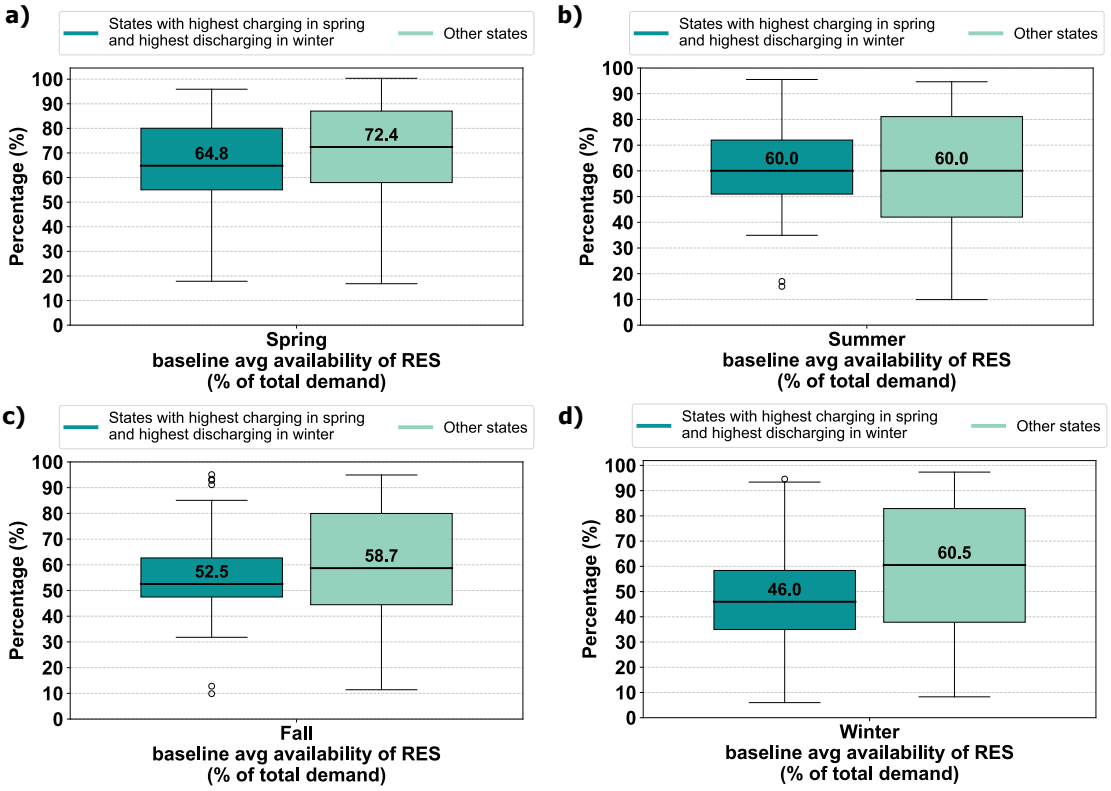

Figure 36 – Average relative availability of RES (in % of total demand) among the 48 states for each meteorological season.

responses of LDES systems under different renewable resource compositions. Utah belongs to the aforementioned group of 22 states and exhibits a seasonal SoC pattern characterized by higher charging during spring and increased discharging during winter. This behavior is consistent with the higher relative availability of renewable generation observed in spring and its reduction during winter, particularly in systems with a predominant contribution from solar resources. In contrast, Vermont, whose renewable generation mix is predominantly wind-based, displays a different seasonal behavior, with comparatively higher charging levels during winter, and more pronounced discharging during summer. This behavior can be associated with increased wind availability during winter in parts of the Northeastern United States and comparatively lower availability during summer [62]. This contrast highlights how regional differences in renewable resource composition and availability can lead to distinct interseasonal SoC profiles.

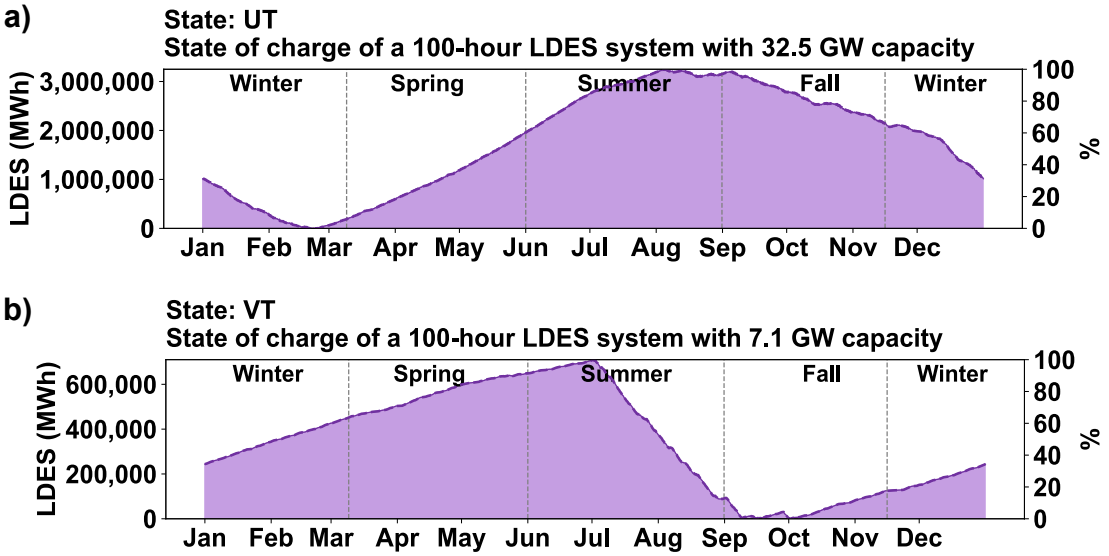

Figure 37 – Different LDES SOC patterns. (a) LDES SoC in Utah throughout the year. (b) LDES SoC throughout the year in Vermont.

3.3.6 Analysis of LDES round-trip efficiency impacts on states with negative boundary costs

As demonstrated in Section 3.3.1, a specific subset of states (AL, NJ, OH, CT, and DE) exhibited negative boundary costs for the 100-hour LDES under the baseline assumption of 42.5% round-trip efficiency. However, as summarized in the literature review, in the Table 1, emerging LDES technologies encompass a wide variety of systems with projected RTEs varying significantly from 20% to 90%. To investigate whether technological advancements in storage efficiency can overcome the economic barriers in these challenging regions, a sensitivity analysis was conducted by incrementally increasing the RTE of the candidate 100-hour LDES to 50%, 60%, and 70%.

The primary objective of this sensitivity assessment is to determine if higher efficiencies can reduce the required renewable capacity expansion and minimize operational energy losses sufficiently to shift the boundary costs into positive territory. Because different LDES power capacities were tested for each state, the analysis focuses on the specific power quantity that yields the maximum boundary cost. The impacts of these varying RTE levels are summarized in Table 10.

Table 10 – Maximum boundary costs ($/kW) and their corresponding optimal LDES power capacities (GW) under different round-trip efficiencies.

State	**42.5% RTE (Ref.)**	**50% RTE**	**60% RTE**	**70% RTE**
Alabama (AL)	-0.60 (150 GW)	15.47 (141 GW)	38.15 (147 GW)	54.03 (150 GW)
Connecticut (CT)	-1.43 (150 GW)	-0.94 (150 GW)	12.19 (45 GW)	37.82 (46 GW)
Delaware (DE)	-0.07 (150 GW)	43.17 (28 GW)	43.17 (28 GW)	43.17 (28 GW)
New Jersey (NJ)	-3.95 (150 GW)	-6.16 (150 GW)	-4.32 (150 GW)	-2.52 (150 GW)
Ohio (OH)	-11.81 (150 GW)	-17.15 (150 GW)	-10.80 (150 GW)	-6.05 (150 GW)

The results demonstrate that increasing the efficiency is sufficient to achieve positive boundary costs for Alabama, Connecticut, and Delaware. The boundary cost curves for the scenarios that achieved economic viability across different RTEs are illustrated in Figure 38. As detailed in Table 10, while Delaware and Alabama become viable at 50% RTE, Connecticut requires a higher efficiency of 60% to reach a positive value.

Conversely, New Jersey and Ohio still present negative boundary costs even at the highest tested efficiency of 70%. This indicates that their economic barriers go beyond storage efficiency limitations. Based on their system indicators, both states rely heavily on thermal generation (50.56% for OH and 30.15% for NJ) with high capacity utilization. Additionally, their thermal FO&M costs represent a relatively low share of the total system cost (6.65% for OH and 7.44% for NJ). Therefore, retiring these cheap and heavily utilized thermal plants requires massive investments in renewable expansion that cannot be financially offset simply by improving LDES efficiency. Ultimately, these findings conclude the state-wise assessments of this study, emphasizing that while technological advancements in storage are crucial, the economic viability of LDES remains fundamentally tied to the unique structural characteristics of each regional grid.

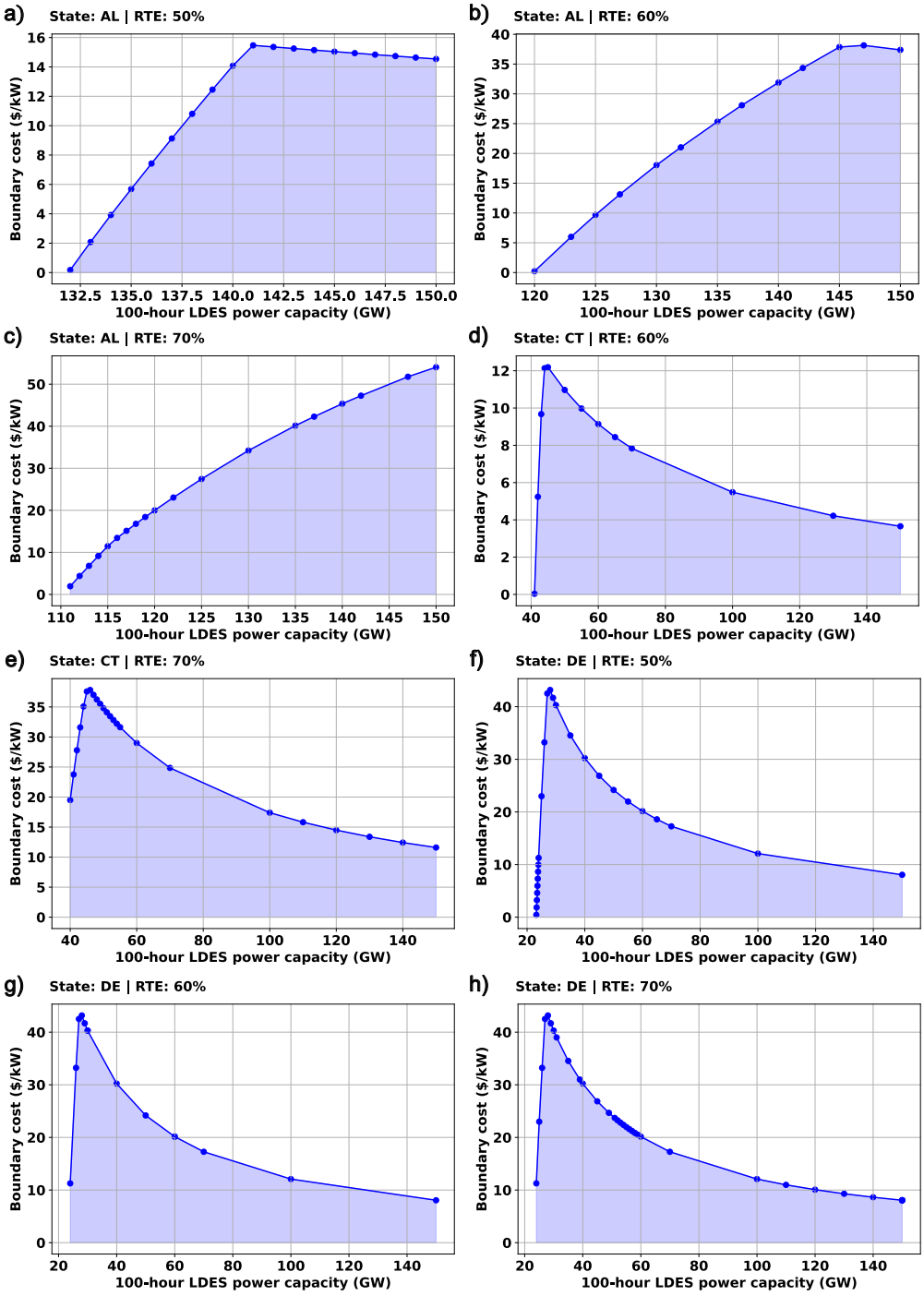

Figure 38 – Boundary cost curves for states that achieved positive values under varying LDES round-trip efficiencies.

4 Conclusion and future work

In this research, we proposed a novel valuation methodology to compute the boundary technology cost of LDES systems, defined as the cost below which these technologies become economically viable in the future. Unlike conventional planning approaches, which are based on assumptions about the value of investment costs, the proposed framework determines the maximum economically viable cost of an emerging and still immature technology by explicitly linking investment decisions to system wide operational benefits. This characteristic is particularly relevant in the context of new technologies, for which cost trajectories are uncertain, and market references are limited.

The methodology consists of a *baseline model* and an *opportunity value maximization model*, which are solved sequentially to quantify the maximum reduction in overall system costs enabled by a given quantity of LDES in terms of energy and power capacity. The proposed approach is general and can be readily extended to other system configurations, decarbonization levels, regions, and emerging technologies whose economic value is primarily driven by system level interactions.

The methodology was first applied to the California power system as an initial and detailed case study, allowing for a comprehensive economic and operational assessment of LDES in a highly renewable and policy driven context. The results demonstrated that full decarbonization in California in 2050 can be cost-effectively achieved if at least 8.7 GW power capacity of a 100-hour LDES is present. At this quantity, if the investment cost of LDES is US$ 13.74 kW^{-1}, the overall annual system costs of the fully decarbonized system will be the same as the reference system, which still relies on gas units to provide firm generation.

Furthermore, we observed that the boundary cost of LDES raises when the power capacity ranges from 8.7 GW to 17 GW. This increase is due to the higher rate of reduction in system costs per additional kW of LDES power capacity within this interval. The quantity with the highest cost to 100-hour LDES systems supports California's power system decarbonization goals and it is in economically viable is around 17 GW which can allow the investment cost to be the maximum US$

512.54 kW^{-1}. Once the LDES power capacity is greater than 17 GW, the rate of reduction declines and the boundary cost of LDES follows the same pattern. These results highlight not only the economic relevance of LDES for deep decarbonization in California, but also the importance of identifying deployment ranges in which storage delivers the greatest system value.

After validating the methodology through the California case study, it was applied to the 48 contiguous United States, enabling a systematic comparison of LDES boundary costs across diverse power system structures. The national level analysis revealed substantial heterogeneity in the economic value of LDES, with boundary cost levels varying widely across states. This variability reflects structural differences in power system configurations, particularly the composition of the generation mix and the characteristics of the existing thermal fleet. States with higher LDES viability tend to exhibit lower shares of thermal generation, greater wind penetration, and higher fixed costs associated with existing thermal assets. Together, these findings highlight the central role of thermal generation characteristics in shaping the economic value of LDES and reinforce the limitations of uniform cost targets when assessing emerging storage technologies.

When compared against national cost benchmarks, the results indicate that the economic viability of 100 h LDES for thermal replacement remains limited under current cost targets. At the US DOE 2030 target of US$ 1100 kW^{-1} for multi day LDES, only 4 states exhibit boundary costs above this threshold. As the assumed investment cost declines, the number of states for which LDES becomes economically viable increases progressively. Under a cost level of US$ 500 kW^{-1}, 9 states surpass this threshold, while a further reduction to US$ 300 kW^{-1} expands economic viability to 17 states. These findings indicate that the competitiveness of LDES at scale is likely to emerge unevenly across regions and remains highly sensitive to state specific system characteristics. This heterogeneity reinforces the importance of system specific valuation frameworks, such as the one proposed in this thesis, to support informed technology development targets and policy decisions for emerging technologies, with LDES serving as an illustrative case under a deeply decarbonized power system scenario.

In addition to the quantitative analyses presented in this thesis, a complemen-

tary interactive dashboard was developed using Tableau to enhance transparency and facilitate the interpretation of the results [61]. The dashboard provides a comprehensive visual exploration of state specific energy system characteristics, allowing users to compare key metrics side by side and to examine both percentage and absolute values associated with generation, reserves, and system costs. By integrating economic and operational indicators in a unified platform, the dashboard enables a more intuitive assessment of how LDES affects system operation and cost composition across states, including variations in overall annual system costs and components such as the opportunity value associated with LDES deployment. Importantly, the platform allows users to directly download all underlying data, supporting reproducibility, independent analysis, and broader use by researchers and decision makers. As such, the dashboard extends the contribution of this thesis beyond static results, reinforcing transparency and accessibility in the evaluation of emerging energy technologies.

Future research can build upon this work by extending the proposed framework along several complementary dimensions. One relevant avenue is the explicit representation of transmission constraints, both within and across states, which would allow for a more detailed assessment of spatial interactions and congestion effects on the economic value of LDES. In addition, while this thesis focuses on scenarios of full power system decarbonization as a policy relevant benchmark, the methodology can be readily applied to alternative transition pathways, including partial decarbonization scenarios and systems with residual thermal generation. Finally, the valuation framework is not limited to long-duration energy storage and can be adapted to assess other emerging and still immature technologies whose system level value arises from complex operational interactions. These extensions would further broaden the applicability of the proposed methodology across different regions, policy contexts, and technological portfolios.

Another relevant direction for future research involves assessing the impact of load growth uncertainties on the economic value of LDES. This study utilized demand projections from the Cambium 2022 dataset; however, emerging external factors, such as the rapid expansion of Artificial Intelligence (AI) data centers, are expected to drastically increase energy consumption in specific regions. For

example, while Virginia already exhibits the highest boundary cost in our findings, its power capacity is anticipated to double in the next decade to meet the growing demand driven by new data center infrastructure [63]. Providing continuous clean power for these intensive, round-the-clock loads makes LDES even more critical. Notably, technology companies are already procuring multi-day battery systems to reliably power new data centers [64]. Future capacity expansion studies should incorporate these aggressive demand scenarios to fully capture how localized load spikes might drive the boundary cost and the overall necessity of LDES even higher.

Beyond addressing demand uncertainties, incorporating detailed operational constraints represents an important next step. While these degradation mechanisms are predominantly analyzed in SDES, they remain highly applicable to LDES contexts. Although LDES systems generally undergo fewer charge-discharge cycles, repeated cycling still drives irreversible physical and chemical changes that reduce overall capacity [65]. Furthermore, the extended idle periods inherent to LDES make the system highly susceptible to time-dependent calendar aging [66]. Specifically, since deeply discharging a battery induces severe mechanical and thermal stress that significantly accelerates both cycle and calendar aging processes [67, 66, 68], a critical direction for future research is to restrict the Depth of Discharge (DoD) by establishing a strict minimum SoC limit [67, 65, 66]. Incorporating these operational boundaries and multi-stress degradation effects in future frameworks is essential to mitigate detrimental degradation, prevent accelerated wear, and ensure a realistic assessment of the energy storage system's true performance and long-term viability [65, 66].

An additional direction for future research relates to the potential contribution of long-duration energy storage to mitigating renewable energy curtailment, particularly in the Brazilian power system. In Brazil, *constrained-off* events result in substantial reimbursement costs to generators, while simultaneously reducing renewable energy utilization and raising concerns regarding system security. By absorbing surplus generation, LDES may contribute to reducing curtailment, improving overall system efficiency, and lowering compensation costs. Nevertheless, the economic viability of LDES in the Brazilian context, its potential benefits to the national electrical system, and the existence of adequate market conditions

remain open research questions. Addressing these aspects constitutes a relevant extension of the present work and motivates the application of the proposed valuation methodology to the Brazilian power system in future studies.

BIBLIOGRAPHY

[1] BOUCKAERT, S. et al. *Net zero by 2050: A roadmap for the global energy sector*. [S.l.], 2021. `https://www.iea.org/`.

[2] UNFCCC. *The United States of America Nationally Determined Contribution*. [S.l.], 2022.

[3] KERRY, J.; MCCARTHY, G. *The Long-Term Strategy of the United States: Pathways to Net-Zero Greenhouse Gas Emissions by 2050*. [S.l.], 2021. Disponível em: <https://www.whitehouse.gov/>.

[4] International Monetary Fund. *United States: 2026 Article IV Consultation—Press Release; Staff Report; and Statement by the Executive Director for the United States*. [S.l.], 2026. (IMF Country Report, 2026/076). Accessed on April 4, 2026. Disponível em: <https://www.imf.org/-/media/files/publications/cr/2026/english/1usaea2026001.pdf>.

[5] GILL, L.; GUTIERREZ, A.; WEEKS, T. *2021 SB 100 Joint Agency Report: achieving 100 Percent Clean Electricity in California, an Initial Assessment*. [S.l.], 2021. Accessed on November 12, 2023. Disponível em: <https://www.energy.ca.gov/publications/2021/2021-sb-100-joint-agency-report-achieving-100-percent-clean-electricity>.

[6] GROTLE, A. O. et al. Economic prospects of flexible nuclear energy operation under different market conditions. In: IEEE. *2024 20th International Conference on the European Energy Market (EEM)*. [S.l.], 2024. p. 1–7.

[7] VECCHI, A.; SCIACOVELLI, A. Long-duration thermo-mechanical energy storage–present and future techno-economic competitiveness. *Appl. Energy*, Elsevier, v. 334, p. 120628, 2023. ISSN 0306-2619.

[8] ASHFAQ, S. et al. Comparing the role of long duration energy storage technologies for zero-carbon electricity systems. *IEEE Access*, IEEE, 2024.

[9] SHAHZAD, S. et al. Unlocking the potential of long-duration energy storage: Pathways to net-zero emissions through global innovation and collaboration. *Journal of Energy Storage*, Elsevier, v. 97, p. 112904, 2024.

[10] ASPITARTE, L.; WOODSIDE, C. R. A techno-economic survey of energy storage media for long-duration energy storage applications. *Cell Reports Sustainability*, Elsevier, v. 1, 2024.

[11] DOWLING, J. A. et al. Role of long-duration energy storage in variable renewable electricity systems. *Joule*, Elsevier, v. 4, p. 1907–1928, 2020. ISSN 2542-4351.

[12] LIU, T. et al. Evaluation of the short-and long-duration energy storage requirements in solar-wind hybrid systems. *Energy Conversion and Management*, Elsevier, v. 314, p. 118635, 2024.

[13] AHMAD, T. et al. Energetics systems and artificial intelligence: Applications of industry 4.0. *Energy Reports*, Elsevier, v. 8, p. 334–361, 2022.

[14] LIU, T.; YANG, Z.; DUAN, Y. Short-and long-duration cooperative energy storage system: Optimizing sizing and comparing rule-based strategies. *Energy*, Elsevier, v. 281, p. 128273, 2023.

[15] MOREIRA, A. et al. On the role of battery energy storage systems in the day-ahead contingency-constrained unit commitment problem under renewable penetration. *Electric Power Systems Research*, Elsevier, v. 235, p. 110856, 2024.

[16] SEPULVEDA, N. A. et al. The role of firm low-carbon electricity resources in deep decarbonization of power generation. *Joule*, Elsevier, v. 2, p. 2403–2420, 2018.

[17] BISTLINE, J. E.; YOUNG, D. T. The role of natural gas in reaching net-zero emissions in the electric sector. *Nature Communications*, Nature Publishing Group UK London, v. 13, p. 4743, 2022.

[18] STAADECKER, M. et al. The value of long-duration energy storage under various grid conditions in a zero-emissions future. *Nature Communications*, Nature Publishing Group UK London, v. 15, p. 9501, 2024.

[19] TWITCHELL, J.; DESOMBER, K.; BHATNAGAR, D. Defining long duration energy storage. *J. Energy Storage*, Elsevier, v. 60, p. 105787, 2023. ISSN 2352-152X.

[20] SEPULVEDA, N. A. et al. The design space for long-duration energy storage in decarbonized power systems. *Nat. Energy*, Nature Publishing Group UK London, v. 6, p. 506–516, 2021.

[21] HUNTER, C. A. et al. Techno-economic analysis of long-duration energy storage and flexible power generation technologies to support high-variable renewable energy grids. *Joule*, Elsevier, v. 5, p. 2077–2101, 2021. ISSN 2542-4351.

[22] YIN, H. et al. Field measurement and analysis of frequency and rocof for low-inertia power systems. *IEEE Transactions on Industrial Electronics*, IEEE, 2024.

[23] GHILOUFI, M.; SBITA, L. Grid-forming and grid-following inverters for virtual inertia emulation in smart grid. In: NATIONAL ENGINEERING SCHOOL OF GABES, TUNISIA. [S.l.], 2025. Formatado como artigo de conferência IEEE.

[24] SAHA, S. et al. Quantifying hourly virtual inertia and battery energy storage system requirements for frequency stability in low-inertia power systems. *Journal of Energy Storage*, Elsevier, v. 153, p. 120853, 2026.

[25] LIU, J. et al. *Inertia Response Comparative Analysis between Grid-Following and Grid-Forming Energy Storage System*. 2025. Documento em formato de artigo/trabalho acadêmico (Afiliações: China Southern Power Grid Co., Ltd. e Huazhong University of Science and Technology).

[26] KAUSHIK, E. et al. Comprehensive overview of power system flexibility during the scenario of high penetration of renewable energy in utility grid. *Energies*, MDPI, v. 15, p. 516, 2022.

[27] ZINGALES, A. Smart storage the key factor of energy transition. In: IOP PUBLISHING. *IOP Conference Series: Earth and Environmental Science*. [S.l.], 2022. v. 1073, p. 012014.

[28] HO, C. K.; MCNAMARA, J. W. The value of long-duration energy storage: Policy and perception. In: AIP PUBLISHING. *AIP Conference Proceedings*. [S.l.], 2023. v. 2815.

[29] U.S. Department of Energy Energy Earthshots. *Long Duration Storage Shot*. 2021. Accessed on January 2, 2024. Disponível em: <https://www.energy.gov/eere/long-duration-storage-shot>.

[30] LDES Council. *Driving to Net Zero Industry Through Long Duration Energy Storage*. [S.l.], 2023. Disponível em: <https://www.ldescouncil.com/>.

[31] ALBERTUS, P.; MANSER, J. S.; LITZELMAN, S. Long-duration electricity storage applications, economics, and technologies. *Joule*, Elsevier, v. 4, p. 21–32, 2020. ISSN 2542-4351.

[32] ZHANG, J. et al. Benefit analysis of long-duration energy storage in power systems with high renewable energy shares. *Front. Energy Res.*, Frontiers Media SA, v. 8, p. 527910, 2020.

[33] SCOTT, K. et al. *Pathways to Commercial Liftoff: Long Duration Energy Storage*. [S.l.], 2023. Disponível em: <https://liftoff.energy.gov/>.

[34] NARAYANAN, S. et al. Materials challenges and technical approaches for realizing inexpensive and robust iron–air batteries for large-scale energy storage. *Solid State Ionics*, Elsevier, v. 216, p. 105–109, 2012. ISSN 0167-2738.

[35] ZIEGLER, M. S. et al. Storage requirements and costs of shaping renewable energy toward grid decarbonization. *Joule*, Elsevier, v. 3, p. 2134–2153, 2019. ISSN 2542-4351.

[36] HARGREAVES, J. J.; JONES, R. A. Long term energy storage in highly renewable systems. *Front. Energy Res.*, Frontiers Media SA, v. 8, p. 219, 2020.

[37] GUERRA, O. J. et al. The value of seasonal energy storage technologies for the integration ofwind and solar power. *Energy Environ. Sci.*, v. 13, p. 1909–1922, 2020.

[38] HUNT, J. D. et al. Compressed air seesaw energy storage: A solution for long-term electricity storage. *Journal of Energy Storage*, Elsevier, v. 60, p. 106638, 2023.

[39] COLOMBO, M.; KURTZ, S. Value of long-duration energy storage and oxy-combustion in renewables driven grids. In: IEEE. *2023 North American Power Symposium (NAPS)*. [S.l.], 2023. p. 1–5.

[40] JÜLCH, V. Comparison of electricity storage options using levelized cost of storage (lcos) method. *Applied Energy*, Elsevier, v. 183, p. 1594–1606, 2016.

[41] KABEYI, M. J. B.; OLANREWAJU, O. A. The levelized cost of energy and modifications for use in electricity generation planning. *Energy Reports*, Elsevier, v. 9, p. 495–534, 2023.

[42] BALDINELLI, A. et al. Economics of innovative high capacity-to-power energy storage technologies pointing at 100% renewable micro-grids. *Journal of Energy Storage*, Elsevier, v. 28, p. 101198, 2020.

[43] WANG, H. et al. System value assessment and heterogeneous cost allocation of long-duration energy storage systems: A public asset perspective. *Energies*, MDPI, 2026.

[44] GAGNON, P.; COWIESTOLL, B.; SCHWARZ, M. *Cambium 2022 Scenario Descriptions and Documentation*. [S.l.], 2023. NREL/TP-6A40-84916. Disponível em: <https://nrel.gov/publications.html>.

[45] DOE. *Long-Duration Energy Storage Demonstrations Program – Multiday Iron Air Demonstration*. 2024. Accessed on March 7, 2025. Disponível em: <https://www.energy.gov/sites/default/files/2024-06/FactSheet_LDESAward_Xcel_6.5.24_v3.pdf>.

[46] MCKERRACHER, R. D. et al. A review of the iron–air secondary battery for energy storage. *ChemPlusChem*, v. 80, 2015.

[47] U.S. Department of Energy Office of Clean Energy Demonstrations. *Long-Duration Energy Storage Demonstrations Program – Multiday Iron Air Demonstration*. 2024. Project Fact Sheet. Available at: `https://www.energy.gov/oced/ldes`. Accessed: April 13, 2026.

[48] Form Energy. *Massachusetts, New England States Selected to Receive $389 Million in Federal Funding for Transformational Transmission and Energy Storage Infrastructure*. 2024. Press Release. Accessed: April 13, 2026.

[49] CUI, X. et al. Analysis of the net present value and equivalent annual cost in optimal machine life. p. 2929–2933, 2022.

[50] GAGNON, P.; COWIESTOLL, B.; SCHWARZ, M. *Cambium 2022 Data*. 2023. Accessed on May 17, 2023. Disponível em: <https://scenarioviewer.nrel.gov>.

[51] HO, J. et al. *Regional Energy Deployment System (ReEDS) Model Documentation: Version 2020*. [S.l.], 2021. NREL/TP-6A20-78195. Disponível em: <https://nrel.gov/publications.html>.

[52] COLE, W. et al. *Regional Energy Deployment System Model 2.0 (ReEDS 2.0)*. 2021. Version 2021.1. Accessed on March 22, 2023. Disponível em: <https://www.nrel.gov/analysis/reeds/index.html>.

[53] NREL. *ATB Electricity Data 2022*. 2022. Accessed on March 29, 2023. Disponível em: <https://atb.nrel.gov/electricity/2022/data>.

[54] U.S. Energy Information Administration. *Annual Energy Outlook 2023*. 2023. Accessed on July 1, 2023. Disponível em: <https://www.eia.gov/outlooks/aeo/>.

[55] GAGNON, P. *Personal communication containing the underlying PLEXOS database for Cambium 2022 scenarios*. 2023. Email. Email received on April 6, 2023.

[56] U.S. Inflation Calculator. *U.S. Inflation Calculator*. 2023. Accessed on May 6, 2023. Disponível em: <https://www.usinflationcalculator.com/>.

[57] HEAD, K. et al. *Summer Market Performance Report: June 2023*. [S.l.], 2023. Disponível em: <https://www.caiso.com/>.

[58] U.S. Energy Information Administration. *State Electricity Profiles 2022*. 2023. Accessed on Mar 4, 2024. Disponível em: <https://www.eia.gov/electricity/state/california/>.

[59] U.S. Energy Information Administration. *Annual Energy Outlook*. [S.l.], 2023. Disponível em: <https://www.eia.gov/outlooks/aeo/pdf/AEO2023_Narrative.pdf>.

[60] TONG, D. et al. Geophysical constraints on the reliability of solar and wind power worldwide. *Nature communications*, Nature Publishing Group, v. 12, p. 1–12, 2021.

[61] SILVA, P. et al. *Economic viability of 100-h long-duration energy storage (LDES) systems in 2050 - Tableau Online*. 2026. Accessed on April 10, 2026. Disponível em: <https://public.tableau.com/app/profile/patricia.silva8551/viz/LDESeconomicviability/Painel_1>.

[62] KLINK, K. Climatological mean and interannual variance of united states surface wind speed, direction and velocity. *International Journal of Climatology*, v. 19, p. 471–488, 1999.

[63] MAIDEN, V. *Virginia's Landscape & Approach: Energy & Data Centers*. 2025. Presentation. Presented at the MEGA-DC Project Team Meeting.

[64] BLOOMBERG. *Crusoe Buys Batteries That Last for Days to Power New Data Centers*. 2026. News article featured by Form Energy. Accessed: April 13, 2026.

[65] GHANAEE, E. et al. Comparative analysis of battery degradation models for optimal operation of a hybrid power plant in the day-ahead market. Universidad Politécnica de Madrid, Spain, 2025.

[66] YAN, Y. et al. A multi-stress universal degradation framework for lithium-ion batteries in diverse energy storage scenarios. *Journal of Energy Storage*, Elsevier, v. 154, p. 121305, 2026.

[67] YÜKSEK, G.; ALKAYA, A. Effect of the depth of discharge and c-rate on battery degradation and cycle life. Mersin University, Turkey, 2023.

[68] ZORDAN, S. et al. A state-dependent experimental model of storage efficiency for optimized battery system operation and revamping of degraded capacity. *Journal of Energy Storage*, Elsevier, v. 153, p. 120922, 2026.

ANNEX A – Graphs on the operation of all the states of the US

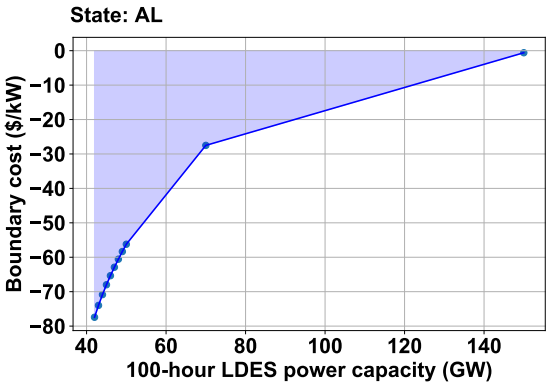

(a) Boundary cost curve.

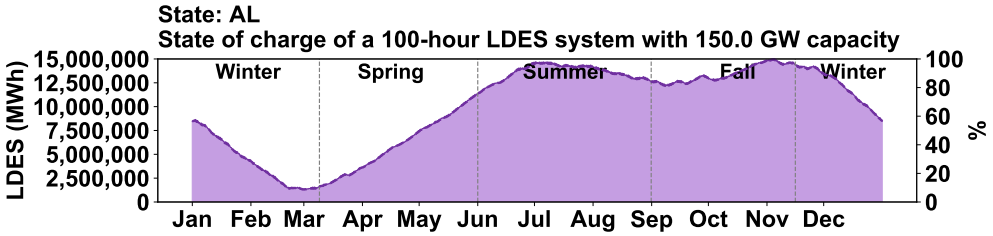

(b) State of charge.

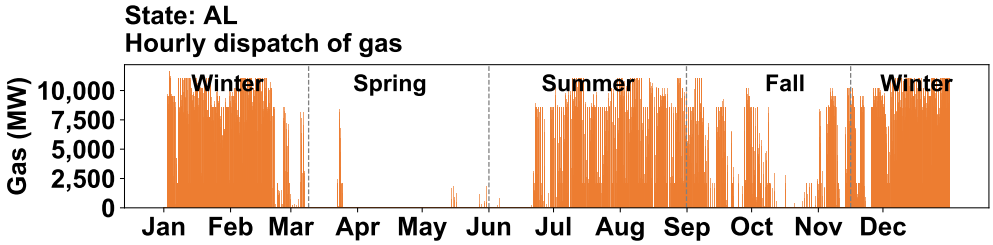

(c) Hourly dispatch of gas.

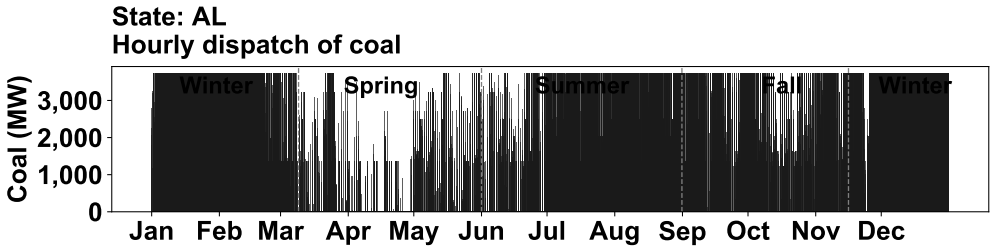

(d) Hourly dispatch of coal.

Figure 39 – Alabama (AL).

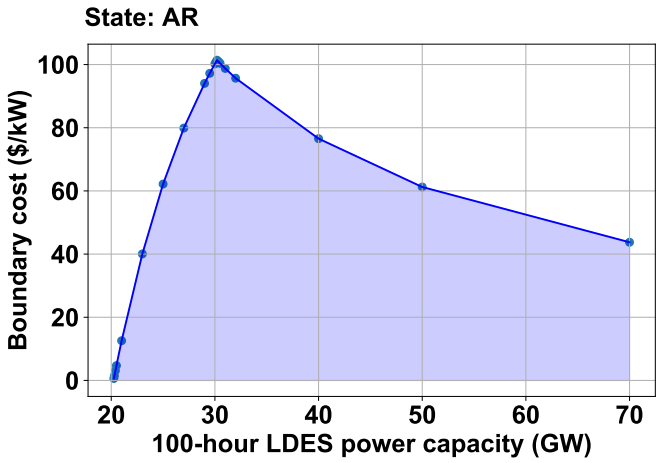

(a) Boundary cost curve.

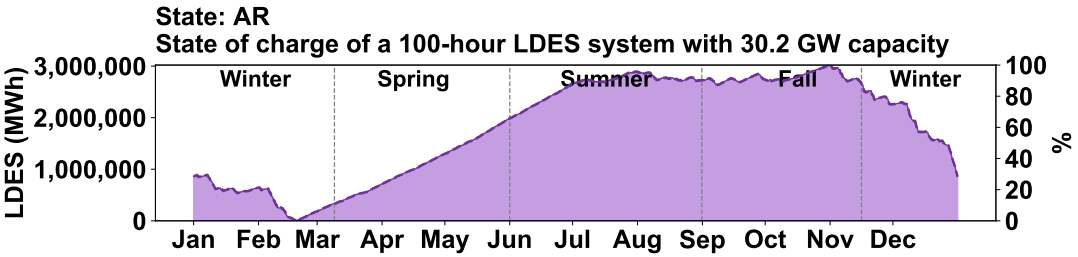

(b) State of charge.

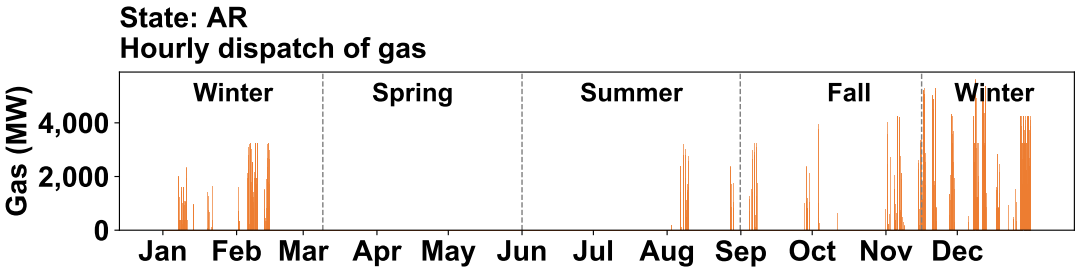

(c) Hourly dispatch of gas.

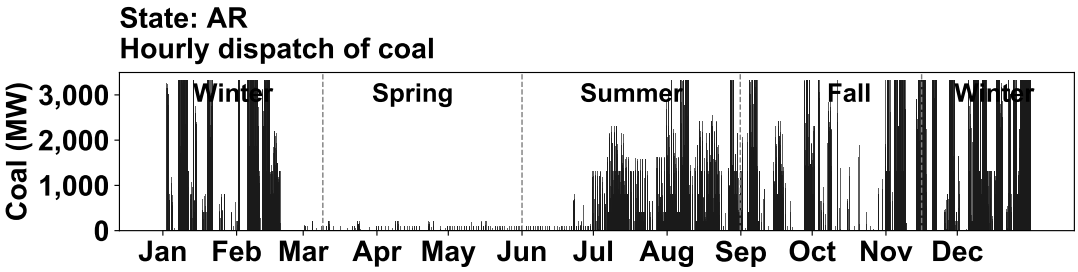

(d) Hourly dispatch of coal.

Figure 40 – Arkansas (AR).

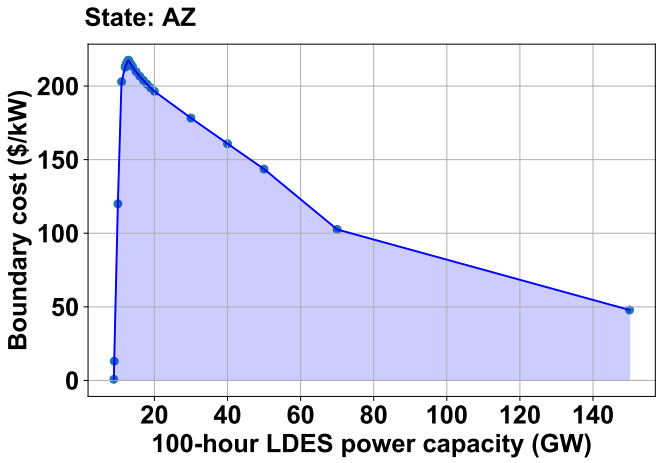

(a) Boundary cost curve.

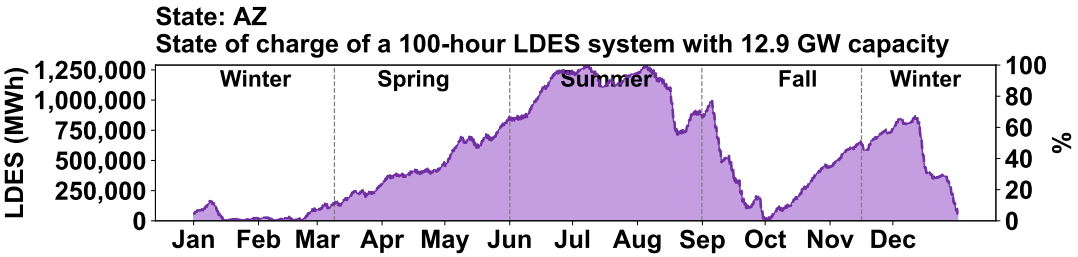

(b) State of charge.

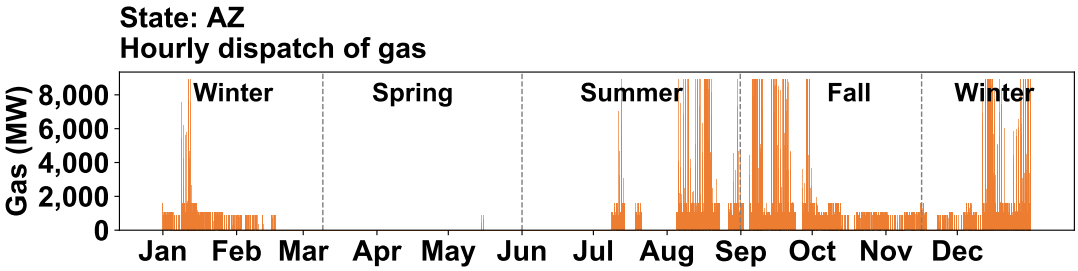

(c) Hourly dispatch of gas.

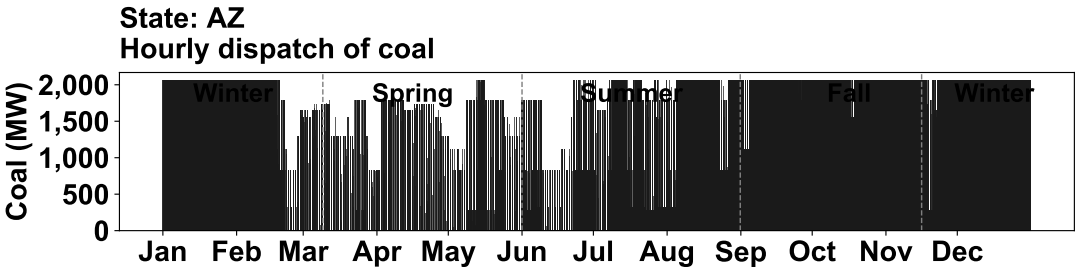

(d) Hourly dispatch of coal.

Figure 41 – Arizona (AZ).

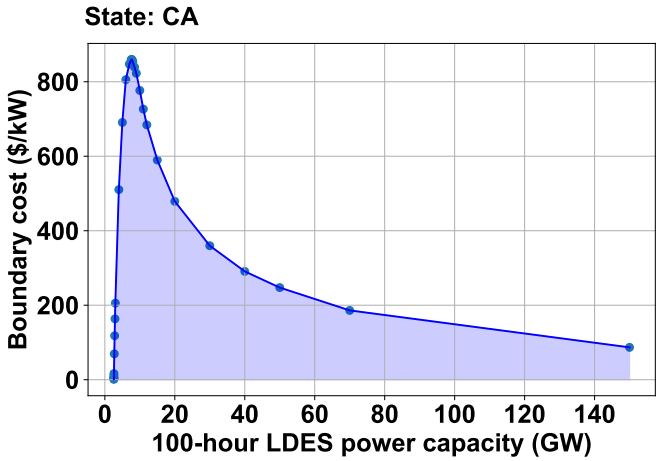

(a) Boundary cost curve.

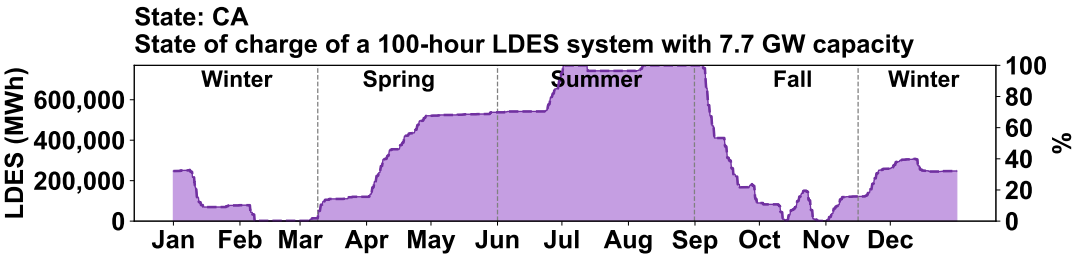

(b) State of charge.

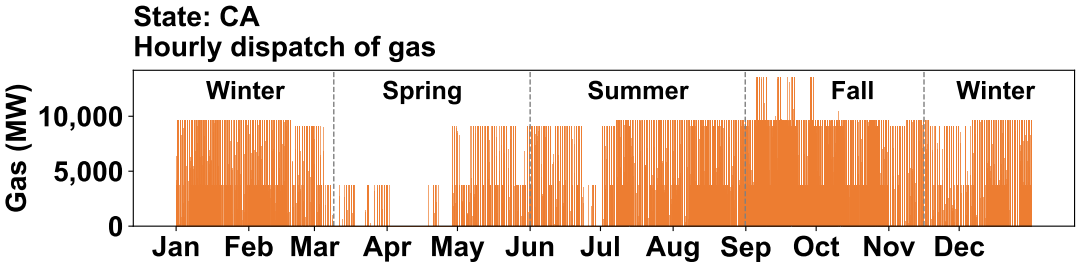

(c) Hourly dispatch of gas.

Figure 42 – California (CA).

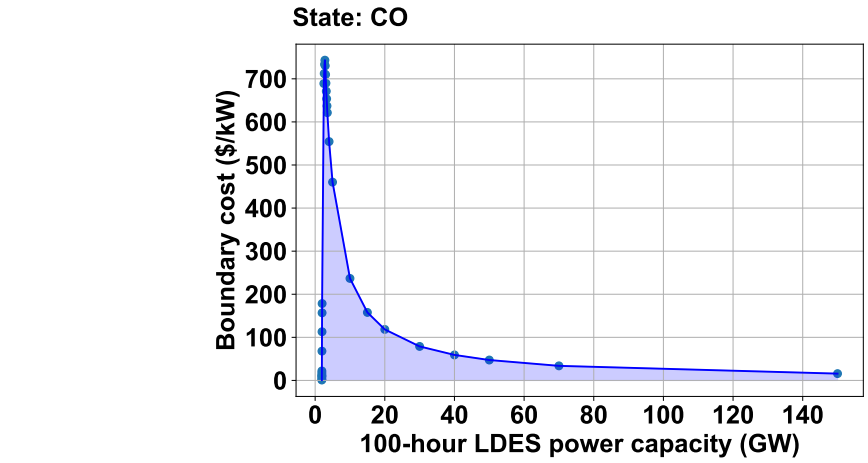

(a) Boundary cost curve.

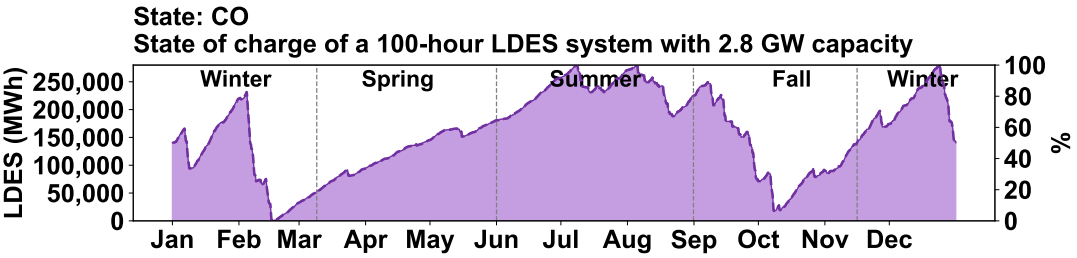

(b) State of charge.

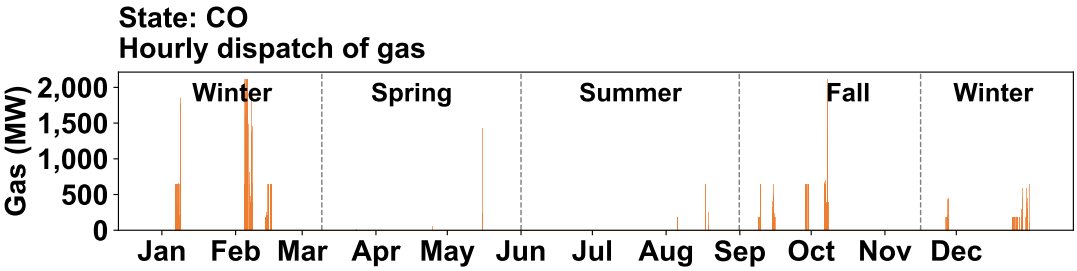

(c) Hourly dispatch of gas.

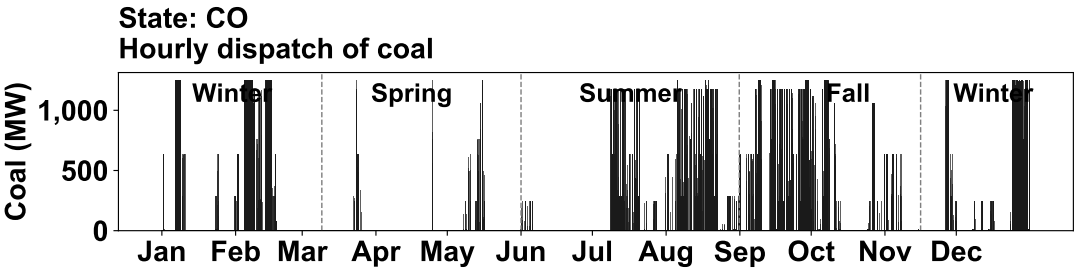

(d) Hourly dispatch of coal.

Figure 43 – Colorado (CO).

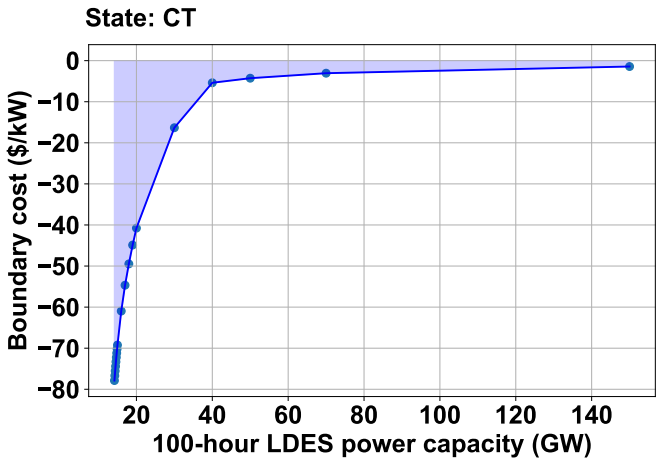

(a) Boundary cost curve.

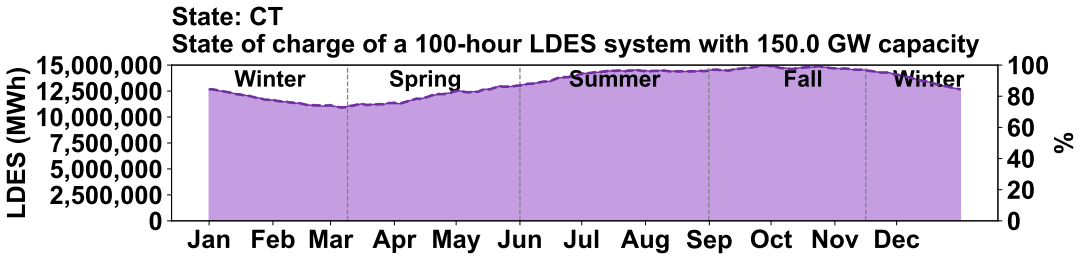

(b) State of charge.

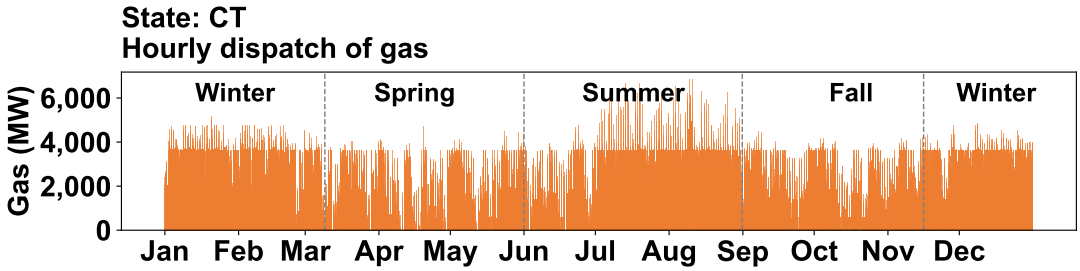

(c) Hourly dispatch of gas.

Figure 44 – Connecticut (CT).

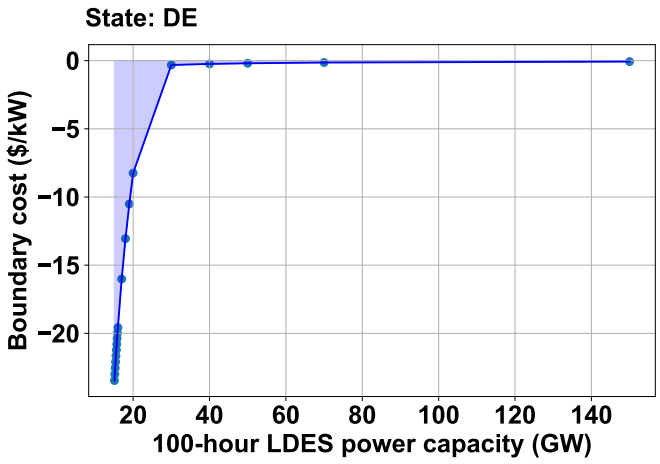

(a) Boundary cost curve.

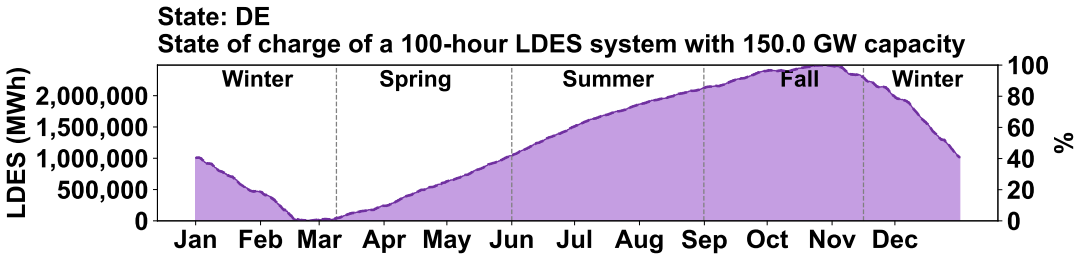

(b) State of charge.

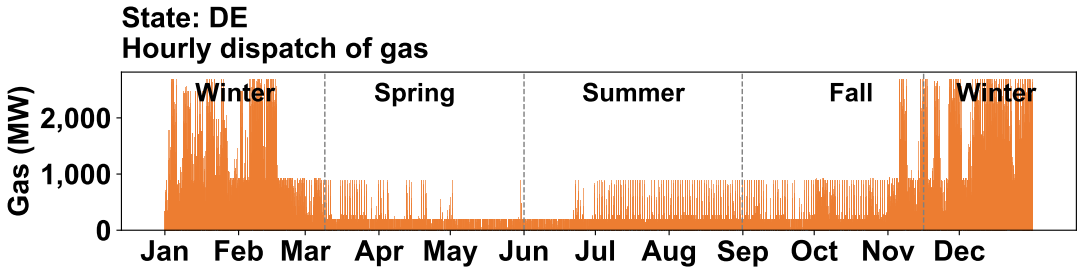

(c) Hourly dispatch of gas.

Figure 45 – Delaware (DE).

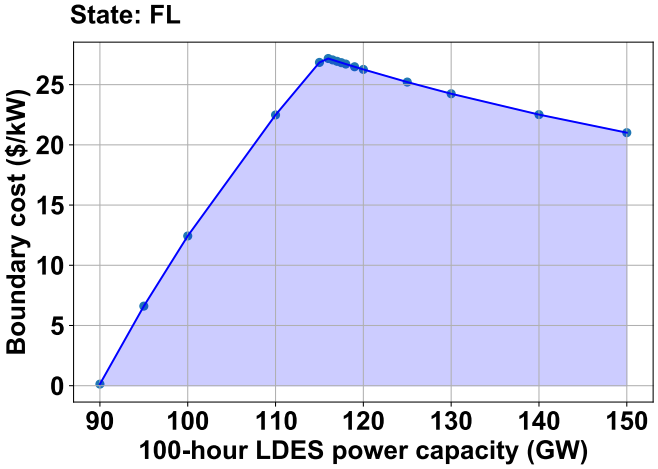

(a) Boundary cost curve.

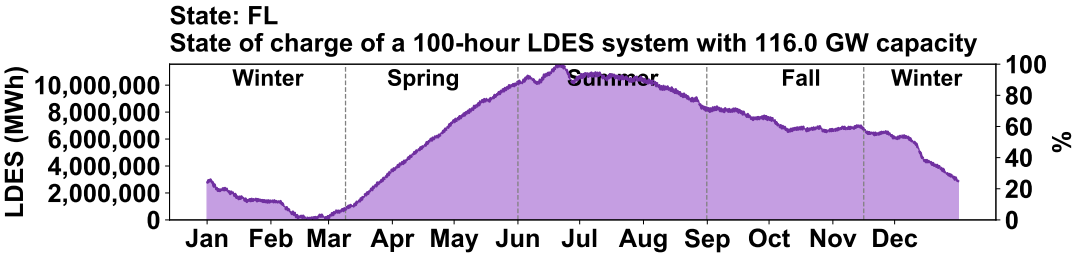

(b) State of charge.

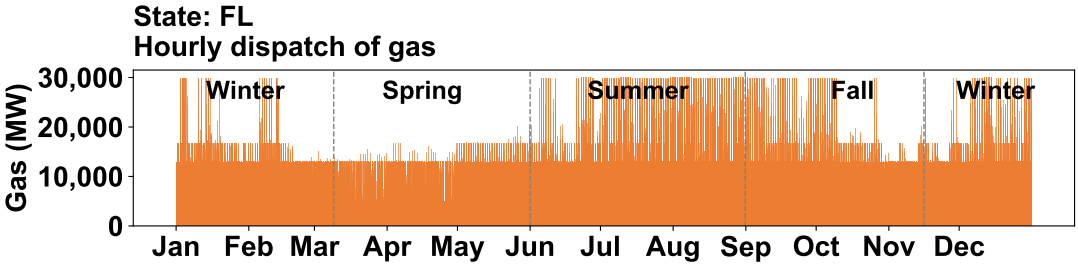

(c) Hourly dispatch of gas.

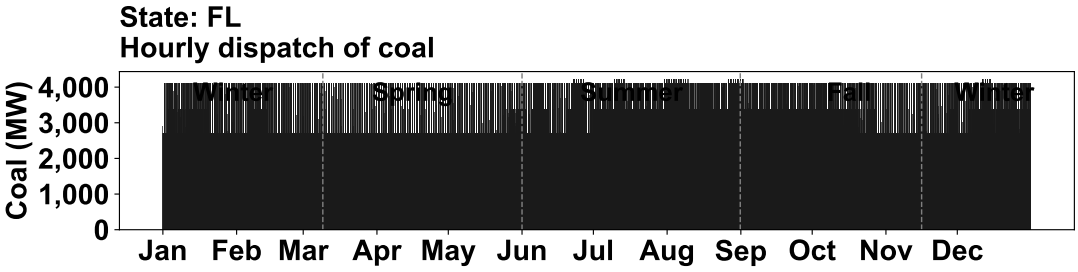

(d) Hourly dispatch of coal.

Figure 46 – Florida (FL).

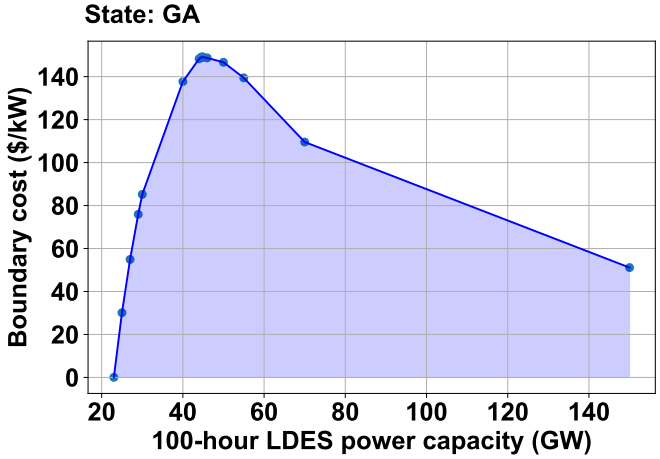

(a) Boundary cost curve.

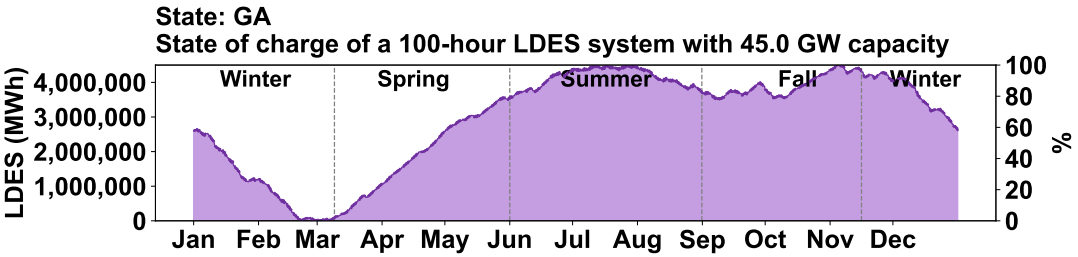

(b) State of charge.

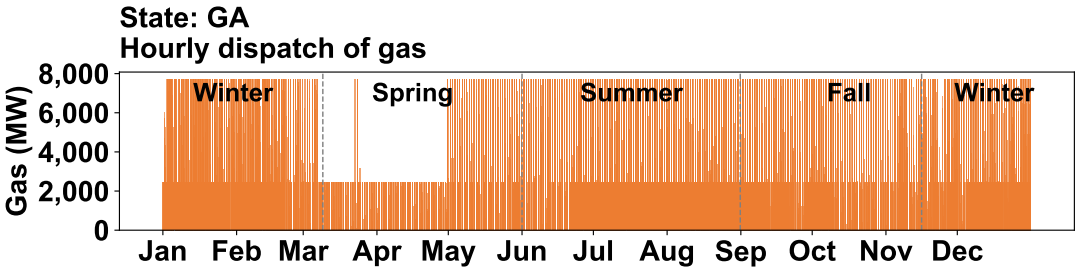

(c) Hourly dispatch of gas.

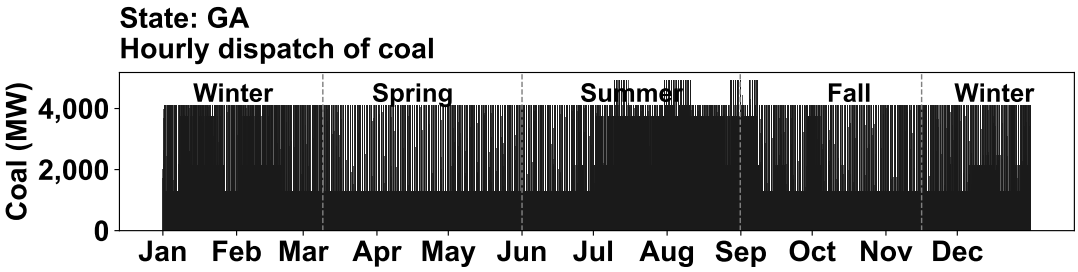

(d) Hourly dispatch of coal.

Figure 47 – Georgia (GA).

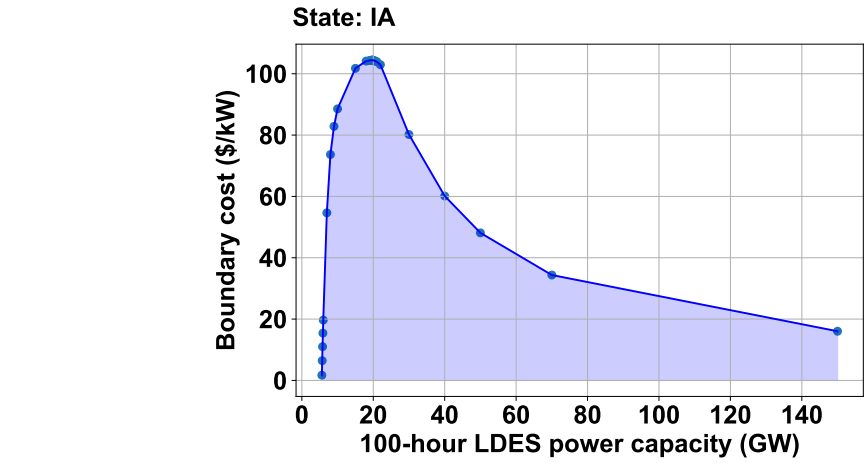

(a) Boundary cost curve.

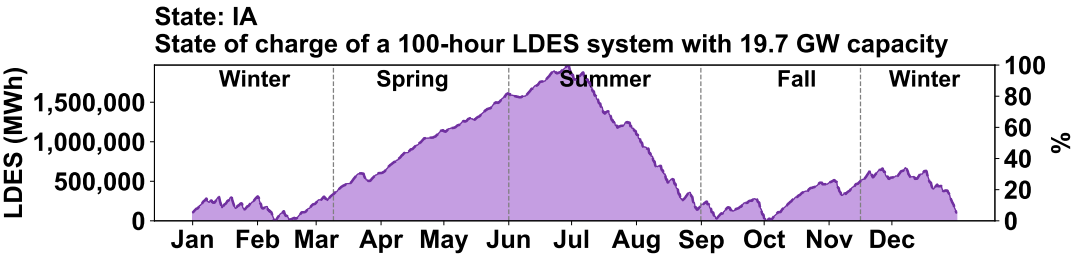

(b) State of charge.

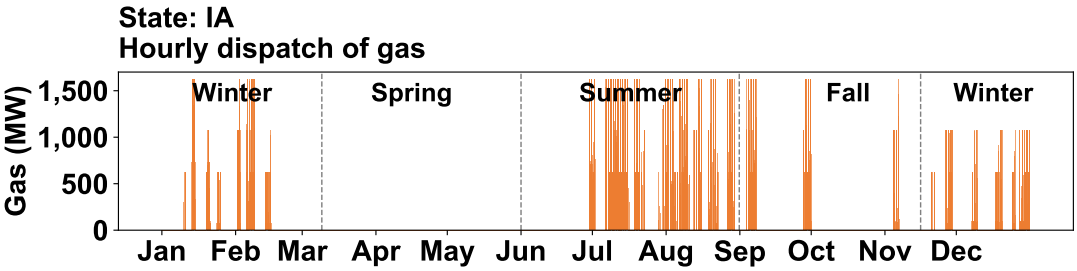

(c) Hourly dispatch of gas.

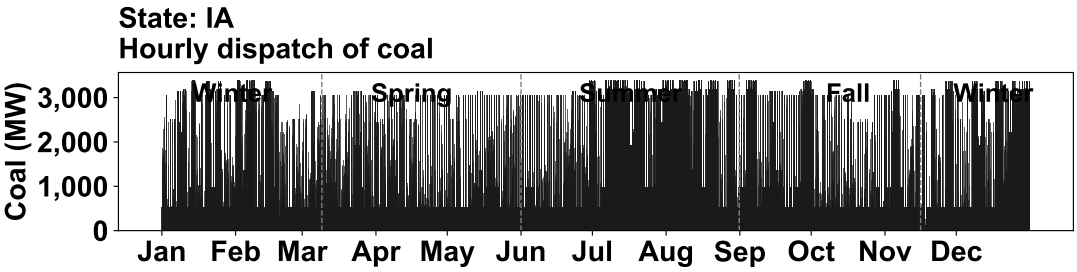

(d) Hourly dispatch of coal.

Figure 48 – Iowa (IA).

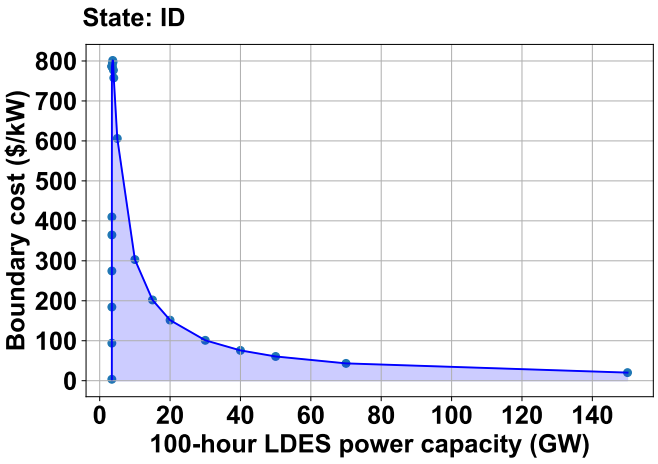

(a) Boundary cost curve.

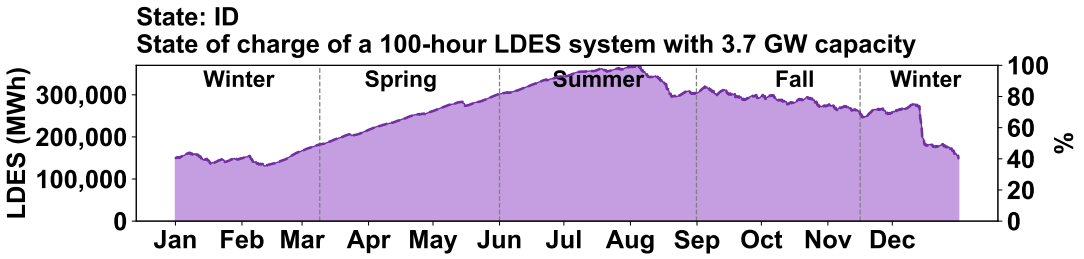

(b) State of charge.

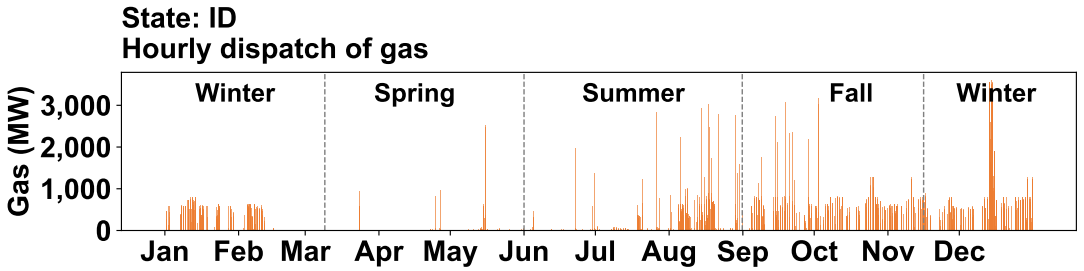

(c) Hourly dispatch of gas.

Figure 49 – Idaho (ID).

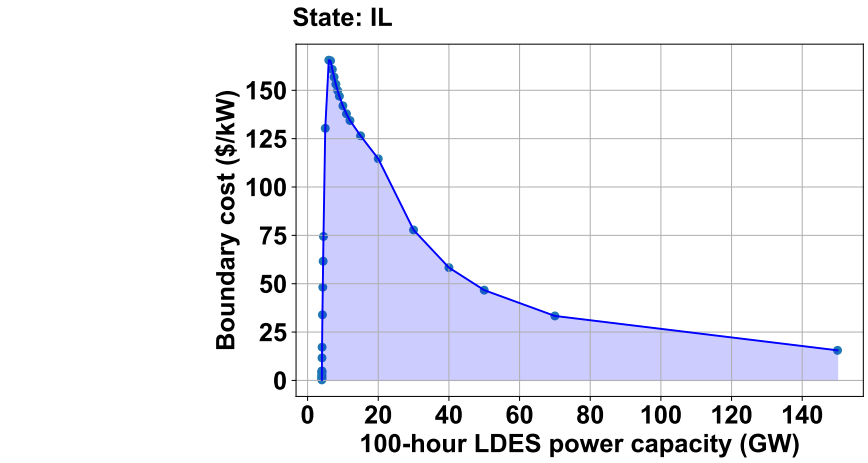

(a) Boundary cost curve.

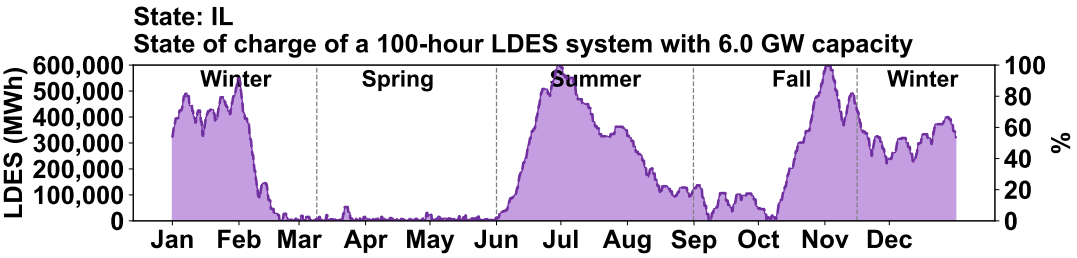

(b) State of charge.

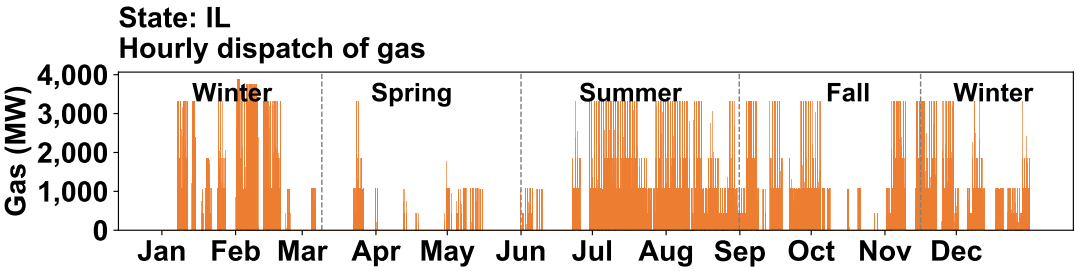

(c) Hourly dispatch of gas.

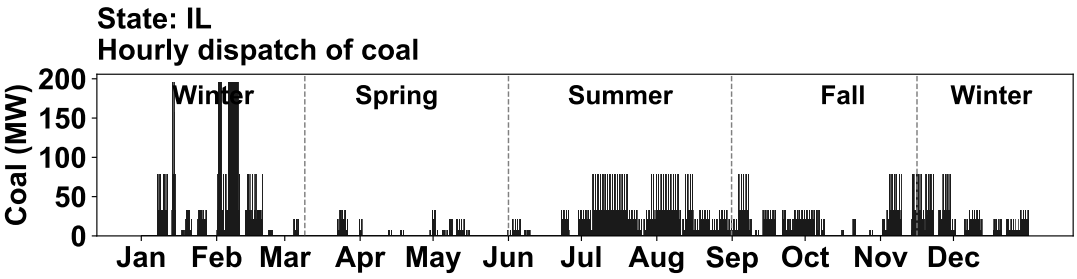

(d) Hourly dispatch of coal.

Figure 50 – Illinois (IL).

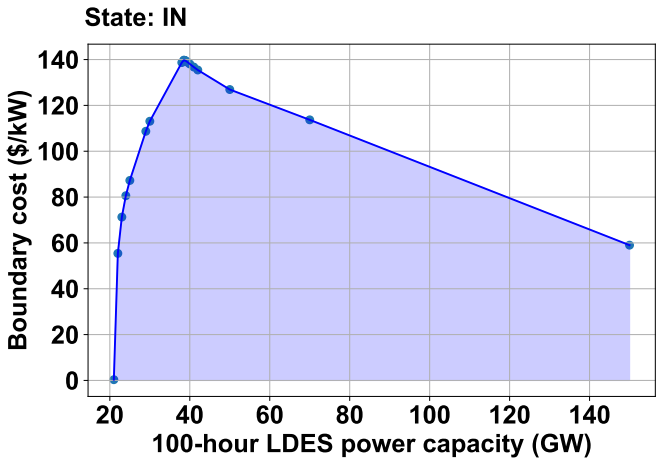

(a) Boundary cost curve.

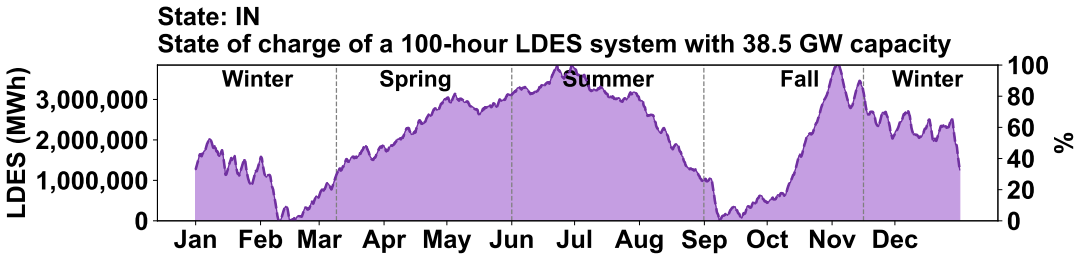

(b) State of charge.

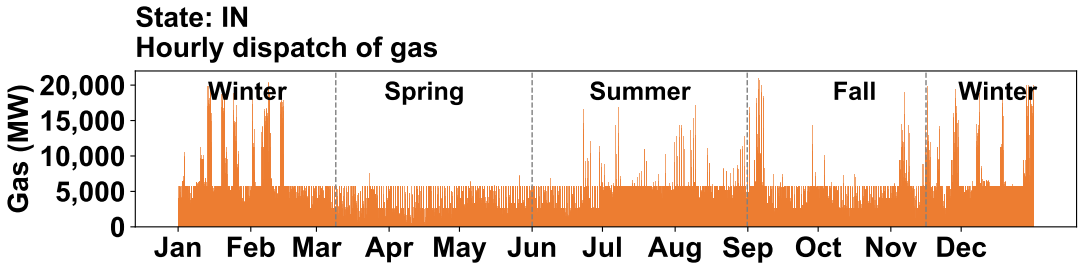

(c) Hourly dispatch of gas.

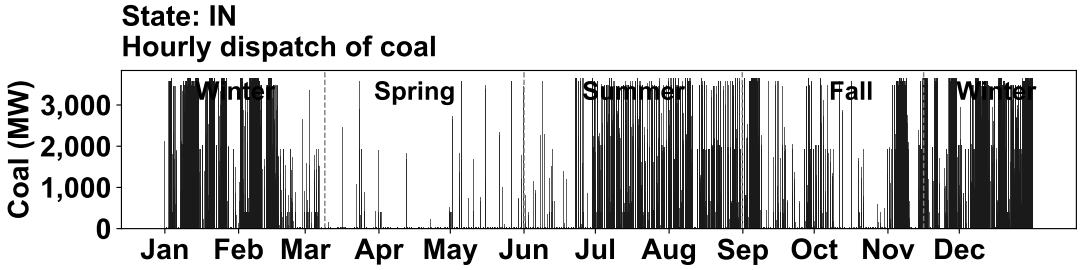

(d) Hourly dispatch of coal.

Figure 51 – Indiana (IN).

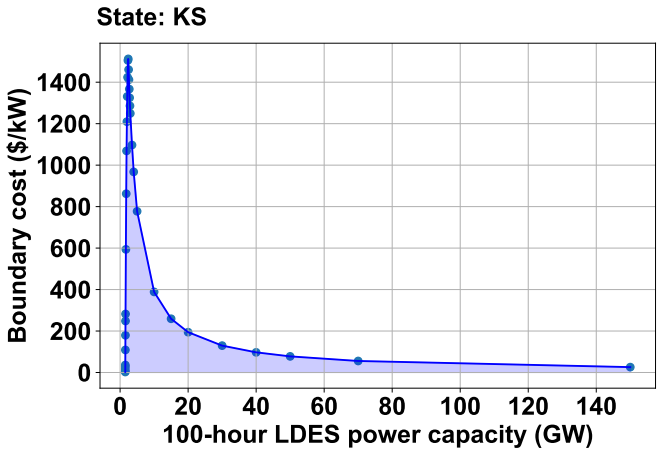

(a) Boundary cost curve.

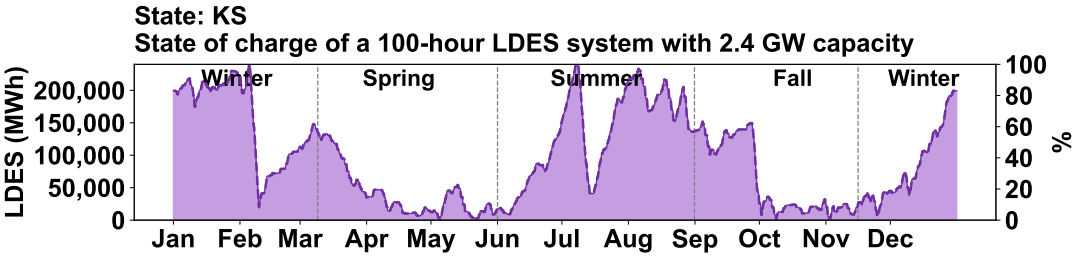

(b) State of charge.

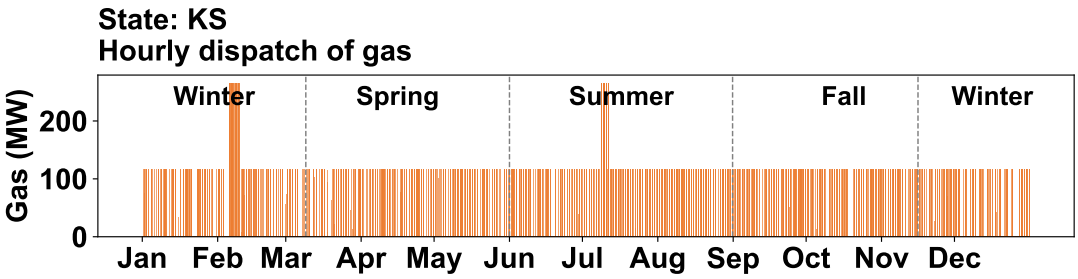

(c) Hourly dispatch of gas.

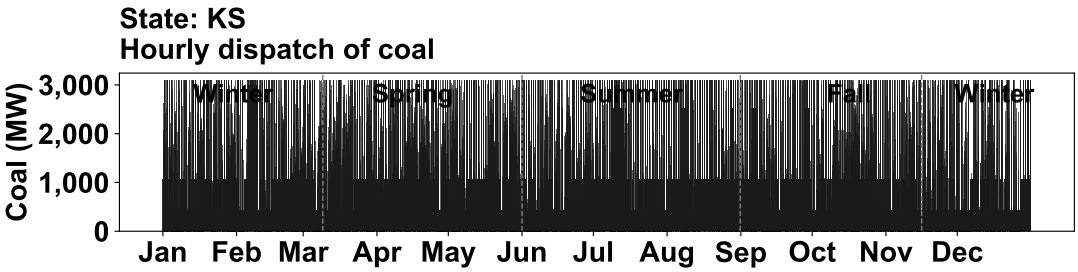

(d) Hourly dispatch of coal.

Figure 52 – Kansas (KS).

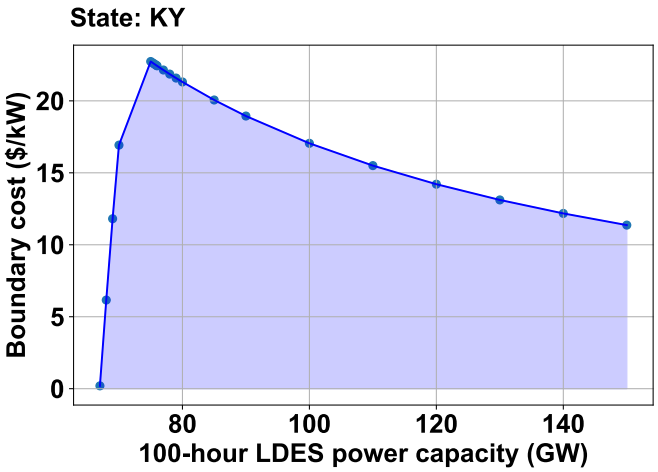

(a) Boundary cost curve.

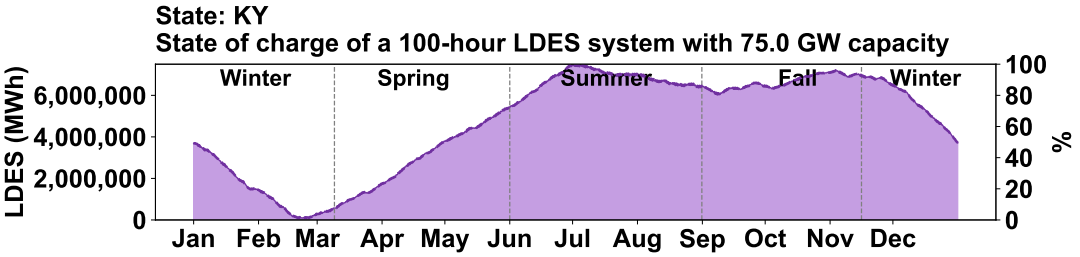

(b) State of charge.

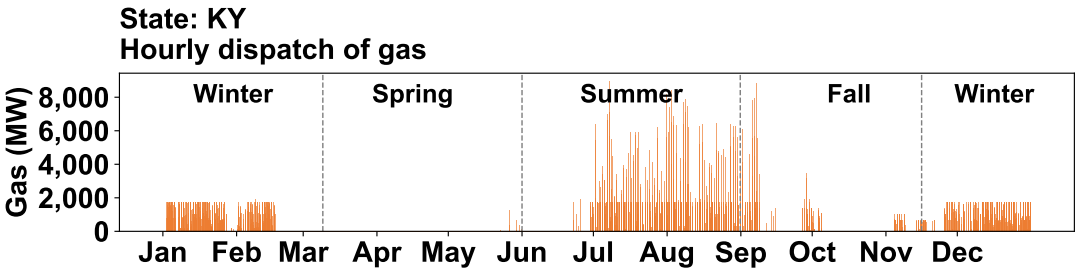

(c) Hourly dispatch of gas.

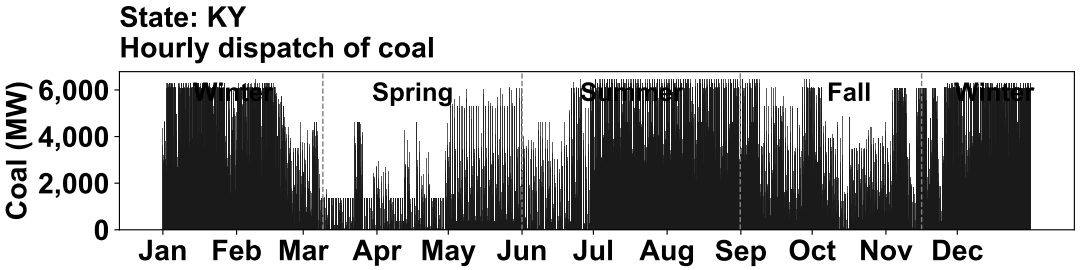

(d) Hourly dispatch of coal.

Figure 53 – Kentucky (KY).

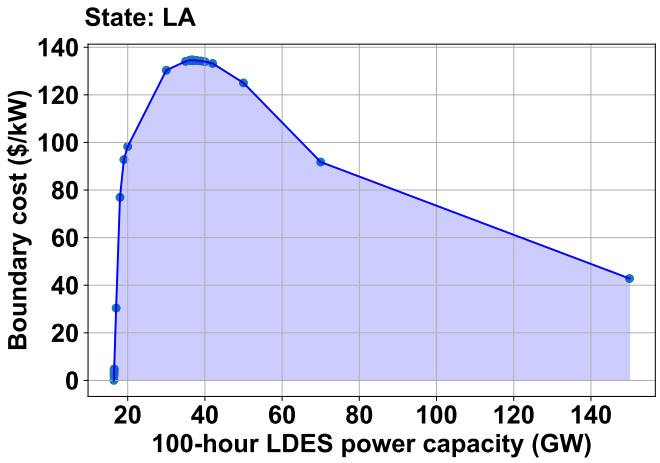

(a) Boundary cost curve.

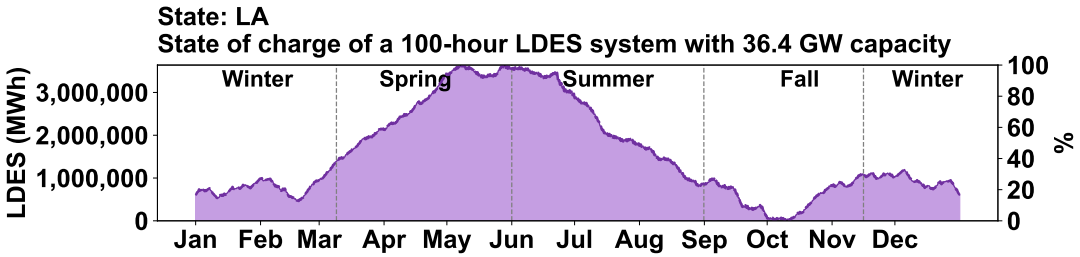

(b) State of charge.

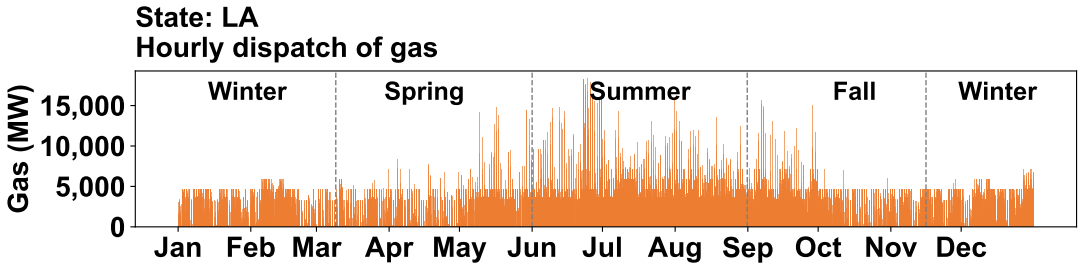

(c) Hourly dispatch of gas.

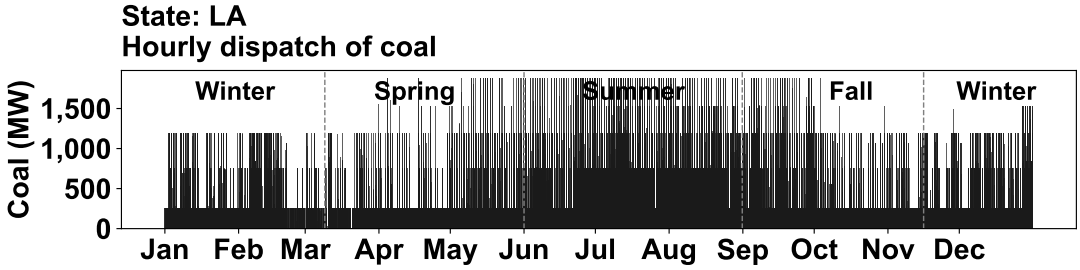

(d) Hourly dispatch of coal.

Figure 54 – Louisiana (LA).

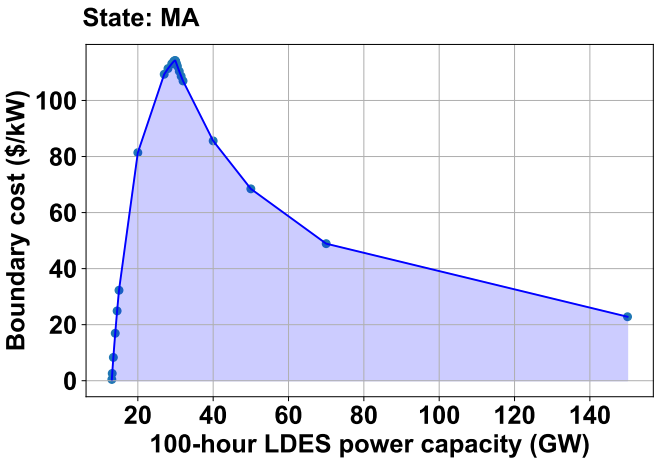

(a) Boundary cost curve.

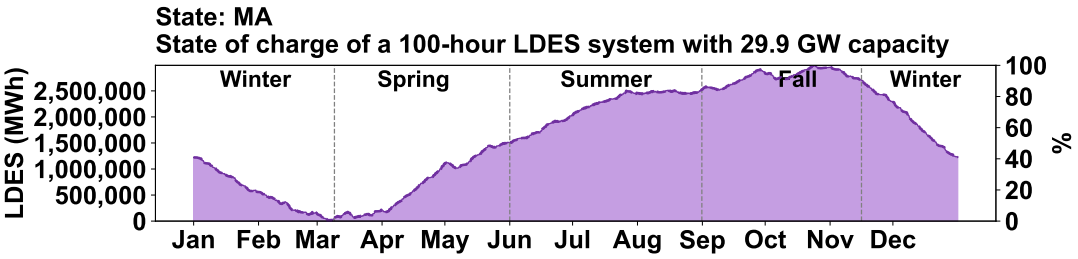

(b) State of charge.

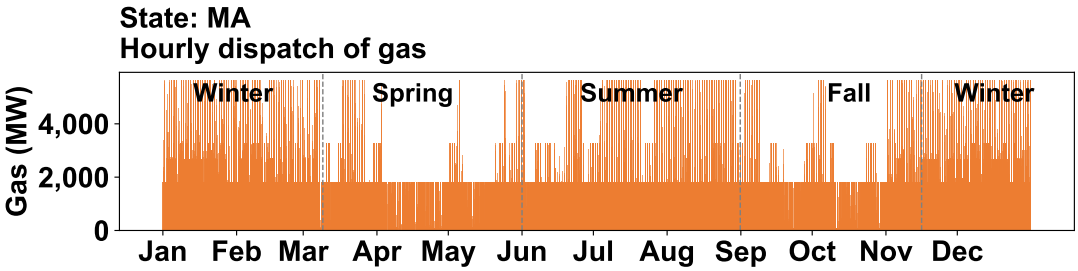

(c) Hourly dispatch of gas.

Figure 55 – Massachusetts (MA).

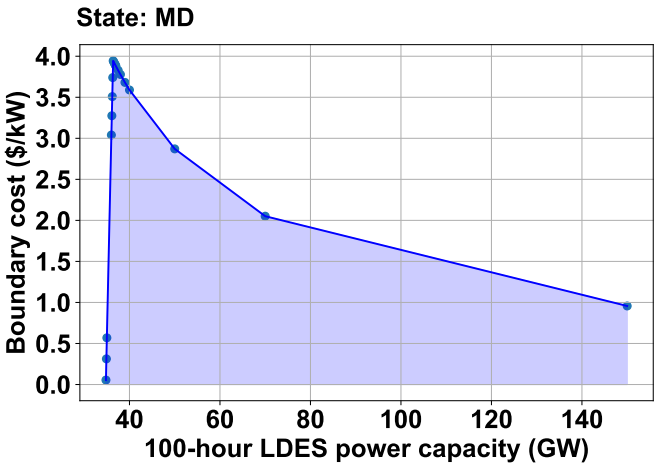

(a) Boundary cost curve.

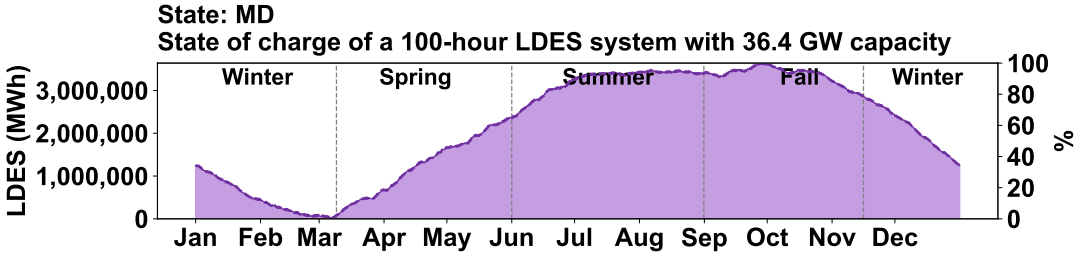

(b) State of charge.

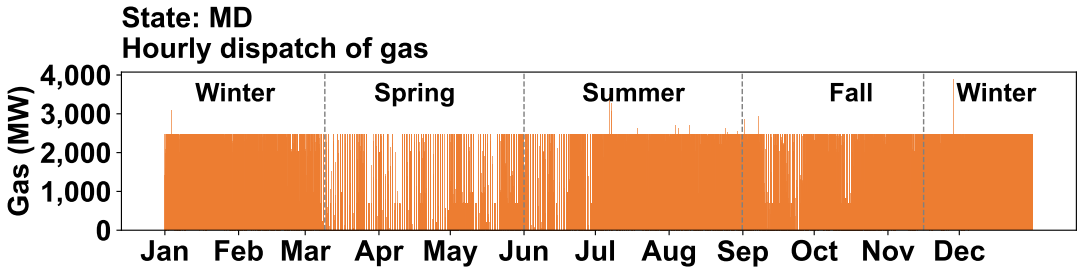

(c) Hourly dispatch of gas.

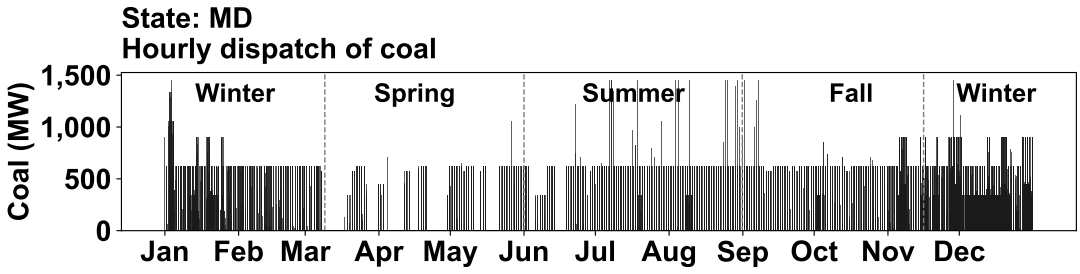

(d) Hourly dispatch of coal.

Figure 56 – Maryland (MD).

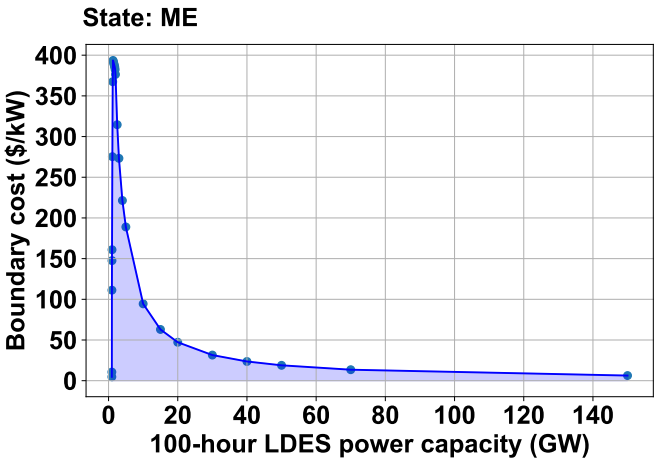

(a) Boundary cost curve.

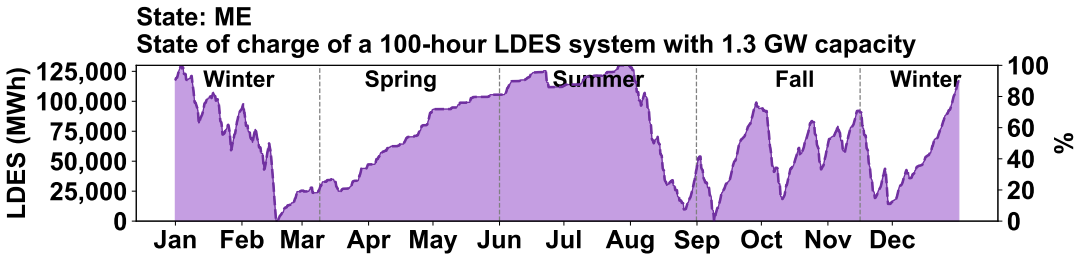

(b) State of charge.

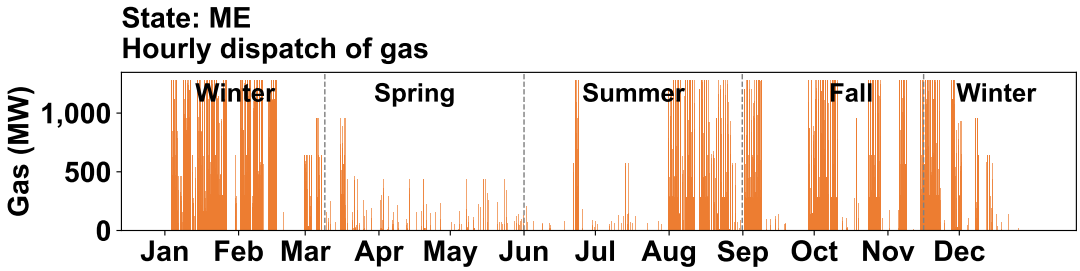

(c) Hourly dispatch of gas.

Figure 57 – Maine (ME).

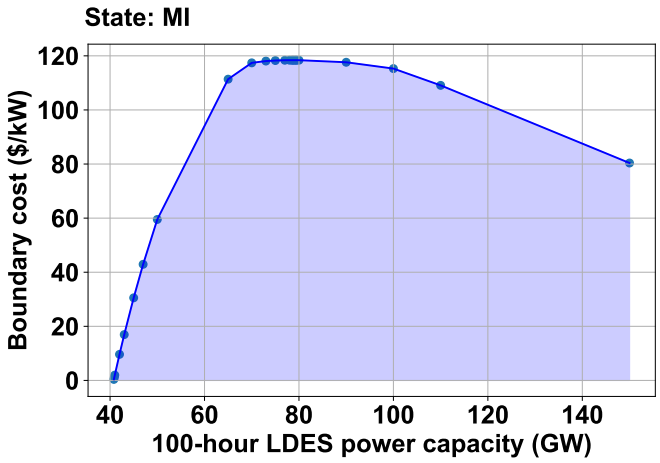

(a) Boundary cost curve.

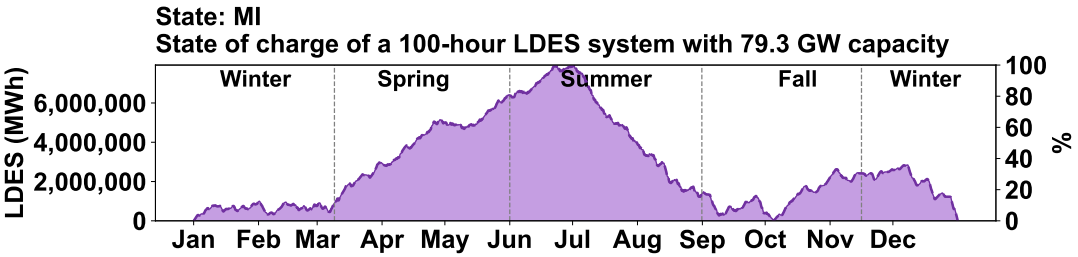

(b) State of charge.

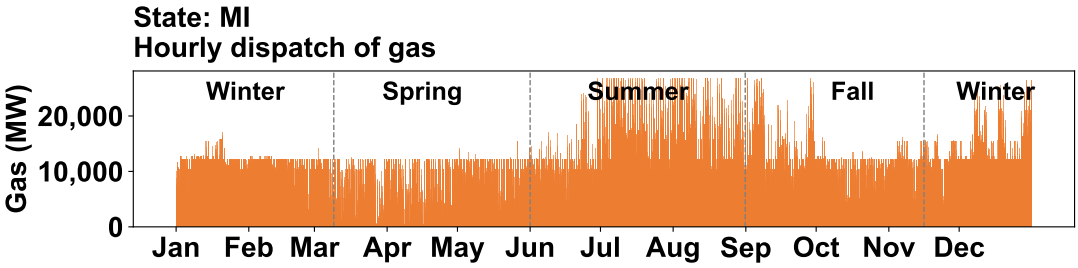

(c) Hourly dispatch of gas.

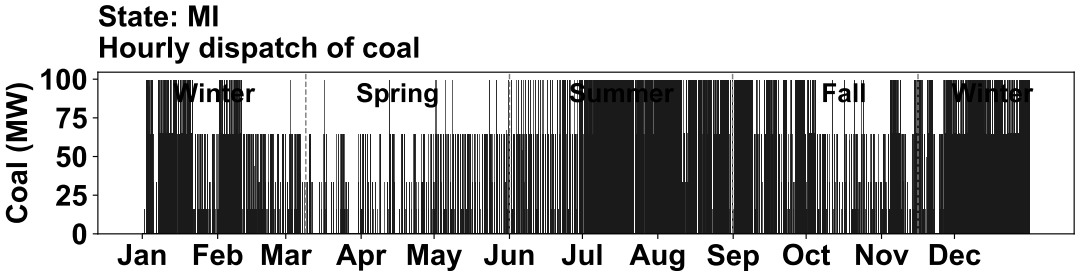

(d) Hourly dispatch of coal.

Figure 58 – Michigan (MI).

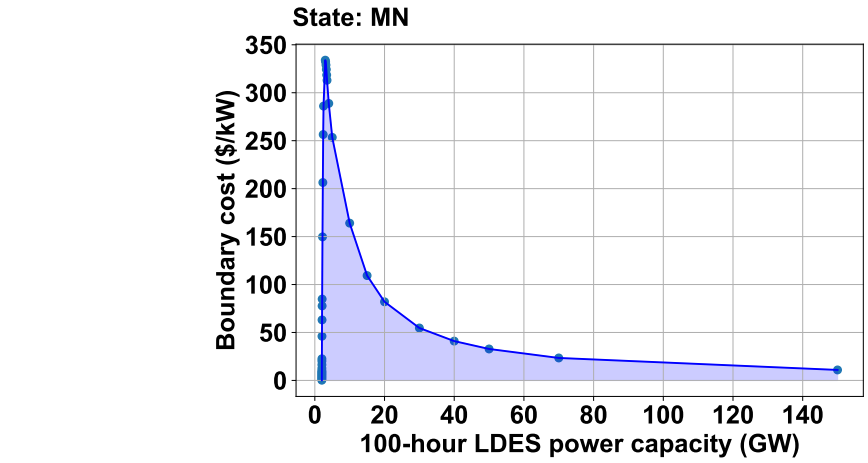

(a) Boundary cost curve.

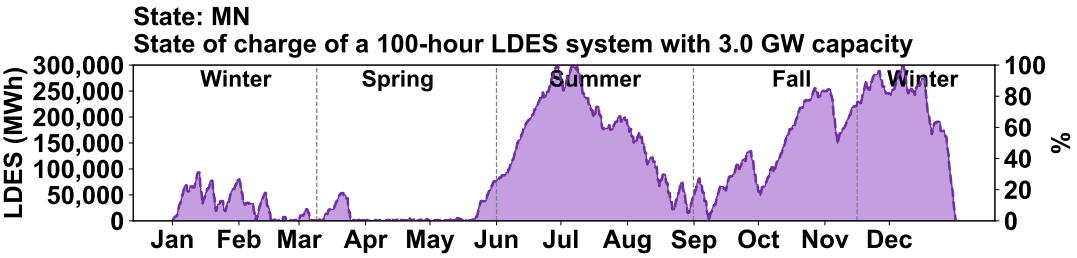

(b) State of charge.

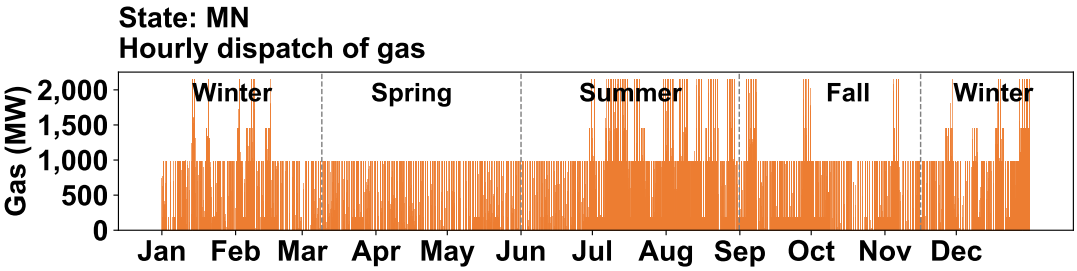

(c) Hourly dispatch of gas.

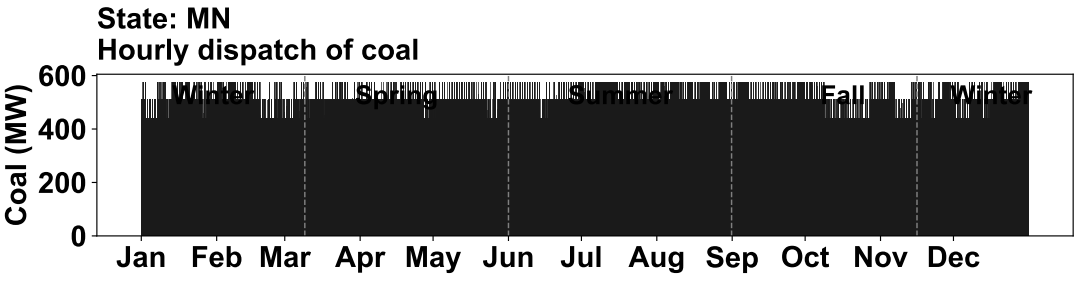

(d) Hourly dispatch of coal.

Figure 59 – Minnesota (MN).

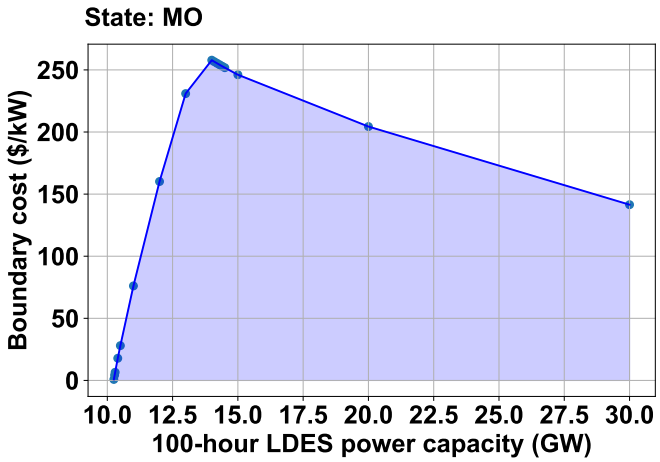

(a) Boundary cost curve.

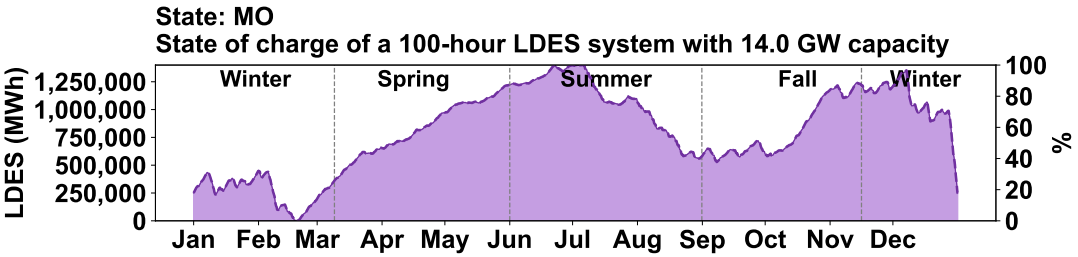

(b) State of charge.

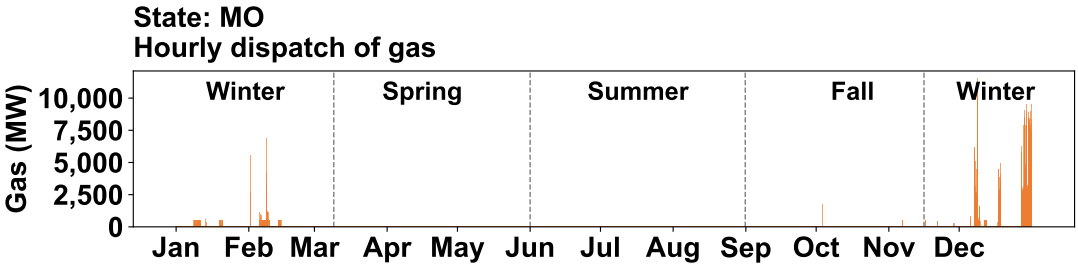

(c) Hourly dispatch of gas.

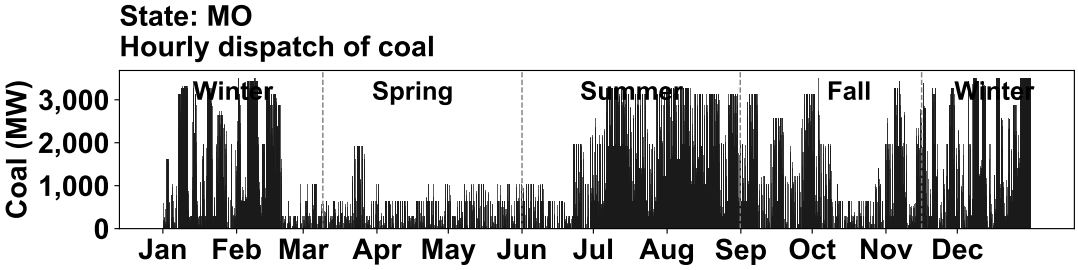

(d) Hourly dispatch of coal.

Figure 60 – Missouri (MO).

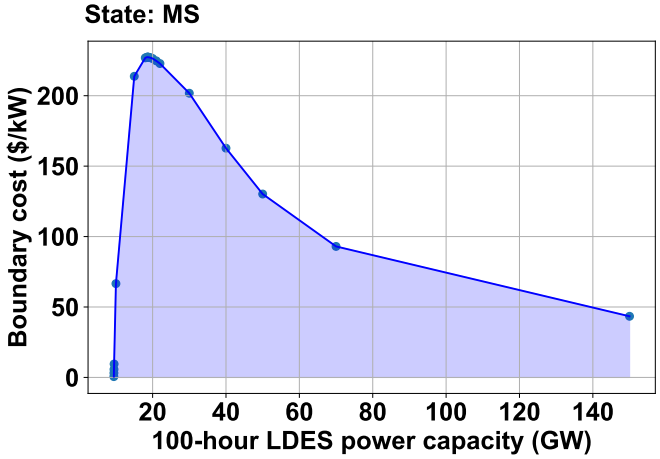

(a) Boundary cost curve.

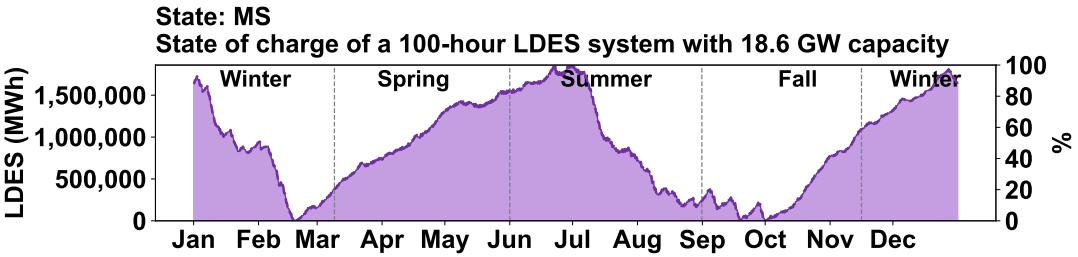

(b) State of charge.

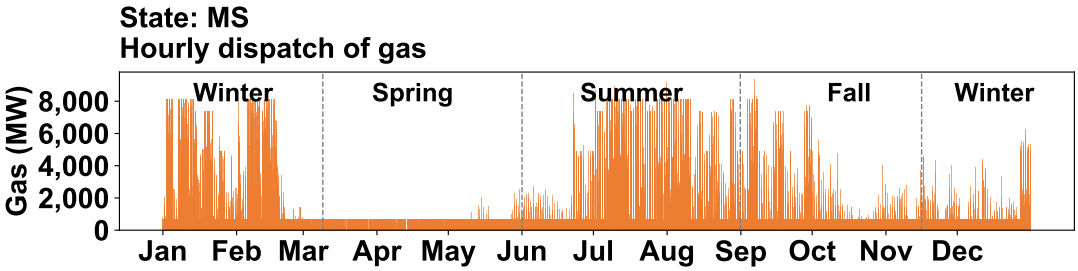

(c) Hourly dispatch of gas.

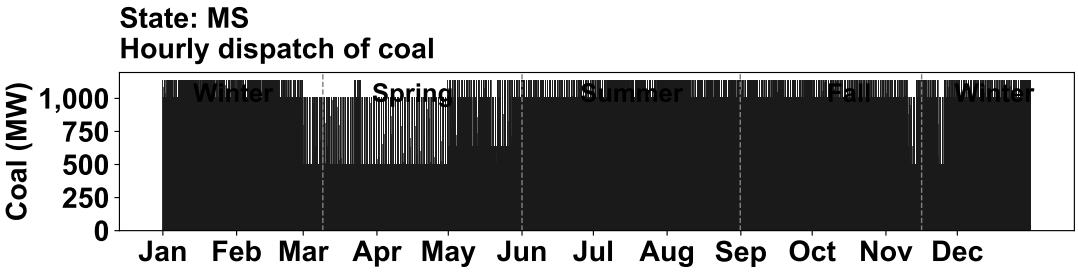

(d) Hourly dispatch of coal.

Figure 61 – Mississippi (MS).

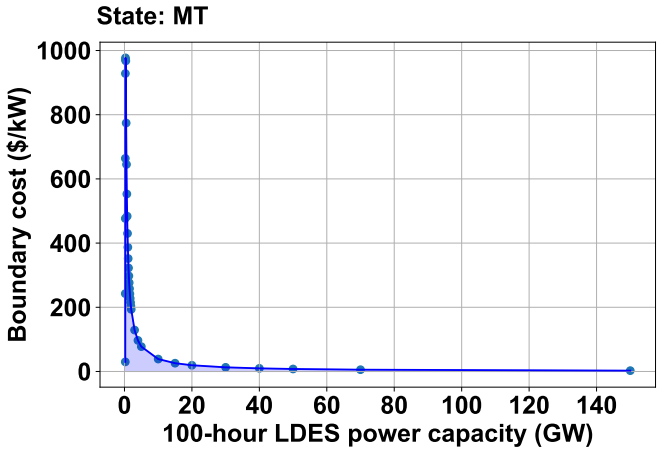

(a) Boundary cost curve.

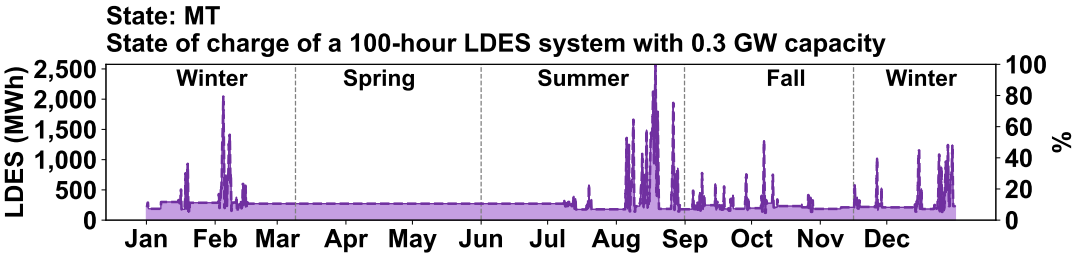

(b) State of charge.

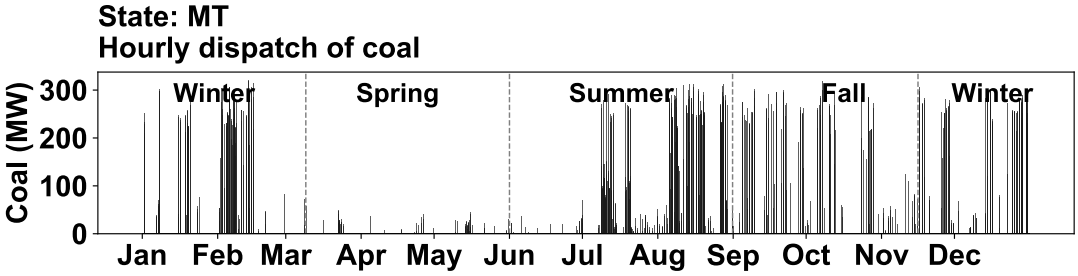

(c) Hourly dispatch of coal.

Figure 62 – Montana (MT).

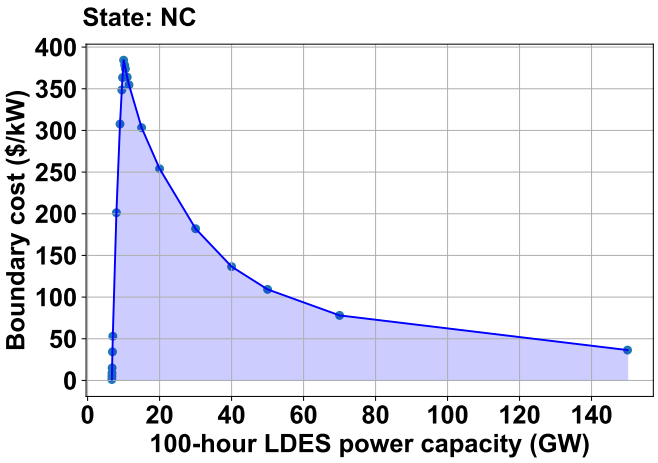

(a) Boundary cost curve.

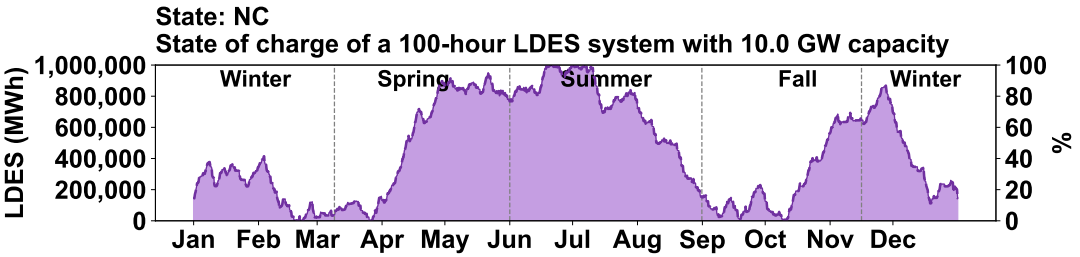

(b) State of charge.

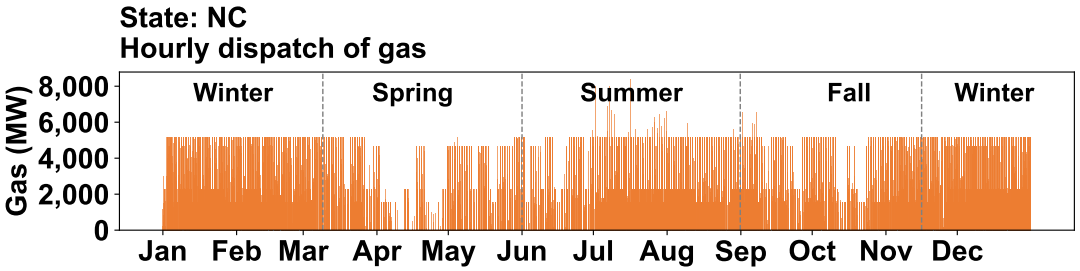

(c) Hourly dispatch of gas.

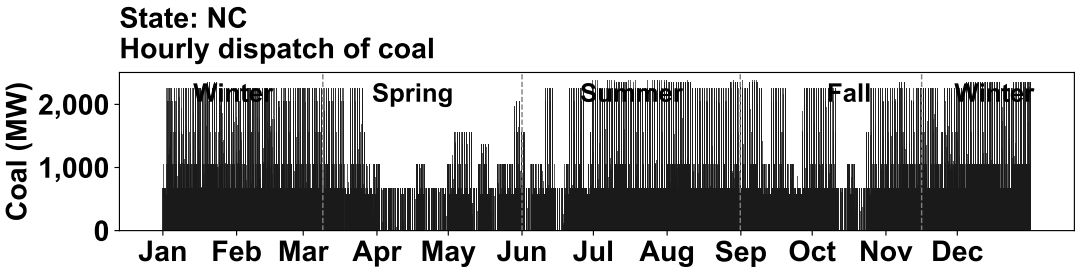

(d) Hourly dispatch of coal.

Figure 63 – North Carolina (NC).

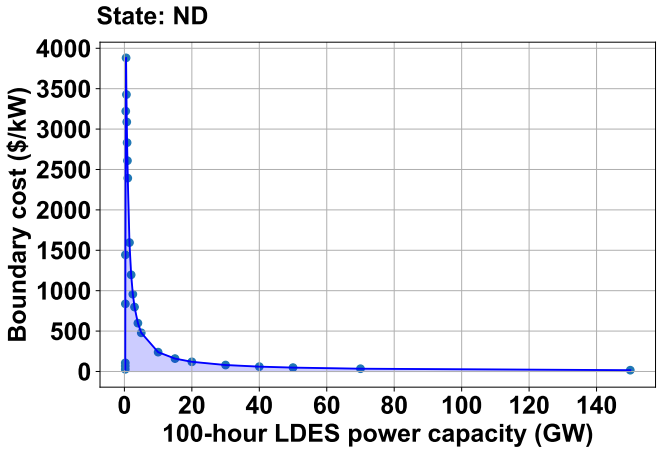

(a) Boundary cost curve.

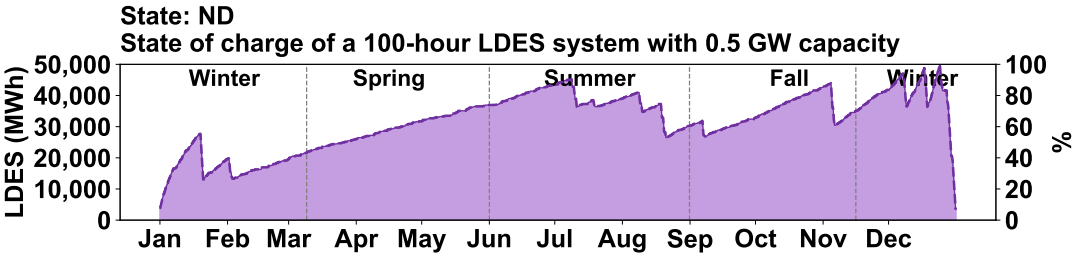

(b) State of charge.

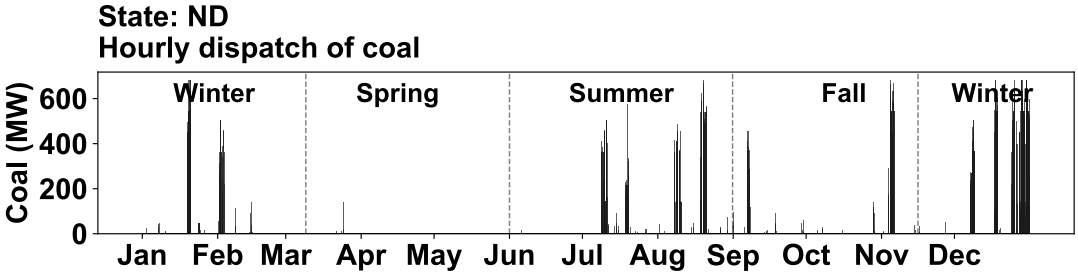

(c) Hourly dispatch of coal.

Figure 64 – North Dakota (ND).

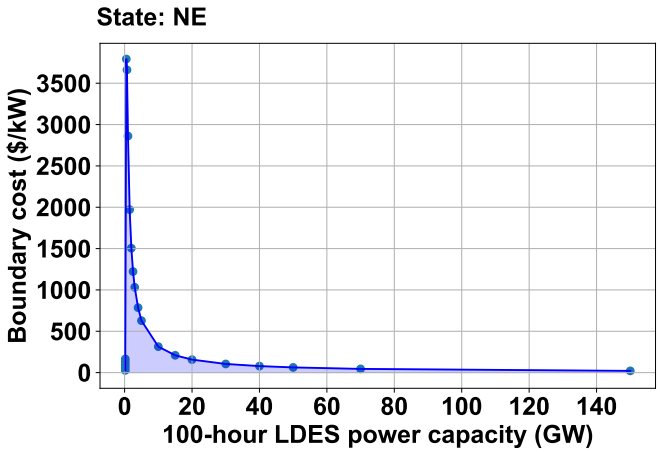

(a) Boundary cost curve.

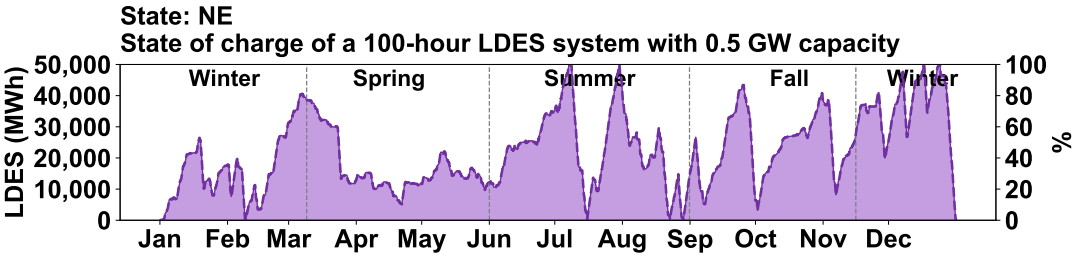

(b) State of charge.

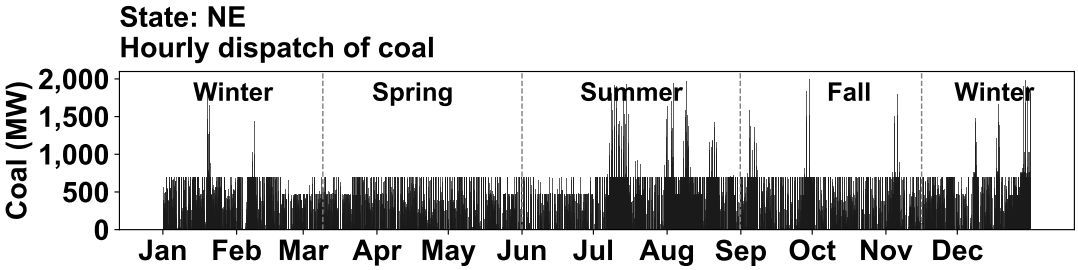

(c) Hourly dispatch of coal.

Figure 65 – Nebraska (NE).

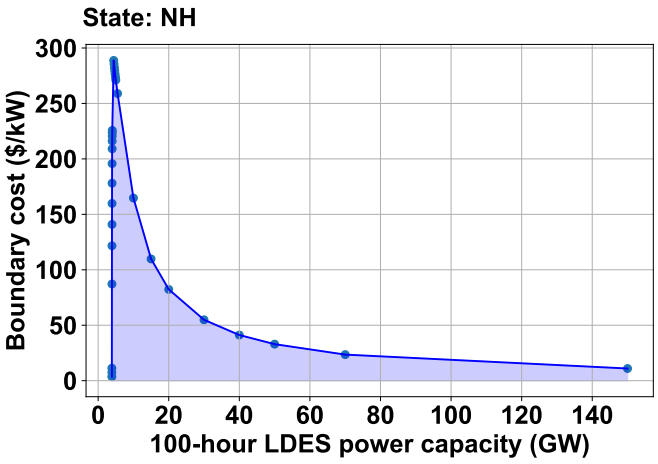

(a) Boundary cost curve.

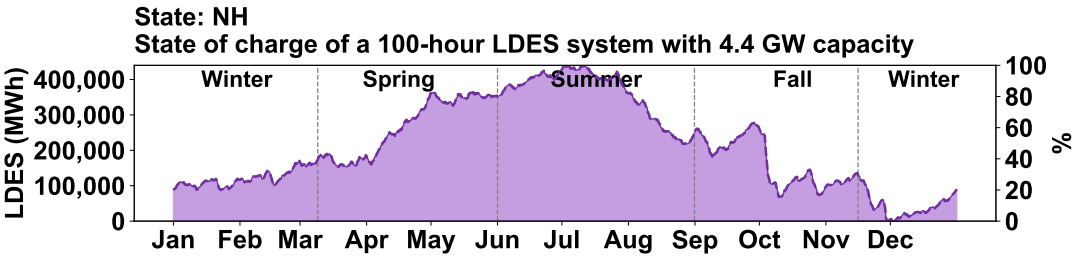

(b) State of charge.

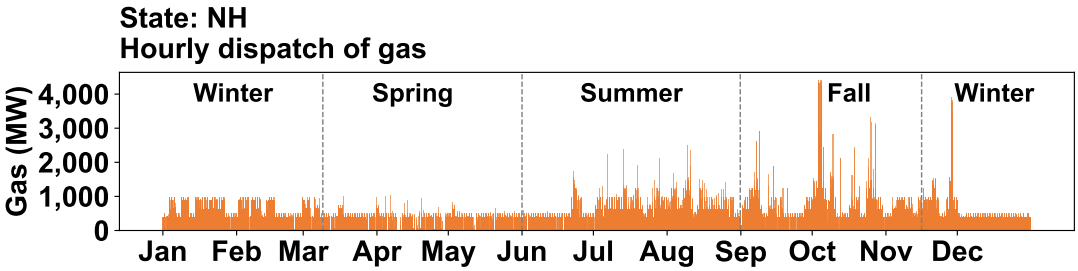

(c) Hourly dispatch of gas.

Figure 66 – New Hampshire (NH).

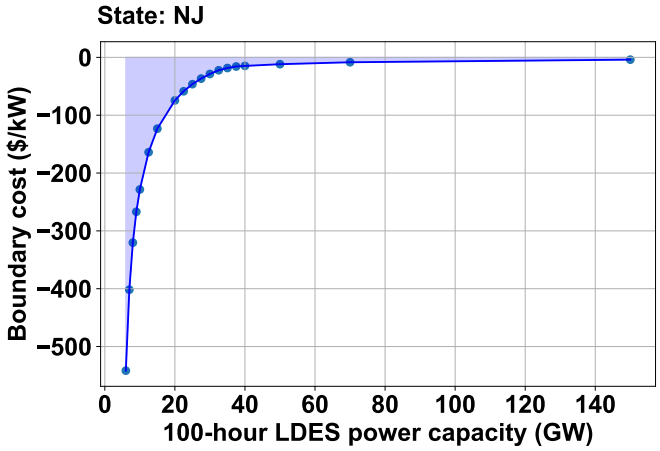

(a) Boundary cost curve.

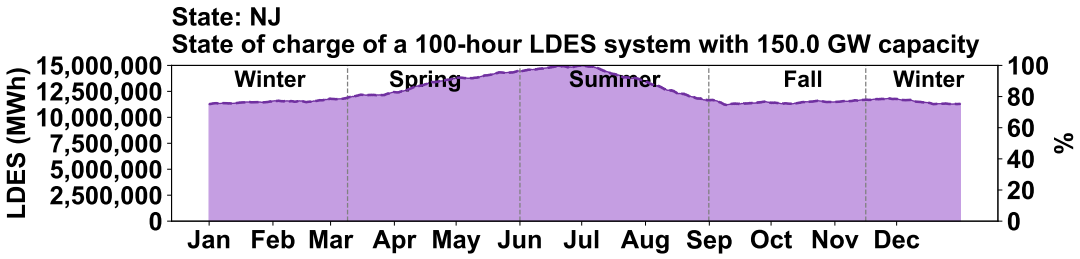

(b) State of charge.

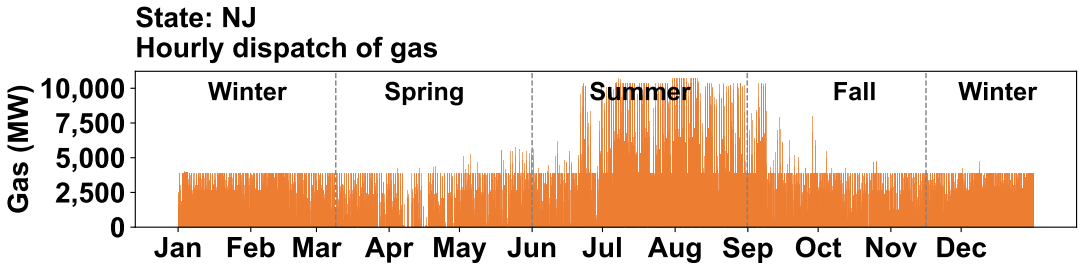

(c) Hourly dispatch of gas.

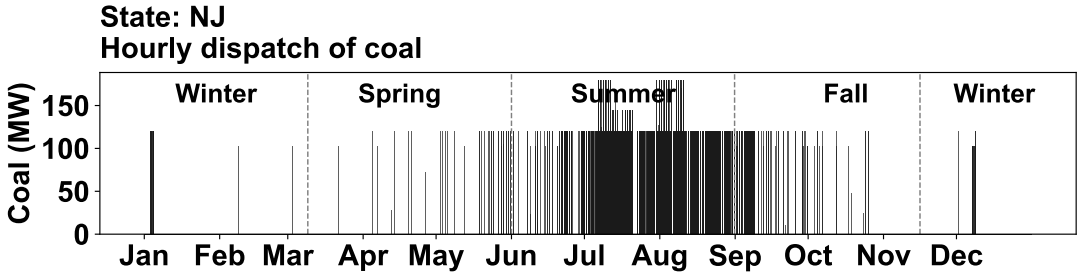

(d) Hourly dispatch of coal.

Figure 67 – New Jersey (NJ).

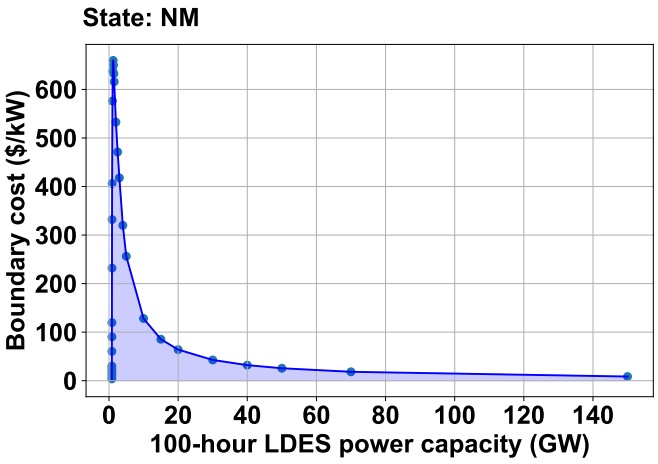

(a) Boundary cost curve.

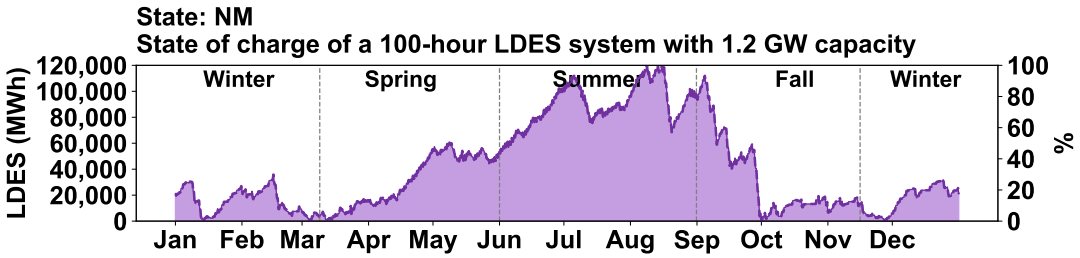

(b) State of charge.

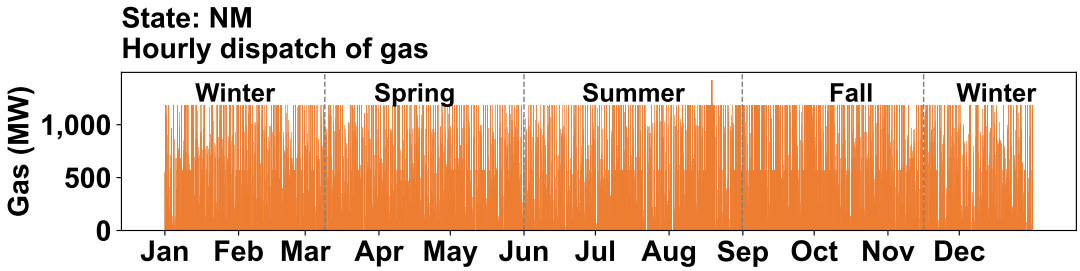

(c) Hourly dispatch of gas.

Figure 68 – New Mexico (NM).

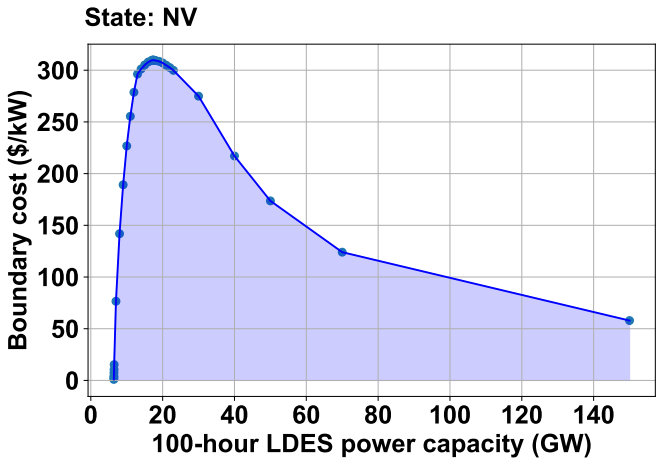

(a) Boundary cost curve.

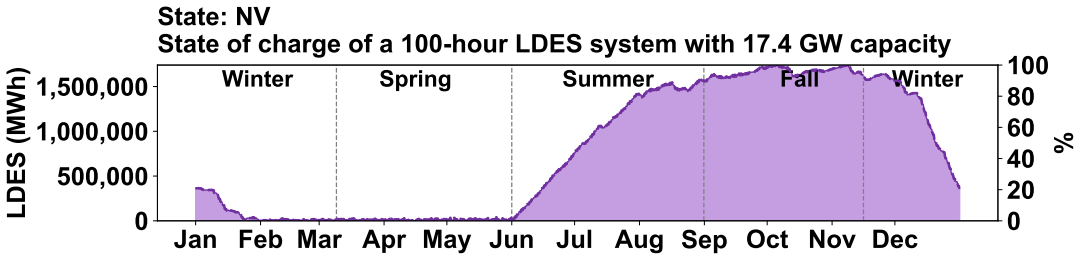

(b) State of charge.

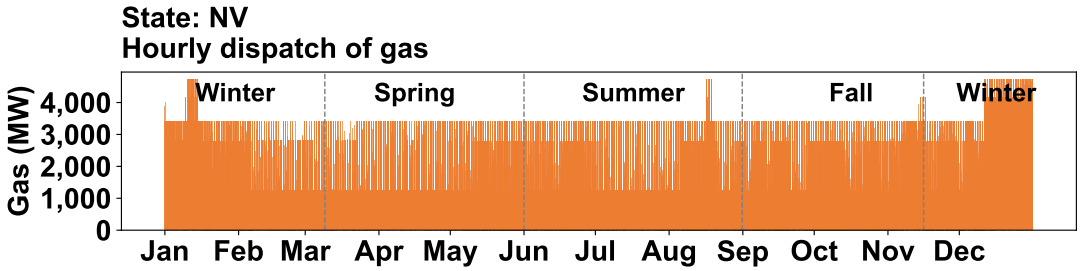

(c) Hourly dispatch of gas.

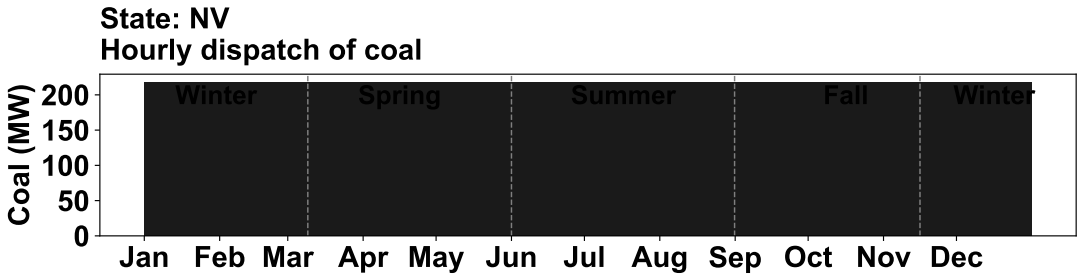

(d) Hourly dispatch of coal.

Figure 69 – Nevada (NV).

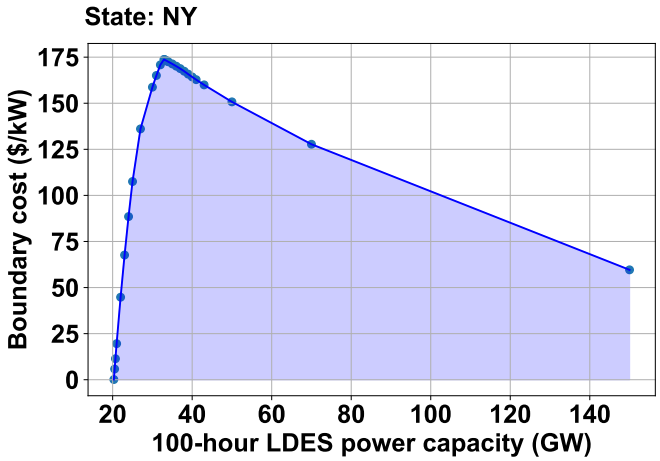

(a) Boundary cost curve.

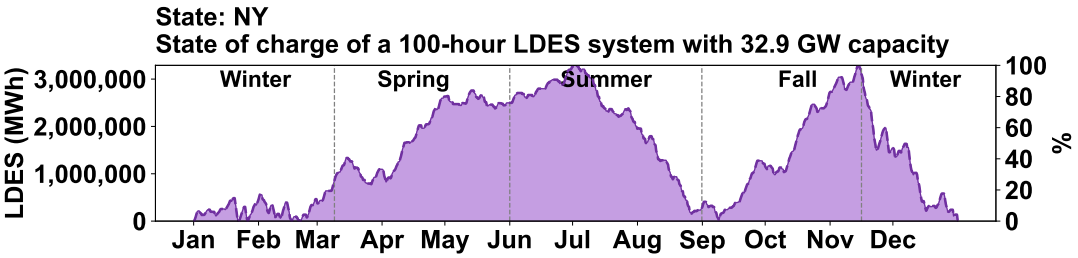

(b) State of charge.

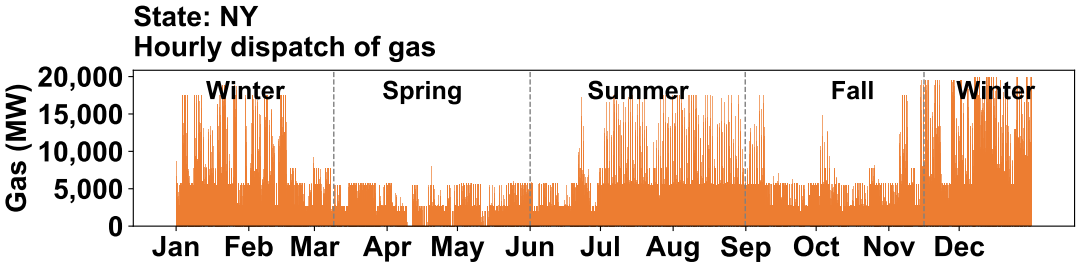

(c) Hourly dispatch of gas.

Figure 70 – New York (NY).

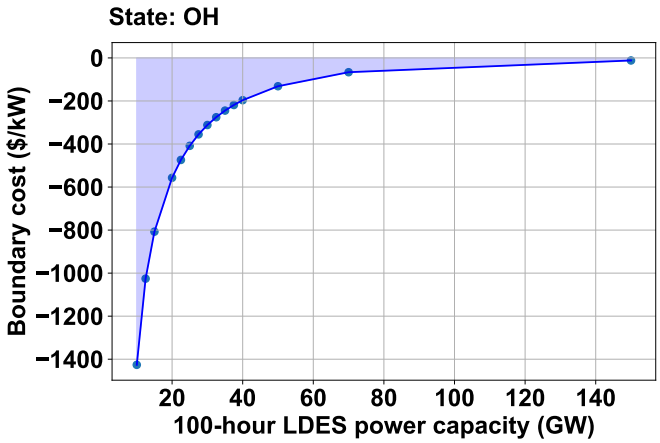

(a) Boundary cost curve.

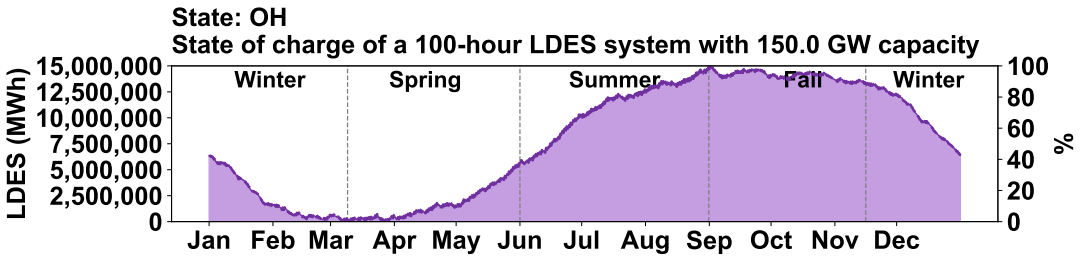

(b) State of charge.

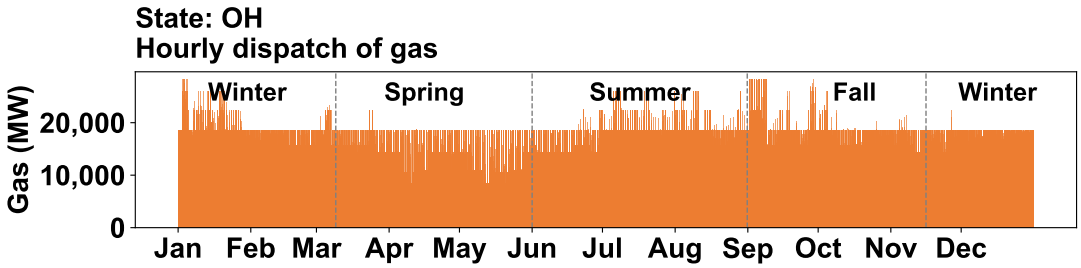

(c) Hourly dispatch of gas.

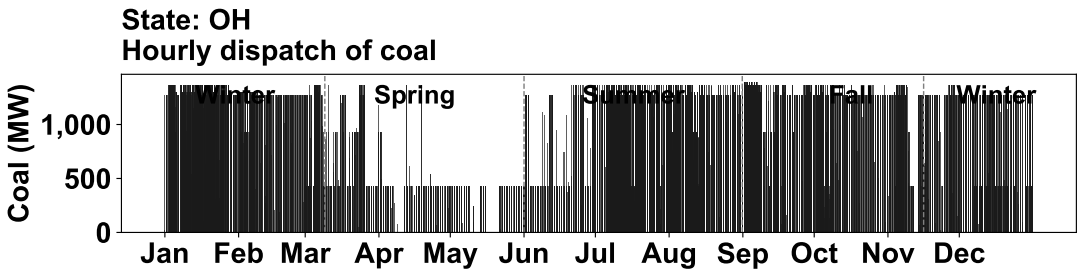

(d) Hourly dispatch of coal.

Figure 71 – Ohio (OH).

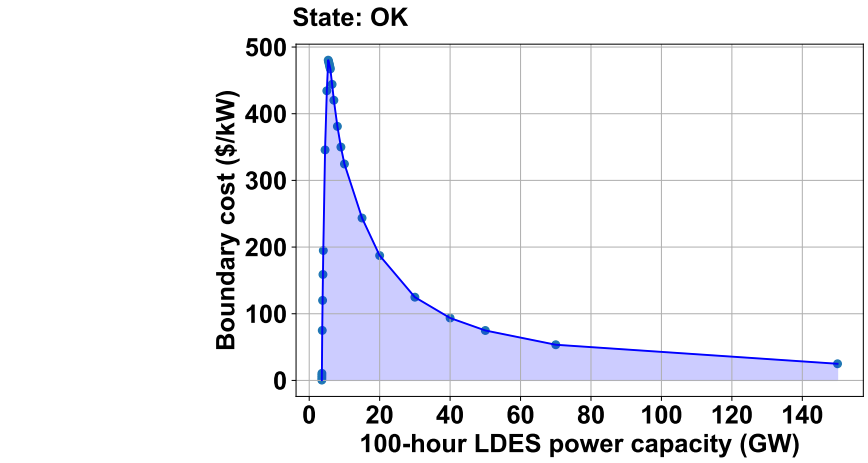

(a) Boundary cost curve.

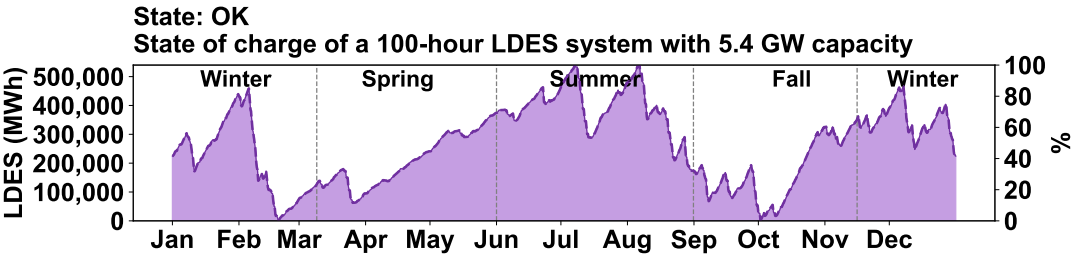

(b) State of charge.

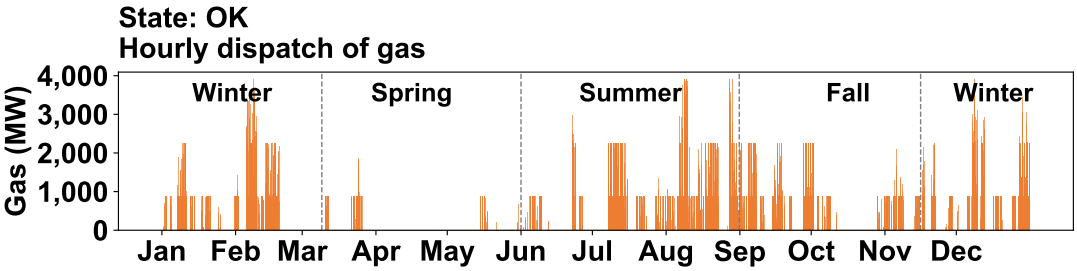

(c) Hourly dispatch of gas.

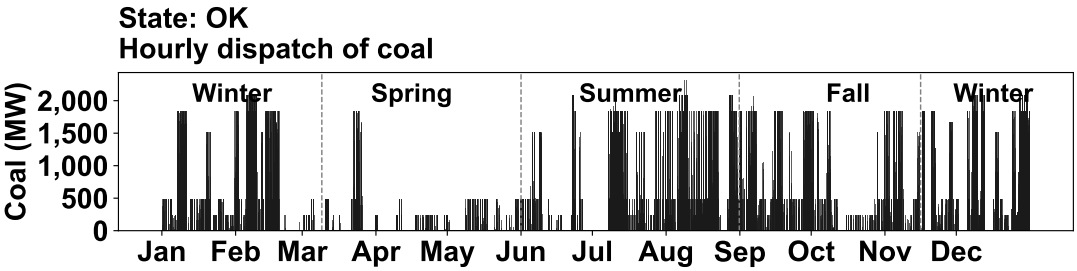

(d) Hourly dispatch of coal.

Figure 72 – Oklahoma (OK).

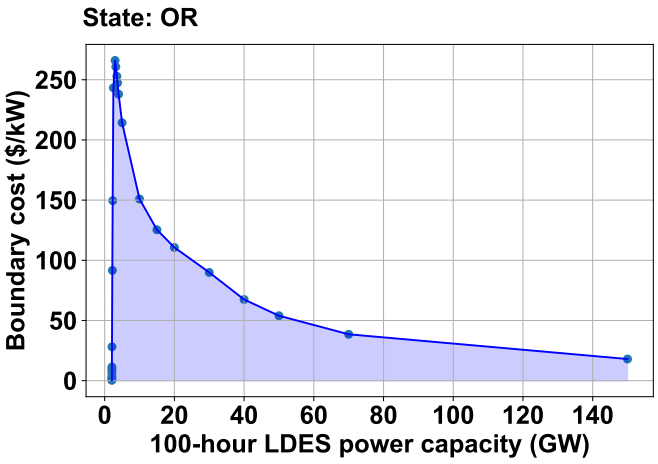

(a) Boundary cost curve.

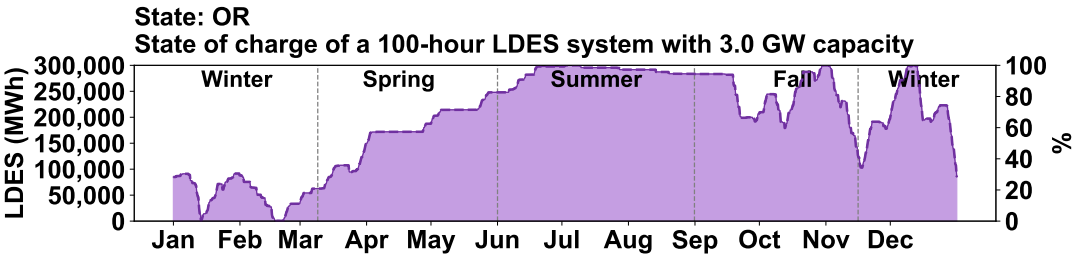

(b) State of charge.

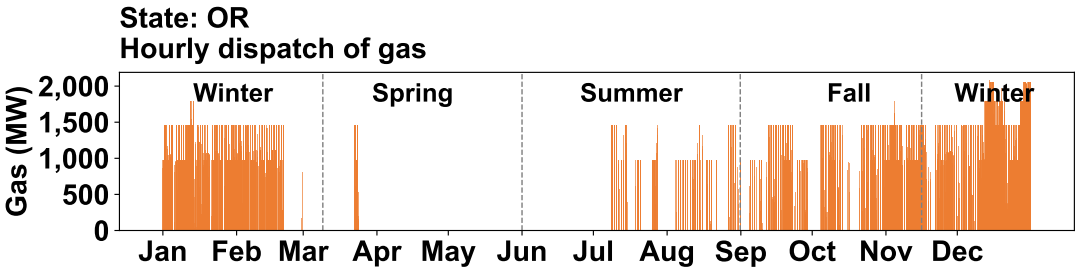

(c) Hourly dispatch of gas.

Figure 73 – Oregon (OR).

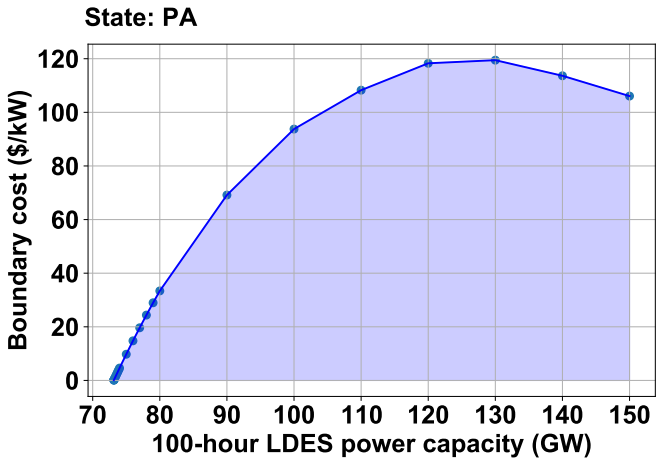

(a) Boundary cost curve.

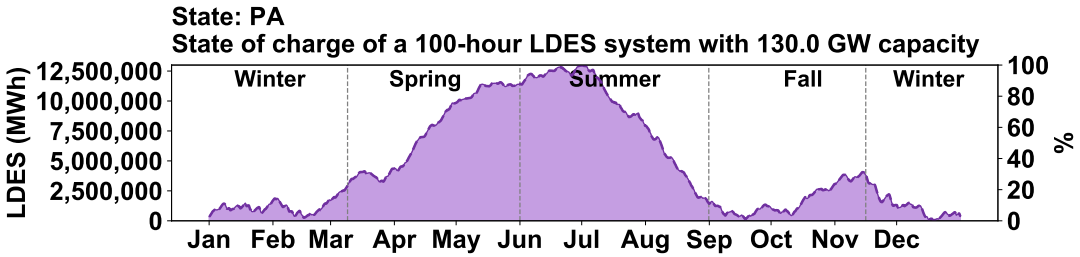

(b) State of charge.

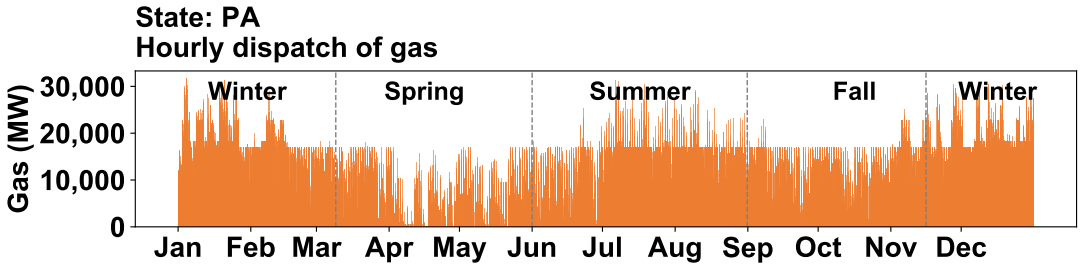

(c) Hourly dispatch of gas.

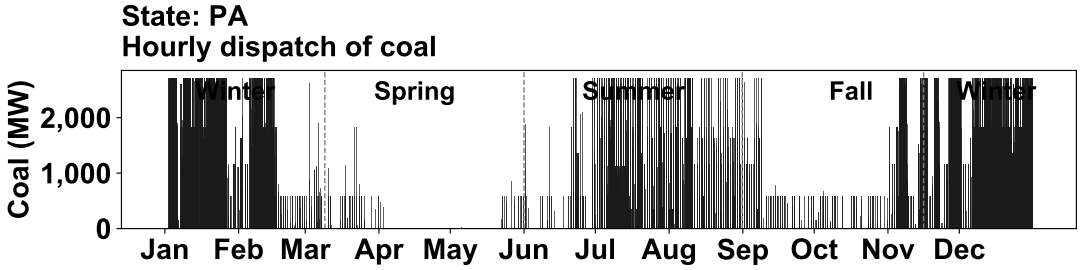

(d) Hourly dispatch of coal.

Figure 74 – Pennsylvania (PA).

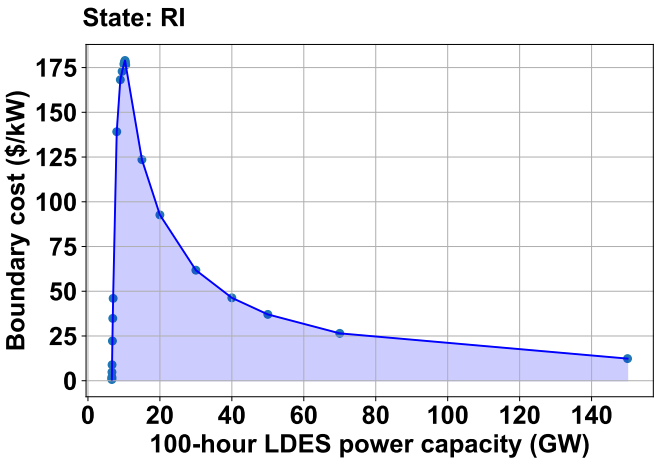

(a) Boundary cost curve.

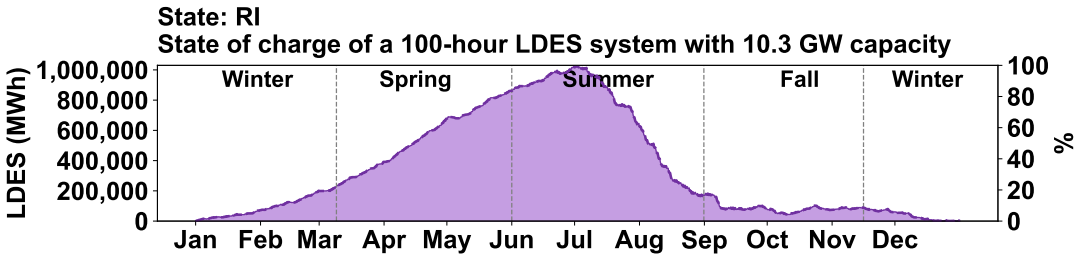

(b) State of charge.

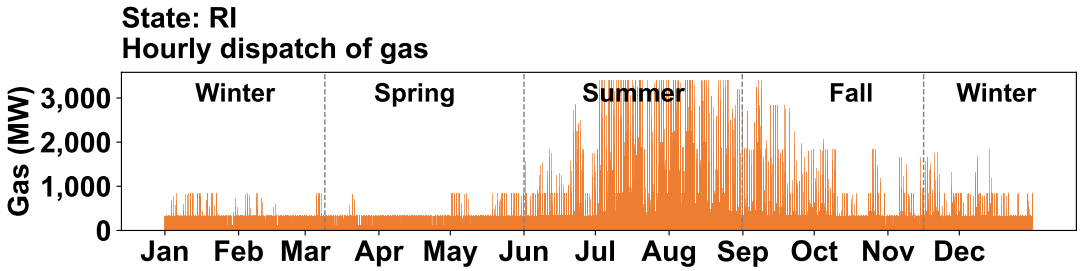

(c) Hourly dispatch of gas.

Figure 75 – Rhode Island (RI).

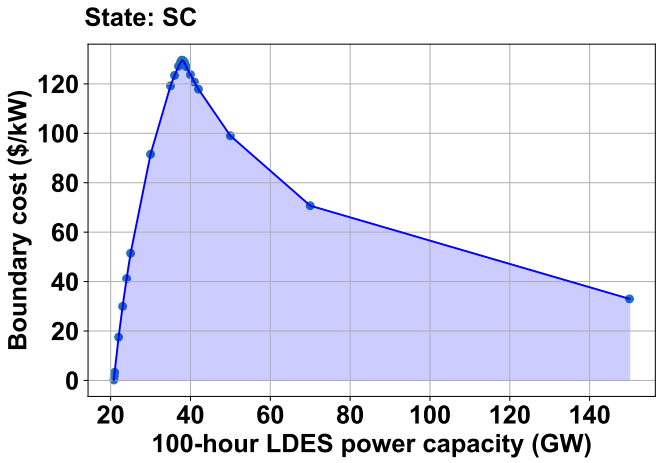

(a) Boundary cost curve.

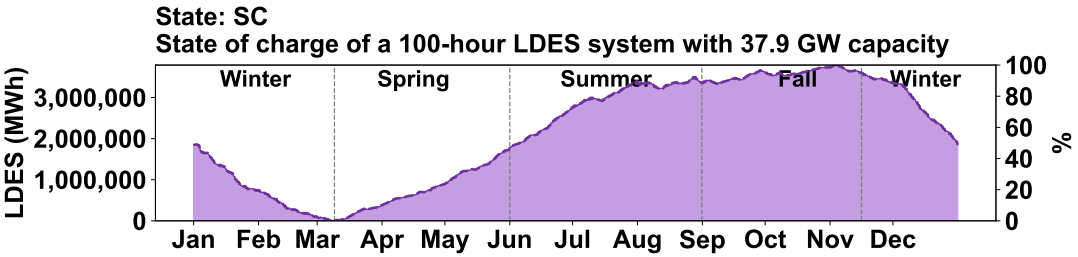

(b) State of charge.

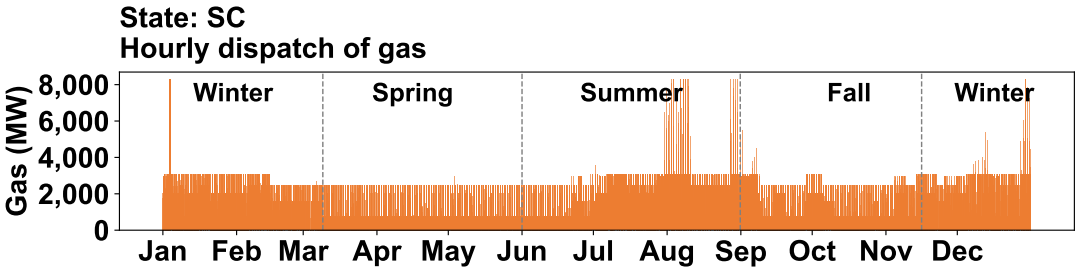

(c) Hourly dispatch of gas.

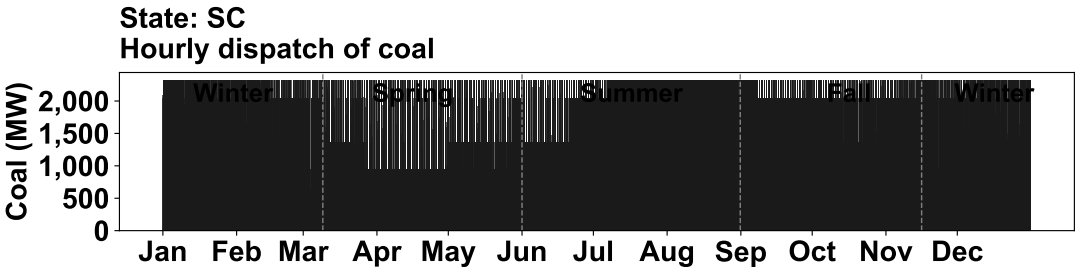

(d) Hourly dispatch of coal.

Figure 76 – South Carolina (SC).

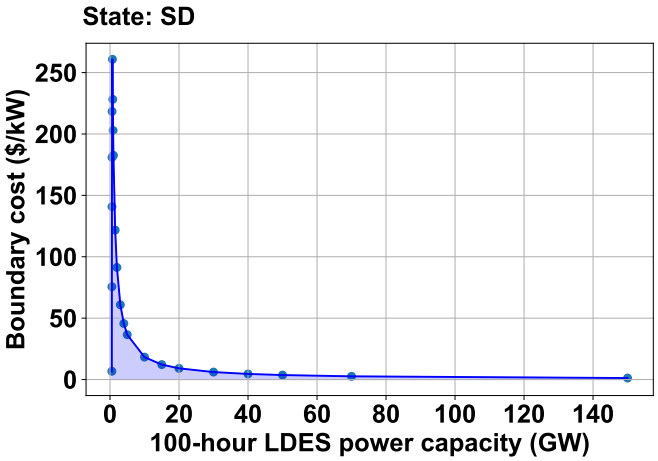

(a) Boundary cost curve.

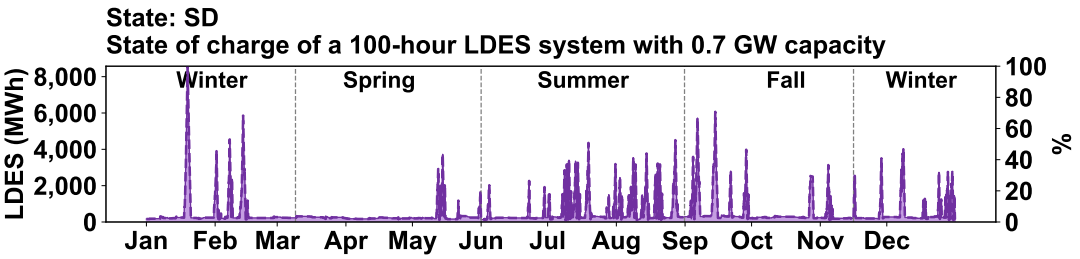

(b) State of charge.

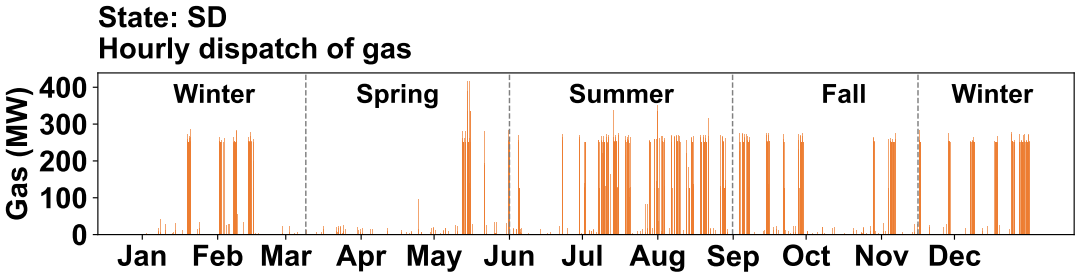

(c) Hourly dispatch of gas.

Figure 77 – South Dakota (SD).

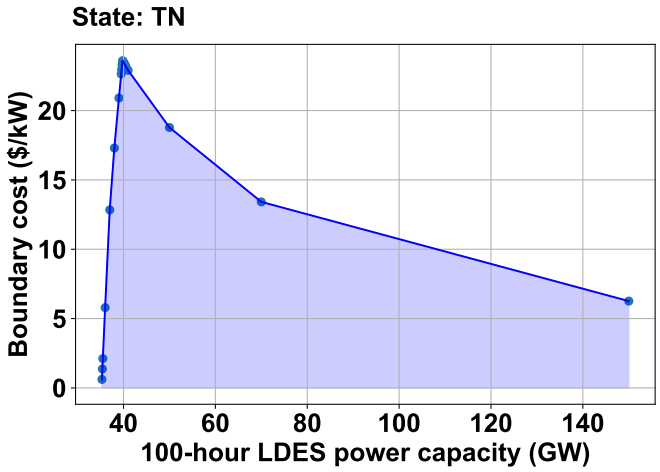

(a) Boundary cost curve.

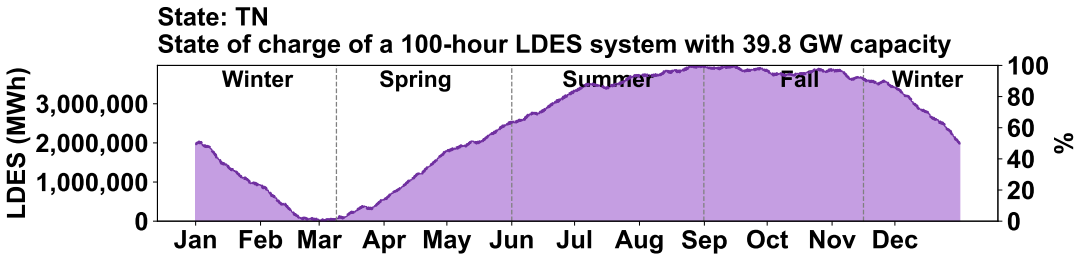

(b) State of charge.

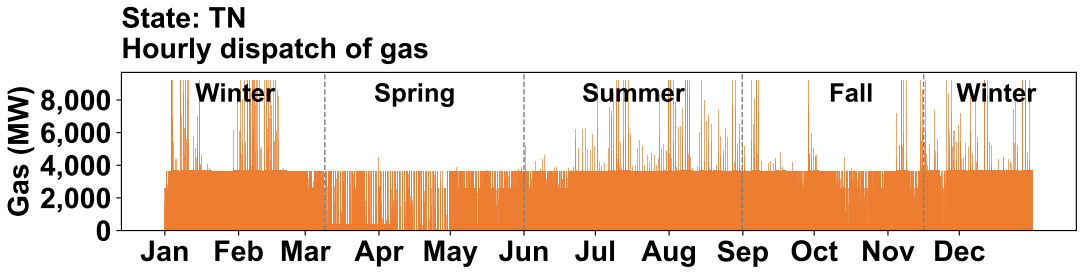

(c) Hourly dispatch of gas.

Figure 78 – Tennessee (TN).

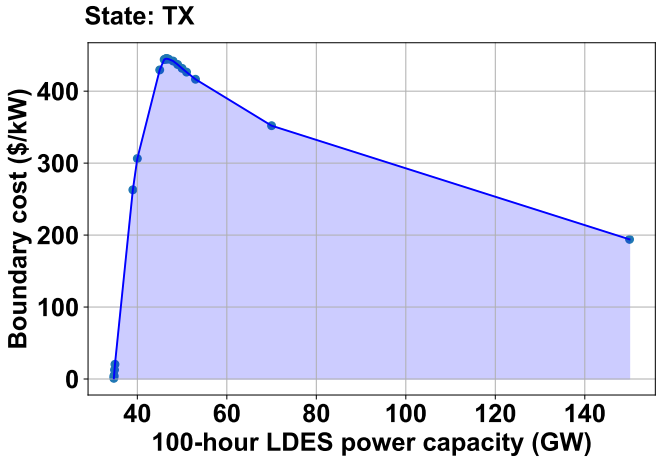

(a) Boundary cost curve.

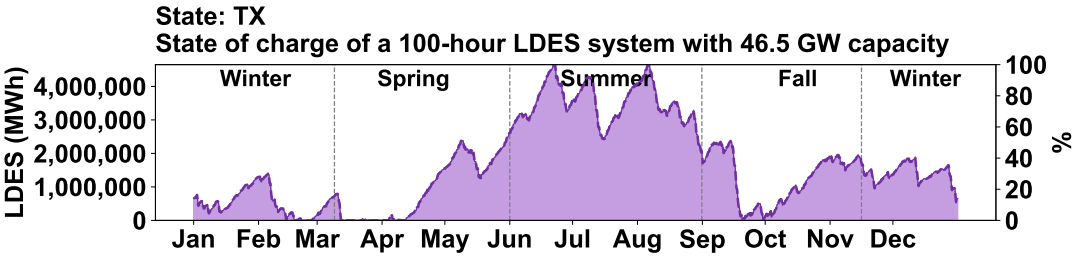

(b) State of charge.

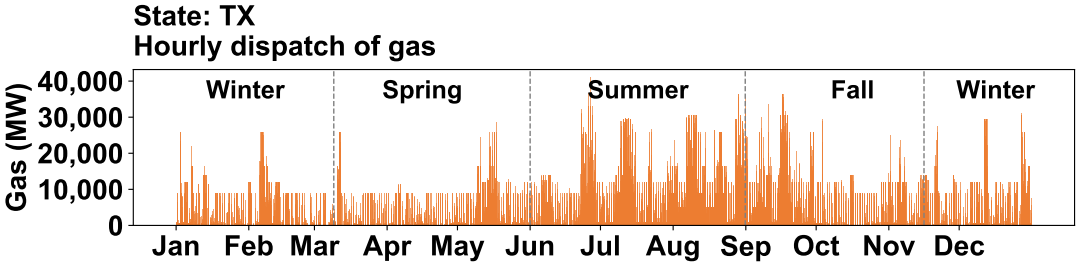

(c) Hourly dispatch of gas.

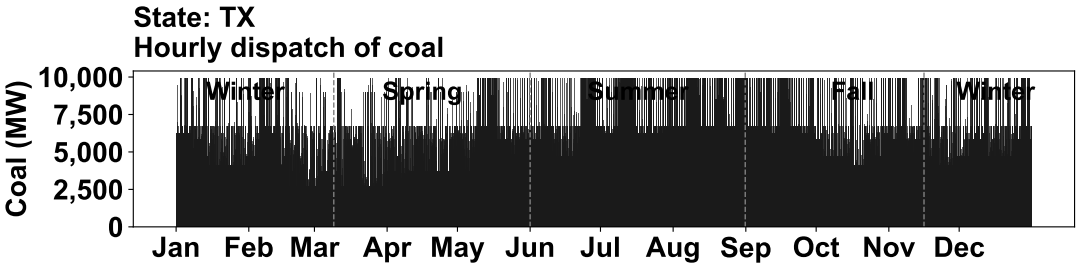

(d) Hourly dispatch of coal.

Figure 79 – Texas (TX).

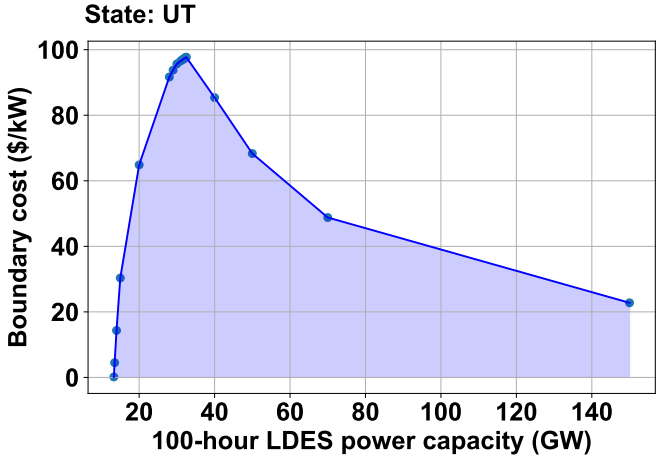

(a) Boundary cost curve.

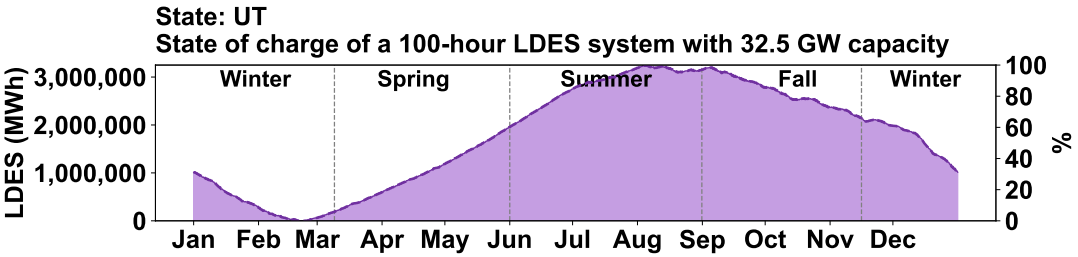

(b) State of charge.

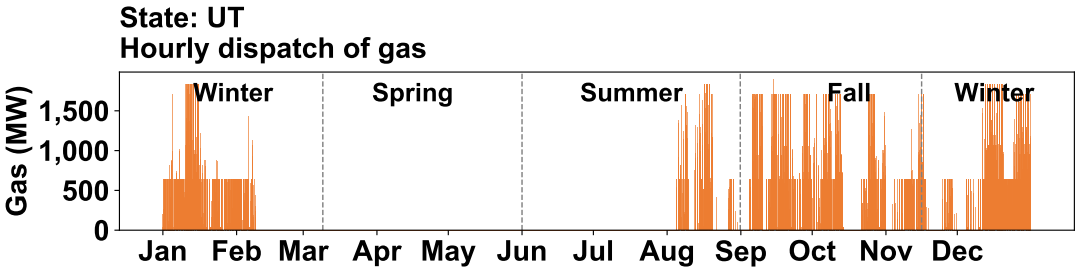

(c) Hourly dispatch of gas.

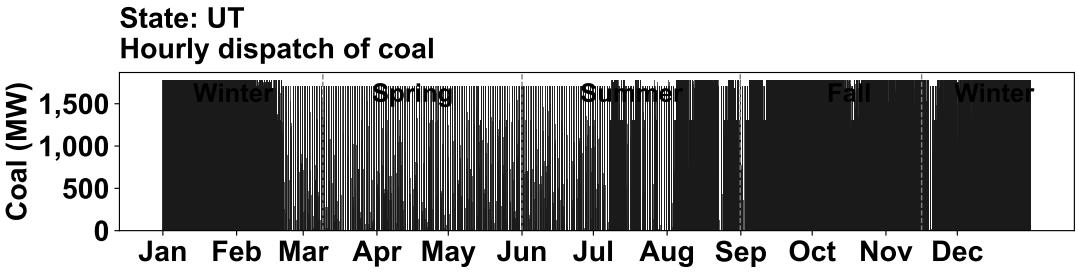

(d) Hourly dispatch of coal.

Figure 80 – Utah (UT).

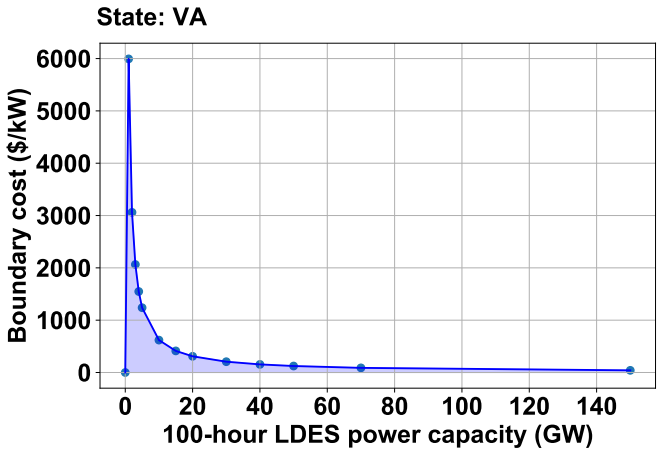

(a) Boundary cost curve.

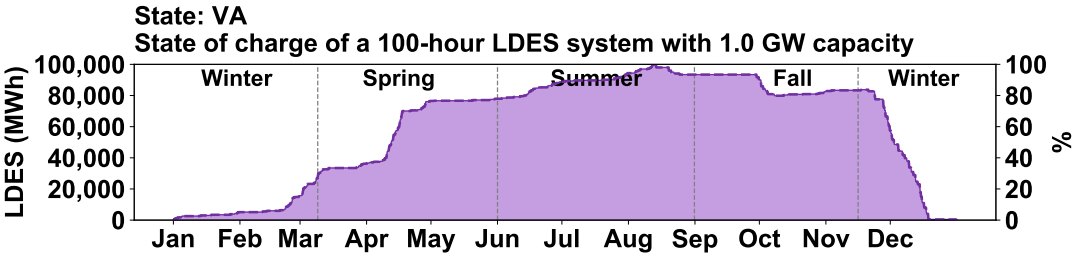

(b) State of charge.

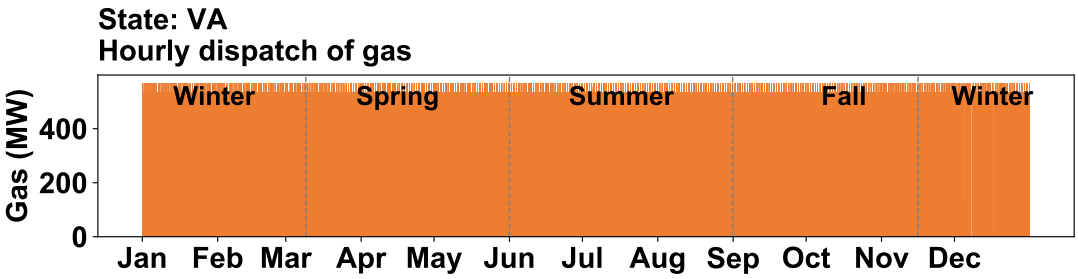

(c) Hourly dispatch of gas.

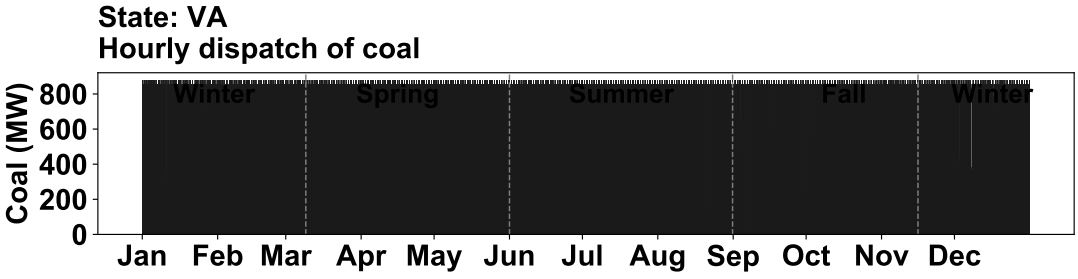

(d) Hourly dispatch of coal.

Figure 81 – Virginia (VA).

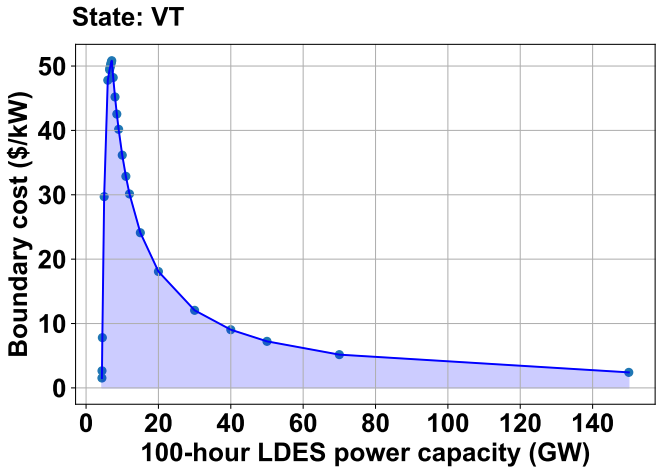

(a) Boundary cost curve.

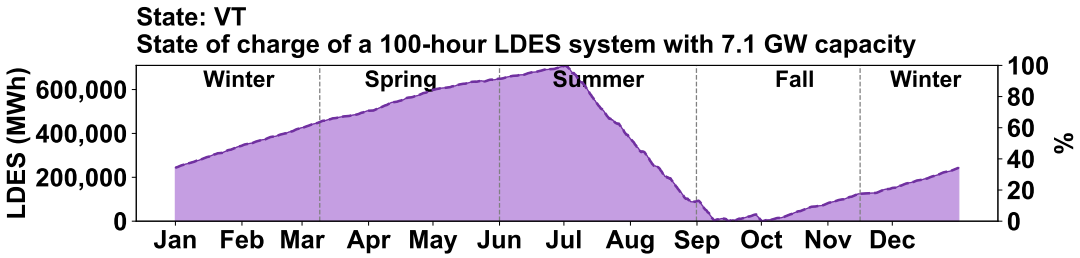

(b) State of charge.

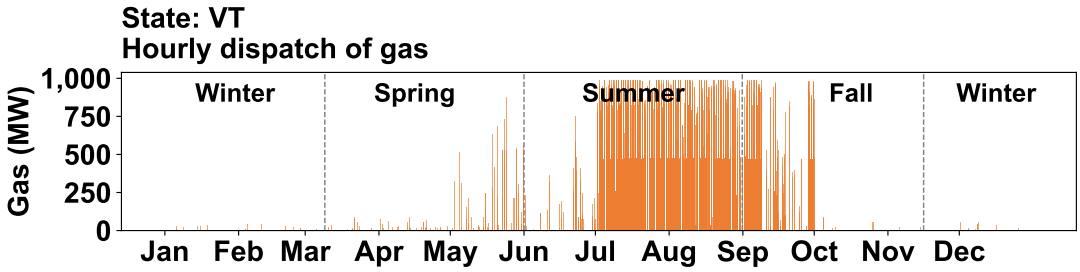

(c) Hourly dispatch of gas.

Figure 82 – Vermont (VT).

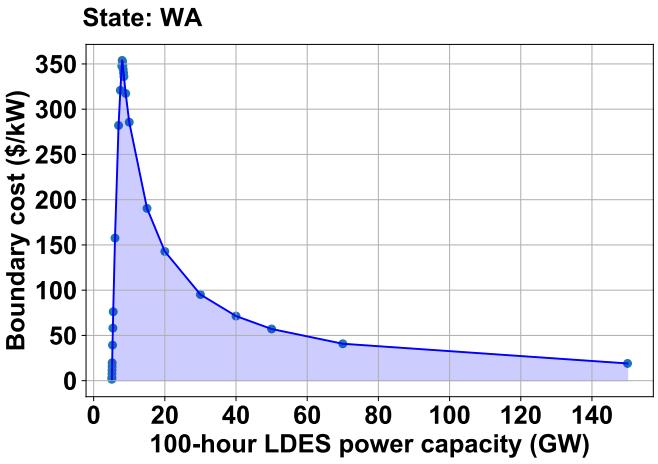

(a) Boundary cost curve.

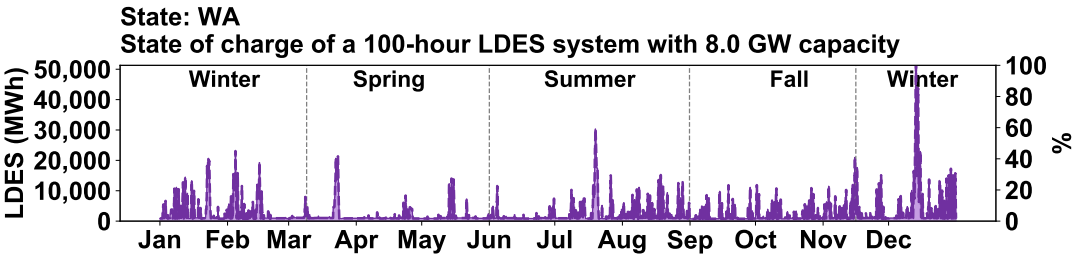

(b) State of charge.

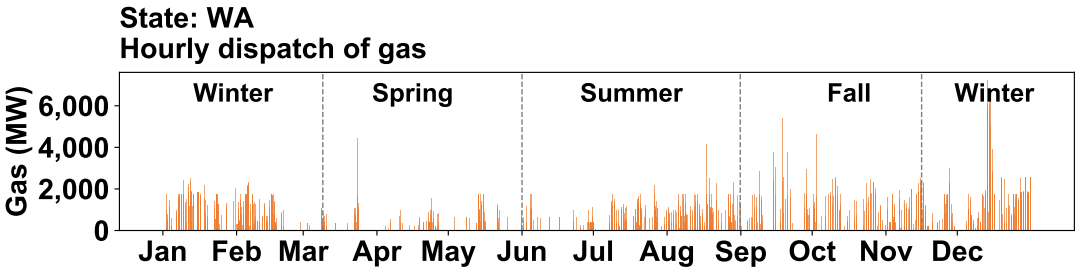

(c) Hourly dispatch of gas.

Figure 83 – Washington (WA).

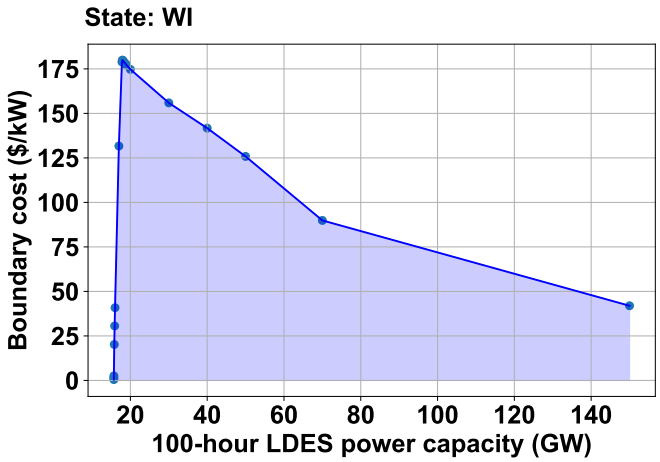

(a) Boundary cost curve.

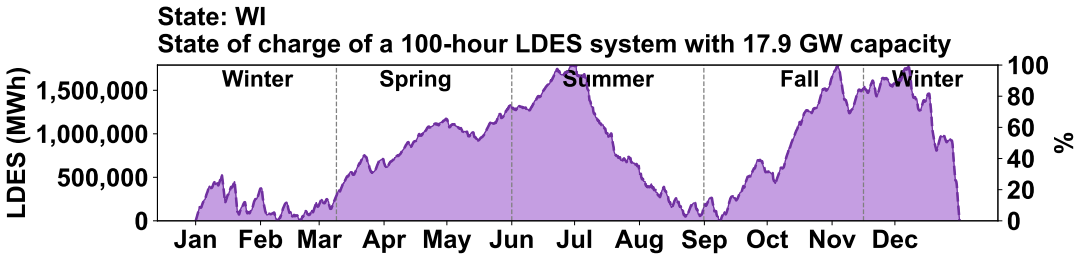

(b) State of charge.

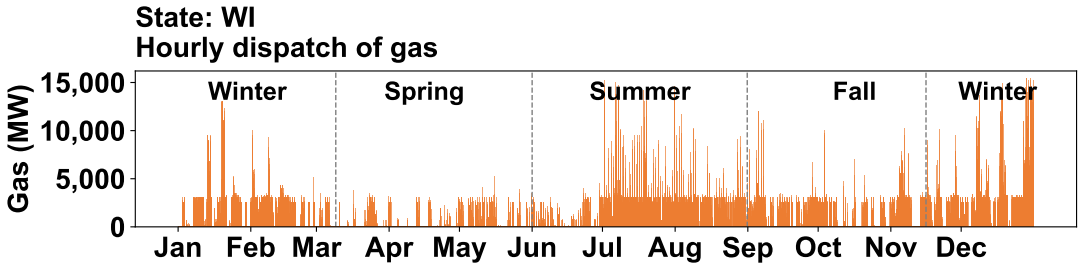

(c) Hourly dispatch of gas.

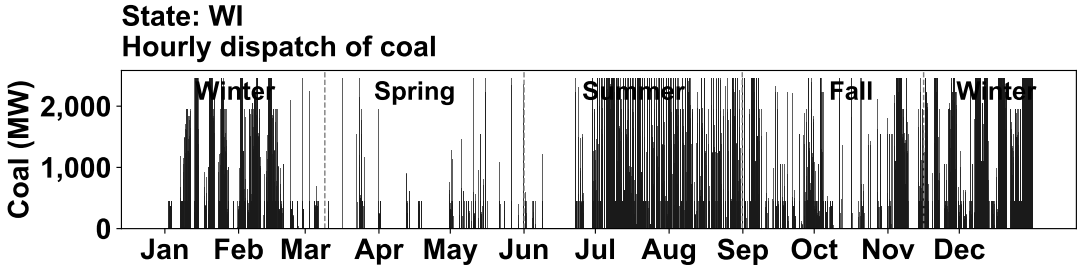

(d) Hourly dispatch of coal.

Figure 84 – Wisconsin (WI).

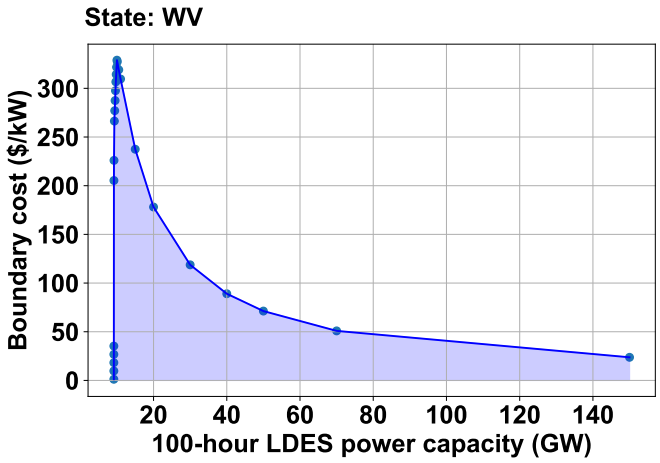

(a) Boundary cost curve.

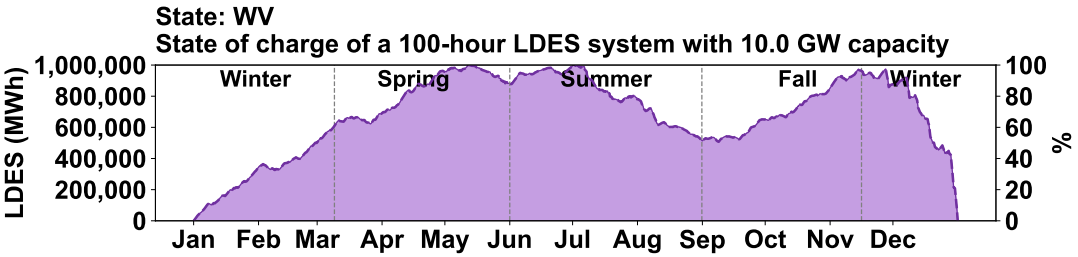

(b) State of charge.

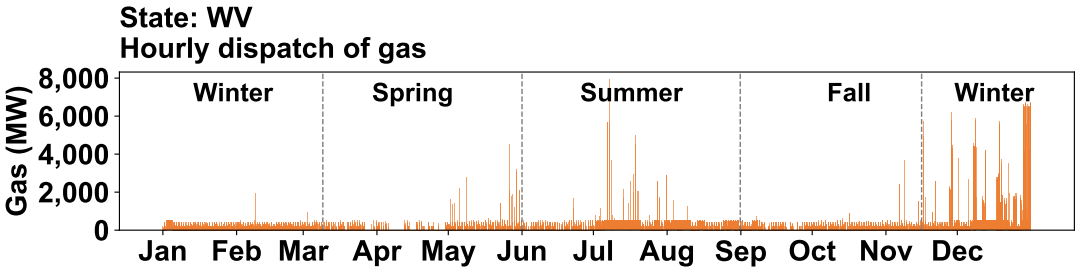

(c) Hourly dispatch of gas.

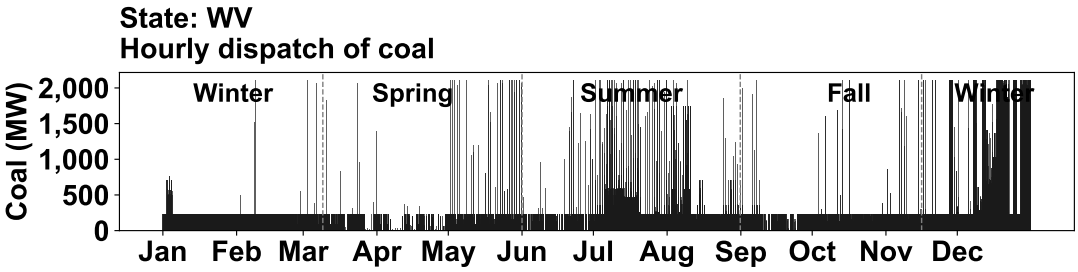

(d) Hourly dispatch of coal.

Figure 85 – West Virginia (WV).

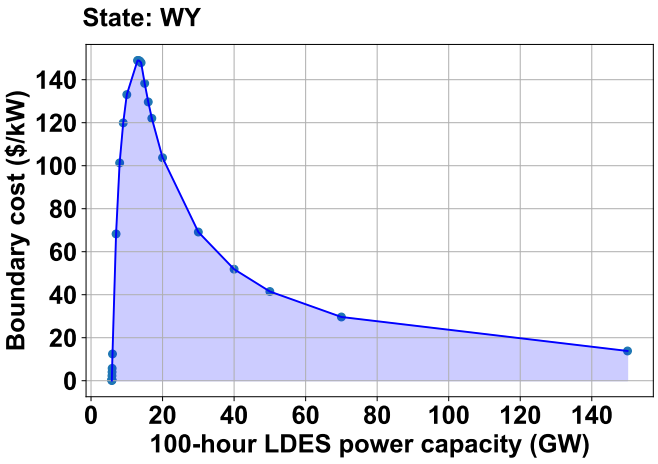

(a) Boundary cost curve.

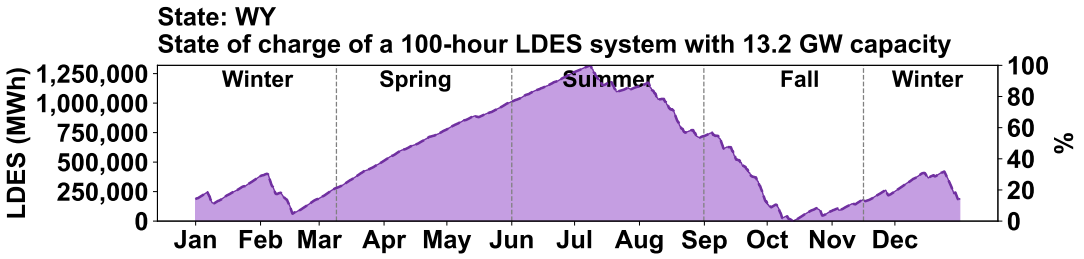

(b) State of charge.

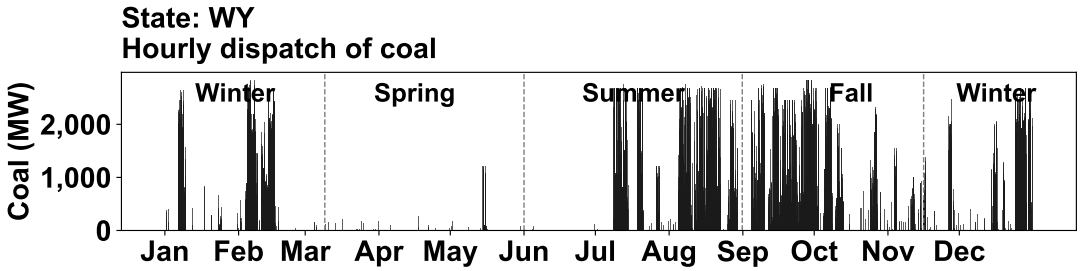

(c) Hourly dispatch of coal.

Figure 86 – Wyoming (WY).